ISSN 1948-9366 (online)

World Journal of

Gastrointestinal Surgery

World J Gastrointest Surg 2022 October 27; 14(10): 1089-1178

Published by Baishideng Publishing Group Inc

World Journal of Gastrointestinal Surgery

Contents

Monthly Volume 14 Number 10 October 27, 2022

REVIEW

ORIGINAL ARTICLE

Retrospective Study

Observational Study

CASE REPORT

World Journal of Gastrointestinal Surgery

Monthly Volume 14 Number 10 October 27, 2022

Contents

ABOUT COVER

Editorial Board Member of *World Journal of Gastrointestinal Surgery*, Anil Kumar Agarwal, FACS, FRCS (Hon), MBBS, MCh, MS, Director, Professor, Surgeon, Department of Gastrointestinal Surgery and Liver Transplant, GB Pant Institute of Postgraduate Medical Education and Research and Maulana Azad Medical College, Delhi University, New Delhi 110002, India. aka.gis@gmail.com

AIMS AND SCOPE

The primary aim of *World Journal of Gastrointestinal Surgery* (*WJGS*, *World J Gastrointest Surg*) is to provide scholars and readers from various fields of gastrointestinal surgery with a platform to publish high-quality basic and clinical research articles and communicate their research findings online.

WJGS mainly publishes articles reporting research results and findings obtained in the field of gastrointestinal surgery and covering a wide range of topics including biliary tract surgical procedures, biliopancreatic diversion, colectomy, esophagectomy, esophagostomy, pancreas transplantation, and pancreatectomy, *etc*.

INDEXING/ABSTRACTING

The *WJGS* is now abstracted and indexed in Science Citation Index Expanded (SCIE, also known as SciSearch®), Current Contents/Clinical Medicine, Journal Citation Reports/Science Edition, PubMed, PubMed Central, Reference Citation Analysis, China National Knowledge Infrastructure, China Science and Technology Journal Database, and Superstar Journals Database. The 2022 Edition of Journal Citation Reports® cites the 2021 impact factor (IF) for *WJGS* as 2.505; IF without journal self cites: 2.473; 5-year IF: 3.099; Journal Citation Indicator: 0.49; Ranking: 104 among 211 journals in surgery; Quartile category: Q2; Ranking: 81 among 93 journals in gastroenterology and hepatology; and Quartile category: Q4.

RESPONSIBLE EDITORS FOR THIS ISSUE

Production Editor: *Rui-Rui Wu*; **Production Department Director:** *Xiang Li*; **Editorial Office Director:** *Jia-Ru Fan*.

NAME OF JOURNAL
World Journal of Gastrointestinal Surgery

ISSN
ISSN 1948-9366 (online)

LAUNCH DATE
November 30, 2009

FREQUENCY
Monthly

EDITORS-IN-CHIEF
Peter Schemmer

EDITORIAL BOARD MEMBERS
https://www.wjgnet.com/1948-9366/editorialboard.htm

PUBLICATION DATE
October 27, 2022

INSTRUCTIONS TO AUTHORS
https://www.wjgnet.com/bpg/gerinfo/204

GUIDELINES FOR ETHICS DOCUMENTS
https://www.wjgnet.com/bpg/GerInfo/287

GUIDELINES FOR NON-NATIVE SPEAKERS OF ENGLISH
https://www.wjgnet.com/bpg/gerinfo/240

PUBLICATION ETHICS
https://www.wjgnet.com/bpg/GerInfo/288

PUBLICATION MISCONDUCT
https://www.wjgnet.com/bpg/gerinfo/208

ARTICLE PROCESSING CHARGE
https://www.wjgnet.com/bpg/gerinfo/242

STEPS FOR SUBMITTING MANUSCRIPTS
https://www.wjgnet.com/bpg/GerInfo/239

ONLINE SUBMISSION
https://www.f6publishing.com

World Journal of Gastrointestinal Surgery

Submit a Manuscript: https://www.f6publishing.com

World J Gastrointest Surg 2022 October 27; 14(10): 1089-1106

DOI: 10.4240/wjgs.v14.i10.1089

ISSN 1948-9366 (online)

REVIEW

Drain fluid biomarkers for prediction and diagnosis of clinically relevant postoperative pancreatic fistula: A narrative review

Nadya Rykina-Tameeva, Jaswinder S Samra, Sumit Sahni, Anubhav Mittal

Specialty type: Surgery

Provenance and peer review: Invited article; Externally peer reviewed.

Peer-review model: Single blind

Peer-review report's scientific quality classification
Grade A (Excellent): A
Grade B (Very good): B
Grade C (Good): C, C
Grade D (Fair): 0
Grade E (Poor): 0

P-Reviewer: Gao W, China; Kitamura K, Japan; Sharma V, India

Received: June 16, 2022
Peer-review started: June 16, 2022
First decision: September 4, 2022
Revised: September 16, 2022
Accepted: October 14, 2022
Article in press: October 14, 2022
Published online: October 27, 2022

Nadya Rykina-Tameeva, Jaswinder S Samra, Sumit Sahni, Anubhav Mittal, Northern Clinical School, University of Sydney, St Leonards 2065, Australia

Corresponding author: Sumit Sahni, PhD, Research Fellow, Senior Research Fellow, Northern Clinical School, University of Sydney, Level 8, Kolling Building, Royal North Shore Hospital Campus, St Leonards 2065, Australia. sumit.sahni@sydney.edu.au

Abstract

Clinically relevant postoperative pancreatic fistula (CR-POPF) has continued to compromise patient recovery post-pancreatectomy despite decades of research seeking to improve risk prediction and diagnosis. The current diagnostic criteria for CR-POPF requires elevated drain fluid amylase to present alongside POPF-related complications including infection, haemorrhage and organ failure. These worrying sequelae necessitate earlier and easily obtainable biomarkers capable of reflecting evolving CR-POPF. Drain fluid has recently emerged as a promising source of biomarkers as it is derived from the pancreas and hence, capable of reflecting its postoperative condition. The present review aims to summarise the current knowledge of CR-POPF drain fluid biomarkers and identify gaps in the field to invigorate future research in this critical area of clinical need. These findings may provide robust diagnostic alternatives for CR-POPF and hence, to clarify their clinical utility require further reports detailing their diagnostic and/or predictive accuracy.

Key Words: Biomarkers; Clinically relevant postoperative pancreatic fistula; Diagnosis; Drain fluid; Prediction

Core Tip: This review demonstrates the potential for drain fluid biomarkers to overcome the limitations of the current diagnostic definition of clinically relevant postoperative pancreatic fistula. Numerous future directions for drain fluid research have been identified, where ideally, new biomarkers would report the accuracy of surgery-specific, risk-stratified cut-offs to clarify their clinical utility. Hence, decisions regarding drain removal and further monitoring can accordingly be made to either expediate or make recovery safer respectively. These improvements will invariably bolster pancreatic ductal adenocarcinoma survival outcomes by tapering the high morbidity of pancreatectomies and ensuring better quality of life for patients.

Citation: Rykina-Tameeva N, Samra JS, Sahni S, Mittal A. Drain fluid biomarkers for prediction and diagnosis of clinically relevant postoperative pancreatic fistula: A narrative review. *World J Gastrointest Surg* 2022; 14(10): 1089-1106
URL: https://www.wjgnet.com/1948-9366/full/v14/i10/1089.htm
DOI: https://dx.doi.org/10.4240/wjgs.v14.i10.1089

INTRODUCTION

Pancreatic cancer represents a grave diagnosis in which incidence closely parallels mortality[1]. Manifesting as adenocarcinomas, neuroendocrine tumors, acinar carcinomas, colloid carcinomas, pancreatoblastomas and solid-pseudopapillary neoplasms, pancreatic cancer is predicted to be the second most diagnosed cancer by 2030[2]. Both the challenges of early diagnosis and treatment contribute to its dismal prognosis, whereby its failure to manifest symptoms early and resistance to conventional treatments leaves surgery as the only curative option[3,4]. The greatest contributor to the burden of pancreatic cancer is pancreatic ductal adenocarcinoma (PDAC) which occurs in 90% of cases and has the highest fatality rate of all solid tumors[3,5]. The majority of PDACs develop in the head of the pancreas (60%-70%) and require pancreaticoduodenectomy. The remainder arise in the body and tail (15% of cases each) which require a distal pancreatectomy to excise the tumor[6] (Figure 1). As only 20%-25% of PDAC patients are diagnosed with resectable disease, maximising their surgical outcomes is of utmost importance, particularly as 5-year survival can improve from < 7% without surgery[3] to 39% after surgery[7]. Necessarily, this involves minimising surgical complications, not only to improve recovery, but to avoid increasing the challenges of cancer which already include compromised nutrition, immunity, metabolism as well as mental and financial wellbeing[8-10]. Clinically relevant postoperative pancreatic fistula (CR-POPF) has persisted as the leading cause of postoperative morbidity and mortality despite decades of improving pancreatectomy techniques and perioperative care[11-15]. Affecting up to 50% of cases[16], CR-POPF has been shown to increase readmission rates, length of stay, health-related costs and particularly relevant for pancreatic cancer patients, potentiate recurrence and delay the delivery of adjuvant therapy, both of which can compromise the curative intent of surgery[17-22].

CR-POPF definition

POPF was initially stratified into grades A-C[23], with grade A since being reclassified by the International Study Group on Pancreatic Surgery (ISGPS) as a biochemical leak in favour of recognising the clinically relevant grades B and C[24]. CR-POPF is diagnosed once drain amylase on postoperative day (POD) three exceeds three times the upper limit of normal for serum amylase and the patient develops a clinically relevant change in their condition, necessitating intervention (Figure 2). Grade B fistulae are characterised by prolonged drainage exceeding three weeks, pharmaceutical interventions, additional imaging and infections. Grade C sequelae are more severe, potentiating sepsis, organ failure and in up to 35% of cases, death[25]. This definition does not require imaging to confirm a diagnosis of CR-POPF, particularly as intra-abdominal fluid collections may be transiently increased after surgery. Imaging, however, may be necessary for planning interventions in confirmed cases[26]. Recently, non-contrast-enhanced computed tomography paired with machine learning has been shown capable of evaluating pancreatic texture to predict CR-POPF, doing so with a sensitivity of 0.96 and specificity of 0.98[27]. Similarly, transabdominal pancreatic ultrasound elastography has been associated with CR-POPF, occurring more in patients with softer parenchyma (P = 0.002)[28].

Pathophysiology of CR-POPF: Pancreatic fistulae often occur in pancreata with preserved exocrine function in which pancreatic enzymes are released and activated, damaging tissues, and potentiating systemic complications. Such glands are characterised by soft texture and at least normal acinar cell density at the surgical margin, both of which have been associated with CR-POPF after pancreatoduodenectomy and distal pancreatectomy[29-33]. In advanced PDAC, obstructive pancreatitis may develop[34], contributing to a firm parenchyma. Recently, neoadjuvant therapy has been explored as a

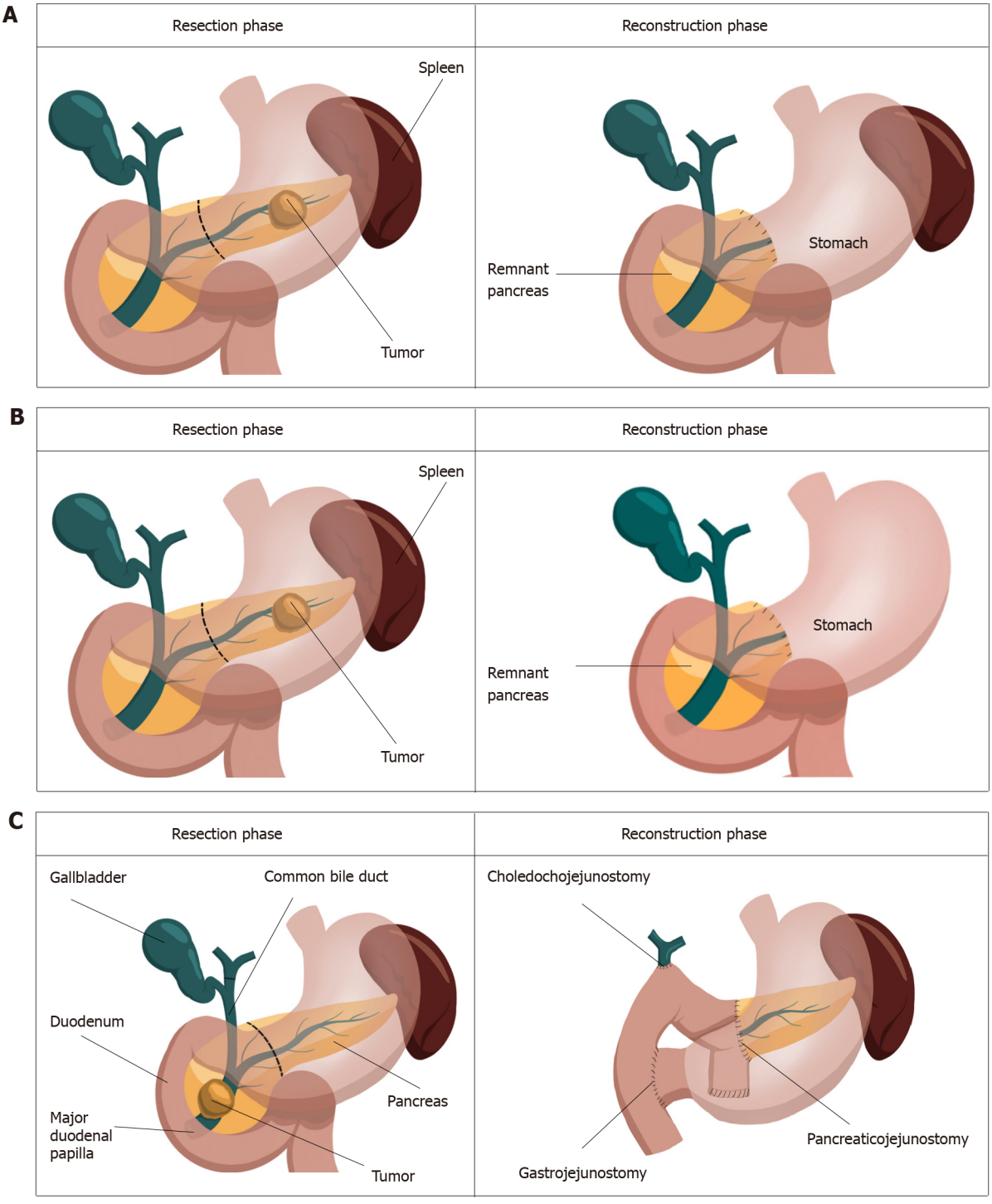

DOI: 10.4240/wjgs.v14.i10.1089

Figure 1 Resection and reconstruction phases of different pancreatic surgeries. A: Resection and reconstruction phases of distal pancreatectomy, the spleen is preserved; B: Resection and reconstruction phases of distal pancreatectomy with splenectomy; C: Resection and reconstruction phases of pancreatoduodenectomy.

potential protector against CR-POPF[35], being shown to favour a more fibrotic and acinar-deplete parenchyma[36]. However, pancreatic texture has been shown to not predict CR-POPF after distal pancreatectomy[37], emphasising the clinical importance of the distinct risk profiles for both resection types.

CR-POPF can develop following the reconstruction phase of surgery (Figure 1). In pancreatoduodenectomy, fistula is often attributed to failure of the pancreatoenteric anastomosis whereby pancreatic fluid destined for the duodenum leaks into the abdomen[38]. Leakage can also occur from the gland itself, in what is referred to as a parenchymal leak[39]. In distal pancreatectomy, increased pressure in the pancreatic duct due to obstruction at the sphincter of Oddi has been thought to result in pancreatic

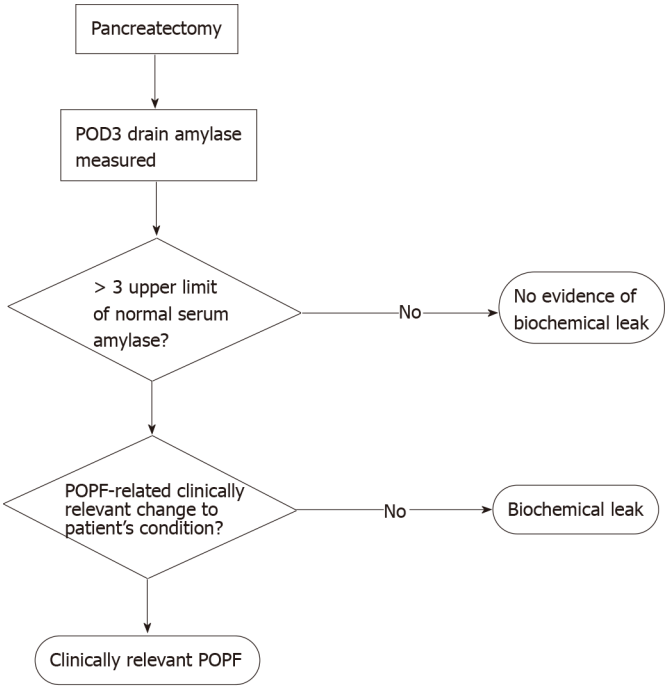

DOI: 10.4240/wjgs.v14.i10.1089

Figure 2 Current standard pathway for the diagnosis of clinically relevant postoperative pancreatic fistula. POD: Postoperative day; POPF: Postoperative pancreatic fistula.

juice leakage[40,41]. As distal resections do not cause downstream obstruction of the pancreatic duct, they are not predisposed to leakage in the same way as pancreases after pancreatoduodenectomy. Splenic preservation has been seen effective in preventing CR-POPF, owing this to the avoidance of pancreatic ischemia secondary to splenic vessel ligation[42,43]. Indeed, the higher morbidity inherent to multi-visceral resection is avoided in spleen-preserving distal pancreatectomy. Moreover, the former facilitates shorter operative times, which may be advantageous given that operations exceeding 480 min were at greater risk of developing pancreatic fistula (P = 0.02)[44]. This finding however did not persist in pancreatoduodenectomy patients[31,45]. Whilst the location of the tumour matters in determining the surgical approach, the size of the tumour has not been shown to influence the development of CR-POPF in pancreatoduodenectomy patients[46] but has so in distal pancreatectomy patients undergoing staple closure (P = 0.009, univariate analysis)[47].

Drain biomarkers for CR-POPF: Predictive biomarkers have commonly been investigated in both drain fluid and blood. The operative placement of drains and close relationship of drain fluid to the pancreas highlights its potential as a convenient biofluid capable of reflecting CR-POPF risk. Hence, the present review synthesises all drain fluid biomarkers identified for the prediction and diagnosis of CR-POPF.

Drain amylase

Drain amylase has been extensively explored given its evaluation being embedded in the current diagnostic pathway (Figure 2). Where diagnostic cut-offs have been defined for drain amylase, many measures of accuracy beyond sensitivity and specificity have been reported[48-57] (Table 1). While postoperative evaluation of drain amylase are common, earlier assessments may represent a simple way to improve the utility of drain amylase observations. Particularly, intraoperative measures provide an immediate assessment of pancreatic exocrine function and hence, its propensity to secrete erosive enzymes and predispose the pancreas to leak and subsequent CR-POPF. Indeed, Nahm *et al*[32] reported a significant association between intraoperative amylase concentration and CR-POPF with an area under the receiver operating characteristic curve (AUC) of 0.76 (P = 0.004) in their cohort of 61 pancreatectomy patients. The accuracy of intraoperative amylase has also been evaluated in surgery-exclusive cohorts with de Reuver *et al*[58] reporting an AUC of 0.83 in their cohort of 62 pancreatoduodenectomy patients. Wang *et al*[59] investigated this time point in 40 distal pancreatectomy patients, obtaining a sensitivity and specificity of 0.846 and 0.889 respectively for a cut-off of > 3089 U/L. These studies indicate that the enzymatic leak which can catalyse the development of a CR-POPF begins at the time of surgery, presenting an opportunity to expediate the diagnostic pathway which currently begins on POD3.

To better facilitate earlier diagnosis of CR-POPF, the sensitivity and specificity of POD1 drain amylase has been widely reported with cut-offs ranging from 282 U/L - 5000U/L[34,49,60-79]. Beyond

Table 1 Drain amylase accuracy evaluated beyond sensitivity and specificity

Ref.	Cut-off (U/L)	Predictive Performance	Evaluated (POD)	Patients *n*	Surgery	CR-POPF (%)	Study design	Publication
Giovinazzo *et al* [48], 2018	350	AUC = 0.92	1	568	PD	NS	R	Abstract
Partelli *et al*[49], 2017	500	AUC = 0.881, OR = 21.72	1	463	PD	13.82	R	Abstract
Kerem *et al*[50], 2018	1363	AUC = 0.91	1	135	PD	13.33	R	Abstract
Kawai *et al*[51], 2009	5000	*P* = 0.1002 (univariate)	1	244	PD	28	R	Full paper
Teixeira *et al*[52], 2018	< 270 271-5000 > 5000	Higher median values statistically predicted CR-POPF	1	102	PD	25.5	P	Full paper
Mimura *et al*[53], 2012	2000	AUC = 0.81	1	240	PD	23.4	R	Abstract
Mimura *et al*[53], 2012	100	AUC = 0.86	5	240	PD	23.4	R	Abstract
Kawaida *et al*[54], 2018	860	*P* = 0.002 (univariate)	3	75	DP	9.3	P	Full paper
Recreo Baquedano *et al*[55], 2019	< 400	NPV = 0.968	3	278	PD	14	P	Abstract
Newhook *et al*[56], 2020	49	Sensitivity = 1	1	45	DP	24	P	Full paper
Newhook *et al*[56], 2020	26	Sensitivity = 1	3	45	DP	24	P	Full paper
van Dongen *et al* [57], 2021	100	Sensitivity = 1	2	285	PD	18.24	R	Abstract

POD: Postoperative day; AUC: Area under the receiver operating characteristic curve; OR: Odds ratio; CR-POPF: Clinically relevant postoperative pancreatic fistula; PD: Pancreatoduodenectomy; DP: Distal pancreatectomy; P: Prospective; R: Retrospective; NS: Not stated; NPV: Negative predictive value.

discrete cut-offs, Hiraki *et al*[80] found median drain amylase concentration in a prospective study of 30 pancreatoduodenectomy patients to have a sensitivity and specificity of 0.933 and 0.867 respectively. Moreover, Kühlbrey *et al*[81] found POD1 drain amylase to effectively predict CR-POPF after pancreatectomy returning AUCs of 0.829 ($P < 0.001$) and 0.637 ($P < 0.01$) for pancreatoduodenectomy and distal pancreatectomy respectively. This was corroborated by Wüster *et al*[82] who reported similar AUCs of 0.830 and 0.854 respectively. POD1 drain amylase concentrations have been noted as significantly higher in CR-POPF patients[32,83], correlated with CR-POPF following univariate analysis [84] and identified as an independent risk factor for CR-POPF after pancreatoduodenectomy[49,85-87]. In contrast, in a cohort of 74 pancreatectomy patients, no significant differences in POD1 drain amylase were found in patients who did and did not develop CR-POPF[88]. However, this study may have been underpowered as only nine (12.2%) patients developed CR-POPF.

The accuracy of POD2 drain amylase has been less explored with all reports evaluating pancreatoduodenectomy patients alongside POD1 drain[65,69] or serum amylase[57]. Sensitivity has been reported by two independent studies as 0.88, with the specificity of 0.83 in Ansorge *et al*'s work[69] surpassing Caputo's group's specificity of 0.74 when cut-offs of 314 U/L and 368 U/L were used respectively[65]. Odds ratios of 35 and 29 have further been reported in prospective studies[89,90]. While measuring on POD2 does allow greater time for the biochemical leak to develop thereby enhancing diagnostic accuracy, it does require a change to monitoring protocols which predominantly sample drain fluid on odd PODs (*e.g.*, POD1, POD3 or POD5). Moreover, this relatively unexamined timepoint reflects current preferences to either assess drain amylase early on POD1 or to abide by the recommended testing day of POD3.

The close relationship of POD3 amylase to the ISGPS definition has resulted in few explorations of its true diagnostic performance[24]. Following pancreatoduodenectomy, POD3 drain amylase has been noted to be significantly higher in CR-POPF patients[91]. Diagnostic cut-offs for POD3 drain amylase have ranged between 26 U/L and 1026 U/L for distal pancreatectomy cohorts[54,56,92,93], 93-2820 U/L

for pancreatoduodenectomy cohorts[55,56,83,84,94-99] and 200-3000 U/L in studies analysing the biomarker in pancreatectomy patients[16,56,75,100-103]. When cut-off accuracy was reported, sensitivity ranged from 0.316-1.00 and specificity, from 0.631-0.968[16,55,75,84,92,94-98,101-103], showing drain amylase alone does not completely include or exclude CR-POPF. This reinforces the importance of clinically relevant sequelae developing for accurate diagnosis as stipulated by the consensus definition [24]. POD4 drain amylase was found by Kosaka *et al*[104] to be significantly elevated in CR-POPF patients after pancreatoduodenectomy later defining a cut-off of 646 U/L as having an AUC of 0.87 [105]. After distal pancreatectomy, Suzumura *et al*[106] identified ≥ 1200 U/L as the predictive cut-off and Hiyoshi's group reported a sensitivity and specificity of 0.938 and 0.7 for a cut-off of ≥ 800 U/L [107]. POD5 drain amylase has been significantly correlated with CR-POPF post-pancreatoduodenectomy[108] where after distal pancreatectomy, a cut-off of > 1000 U/L was significantly associated with CR-POPF[109], with the cut-off of > 538 U/L by Coayla *et al*[98] predicting CR-POPF with a sensitivity and specificity of 0.86 and 0.91 respectively.

Median drain amylase levels post-pancreatoduodenectomy have been observed as significantly higher in CR-POPF patients[110] on POD1[52], POD2[57] and POD3[69]. Similarly, Moskovic *et al*[111] found median drain amylase concentration post-pancreatectomy to be significantly elevated on PODs 1-6 in CR-POPF patients. However, this offered no diagnostic advantage and given the wide day range, would prevent diagnosis on a designated day and limit early intervention. Both median and statistically derived cut-offs are limited in their ability to determine specific patient risk as they are summarised from entire patient cohorts which exhibit a spectrum of risk profiles.

Studies stratifying CR-POPF risk using drain amylase have been few and pancreatoduodenectomy exclusive. On POD1, Sutcliffe's group reported drain amylase < 2000 U/L excluded grade C POPF with a negative predictive value (NPV) of 0.99[112], whereas Caputo *et al*[113] found POD1 drain amylase ≥ 807 U/L to significantly predict grade C POPF with a sensitivity and specificity of 0.727 and 0.644 respectively. However, Chiba *et al*[114] did not find drain amylase to be a significant grade C POPF risk factor during the first postoperative week, owing this potentially to the difficulty of ensuring adequate pancreatic juice drainage post-operatively. Drain amylase was similarly examined by Li *et al*[115] to better identify low and high-risk patients. Here, a POD1 cut-off of 921.7 U/L (AUC = 0.85) had a sensitivity and specificity of 0.789 and 0.828 whereas their POD3 cut-off of 4021.5 U/L had overall higher accuracy favouring specificity at 0.954 (sensitivity = 0.778). In low-risk patients undergoing PD, Newhook *et al*[56] reported a POD1 cut-off of 661 U/L and POD3 cut-off of 141 U/L could completely exclude CR-POPF when drain amylase was below these levels (sensitivity = 1). Amongst high-risk PD patients, the POD1 and POD3 cut-offs to exclude CR-POPF were < 136 U/L and < 93 U/L respectively. Whilst these cut-offs ensure no false negative results, they may be rarely encountered and hence, rarely utilised. As such, clinicians may prefer higher cut-offs, compromising on sensitivity, to clarify the danger of higher amylase levels more likely to be encountered in clinical practice. These risk-stratified approaches are a welcome advance on previous reports which have predominantly derived predictive cut-offs from entire patient populations, limiting targeted risk prediction. Similar investigations should be conducted in distal pancreatectomy cohorts to define risk-specific cut-offs in these patients. As such, accounting for the operation, patient risk and corresponding predictive drain amylase levels will help refine CR-POPF diagnosis, ultimately decreasing complication rates.

The majority of drain amylase investigations have reported the biomarker at singular timepoints, with others considering its accuracy across multiple PODs. Tzedakis' group found in their cohort of pancreatectomy patients that drain amylase elevated beyond three times the upper limit of normal on POD1 and POD3 had a sensitivity of 0.974 and NPV of 0.971[101]. Similarly, Linnemann *et al*[116] reported a NPV of 0.95 in pancreatoduodenectomy patients with a peak drain amylase of 1000 U/L on PODs 1-3. These studies evidence a superior ability to exclude CR-POPF which may justify the additional monitoring of drain amylase which differs from the popular, singular day approach. Hence, early, and continued monitoring can strengthen the identification and selection of low-risk patients for accelerated recovery pathways. In pancreatoduodenectomy cohorts, numerous reports have investigated changes in drain amylase across the postoperative period. This measure possesses the potential to reflect existing and imminent CR-POPF risk. Dugalic *et al*[110] reported a moderate decline of < 50% between POD 1 and POD3 to be significantly associated with CR-POPF. Seemingly supporting these findings, Koizumi *et al*[117] found a notable decrease in drain amylase between POD1 and POD5 in patients without CR-POPF. This suggests the relative persistence of elevated drain amylase may be predictive of CR-POPF, a finding which corroborates reports of drain amylase being significantly elevated in CR-POPF patients during this time period[118,119]. However, Furukawa *et al*[120] identified a decline of pancreatic amylase of greater than 80% between POD1 and POD3 to be predictive of CR-POPF after pancreatoduodenectomy. Further into the postoperative period, Kuhara *et al*[121] appear to support this in identifying a decrease in drain POD5 amylase to a third of the POD3 level to be a significant risk factor for CR-POPF. To bolster day-specific tracing of CR-POPF risk, future studies should clarify these discrepancies and quantify the drain amylase changes that would indicate impending CR-POPF. Similar investigations in distal pancreatectomy cohorts are also warranted. Nobuoka *et al*[122] evaluated CR-POPF risk by considering the product of drain amylase and volume. This combined variable was found to be significantly higher in CR-POPF patients on POD1 and POD7. Extending this, Okano *et al*[119] evaluated the product of drain amylase and volume on POD3 and

POD1 in ratio. Here, patients who did not develop CR-POPF had significantly lower values. Together, these indicate that involving drain volume in the assessment of CR-POPF risk may provide opposite findings to when drain amylase is exclusively evaluated, persisting at elevated levels and potentially decreasing, respectively.

Drain lipase

Drain lipase has gained momentum as a potential accompaniment or replacement for drain amylase in diagnosing CR-POPF given its similar ability to capture the exocrine function of the remnant pancreas. Moreover, serum lipase assists in acute pancreatitis diagnosis[123,124], a postoperative complication which itself has been shown to independently predict CR-POPF[125,126]. Lipase drives intraperitoneal lipolysis which can exacerbate systemic inflammation and trigger multi-organ dysfunction specifically as the subsequent high systemic unsaturated fatty acid levels can cause mitochondrial toxicity[127], lipotoxicity[128] and kidney[129,130] or liver damage[131]. Diagnostic cut-offs have ranged from 4.88 U/L to 1000 U/L with the majority exploring both pancreatoduodenectomy and distal pancreatectomy patients[100-102,132]. However, pancreatoduodenectomy[97] and distal pancreatectomy[107] exclusive studies have also been conducted. Amongst these reports, the sensitivity and specificity has ranged from 0.8-0.938 and 0.649-0.95, respectively[97,100-102,107,132]. Suzuki *et al*[133] reported POD1 drain lipase levels to be an independent risk factor for CR-POPF (P = 0.037). Tzedakis *et al*[101] further considered the evolution of drain lipase and its relation to CR-POPF risk with sustained elevation of drain lipase across POD1 and POD3 having a sensitivity of 0.948 which was then confirmed in their validation cohort.

In the way of risk stratification, Frymerman *et al*[134] identified the combination of elevated POD3 and POD5 drain lipase (> 5000 U/L) and soft pancreatic texture to be predictive of grade C fistula. As this combination includes the most widely reported risk factor for CR-POPF, soft parenchyma, the contribution of elevated drain lipase to overall grade C risk remains unclear. Hence, drain lipase-exclusive risk stratification requires further investigation particularly during the early postoperative period as the majority of the aforementioned studies evaluated drain lipase on or after POD3.

Drain culture

The extent and character of drain fluid infection has been explored in surgery-specific and all-inclusive analyses of CR-POPF patients (Table 2). Pancreatoduodenectomy has been more extensively explored, with infection of the ascitic fluid and surgical site potentially explained by preoperative bile duct infection[135,136]. Moreover, the construction of the gastrointestinal anastomosis exposes the pancreas to the densely colonised duodenum and jejunum, causing intra-abdominal translocation of species that is further facilitated by bile and pancreatic outflow[137].

Investigations in pancreatoduodenectomy cohorts: A significantly higher prevalence of CR-POPF in pancreatoduodenectomy patients with positive drain culture has been widely reported[138-144], where internal and preoperative biliary drainage, elevated drain amylase, combined colectomy and a longer duration of surgery have been identified as significant risk factors for contaminated drain fluid[140,145].

Kimura *et al*[146] identified contaminated drain fluid on POD1 and POD3 to be an independent risk factor for CR-POPF which has since been corroborated in the early postoperative period PODs 1-3[139], POD1[147,148] and POD3[142,149]. The accuracy of POD1 drain culture was reported by Hata *et al*[145] as having a sensitivity of 0.45 and specificity of 0.813 resulting in a positive predictive value (PPV) of 0.479, with specificity (0.99) similarly prevailing over sensitivity (0.32) in Morimoto *et al*'s analysis of POD3 drain fluid smear tests which reported a superior PPV of 0.89[142].

The great diversity of microorganisms in post-pancreatoduodenectomy drain fluid is evident in the wide identification of *Enterococcus*[137-139,141,148,150-153], *Enterobacter*[138,141,148,151,152], *Pseudomonas*[151,153,154], *Klebsiella*[137,153], Methicillin-resistant *Staphylococcus aureus*[153], *Candida*[150,151], *Citrobacter* and *Escherichia coli* (*E. coli*)[137,155]. Yang *et al*[139] identified fungi, *Staphylococcus*, *Enterococcus*, *Pseudomonas*, *Acinetobacter*, *Stenotrophomonas*, *E. coli* and *Klebsiella* significantly more often in their CR-POPF patients. *E. coli* has specifically been implicated in bacterobilia whereby its colonisation of the bile stent has been significantly associated with grade C POPF (P = 0.028, odds ratio = 4.07)[156].

During the first postoperative week, Chiba *et al*[114] found gram-positive bacteria to predominate in grade B POPF patients while gram-negative rods were identified an independent predictor for grade C fistula. As McMillan's group isolated gram-negative organisms more commonly than gram positive (78.3% *vs* 68.1% respectively)[157], this could indicate that infections, being more commonly comprised of high-risk bacteria, predispose patients to more severe POPF. Indeed, Yamashita *et al*[154] isolated *Pseudomonas aeruginosa* exclusively in CR-POPF patients and identified the bacteria as the source of proteases which activated trypsin from trypsinogen. Belmouhand's group corroborated this latter finding and further identified drain *Enterobacter cloacae* as a source of trypsin-activating proteases thereby contextualising the role of gram-negative rods in CR-POPF development[150].

Nagakawa *et al*[141] found the bacteria detected on POD1 and POD3 to be similar in CR-POPF patients. This taken with the consistent number of non-intestinal bacterium observed on POD3 and POD7 highlights an opportunity for early risk assessment on POD3 as clinicians could anticipate a CR-

Table 2 Investigations of drain culture across different pancreatic surgery cohorts

Clinical condition	Pancreatoduodenectomy patients	Distal pancreatectomy patients
Present in CR-POPF patients	Fungi, gram-positive bacteria, *Acinetobacter*, *Stenotrophomonas*, *Citrobacter spp*, *Staphylococcus*, *Enterococcus*, *Enterococcus faecalis Candida spp.*, *Klebsiella*, *Klebsiella pneumoniae*, *Pseudomonas*, *Pseudomonas aeruginosa*, *Escherichia coli*, *Enterobacter cloacae*	Fungi, *Staphylococcus*, *Enterococcus*, *Pseudomonas*, *Acinetobacter*, *Stenotrophomonas*, *Escherichia coli and Klebsiella spp*
Predictor of CR-POPF	Polymicrobial infections, *Candida*	
Predictor of grade C	Gram-negative rods, *Candida*	

CR-POPF: Clinically relevant postoperative pancreatic fistula.

POPF diagnosis when diagnostic bacteria are first detected[149]. Hence, the concurrent assessment of drain culture alongside POD3 drain amylase may assist earlier CR-POPF diagnosis, potentially reducing the reliance on complication development as is stipulated by the current consensus definition. Hence, patient safety will be increased as despite developing CR-POPF, patients will not have to endure challenging sequelae prior to diagnosis.

Beyond individual microorganisms, Demir *et al*[158] reported patients presenting with both CR-POPF and positive drain culture had significantly more polymicrobial infections with De Pastena's group noting the number of CR-POPF patients with polymicrobial infections to be significantly higher than those with biochemical leak (P = 0.003)[159]. The prevalence of polymicrobial infections in CR-POPF patients has ranged from 0.478-0.681, however their association with the complication has not been noted[157,159,160]. Belmouhand's group did not find polymicrobial drain fluid infections to be associated with anastomosis leakage[150], neither did Maatman *et al*[161] find this for any postoperative complication.

Rather than investigating polymicrobial infections as a risk factor for CR-POPF, risk stratification would be best assisted by the specific identification of problematic bacteria within polymicrobial drain fluid samples. Hence, an exploration of microorganisms associated with CR-POPF naturally assists in this. Abe *et al*[162] reported *Candida* to be significantly associated with CR-POPF and an independent risk factor for grade C fistulae (P = 0.043) which supported McMillan *et al*'s findings where *Candida* was found in 87.3% of grade C cases for which microbiological data was available[157]. Here, *Enterococcus* and *Staphylococcus* were also detected, conflicting later findings by Belmouhand's group who reported no significant difference in the severity of POPF when drain fluid was similarly contaminated[150]. The commonly identified *Enterococcus* and *Enterobacter* species have been detected on POD1[146] and proposed to originate from bile[140]. Abe *et al*[162] detected *Enterococcus* and *Enterobacter* species in drain fluid with Yamashita *et al*[138] specifically identifying *Enterococcus faecalis* and *Enterobacter cloacae* as precipitating CR-POPF. Interestingly, McMillan *et al*[157] found mortality to be significantly lower in patients with *Enterobacter* positive cultures despite it being widely identified in the drain fluid of CR-POPF patients. The inconclusive relevance of *Enterobacter, Enterococcus* and *Staphylococcus* to CR-POPF risk and concurrent identification of *Candida* in drain fluid confirms the findings of *Candida* as characteristic of polymicrobial infections[150] and more likely to appear in grade C POPF[162].

Investigations in distal pancreatectomy cohorts: Similar to pancreatoduodenectomy studies, distal pancreatectomy patients with positive drain culture have been associated with significantly higher rates of CR-POPF[163,164] with positive drain culture being an independent risk factor for the complication before POD3[165] and on POD4[166]. However, abdominal infection was not found to be a risk factor for CR-POPF by Sato *et al*[167] in their cohort of 49 patients which may have been underpowered. Yang *et al*[165] identified *Staphylococcus*, *Enterococcus*, *Pseudomonas*, *Acinetobacter*, *Stenotrophomonas*, *E. coli* and *Klebsiella spp* significantly more often in their CR-POPF patients. Here, 74.2% of patients contaminated with *Staphylococcus* and 92.9% of patients with *Klebsiella* subsequently developed CR-POPF. Loos *et al*[137] similarly identified *Staphylococcus spp.* and *Enterococcus spp.* most frequently in the drain fluid of CR-POPF patients. Harino *et al*[163] found *Staphylococcus* numbers to increase in patients when drains were removed after POD5, with Yang's group reporting rapid increases in positive drain culture when drains remained between POD3 and POD7 with a prevalence of 21.6% and 73.3% respectively[165]. Hence, earlier drain removal may assist in curbing the growth of bacteria and its subsequent role in CR-POPF development.

Yang *et al*[165] also found fungi to be isolated significantly more often in distal pancreatectomy patients who developed CR-POPF, while Abe *et al*[162] noted the absence of *Candida* which contrasted findings after pancreatoduodenectomy. Hence, the distinct drain culture portfolios following each resection type facilitate the identification of specific high-risk bacteria, the predictive potential of which would be enhanced by identifying the day of earliest detection and strongest association with CR-POPF. Moreover, it should be investigated whether mere presence of certain bacteria is predictive of CR-POPF

Table 3 Recommendations for future research

Drain biomarker	To investigate	To confirm
Amylase	Accuracy of intraoperative predictive cut-offs in pancreatoduodenectomy patients	Diagnostic accuracy of proposed cut-offs
	Accuracy of POD2 cut-offs in distal pancreatectomy patients	The change in postoperative drain amylase required to be predictive of CR-POPF in pancreatoduodenectomy patients
	Accuracy of POD4 cut-offs in surgery specific cohorts	If a persistently high value for drain amylase x drain volume postoperatively is predictive of CR-POPF
	Accuracy of risk-stratified cut-offs in distal pancreatectomy patients	
	The change in postoperative drain amylase required to be predictive of CR-POPF in distal pancreatectomy patients	
	When drain amylase has the highest predictive accuracy	
Lipase	The change in postoperative drain lipase required to be predictive of CR-POPF in surgery specific cohorts and its accuracy	Diagnostic accuracy of proposed cut-offs
	The accuracy of predictive cut-offs before POD3 in surgery specific cohorts	Diagnostic value of drain lipase in multi-factorial predictive models
	Accuracy of risk-stratified cut-offs in surgery specific cohorts	When drain amylase has the highest predictive accuracy
Drain culture	Bacteria within polymicrobial drain fluid samples which predict grade B and C POPF in surgery specific cohorts	Clinical relevance of *Enterobacter, Enterococcus* and *Staphylococcus* to CR-POPF risk in pancreatoduodenectomy patients
	When particular microorganisms are most predictive of CR-POPF	
	The concentrations of high-risk bacteria that accurately predict CR-POPF in surgery specific cohorts	
Other biomolecules	Accuracy of predictive cut-offs for each biomarker in surgery specific cohorts	
	Accuracy of novel enzymes compared to drain amylase and lipase in matched surgical cohorts and PODs	
Fluid appearance	Accuracy on specific days before POD3	

POD: Postoperative day; CR-POPF: Clinically relevant postoperative pancreatic fistula.

or if there is a level at which risk is higher. Here, additional understanding of the time course for bacterial growth would assist close monitoring of colony numbers to facilitate better complication anticipation and prevention.

Miscellaneous drain biomarkers

Other biomolecules: Drain lipase activity has been indirectly explored through alternate biomarkers for CR-POPF. Indeed, POD1 drain glycerol (> 800 μmol/L) has been associated with CR-POPF after pancreatoduodenectomy[168]. Similarly, drain free fatty acid has been significantly associated with CR-POPF. In an ensuing rat model, intraperitoneal lipolysis resulted in greater pancreatic juice leakage which risks CR-POPF by eroding the parenchyma and irritating acute pancreatitis[131]. Being products of lipolysis, drain glycerol and free fatty acids could serve as surrogate biomarkers for drain lipase, and hence CR-POPF. To effectively compare the predictive performance of these newer biomarkers however, a better understanding of their accuracy is required. To determine their clinical utility, their accuracy should also be compared against drain amylase and lipase.

Further, trypsin activation peptide (TAP) as a surrogate measure for protease activation has been explored. Xiu *et al*[169] found the TAP to drain amylase ratio in pancreatoduodenectomy patients to be significantly higher in CR-POPF patients, with this predictive measure being significantly higher when compared to distal pancreatectomy and biochemical leak patients. Wüster's group identified TAP and chymotrypsin elevation to be uniquely associated with distal pancreatectomy and pancreatoduodenectomy CR-POPF patients, respectively[82]. Irrespective of resection type, myeloperoxidase and trypsin activity were significantly elevated on PODs 1-2 and PODs 1-7, respectively. However, amongst the CR-POPF patients, elastase was not found to be significantly associated with the complication[82]. Ansorge *et al*[168] identified a significantly higher intraperitoneal lactate to pyruvate ratio in CR-POPF patients which increased significantly between POD1 and POD2 due to increased lactate and decreased pyruvate, thereby implicating metabolic disruption in the pathophysiology of CR-POPF. Hence, these emerging biomarkers may offer new opportunities for bolstering CR-POPF prediction particularly if

combined with established risk factors in future predictive models.

Drain fluid appearance: Observations of "sinister" drain effluent are often relied upon to inform an assessment of CR-POPF risk[76] and were a criteria of the initial consensus definition[23]. Abnormal drain fluid can be brown, green, milky or unusually clear[65]. Non-serous fluid following pancreatoduodenectomy has been independently associated with CR-POPF on POD1, POD3 and POD4[170]. However, Kosaka *et al*[105] did not find drain fluid colour to significantly differ between CR-POPF and non-CR-POPF pancreatoduodenectomy patients on POD4 on multivariate analysis agreeing with Suzumura *et al*'s findings following distal pancreatectomy[106]. Drain turbidity has been significantly correlated with drain fluid amylase on POD5 and beyond[108], suggesting its early observation could anticipate later development of CR-POPF.

CONCLUSION

This review revealed the potential for drain fluid biomarkers to overcome the limitations of the current diagnostic definition which necessitates a reactive management approach[24]. Numerous future directions for drain fluid research include investigating and confirming the accuracy of drain biomarkers in novel and established contexts respectively (Table 3). Through this, reports of biomarkers can specifically detail the accuracy of surgery-specific, risk-stratified cut-offs to clarify their clinical utility. Hence, decisions regarding drain removal and further monitoring can accordingly be made to either expediate or protect patient recovery respectively. Clarifying the clinical utility of drain biomarkers, could also facilitate their inclusion as variables in predictive models alongside blood biomarkers and medical imaging. This would complement recent efforts in which predictive models have sought to improve and expediate diagnosis when compared to the evaluation of individual variables[171-173]. As such, progress can continue to be made towards risk-stratifying patients according to pre- and intra-operative variables.

FOOTNOTES

Author contributions: Rykina-Tameeva N wrote the paper; Samra JS, Sahni S and Mittal A provided feedback and revised the paper; Sahni S and Mittal A have contributed equally as senior authors.

Conflict-of-interest statement: All the authors report no relevant conflicts of interest for this article.

Country/Territory of origin: Australia

ORCID number: Sumit Sahni 0000-0002-2900-8845; Anubhav Mittal 0000-0003-3960-2968.

S-Editor: Wang JJ
L-Editor: A
P-Editor: Wang JJ

REFERENCES

1 **Bray F**, Ferlay J, Soerjomataram I, Siegel RL, Torre LA, Jemal A. Global cancer statistics 2018: GLOBOCAN estimates of incidence and mortality worldwide for 36 cancers in 185 countries. *CA Cancer J Clin* 2018; **68**: 394-424 [PMID: 30207593 DOI: 10.3322/caac.21492]

2 **Rahib L**, Smith BD, Aizenberg R, Rosenzweig AB, Fleshman JM, Matrisian LM. Projecting cancer incidence and deaths to 2030: the unexpected burden of thyroid, liver, and pancreas cancers in the United States. *Cancer Res* 2014; **74**: 2913-2921 [PMID: 24840647 DOI: 10.1158/0008-5472.CAN-14-0155]

3 **Kleeff J**, Korc M, Apte M, La Vecchia C, Johnson CD, Biankin AV, Neale RE, Tempero M, Tuveson DA, Hruban RH, Neoptolemos JP. Pancreatic cancer. *Nat Rev Dis Primers* 2016; **2**: 16022 [PMID: 27158978 DOI: 10.1038/nrdp.2016.22]

4 **Kamisawa T**, Wood LD, Itoi T, Takaori K. Pancreatic cancer. *Lancet* 2016; **388**: 73-85 [PMID: 26830752 DOI: 10.1016/S0140-6736(16)00141-0]

5 **Christenson ES**, Jaffee E, Azad NS. Current and emerging therapies for patients with advanced pancreatic ductal adenocarcinoma: a bright future. *Lancet Oncol* 2020; **21**: e135-e145 [PMID: 32135117 DOI:

10.1016/S1470-2045(19)30795-8]
6 **McGuigan A**, Kelly P, Turkington RC, Jones C, Coleman HG, McCain RS. Pancreatic cancer: A review of clinical diagnosis, epidemiology, treatment and outcomes. *World J Gastroenterol* 2018; **24**: 4846-4861 [PMID: 30487695 DOI: 10.3748/wjg.v24.i43.4846]
7 **Cameron JL**, He J. Two thousand consecutive pancreaticoduodenectomies. *J Am Coll Surg* 2015; **220**: 530-536 [PMID: 25724606 DOI: 10.1016/j.jamcollsurg.2014.12.031]
8 **Tumas J**, Tumiene B, Jurkeviciene J, Jasiunas E, Sileikis A. Nutritional and immune impairments and their effects on outcomes in early pancreatic cancer patients undergoing pancreatoduodenectomy. *Clin Nutr* 2020; **39**: 3385-3394 [PMID: 32184025 DOI: 10.1016/j.clnu.2020.02.029]
9 **Carrato A**, Falcone A, Ducreux M, Valle JW, Parnaby A, Djazouli K, Alnwick-Allu K, Hutchings A, Palaska C, Parthenaki I. A Systematic Review of the Burden of Pancreatic Cancer in Europe: Real-World Impact on Survival, Quality of Life and Costs. *J Gastrointest Cancer* 2015; **46**: 201-211 [PMID: 25972062 DOI: 10.1007/s12029-015-9724-1]
10 **Gilliland TM**, Villafane-Ferriol N, Shah KP, Shah RM, Tran Cao HS, Massarweh NN, Silberfein EJ, Choi EA, Hsu C, McElhany AL, Barakat O, Fisher W, Van Buren G. Nutritional and Metabolic Derangements in Pancreatic Cancer and Pancreatic Resection. *Nutrients* 2017; **9** [PMID: 28272344 DOI: 10.3390/nu9030243]
11 **Peters JH**, Carey LC. Historical review of pancreaticoduodenectomy. *Am J Surg* 1991; **161**: 219-225 [PMID: 1990875 DOI: 10.1016/0002-9610(91)91134-5]
12 **McPhee JT**, Hill JS, Whalen GF, Zayaruzny M, Litwin DE, Sullivan ME, Anderson FA, Tseng JF. Perioperative mortality for pancreatectomy: a national perspective. *Ann Surg* 2007; **246**: 246-253 [PMID: 17667503 DOI: 10.1097/01.sla.0000259993.17350.3a]
13 **Gleeson EM**, Shaikh MF, Shewokis PA, Clarke JR, Meyers WC, Pitt HA, Bowne WB. WHipple-ABACUS, a simple, validated risk score for 30-day mortality after pancreaticoduodenectomy developed using the ACS-NSQIP database. *Surgery* 2016; **160**: 1279-1287 [PMID: 27544541 DOI: 10.1016/j.surg.2016.06.040]
14 **Ecker BL**, McMillan MT, Allegrini V, Bassi C, Beane JD, Beckman RM, Behrman SW, Dickson EJ, Callery MP, Christein JD, Drebin JA, Hollis RH, House MG, Jamieson NB, Javed AA, Kent TS, Kluger MD, Kowalsky SJ, Maggino L, Malleo G, Valero V 3rd, Velu LKP, Watkins AA, Wolfgang CL, Zureikat AH, Vollmer CM Jr. Risk Factors and Mitigation Strategies for Pancreatic Fistula After Distal Pancreatectomy: Analysis of 2026 Resections From the International, Multi-institutional Distal Pancreatectomy Study Group. *Ann Surg* 2019; **269**: 143-149 [PMID: 28857813 DOI: 10.1097/SLA.0000000000002491]
15 **Pedrazzoli S**. Pancreatoduodenectomy (PD) and postoperative pancreatic fistula (POPF): A systematic review and analysis of the POPF-related mortality rate in 60,739 patients retrieved from the English literature published between 1990 and 2015. *Medicine (Baltimore)* 2017; **96**: e6858 [PMID: 28489778 DOI: 10.1097/MD.0000000000006858]
16 **Kanda M**, Fujii T, Takami H, Suenaga M, Inokawa Y, Yamada S, Kobayashi D, Tanaka C, Sugimoto H, Koike M, Nomoto S, Fujiwara M, Kodera Y. Novel diagnostics for aggravating pancreatic fistulas at the acute phase after pancreatectomy. *World J Gastroenterol* 2014; **20**: 8535-8544 [PMID: 25024608 DOI: 10.3748/wjg.v20.i26.8535]
17 **Nagai S**, Fujii T, Kodera Y, Kanda M, Sahin TT, Kanzaki A, Hayashi M, Sugimoto H, Nomoto S, Takeda S, Morita S, Nakao A. Recurrence pattern and prognosis of pancreatic cancer after pancreatic fistula. *Ann Surg Oncol* 2011; **18**: 2329-2337 [PMID: 21327822 DOI: 10.1245/s10434-011-1604-8]
18 **Mosquera C**, Vohra NA, Fitzgerald TL, Zervos EE. Discharge with Pancreatic Fistula after Pancreaticoduodenectomy Independently Predicts Hospital Readmission. *Am Surg* 2016; **82**: 698-703 [PMID: 27657584 DOI: 10.1177/000313481608200827]
19 **Williamsson C**, Ansari D, Andersson R, Tingstedt B. Postoperative pancreatic fistula-impact on outcome, hospital cost and effects of centralization. *HPB (Oxford)* 2017; **19**: 436-442 [PMID: 28161218 DOI: 10.1016/j.hpb.2017.01.004]
20 **Watanabe Y**, Nishihara K, Matsumoto S, Okayama T, Abe Y, Nakano T. Effect of postoperative major complications on prognosis after pancreatectomy for pancreatic cancer: a retrospective review. *Surg Today* 2017; **47**: 555-567 [PMID: 27704248 DOI: 10.1007/s00595-016-1426-1]
21 **Mackay TM**, Smits FJ, Roos D, Bonsing BA, Bosscha K, Busch OR, Creemers GJ, van Dam RM, van Eijck CHJ, Gerhards MF, de Groot JWB, Groot Koerkamp B, Haj Mohammad N, van der Harst E, de Hingh IHJT, Homs MYV, Kazemier G, Liem MSL, de Meijer VE, Molenaar IQ, Nieuwenhuijs VB, van Santvoort HC, van der Schelling GP, Stommel MWJ, Ten Tije AJ, de Vos-Geelen J, Wit F, Wilmink JW, van Laarhoven HWM, Besselink MG; Dutch Pancreatic Cancer Group. The risk of not receiving adjuvant chemotherapy after resection of pancreatic ductal adenocarcinoma: a nationwide analysis. *HPB (Oxford)* 2020; **22**: 233-240 [PMID: 31439478 DOI: 10.1016/j.hpb.2019.06.019]
22 **Dhayat SA**, Tamim ANJ, Jacob M, Ebeling G, Kerschke L, Kabar I, Senninger N. Postoperative pancreatic fistula affects recurrence-free survival of pancreatic cancer patients. *PLoS One* 2021; **16**: e0252727 [PMID: 34086792 DOI: 10.1371/journal.pone.0252727]
23 **Bassi C**, Dervenis C, Butturini G, Fingerhut A, Yeo C, Izbicki J, Neoptolemos J, Sarr M, Traverso W, Buchler M; International Study Group on Pancreatic Fistula Definition. Postoperative pancreatic fistula: an international study group (ISGPF) definition. *Surgery* 2005; **138**: 8-13 [PMID: 16003309 DOI: 10.1016/j.surg.2005.05.001]
24 **Bassi C**, Marchegiani G, Dervenis C, Sarr M, Abu Hilal M, Adham M, Allen P, Andersson R, Asbun HJ, Besselink MG, Conlon K, Del Chiaro M, Falconi M, Fernandez-Cruz L, Fernandez-Del Castillo C, Fingerhut A, Friess H, Gouma DJ, Hackert T, Izbicki J, Lillemoe KD, Neoptolemos JP, Olah A, Schulick R, Shrikhande SV, Takada T, Takaori K, Traverso W, Vollmer CR, Wolfgang CL, Yeo CJ, Salvia R, Buchler M; International Study Group on Pancreatic Surgery (ISGPS). The 2016 update of the International Study Group (ISGPS) definition and grading of postoperative pancreatic fistula: 11 Years After. *Surgery* 2017; **161**: 584-591 [PMID: 28040257 DOI: 10.1016/j.surg.2016.11.014]
25 **McMillan MT**, Allegrini V, Asbun HJ, Ball CG, Bassi C, Beane JD, Behrman SW, Berger AC, Bloomston M, Callery MP, Christein JD, Dickson E, Dixon E, Drebin JA, Fernandez-Del Castillo C, Fisher WE, Fong ZV, Haverick E, Hollis RH, House MG, Hughes SJ, Jamieson NB, Kent TS, Kowalsky SJ, Kunstman JW, Malleo G, McElhany AL, Salem RR, Soares KC, Sprys MH, Valero V 3rd, Watkins AA, Wolfgang CL, Zureikat AH, Vollmer CM Jr. Incorporation of

Procedure-specific Risk Into the ACS-NSQIP Surgical Risk Calculator Improves the Prediction of Morbidity and Mortality After Pancreatoduodenectomy. *Ann Surg* 2017; **265**: 978-986 [PMID: 27232260 DOI: 10.1097/SLA.0000000000001796]

26 **Malleo G**, Pulvirenti A, Marchegiani G, Butturini G, Salvia R, Bassi C. Diagnosis and management of postoperative pancreatic fistula. *Langenbecks Arch Surg* 2014; **399**: 801-810 [PMID: 25173359 DOI: 10.1007/s00423-014-1242-2]

27 **Kambakamba P**, Mannil M, Herrera PE, Müller PC, Kuemmerli C, Linecker M, von Spiczak J, Hüllner MW, Raptis DA, Petrowsky H, Clavien PA, Alkadhi H. The potential of machine learning to predict postoperative pancreatic fistula based on preoperative, non-contrast-enhanced CT: A proof-of-principle study. *Surgery* 2020; **167**: 448-454 [PMID: 31727325 DOI: 10.1016/j.surg.2019.09.019]

28 **Marasco G**, Ricci C, Buttitta F, Dajti E, Ravaioli F, Ingaldi C, Alberici L, Serra C, Festi D, Colecchia A, Casadei R. Is Ultrasound Elastography Useful in Predicting Clinically Relevant Pancreatic Fistula After Pancreatic Resection? *Pancreas* 2020; **49**: 1342-1347 [PMID: 33122523 DOI: 10.1097/MPA.0000000000001685]

29 **Peng YP**, Zhu XL, Yin LD, Zhu Y, Wei JS, Wu JL, Miao Y. Risk factors of postoperative pancreatic fistula in patients after distal pancreatectomy: a systematic review and meta-analysis. *Sci Rep* 2017; **7**: 185 [PMID: 28298641 DOI: 10.1038/s41598-017-00311-8]

30 **Wang GQ**, Yadav DK, Jiang W, Hua YF, Lu C. Risk Factors for Clinically Relevant Postoperative Pancreatic Fistula (CR-POPF) after Distal Pancreatectomy: A Single Center Retrospective Study. *Can J Gastroenterol Hepatol* 2021; **2021**: 8874504 [PMID: 33542910 DOI: 10.1155/2021/8874504]

31 **Callery MP**, Pratt WB, Kent TS, Chaikof EL, Vollmer CM Jr. A prospectively validated clinical risk score accurately predicts pancreatic fistula after pancreatoduodenectomy. *J Am Coll Surg* 2013; **216**: 1-14 [PMID: 23122535 DOI: 10.1016/j.jamcollsurg.2012.09.002]

32 **Nahm CB**, Brown KM, Townend PJ, Colvin E, Howell VM, Gill AJ, Connor S, Samra JS, Mittal A. Acinar cell density at the pancreatic resection margin is associated with post-pancreatectomy pancreatitis and the development of postoperative pancreatic fistula. *HPB (Oxford)* 2018; **20**: 432-440 [PMID: 29307511 DOI: 10.1016/j.hpb.2017.11.003]

33 **Laaninen M**, Bläuer M, Vasama K, Jin H, Räty S, Sand J, Nordback I, Laukkarinen J. The risk for immediate postoperative complications after pancreaticoduodenectomy is increased by high frequency of acinar cells and decreased by prevalent fibrosis of the cut edge of pancreas. *Pancreas* 2012; **41**: 957-961 [PMID: 22699198 DOI: 10.1097/MPA.0b013e3182480b81]

34 **Kawai M**, Kondo S, Yamaue H, Wada K, Sano K, Motoi F, Unno M, Satoi S, Kwon AH, Hatori T, Yamamoto M, Matsumoto J, Murakami Y, Doi R, Ito M, Miyakawa S, Shinchi H, Natsugoe S, Nakagawara H, Ohta T, Takada T. Predictive risk factors for clinically relevant pancreatic fistula analyzed in 1,239 patients with pancreaticoduodenectomy: multicenter data collection as a project study of pancreatic surgery by the Japanese Society of Hepato-Biliary-Pancreatic Surgery. *J Hepatobiliary Pancreat Sci* 2011; **18**: 601-608 [PMID: 21491103 DOI: 10.1007/s00534-011-0373-x]

35 **Dahdaleh FS**, Naffouje SA, Hanna MH, Salti GI. Impact of Neoadjuvant Systemic Therapy on Pancreatic Fistula Rates Following Pancreatectomy: a Population-Based Propensity-Matched Analysis. *J Gastrointest Surg* 2021; **25**: 747-756 [PMID: 32253648 DOI: 10.1007/s11605-020-04581-y]

36 **Rykina-Tameeva N**, Nahm CB, Mehta S, Gill AJ, Samra JS, Mittal A. Neoadjuvant therapy for pancreatic cancer changes the composition of the pancreatic parenchyma. *HPB (Oxford)* 2020; **22**: 1631-1636 [PMID: 32247587 DOI: 10.1016/j.hpb.2020.03.007]

37 **Eshmuminov D**, Karpovich I, Kapp J, Töpfer A, Endhardt K, Oberkofler C, Petrowsky H, Lenggenhager D, Tschuor C, Clavien PA. Pancreatic fistulas following distal pancreatectomy are unrelated to the texture quality of the pancreas. *Langenbecks Arch Surg* 2021; **406**: 729-734 [PMID: 33420516 DOI: 10.1007/s00423-020-02071-y]

38 **Nahm CB**, Connor SJ, Samra JS, Mittal A. Postoperative pancreatic fistula: a review of traditional and emerging concepts. *Clin Exp Gastroenterol* 2018; **11**: 105-118 [PMID: 29588609 DOI: 10.2147/CEG.S120217]

39 **Nguyen JH**. Distinguishing between parenchymal and anastomotic leakage at duct-to-mucosa pancreatic reconstruction in pancreaticoduodenectomy. *World J Gastroenterol* 2008; **14**: 6648-6654 [PMID: 19034967 DOI: 10.3748/wjg.14.6648]

40 **Hashimoto Y**, Traverso LW. After distal pancreatectomy pancreatic leakage from the stump of the pancreas may be due to drain failure or pancreatic ductal back pressure. *J Gastrointest Surg* 2012; **16**: 993-1003 [PMID: 22392088 DOI: 10.1007/s11605-012-1849-y]

41 **Hackert T**, Klaiber U, Hinz U, Kehayova T, Probst P, Knebel P, Diener MK, Schneider L, Strobel O, Michalski CW, Ulrich A, Sauer P, Büchler MW. Sphincter of Oddi botulinum toxin injection to prevent pancreatic fistula after distal pancreatectomy. *Surgery* 2017; **161**: 1444-1450 [PMID: 27865590 DOI: 10.1016/j.surg.2016.09.005]

42 **Shoup M**, Brennan MF, McWhite K, Leung DH, Klimstra D, Conlon KC. The value of splenic preservation with distal pancreatectomy. *Arch Surg* 2002; **137**: 164-168 [PMID: 11822953 DOI: 10.1001/archsurg.137.2.164]

43 **Balzano G**, Zerbi A, Cristallo M, Di Carlo V. The unsolved problem of fistula after left pancreatectomy: the benefit of cautious drain management. *J Gastrointest Surg* 2005; **9**: 837-842 [PMID: 15985241 DOI: 10.1016/j.gassur.2005.01.287]

44 **Kleeff J**, Diener MK, Z'graggen K, Hinz U, Wagner M, Bachmann J, Zehetner J, Müller MW, Friess H, Büchler MW. Distal pancreatectomy: risk factors for surgical failure in 302 consecutive cases. *Ann Surg* 2007; **245**: 573-582 [PMID: 17414606 DOI: 10.1097/01.sla.0000251438.43135.fb]

45 **Chen JY**, Feng J, Wang XQ, Cai SW, Dong JH, Chen YL. Risk scoring system and predictor for clinically relevant pancreatic fistula after pancreaticoduodenectomy. *World J Gastroenterol* 2015; **21**: 5926-5933 [PMID: 26019457 DOI: 10.3748/wjg.v21.i19.5926]

46 **Tang T**, Tan Y, Xiao B, Zu G, An Y, Zhang Y, Chen W, Chen X. Influence of Body Mass Index on Perioperative Outcomes Following Pancreaticoduodenectomy. *J Laparoendosc Adv Surg Tech A* 2021; **31**: 999-1005 [PMID: 33181060 DOI: 10.1089/lap.2020.0703]

47 **Yoo HJ**, Paik KY, Oh JS. Is there any different risk factor for clinical relevant pancreatic fistula according to the stump closure method following left-sided pancreatectomy? *Ann Hepatobiliary Pancreat Surg* 2019; **23**: 385-391 [PMID: 31825006 DOI: 10.14701/ahbps.2019.23.4.385]

48 **Giovinazzo F**, Dalla Riva GV, Greener D, Morano C, Linneman R, Besselink M, Abu Hilal M. A learning machine

method to predict post-operative pancreatic fistula after pancreaticoduodenectomy based on amylases value in the drains: A multicentre database analysis of 1638 patients. *HPB* 2018; **20**: S828 [DOI: 10.1016/j.hpb.2018.06.1817]

49 **Partelli S**, Pecorelli N, Muffatti F, Belfiori G, Crippa S, Piazzai F, Castoldi R, Marmorale C, Balzano G, Falconi M. Early Postoperative Prediction of Clinically Relevant Pancreatic Fistula after Pancreaticoduodenectomy: usefulness of C-reactive Protein. *HPB (Oxford)* 2017; **19**: 580-586 [PMID: 28392159 DOI: 10.1016/j.hpb.2017.03.001]

50 **Kerem M**, Dikmen K, Bostanci H, Ermis I, Buyukkasap AC. Predictive effect of postoperative 1st day drain amylase value on the development of pancreatic fistula that occurs after pancreaticoduodenectomy: A prospective clinicalal study. *HPB* 2018; **20**: S645 [DOI: 10.1016/j.hpb.2018.06.2253]

51 **Kawai M**, Tani M, Hirono S, Ina S, Miyazawa M, Yamaue H. How do we predict the clinically relevant pancreatic fistula after pancreaticoduodenectomy? *World J Surg* 2009; **33**: 2670-2678 [PMID: 19774410 DOI: 10.1007/s00268-009-0220-2]

52 **Teixeira UF**, Rodrigues PD, Goldoni MB, Sampaio JA, Fontes PRO, Waechter FL. Early drain fluid amylase is useful to predict pancreatic fistula after pancreatoduodenectomy: Lessons learned from a southern brazilian center. *Arq Gastroenterol* 2018; **55**: 160-163 [PMID: 30043866 DOI: 10.1590/S0004-2803.201800000-28]

53 **Mimura T**, Niguma T, Kojima T. Free orals: Biliary. *HPB* 2012; **14** (Suppl 2): 107-287 [DOI: 10.1111/j.1477-2574.2012.00511.x]

54 **Kawaida H**, Kono H, Watanabe M, Hosomura N, Amemiya H, Fujii H. Risk factors of postoperative pancreatic fistula after distal pancreatectomy using a triple-row stapler. *Surg Today* 2018; **48**: 95-100 [PMID: 28600634 DOI: 10.1007/s00595-017-1554-2]

55 **Recreo Baquedano A**, Sánchez Acedo P, Zazpe Ripa C, Herrera J, Tarifa Castilla A, Fernández San José B, Pelegrín Esteban I. Predictive value of amylase determination in drainages for pancreatic fistula after pancreaticoduodenectomy. *Pancreatology* 2019; **19** (Suppl 2): S183 [DOI: 10.1016/j.pan.2019.07.011]

56 **Newhook TE**, Vega EA, Vreeland TJ, Prakash L, Dewhurst WL, Bruno ML, Kim MP, Ikoma N, Vauthey JN, Katz MH, Lee JE, Tzeng CD. Early postoperative drain fluid amylase in risk-stratified patients promotes tailored post-pancreatectomy drain management and potential for accelerated discharge. *Surgery* 2020; **167**: 442-447 [PMID: 31727324 DOI: 10.1016/j.surg.2019.09.015]

57 **van Dongen JC**, Merkens S, Aziz MH, Groot Koerkamp B, van Eijck CHJ. The value of serum amylase and drain fluid amylase to predict postoperative pancreatic fistula after pancreatoduodenectomy: a retrospective cohort study. *Langenbecks Arch Surg* 2021; **406**: 2333-2341 [PMID: 33990865 DOI: 10.1007/s00423-021-02192-y]

58 **de Reuver PR**, Gundara J, Hugh TJ, Samra JS, Mittal A. Intra-operative amylase in peri-pancreatic fluid independently predicts for pancreatic fistula post pancreaticoduodectomy. *HPB (Oxford)* 2016; **18**: 608-614 [PMID: 27346142 DOI: 10.1016/j.hpb.2016.05.007]

59 **Wang W**, Qian H, Lin J, Weng Y, Zhang J, Wang J. Has the pancreatic fistula already occurred in the operation? *Surg Open Sci* 2019; **1**: 38-42 [PMID: 32754691 DOI: 10.1016/j.sopen.2019.04.003]

60 **Yu YD**, Kim DS, Jung SW, Yoon YI. "Detecting pancreatic fistula beforehand": Utilization of drain fluid amylase measurement on the first postoperative day following pancreaticoduodenectomy. *Korean Liver Society Spring/Autumn Conference (KASL)* 2017; **1**: 53-54

61 **Pinter Carvalheiro da Silva Boteon A**, Longatto Boteon Y, Dasari B, Isaac J, Marudanayagam R, Mirza DF, Muiesan P, John Roberts K, Sutcliffe RP. Early predictors of clinically relevant post-operative pancreatic fistula after pancreaticoduodenectomy. *HPB* 2018; **20** (Suppl 2): S625 [DOI: 10.1016/j.hpb.2018.06.2198]

62 **Mintziras I**, Maurer E, Kanngiesser V, Bartsch DK. C-reactive protein and drain amylase accurately predict clinically relevant pancreatic fistula after partial pancreaticoduodenectomy. *Int J Surg* 2020; **76**: 53-58 [PMID: 32109648 DOI: 10.1016/j.ijsu.2020.02.025]

63 **Bertens KA**, Crown A, Clanton J, Alemi F, Alseidi AA, Biehl T, Helton WS, Rocha FG. What is a better predictor of clinically relevant postoperative pancreatic fistula (CR-POPF) following pancreaticoduodenectomy (PD): postoperative day one drain amylase (POD1DA) or the fistula risk score (FRS)? *HPB (Oxford)* 2017; **19**: 75-81 [PMID: 27825541 DOI: 10.1016/j.hpb.2016.10.001]

64 **Ven Fong Z**, Correa-Gallego C, Ferrone CR, Veillette GR, Warshaw AL, Lillemoe KD, Fernández-del Castillo C. Early Drain Removal--The Middle Ground Between the Drain Versus No Drain Debate in Patients Undergoing Pancreaticoduodenectomy: A Prospective Validation Study. *Ann Surg* 2015; **262**: 378-383 [PMID: 25563864 DOI: 10.1097/SLA.0000000000001038]

65 **Caputo D**, Angeletti S, Ciccozzi M, Cartillone M, Cascone C, La Vaccara V, Coppola A, Coppola R. Role of drain amylase levels assay and routinary postoperative day 3 abdominal CT scan in prevention of complications and management of surgical drains after pancreaticoduodenectomy. *Updates Surg* 2020; **72**: 727-741 [PMID: 32410161 DOI: 10.1007/s13304-020-00784-9]

66 **Aleassa EM**, Sharma G, Malik S, Morris-Stiff G. Lower is high enough: New suggested threshold for postoperative day 1 drain-fluid-amylase post pancreatoduodenectomy. *HPB* 2018; **20** (Suppl 2): S633 [DOI: 10.1016/j.hpb.2018.06.2219]

67 **Peng JS**, Ko JS, Chalikonda S, Wey JS, Walsh RM, Morris-Stiff G. Use of postoperative day 1 drain amylase levels to predict postoperative pancreatic fistulas. *J Am Coll Surg* 2016; **223**: e147-e148 [DOI: 10.1016/j.jamcollsurg.2016.08.378]

68 **Takeishi K**, Maeda T, Yamashita Y, Tsujita E, Itoh S, Harimoto N, Ikegami T, Yoshizumi T, Shirabe K, Maehara Y. A Cohort Study for Derivation and Validation of Early Detection of Pancreatic Fistula After Pancreaticoduodenectomy. *J Gastrointest Surg* 2016; **20**: 385-391 [PMID: 26597269 DOI: 10.1007/s11605-015-3030-x]

69 **Ansorge C**, Nordin J, Strommer L, Lundell Lars, Rangelova E, Blomberg J, Del Chiaro M, Segersvard R. The diagnostic value of pancreatic amylase analyses from prophylactic abdominal drainage in identifying pancreatic fistula following pancreaticoduodenectomy. *Pancreatology* 2013; **13**: S82 [DOI: 10.1016/j.pan.2013.04.286]

70 **Daniel F**, Tamim H, Hosni M. Ueg week 2018 poster presentations. *UEG* 2018; **6**: A423 [DOI: 10.1177/2050640618792819]

71 **Maggino L**, Malleo G, Bassi C, Allegrini V, Beane JD, Beckman RM, Chen B, Dickson EJ, Drebin JA, Ecker BL, Fraker DL, House MG, Jamieson NB, Javed AA, Kowalsky SJ, Lee MK, McMillan MT, Roses RE, Salvia R, Valero V 3rd, Velu LKP, Wolfgang CL, Zureikat AH, Vollmer CM Jr. Identification of an Optimal Cut-off for Drain Fluid Amylase on

Postoperative Day 1 for Predicting Clinically Relevant Fistula After Distal Pancreatectomy: A Multi-institutional Analysis and External Validation. *Ann Surg* 2019; **269**: 337-343 [PMID: 28938266 DOI: 10.1097/SLA.0000000000002532]

72 **Lee CW**, Pitt HA, Riall TS, Ronnekleiv-Kelly SS, Israel JS, Leverson GE, Parmar AD, Kilbane EM, Hall BL, Weber SM. Low drain fluid amylase predicts absence of pancreatic fistula following pancreatectomy. *J Gastrointest Surg* 2014; **18**: 1902-1910 [PMID: 25112411 DOI: 10.1007/s11605-014-2601-6]

73 **El Nakeeb A**, Salah T, Sultan A, El Hemaly M, Askr W, Ezzat H, Hamdy E, Atef E, El Hanafy E, El-Geidie A, Abdel Wahab M, Abdallah T. Pancreatic anastomotic leakage after pancreaticoduodenectomy. Risk factors, clinical predictors, and management (single center experience). *World J Surg* 2013; **37**: 1405-1418 [PMID: 23494109 DOI: 10.1007/s00268-013-1998-5]

74 **Casadei R**, Ricci C, Taffurelli G, Pacilio CA, Di Marco M, Pagano N, Serra C, Calculli L, Santini D, Minni F. Prospective validation of a preoperative risk score model based on pancreatic texture to predict postoperative pancreatic fistula after pancreaticoduodenectomy. *Int J Surg* 2017; **48**: 189-194 [PMID: 28987563 DOI: 10.1016/j.ijsu.2017.09.070]

75 **Kosaka H**, Satoi S, Yamamoto T, Hirooka S, Yamaki S, Kotsuka M, Sakaguchi T, Inoue K, Matsui Y, Sekimoto M. Clinical impact of the sequentially-checked drain removal criteria on postoperative outcomes after pancreatectomy: a retrospective study. *J Hepatobiliary Pancreat Sci* 2019; **26**: 426-434 [PMID: 31237409 DOI: 10.1002/jhbp.649]

76 **McMillan MT**, Malleo G, Bassi C, Allegrini V, Casetti L, Drebin JA, Esposito A, Landoni L, Lee MK, Pulvirenti A, Roses RE, Salvia R, Vollmer CM Jr. Multicenter, Prospective Trial of Selective Drain Management for Pancreatoduodenectomy Using Risk Stratification. *Ann Surg* 2017; **265**: 1209-1218 [PMID: 27280502 DOI: 10.1097/SLA.0000000000001832]

77 **McMillan MT**, Malleo G, Bassi C, Butturini G, Salvia R, Roses RE, Lee MK, Fraker DL, Drebin JA, Vollmer CM Jr. Drain Management after Pancreatoduodenectomy: Reappraisal of a Prospective Randomized Trial Using Risk Stratification. *J Am Coll Surg* 2015; **221**: 798-809 [PMID: 26278037 DOI: 10.1016/j.jamcollsurg.2015.07.005]

78 **Trudeau MT**, Casciani F, Ecker BL, Maggino L, Seykora TF, Puri P, McMillan MT, Miller B, Pratt WB, Asbun HJ, Ball CG, Bassi C, Behrman SW, Berger AC, Bloomston MP, Callery MP, Castillo CF, Christein JD, Dillhoff ME, Dickson EJ, Dixon E, Fisher WE, House MG, Hughes SJ, Kent TS, Malleo G, Salem RR, Wolfgang CL, Zureikat AH, Vollmer CM; on the behalf of the Pancreas Fistula Study Group. The Fistula Risk Score Catalog: Toward Precision Medicine for Pancreatic Fistula After Pancreatoduodenectomy. *Ann Surg* 2022; **275**: e463-e472 [PMID: 32541227 DOI: 10.1097/SLA.0000000000004068]

79 **Yamane H**, Abe T, Amano H, Hanada K, Minami T, Kobayashi T, Fukuda T, Yonehara S, Nakahara M, Ohdan H, Noriyuki T. Visceral Adipose Tissue and Skeletal Muscle Index Distribution Predicts Severe Pancreatic Fistula Development After Pancreaticoduodenectomy. *Anticancer Res* 2018; **38**: 1061-1066 [PMID: 29374741 DOI: 10.1016/j.hpb.2019.10.1207]

80 **Hiraki M**, Miyoshi A, Sadashima E, Shinkai Y, Yasunami M, Manabe T, Kitahara K, Noshiro H. The novel early predictive marker presepsin for postoperative pancreatic fistula: A pilot study. *Exp Ther Med* 2020; **20**: 2298-2304 [PMID: 32765708 DOI: 10.3892/etm.2020.8919]

81 **Kühlbrey CM**, Samiei N, Sick O, Makowiec F, Hopt UT, Wittel UA. Pancreatitis After Pancreatoduodenectomy Predicts Clinically Relevant Postoperative Pancreatic Fistula. *J Gastrointest Surg* 2017; **21**: 330-338 [PMID: 27896656 DOI: 10.1007/s11605-016-3305-x]

82 **Wüster C**, Shi H, Kühlbrey CM, Biesel EA, Hopt UT, Fichtner-Feigl S, Wittel UA. Pancreatic Inflammation and Proenzyme Activation Are Associated With Clinically Relevant Postoperative Pancreatic Fistulas After Pancreas Resection. *Ann Surg* 2020; **272**: 863-870 [PMID: 32833754 DOI: 10.1097/SLA.0000000000004257]

83 **Sugimoto M**, Takahashi S, Gotohda N, Kato Y, Kinoshita T, Shibasaki H, Konishi M. Schematic pancreatic configuration: a risk assessment for postoperative pancreatic fistula after pancreaticoduodenectomy. *J Gastrointest Surg* 2013; **17**: 1744-1751 [PMID: 23975030 DOI: 10.1007/s11605-013-2320-4]

84 **Gruppo M**, Angriman I, Martella B, Spolverato YC, Zingales F, Bardini R. Perioperative albumin ratio is associated with post-operative pancreatic fistula. *ANZ J Surg* 2018; **88**: E602-E605 [PMID: 29194898 DOI: 10.1111/ans.14262]

85 **Hanaki T**, Uejima C, Amisaki M, Yosuke A, Tokuyasu N, Honjo S, Sakamoto T, Saito H, Ikeguchi M, Fujiwara Y. The attenuation value of preoperative computed tomography as a novel predictor for pancreatic fistula after pancreaticoduodenectomy. *Surg Today* 2018; **48**: 598-608 [PMID: 29383597 DOI: 10.1007/s00595-018-1626-y]

86 **Iida H**, Tani M, Maehira H, Mori H, Kitamura N, Miyake T, Kaida S, Shimizu T. Postoperative Pancreatic Swelling Predicts Pancreatic Fistula after Pancreaticoduodenectomy. *Am Surg* 2019; **85**: 321-326 [PMID: 31043189 DOI: 10.1177/000313481908500419]

87 **Sakamoto K**, Tokuhisa Y, Tokumitsu Y. Risk factors of pancreatic fistula after pancreaticoduodenectomy. *J Hepatobiliary Pancreat Sci* 2017; **24**: A387 [DOI: 10.1002/jhbp.480]

88 **Singh H**, Singh MK, Gupta V, Kochhar R, Medhi B, Yadav TD. The value of post-operative measurement of day one drain fluid amylase, serum amylase and serum crp as predictor of pancreatic fistula in pancreatic surgery. *HPB* 2018; **20** (Suppl 2): S617 [DOI: 10.1016/j.hpb.2018.06.2176]

89 **Segersvard R**, Blomberg J, Del Chiaro M, Rengelova E, Ansorge C. The diagnostic value of abdominal drainage in the individual risk assessment for pancreatic fistula following pancreaticoduodenectomy. *Pancreatology* 2013; **13**: S8-S9 [DOI: 10.1016/J.PAN.2013.07.083]

90 **Ansorge C**, Nordin JZ, Lundell L, Strömmer L, Rangelova E, Blomberg J, Del Chiaro M, Segersvärd R. Diagnostic value of abdominal drainage in individual risk assessment of pancreatic fistula following pancreaticoduodenectomy. *Br J Surg* 2014; **101**: 100-108 [PMID: 24306817 DOI: 10.1002/bjs.9362]

91 **Kawaida H**, Watanabe M, Hosomura N. The predictive factors for postoperative pancreatic fistula after pancreaticoduodenectomy for soft pancreas. *J Hepatobiliary Pancreat Sci* 2017; **24** (Suppl 1): A278 [DOI: 10.1002/jhbp.480]

92 **Yoshino J**, Ban D, Ogura T, Ogawa K, Ono H, Mitsunori Y, Kudo A, Tanaka S, Tanabe M. The Clinical Implications of Peripancreatic Fluid Collection After Distal Pancreatectomy. *World J Surg* 2019; **43**: 2069-2076 [PMID: 31004209 DOI: 10.1007/s00268-019-05009-8]

93 **Ohira G**, Amano R, Kimura K. Analysis of pancreatic fistula after distal pancreatectomy. *J Hepatobiliary Pancreat Sci* 2017; **24** (Suppl 1): A279 [DOI: 10.1002/jhbp.480]

94 **Iwasaki T**, Nara S, Kishi Y, Esaki M, Takamoto T, Shimada K. Proposal of a Clinically Useful Criterion for Early Drain Removal After Pancreaticoduodenectomy. *J Gastrointest Surg* 2021; **25**: 737-746 [PMID: 32221781 DOI: 10.1007/s11605-020-04565-y]

95 **Araki M**, Yasuda T, Yoshioka Y. Abstracts of papers submitted to the joint 43rd meeting of the american pancreatic association and the 17th meeting of the international association of pancreatology, october 31-november 3, 2012, miami, florida. *Pancreas* 2012; **41**: 1344-1416 [DOI: 10.1097/MPA.0b013e318270446a]

96 **Srivastava M**, Kumaran V, Nundy S. Does drain amylase <666 iu/L on the third post-operative day effectively predicts the absence of a high-impact postoperative pancreatic fistula following pancreaticoduodenectomy? *HPB* 2016; **18** (Suppl 1): e111 [DOI: 10.1016/j.hpb.2016.02.260]

97 **Facy O**, Chalumeau C, Poussier M, Binquet C, Rat P, Ortega-Deballon P. Diagnosis of postoperative pancreatic fistula. *Br J Surg* 2012; **99**: 1072-1075 [PMID: 22539219 DOI: 10.1002/bjs.8774]

98 **Coayla G**, Rodriguez C, Targarona J, Marcos JC, Hernandez R, Quijano J, Rivero L, Barreda L. Amylase value in drains after pancreatoduodenectomy as predictive factor of postoperative pancreatic fistula. *Pancreatology* 2017; **17**: S39 [DOI: 10.1016/j.pan.2017.07.129]

99 **Ceroni M**, Galindo J, Guerra JF, Salinas J, Martínez J, Jarufe N. Amylase level in drains after pancreatoduodenectomy as a predictor of clinically significant pancreatic fistula. *Pancreas* 2014; **43**: 462-464 [PMID: 24622080 DOI: 10.1097/MPA.0000000000000060]

100 **Griffith D**, Hanna T, Wong K, Reece-Smith A, Aroori S, Bowles M, Stell D, Briggs C. Comparison of lipase and amylase for diagnosing post-operative pancreatic fistulae. *ANZ J Surg* 2018 [PMID: 29882290 DOI: 10.1111/ans.14266]

101 **Tzedakis S**, Sauvanet A, Schiavone R, Razafinimanana M, Cauchy F, Rouet J, Dousset B, Gaujoux S. What should we trust to define, predict and assess pancreatic fistula after pancreatectomy? *Pancreatology* 2020; **20**: 1779-1785 [PMID: 33077382 DOI: 10.1016/j.pan.2020.10.036]

102 **Roy M**, Ban E, Mohandas S, Mownah O, Banerjee A, Valente R, Abraham AT, Kocher H, Bhattacharya S, Hutchins RR. Comparison of drain fluid lipase with drain fluid amylase in the context of post-operative pancreatic fistula. *HPB* 2018; **20**: S674 [DOI: 10.1016/j.hpb.2018.06.2334]

103 **Noji T**, Nakamura T, Ambo Y, Suzuki O, Nakamura F, Kishida A, Hirano S, Kondo S, Kashimura N. Clinically relevant pancreas-related infectious complication after pancreaticoenteral anastomosis could be predicted by the parameters obtained on postoperative day 3. *Pancreas* 2012; **41**: 916-921 [PMID: 22481291 DOI: 10.1097/MPA.0b013e31823e7705]

104 **Kosaka H**, Kuroda N, Suzumura K. Abstracts of papers submitted to the international symposium on pancreas cancer 2012, cosponsored by the japan pancreas society, october 4-6, 2012, kyoto, japan. *Pancreas* 2012; **41**: 1140-1163 [DOI: 10.1097/MPA.0b013e31826a15f2]

105 **Kosaka H**, Kuroda N, Suzumura K, Asano Y, Okada T, Fujimoto J. Multivariate logistic regression analysis for prediction of clinically relevant pancreatic fistula in the early phase after pancreaticoduodenectomy. *J Hepatobiliary Pancreat Sci* 2014; **21**: 128-133 [PMID: 23804410 DOI: 10.1002/jhbp.11]

106 **Suzumura K**, Iida K, Iwama H, Kawabata Y. Prediction of clinically relevant pancreatic fistula in the early phase after distal pancreatectomy. *J Pancreas* 2019; **20**: 121-125

107 **Hiyoshi M**, Wada T, Tsuchimochi Y, Hamada T, Yano K, Imamura N, Fujii Y, Nanashima A. Usefulness of drain lipase to predict postoperative pancreatic fistula after distal pancreatectomy. *Indian J Surg* 2020; **82**: 1-2 [DOI: 10.1007/s12262-020-02128-8]

108 **Rajkamal R**, Mathew J, Subramaniayer M, Ramesh H. Drain fluid amylase levels after pancreaticoduodenectomy for cancer: Correlation with outcomes and complications and evolution of a uniform grading system. *HPB* 2019; **21**: S416-S417 [DOI: 10.1016/j.hpb.2019.10.2134]

109 **Ridaura Capellino N**, Protti Ruiz GP, Dopazo Taboada C, Blanco Cuso L, Pando E, Caralt M, Balsells J, Charco R. Drain fluid amylase on post-operative day 5 as pronostic factor of grade b-c pancreatic fistula after distal pancreatectomy. *HPB* 2018; **20**: S601-S602 [DOI: 10.1016/j.hpb.2018.06.2136]

110 **Dugalic VD**, Knezevic DM, Obradovic VN, Gojnic-Dugalic MG, Matic SV, Pavlovic-Markovic AR, Dugalic PD, Knezevic SM. Drain amylase value as an early predictor of pancreatic fistula after cephalic duodenopancreatectomy. *World J Gastroenterol* 2014; **20**: 8691-8699 [PMID: 25024627 DOI: 10.3748/wjg.v20.i26.8691]

111 **Moskovic DJ**, Hodges SE, Wu MF, Brunicardi FC, Hilsenbeck SG, Fisher WE. Drain data to predict clinically relevant pancreatic fistula. *HPB (Oxford)* 2010; **12**: 472-481 [PMID: 20815856 DOI: 10.1111/j.1477-2574.2010.00212.x]

112 **Sutcliffe RP**, Hamoui M, Pitchaimuthu M, Isaac J, Marudanayagam R, Mirza DF, Muiesan P, John Roberts K. First postoperative day drain fluid amylase greater than 2000 iu/L predicts grade c pancreatic fistula after pancreaticoduodenectomy. *Br J Surg* 2014; **101**: 7 [DOI: 10.1002/bjs.9694]

113 **Caputo D**, Coppola A, Cascone C, Angeletti S, Ciccozzi M, La Vaccara V, Coppola R. Preoperative systemic inflammatory biomarkers and postoperative day 1 drain amylase value predict grade C pancreatic fistula after pancreaticoduodenectomy. *Ann Med Surg (Lond)* 2020; **57**: 56-61 [PMID: 32714527 DOI: 10.1016/j.amsu.2020.07.018]

114 **Chiba N**, Ochiai S, Yokozuka K, Gunji T, Sano T, Tomita K, Tsutsui R, Kawachi S. Risk Factors for Life-threatening Grade C Postoperative Pancreatic Fistula After Pancreatoduodenectomy Compared to Grade B. *Anticancer Res* 2019; **39**: 2199-2205 [PMID: 30952768 DOI: 10.21873/anticanres.13335]

115 **Li Y**, Zhou F, Zhu DM, Zhang ZX, Yang J, Yao J, Wei YJ, Xu YL, Li DC, Zhou J. Novel risk scoring system for prediction of pancreatic fistula after pancreaticoduodenectomy. *World J Gastroenterol* 2019; **25**: 2650-2664 [PMID: 31210716 DOI: 10.3748/wjg.v25.i21.2650]

116 **Linnemann RJA**, Patijn GA, van Rijssen LB, Besselink MG, Mungroop TH, de Hingh IH, Kazemier G, Festen S, de Jong KP, van Eijck CHJ, Scheepers JJG, van der Kolk M, Dulk MD, Bosscha K, Busch OR, Boerma D, van der Harst E, Nieuwenhuijs VB; Dutch Pancreatic Cancer Group. The role of abdominal drainage in pancreatic resection - A multicenter validation study for early drain removal. *Pancreatology* 2019; **19**: 888-896 [PMID: 31378583 DOI: 10.1016/j.pan.2019.07.041]

117 **Koizumi M**, Sata N, Taguchi M. Management of pancreatic anastomotic leakage by measuring drainage amylase and volume after pylorus preserving pancreatoduodenectomy. *Pancreas* 2015; **44**: 1387-1388 [DOI: 10.1097/MPA.0000000000000551]

118 **Hiyoshi M**, Chijiiwa K, Fujii Y, Imamura N, Nagano M, Ohuchida J. Usefulness of drain amylase, serum C-reactive protein levels and body temperature to predict postoperative pancreatic fistula after pancreaticoduodenectomy. *World J Surg* 2013; **37**: 2436-2442 [PMID: 23838932 DOI: 10.1007/s00268-013-2149-8]

119 **Okano K**, Kakinoki K, Suto H, Oshima M, Kashiwagi H, Yamamoto N, Akamoto S, Fujiwara M, Takama T, Usuki H, Hagiike M, Suzuki Y. Persisting ratio of total amylase output in drain fluid can predict postoperative clinical pancreatic fistula. *J Hepatobiliary Pancreat Sci* 2011; **18**: 815-820 [PMID: 21594559 DOI: 10.1007/s00534-011-0393-6]

120 **Furukawa K**, Gocho T, Shirai Y, Iwase R, Haruki K, Fujiwara Y, Shiba H, Misawa T, Yanaga K. The Decline of Amylase Level of Pancreatic Juice After Pancreaticoduodenectomy Predicts Postoperative Pancreatic Fistula. *Pancreas* 2016; **45**: 1474-1477 [PMID: 27518469 DOI: 10.1097/MPA.0000000000000691]

121 **Kuhara K**, Shiozawa S, Usui T, Tsuchiya A, Miyauchi T, Kono T, Shimojima Y, Yamaguchi K, Yokomizo H, Shimakawa T, Yoshimatsu K, Katsube T, Naritaka Y. [Analysis of the Relationship between the Change of Drain Amylase Value and Postoperative Pancreatic Fistula after Pancreaticoduodenectomy]. *Gan To Kagaku Ryoho* 2017; **44**: 1729-1731 [PMID: 29394757]

122 **Nobuoka D**, Gotohda N, Konishi M, Nakagohri T, Takahashi S, Kinoshita T. The correlation between postoperative pancreatic fistula and volume of amylase discharge in drainage fluid after pancreaticoduodenectomy. *Japanese J Gastroenter Surg* 2010; **43**: 351-358 [DOI: 10.5833/jjgs.43.351]

123 **Connor S**. Defining post-operative pancreatitis as a new pancreatic specific complication following pancreatic resection. *HPB (Oxford)* 2016; **18**: 642-651 [PMID: 27485058 DOI: 10.1016/j.hpb.2016.05.006]

124 **Birgin E**, Reeg A, Téoule P, Rahbari NN, Post S, Reissfelder C, Rückert F. Early postoperative pancreatitis following pancreaticoduodenectomy: what is clinically relevant postoperative pancreatitis? *HPB (Oxford)* 2019; **21**: 972-980 [PMID: 30591305 DOI: 10.1016/j.hpb.2018.11.006]

125 **Andrianello S**, Bannone E, Marchegiani G, Malleo G, Paiella S, Esposito A, Salvia R, Bassi C. Characterization of postoperative acute pancreatitis (POAP) after distal pancreatectomy. *Surgery* 2021; **169**: 724-731 [PMID: 33268073 DOI: 10.1016/j.surg.2020.09.008]

126 **Ikenaga N**, Ohtsuka T, Nakata K, Watanabe Y, Mori Y, Nakamura M. Clinical significance of postoperative acute pancreatitis after pancreatoduodenectomy and distal pancreatectomy. *Surgery* 2021; **169**: 732-737 [PMID: 32893007 DOI: 10.1016/j.surg.2020.06.040]

127 **Noel P**, Patel K, Durgampudi C, Trivedi RN, de Oliveira C, Crowell MD, Pannala R, Lee K, Brand R, Chennat J, Slivka A, Papachristou GI, Khalid A, Whitcomb DC, DeLany JP, Cline RA, Acharya C, Jaligama D, Murad FM, Yadav D, Navina S, Singh VP. Peripancreatic fat necrosis worsens acute pancreatitis independent of pancreatic necrosis *via* unsaturated fatty acids increased in human pancreatic necrosis collections. *Gut* 2016; **65**: 100-111 [PMID: 25500204 DOI: 10.1136/gutjnl-2014-308043]

128 **Navina S**, Acharya C, DeLany JP, Orlichenko LS, Baty CJ, Shiva SS, Durgampudi C, Karlsson JM, Lee K, Bae KT, Furlan A, Behari J, Liu S, McHale T, Nichols L, Papachristou GI, Yadav D, Singh VP. Lipotoxicity causes multisystem organ failure and exacerbates acute pancreatitis in obesity. *Sci Transl Med* 2011; **3**: 107ra110 [PMID: 22049070 DOI: 10.1126/scitranslmed.3002573]

129 **Ishola DA Jr**, Post JA, van Timmeren MM, Bakker SJ, Goldschmeding R, Koomans HA, Braam B, Joles JA. Albumin-bound fatty acids induce mitochondrial oxidant stress and impair antioxidant responses in proximal tubular cells. *Kidney Int* 2006; **70**: 724-731 [PMID: 16837928 DOI: 10.1038/sj.ki.5001629]

130 **Arany I**, Clark JS, Reed DK, Juncos LA, Dixit M. Role of p66shc in renal toxicity of oleic acid. *Am J Nephrol* 2013; **38**: 226-232 [PMID: 23988748 DOI: 10.1159/000354357]

131 **Uchida Y**, Masui T, Nakano K, Yogo A, Sato A, Nagai K, Anazawa T, Takaori K, Tabata Y, Uemoto S. Clinical and experimental studies of intraperitoneal lipolysis and the development of clinically relevant pancreatic fistula after pancreatic surgery. *Br J Surg* 2019; **106**: 616-625 [PMID: 30725479 DOI: 10.1002/bjs.11075]

132 **Müssle B**, Oehme F, Schade S, Sommer M, Bogner A, Hempel S, Pochhammer J, Kahlert C, Distler M, Weitz J, Welsch T. Drain Amylase or Lipase for the Detection of POPF-Adding Evidence to an Ongoing Discussion. *J Clin Med* 2019; **9** [PMID: 31861508 DOI: 10.3390/jcm9010007]

133 **Suzuki S**, Shimoda M, Shimazaki J, Oshiro Y, Nishida K, Shiihara M, Izumo W, Yamamoto M. Drain Lipase Levels and Decreased Rate of Drain Amylase Levels as Independent Predictors of Pancreatic Fistula with Nomogram After Pancreaticoduodenectomy. *World J Surg* 2021; **45**: 1921-1928 [PMID: 33721069 DOI: 10.1007/s00268-021-06038-y]

134 **Frymerman AS**, Schuld J, Ziehen P, Kollmar O, Justinger C, Merai M, Richter S, Schilling MK, Moussavian MR. Impact of postoperative pancreatic fistula on surgical outcome--the need for a classification-driven risk management. *J Gastrointest Surg* 2010; **14**: 711-718 [PMID: 20094814 DOI: 10.1007/s11605-009-1147-5]

135 **Kitahata Y**, Kawai M, Tani M, Hirono S, Okada K, Miyazawa M, Shimizu A, Yamaue H. Preoperative cholangitis during biliary drainage increases the incidence of postoperative severe complications after pancreaticoduodenectomy. *Am J Surg* 2014; **208**: 1-10 [PMID: 24530042 DOI: 10.1016/j.amjsurg.2013.10.021]

136 **Akashi M**, Nagakawa Y, Hosokawa Y, Takishita C, Osakabe H, Nishino H, Katsumata K, Akagi Y, Itoi T, Tsuchida A. Preoperative cholangitis is associated with increased surgical site infection following pancreaticoduodenectomy. *J Hepatobiliary Pancreat Sci* 2020; **27**: 640-647 [PMID: 32506646 DOI: 10.1002/jhbp.783]

137 **Loos M**, Strobel O, Legominski M, Dietrich M, Hinz U, Brenner T, Heininger A, Weigand MA, Büchler MW, Hackert T. Postoperative pancreatic fistula: Microbial growth determines outcome. *Surgery* 2018; **164**: 1185-1190 [PMID: 30217397 DOI: 10.1016/j.surg.2018.07.024]

138 **Yamashita K**, Kato D, Sasaki T, Shiwaku H, Ishii F, Naito S, Yamashita Y, Hasegawa S. Contaminated drainage fluid and pancreatic fistula after pancreatoduodenectomy: A retrospective study. *Int J Surg* 2018; **52**: 314-319 [PMID: 29530827 DOI: 10.1016/j.ijsu.2018.02.057]

139 **Yang F**, Jin C, Li J, Di Y, Zhang J, Fu D. Clinical significance of drain fluid culture after pancreaticoduodenectomy. *J*

Hepatobiliary Pancreat Sci 2018; **25**: 508-517 [PMID: 30328297 DOI: 10.1002/jhbp.589]

140 **Sugiura T**, Mizuno T, Okamura Y, Ito T, Yamamoto Y, Kawamura I, Kurai H, Uesaka K. Impact of bacterial contamination of the abdominal cavity during pancreaticoduodenectomy on surgical-site infection. *Br J Surg* 2015; **102**: 1561-1566 [PMID: 26206386 DOI: 10.1002/bjs.9899]

141 **Nagakawa Y**, Matsudo T, Hijikata Y, Kikuchi S, Bunso K, Suzuki Y, Kasuya K, Tsuchida A. Bacterial contamination in ascitic fluid is associated with the development of clinically relevant pancreatic fistula after pancreatoduodenectomy. *Pancreas* 2013; **42**: 701-706 [PMID: 23429497 DOI: 10.1097/MPA.0b013e31826d3a41]

142 **Morimoto M**, Honjo S, Sakamoto T, Yagyu T, Uchinaka E, Amisaki M, Watanabe J, Yamamoto M, Fukumoto Y, Tokuyasu N, Ashida K, Saito H, Fujiwara Y. Bacterial smear test of drainage fluid after pancreaticoduodenectomy can predict postoperative pancreatic fistula. *Pancreatology* 2019; **19**: 274-279 [PMID: 30718188 DOI: 10.1016/j.pan.2019.01.018]

143 **Sato A**, Masui T, Nakano K, Sankoda N, Anazawa T, Takaori K, Kawaguchi Y, Uemoto S. Abdominal contamination with Candida albicans after pancreaticoduodenectomy is related to hemorrhage associated with pancreatic fistulas. *Pancreatology* 2017; **17**: 484-489 [PMID: 28336225 DOI: 10.1016/j.pan.2017.03.007]

144 **Uemura K**, Murakami Y, Sudo T, Hashimoto Y, Kondo N, Nakagawa N, Sasaki H, Okada K, Ohge H, Sueda T. Activation of pancreatic enzyme plus bacterial infection plays an important role in the pathogenic mechanism of clinically relevant popf after pancreaticoduodenectomy. *Gastroenterology* 2013; **144**: S1082 [DOI: 10.1016/S0016-5085(13)64034-2]

145 **Hata T**, Mizuma M, Motoi F, Nakagawa K, Masuda K, Ishida M, Morikawa T, Hayashi H, Kamei T, Naitoh T, Unno M. Early postoperative drainage fluid culture positivity from contaminated bile juice is predictive of pancreatic fistula after pancreaticoduodenectomy. *Surg Today* 2020; **50**: 248-257 [PMID: 31583471 DOI: 10.1007/s00595-019-01885-8]

146 **Kimura N**, Ishido K, Kudo D, Wakiya T, Odagiri T, Wakasa T, Toyoki Y, Hakamada K. Causative effect of bacterial infection on pancreatic fistula and appropriate timing of drain removal after pancreaticoduodenectomy. *Pancreatology* 2016; **16**: S109-S110 [DOI: 10.1016/j.pan.2016.05.367]

147 **Taniguchi K**, Matsuyama R, Yabushita Y, Homma Y, Ota Y, Mori R, Morioka D, Endo I. Prophylactic drain management after pancreaticoduodenectomy without focusing on the drain fluid amylase level: A prospective validation study regarding criteria for early drain removal that do not include the drain fluid amylase level. *J Hepatobiliary Pancreat Sci* 2020; **27**: 950-961 [PMID: 32357279 DOI: 10.1002/jhbp.746]

148 **Osakabe H**, Nagakawa Y, Takishita C, Hijikata Y, Kiya Y, Akashi M, Nishino H, Nakajima T, Shirota T, Sahara Y, Hosokawa Y. Relationship Between Drain Fluid Culture and Clinically Relevant Post-Operative Pancreatic Fistula After Pancreatectomy. Proceedings of the joint 50th anniversary meeting of the American pancreatic association and Japan pancreas society; 2019 Nov 6-9; Maui, Hawaii. Miami: American Pancreatic Association, 2019: 1401-1564

149 Abstracts of the Twelfth Annual Americas Hepato-Pancreato-Biliary Congress. March 7-11, 2012. Miami Beach, Florida, USA. *HPB (Oxford)* 2012; **14** Suppl 1: 1-91 [PMID: 22356212 DOI: 10.1111/j.1477-2574.2012.00437.x]

150 **Belmouhand M**, Krohn PS, Svendsen LB, Henriksen A, Hansen CP, Achiam MP. The occurrence of Enterococcus faecium and faecalis is significantly associated with anastomotic leakage after pancreaticoduodenectomy. *Scand J Surg* 2018; **107**: 107-113 [PMID: 28980499 DOI: 10.1177/1457496917731188]

151 **Kimura N**, Ishido K, Nagase H, Kudo K, Hakamada K. Peripancreatic bacterial contamination can trigger the development of pancreatic fistula after pancreaticoduodenectomy. *HPB* 2019; **21**: S453-S454 [DOI: 10.1016/j.hpb.2019.10.2236]

152 **Imamura M**, Kimura Y, Meguro M, Nishidate T, Ito T, Kyuno D, Ishii M, Kawamoto M, Mizuguchi T, Hirata K. The correlation between postoperative pancreatic fistula and bacterial infection after the pancreatoduodenectomy: Importance of the ivr of the early postoperative period. *HPB* 2014; **16**: 626 [DOI: 10.1111/hpb.12236]

153 **Ikoma H**, Yusuke Y, Morimura R. Poster presentation: Biliary. *HBP* 2012; **14**: 288-699

154 **Yamashita K**, Sasaki T, Itoh R, Kato D, Hatano N, Soejima T, Ishii K, Takenawa T, Hiromatsu K, Yamashita Y. Pancreatic fistulae secondary to trypsinogen activation by Pseudomonas aeruginosa infection after pancreatoduodenectomy. *J Hepatobiliary Pancreat Sci* 2015; **22**: 454-462 [PMID: 25678202 DOI: 10.1002/jhbp.223]

155 **Yamashita K**, Kato D, Sasaki T, Ishii F, Okada H, Hirano Y, Hayashi T, Yamada T, Hasegawa S. Clinical impact of bacterial contamination of intra-abdominal discharge on the incidence of pancreatic fistula after pancreati coduodenectomy. *United European Gastroenterol J* 2019; **7**: 303 [DOI: 10.1177/2050640619854671]

156 Abstracts of Papers Submitted to the 49th Annual Meeting of the American Pancreatic Association, October 31-November 3, 2018, Miami Beach, Florida. *Pancreas* 2018; **47**: 1370-1436 [PMID: 30383711 DOI: 10.1097/MPA.0000000000001177]

157 **McMillan MT**, Vollmer CM Jr, Asbun HJ, Ball CG, Bassi C, Beane JD, Berger AC, Bloomston M, Callery MP, Christein JD, Dixon E, Drebin JA, Castillo CF, Fisher WE, Fong ZV, Haverick E, House MG, Hughes SJ, Kent TS, Kunstman JW, Malleo G, McElhany AL, Salem RR, Soares K, Sprys MH, Valero V 3rd, Watkins AA, Wolfgang CL, Behrman SW. The Characterization and Prediction of ISGPF Grade C Fistulas Following Pancreatoduodenectomy. *J Gastrointest Surg* 2016; **20**: 262-276 [PMID: 26162925 DOI: 10.1007/s11605-015-2884-2]

158 **Demir E**, Abdelhai K, Demir IE, Jäger C, Scheufele F, Schorn S, Rothe K, Friess H, Ceyhan GO. Association of bacteria in pancreatic fistula fluid with complications after pancreatic surgery. *BJS Open* 2020; **4**: 432-437 [PMID: 32297478 DOI: 10.1002/bjs5.50272]

159 **De Pastena M**, Paiella S, Marchegiani G, Malleo G, Ciprani D, Gasparini C, Secchettin E, Salvia R, Bassi C. Postoperative infections represent a major determinant of outcome after pancreaticoduodenectomy: Results from a high-volume center. *Surgery* 2017; **162**: 792-801 [PMID: 28676333 DOI: 10.1016/j.surg.2017.05.016]

160 **Takishita C**. Preoperative cholangitis is associated with the development of clinically relevant surgical site infection (ssi) that cause pancreatic fistula after pancreatoduodenectomy. *HPB* 2016; **18**: e455 [DOI: 10.1016/j.hpb.2016.03.196]

161 **Maatman TK**, Weber DJ, Qureshi B, Ceppa EP, Nakeeb A, Schmidt CM, Zyromski NJ, House MG. Does the Microbiology of Bactibilia Drive Postoperative Complications After Pancreatoduodenectomy? *J Gastrointest Surg* 2020; **24**: 2544-2550 [PMID: 31745903 DOI: 10.1007/s11605-019-04432-5]

162 **Abe K**, Kitago M, Shinoda M, Yagi H, Abe Y, Oshima G, Hori S, Yokose T, Endo Y, Kitagawa Y. High risk pathogens and risk factors for postoperative pancreatic fistula after pancreatectomy; a retrospective case-controlled study. *Int J Surg* 2020; **82**: 136-142 [PMID: 32861892 DOI: 10.1016/j.ijsu.2020.08.035]

163 **Harino T**, Noguchi K, Yanagimoto Y. Clinical Significance of Drainage Culture Contamination in Pancreatic Fistula After Distal Pancreatectomy. Proceedings of the joint 50th anniversary meeting of the American pancreatic association and Japan pancreas society, November 6-9, 2019, Maui, Hawaii. Miami: American Pancreatic Association, 2019: 1401-1564

164 **Mori R**, Matsuyama R, Ota Y, Hiratani S, Goto K, Miyake K, Sawada Y, Kumamoto T, Takeda K, Endo I. The risk factors of postoperative pancreatic fistula after distal pancreatectomy. *Pancreatology* 2016; **16**: S127 [DOI: 10.1016/j.pan.2016.06.458]

165 **Yang F**, Jin C, Hao S, Fu D. Drain Contamination after Distal Pancreatectomy: Incidence, Risk Factors, and Association with Postoperative Pancreatic Fistula. *J Gastrointest Surg* 2019; **23**: 2449-2458 [PMID: 30815778 DOI: 10.1007/s11605-019-04155-7]

166 **Osakabe H**, Nagakawa Y, Kozono S, Takishita C, Nakagawa N, Nishino H, Suzuki K, Shirota T, Hosokawa Y, Akashi M, Ishizaki T, Katsumata K, Tsuchida A. Causative bacteria associated with a clinically relevant postoperative pancreatic fistula infection after distal pancreatectomy. *Surg Today* 2021; **51**: 1813-1818 [PMID: 33907898 DOI: 10.1007/s00595-021-02287-5]

167 **Sato A**, Masui T, Nakano K, Ito T, Anazawa T, Kawaguchi M, Kawaguchi Y, Takaori K, Uemoto S. Is drainage culture useful in predicting postoperative pancreatic fistula after distal pancreatectomy? *Pancreatology* 2016; **16**: S79 [DOI: 10.1016/j.pan.2016.06.283]

168 **Ansorge C**, Regner S, Segersvärd R, Strömmer L. Early intraperitoneal metabolic changes and protease activation as indicators of pancreatic fistula after pancreaticoduodenectomy. *Br J Surg* 2012; **99**: 104-111 [PMID: 22052299 DOI: 10.1002/bjs.7730]

169 **Xiu D**, Wang H, Li M. The research of drainage trypsin activation peptide (TAP) in post-operation pancreatic fistula (POPF). *HPB* 2019; **21**: S446 [DOI: 10.1016/j.hpb.2019.10.2214]

170 **Uemura K**, Murakami Y, Sudo T, Hashimoto Y, Kondo N, Nakagawa N, Sasaki H, Ohge H, Sueda T. Indicators for proper management of surgical drains following pancreaticoduodenectomy. *J Surg Oncol* 2014; **109**: 702-707 [PMID: 24420007 DOI: 10.1002/jso.23561]

171 **Rollin N**, Cassese G, Pineton DE Chambrun G, Serrand C, Navarro F, Blanc P, Panaro F, Valats JC. An easy-to-use score to predict clinically relevant postoperative pancreatic fistula after distal pancreatectomy. *Minerva Surg* 2022; **77**: 354-359 [PMID: 34693675 DOI: 10.23736/S2724-5691.21.09001-8]

172 **Li B**, Pu N, Chen Q, Mei Y, Wang D, Jin D, Wu W, Zhang L, Lou W. Comprehensive Diagnostic Nomogram for Predicting Clinically Relevant Postoperative Pancreatic Fistula After Pancreatoduodenectomy. *Front Oncol* 2021; **11**: 717087 [PMID: 34277458 DOI: 10.3389/fonc.2021.717087]

173 **Shen J**, Guo F, Sun Y, Zhao J, Hu J, Ke Z, Zhang Y, Jin X, Wu H. Predictive nomogram for postoperative pancreatic fistula following pancreaticoduodenectomy: a retrospective study. *BMC Cancer* 2021; **21**: 550 [PMID: 33992090 DOI: 10.1186/s12885-021-08201-z]

World Journal of Gastrointestinal Surgery

Submit a Manuscript: https://www.f6publishing.com

World J Gastrointest Surg 2022 October 27; 14(10): 1107-1119

DOI: 10.4240/wjgs.v14.i10.1107

ISSN 1948-9366 (online)

ORIGINAL ARTICLE

Retrospective Study

Performing robot-assisted pylorus and vagus nerve-preserving gastrectomy for early gastric cancer: A case series of initial experience

Chi Zhang, Mao-Hua Wei, Liang Cao, Yan-Feng Liu, Pin Liang, Xiang Hu

Specialty type: Surgery

Provenance and peer review: Unsolicited article; Externally peer reviewed.

Peer-review model: Single blind

Peer-review report's scientific quality classification

Grade A (Excellent): 0
Grade B (Very good): B
Grade C (Good): C
Grade D (Fair): 0
Grade E (Poor): 0

P-Reviewer: Shah OJ, India; Tanabe H, Japan

Received: February 21, 2022
Peer-review started: February 21, 2022
First decision: April 19, 2022
Revised: May 15, 2022
Accepted: July 19, 2022
Article in press: July 19, 2022
Published online: October 27, 2022

Chi Zhang, Mao-Hua Wei, Liang Cao, Yan-Feng Liu, Pin Liang, Xiang Hu, Department of Gastrointestinal Surgery, The First Affiliated Hospital of Dalian Medical University, Dalian 116011, Liaoning Province, China

Corresponding author: Chi Zhang, MD, Doctor, Department of Gastrointestinal Surgery, The First Affiliated Hospital of Dalian Medical University, No. 222 Zhongshan Road, Xigang District, Dalian 116011, Liaoning Province, China. 18098875983@163.com

Abstract

BACKGROUND

Pylorus and vagus nerve-preserving gastrectomy (PPG) is a function-preserving surgery for early gastric cancer (GC) that has gained considerable interest in the recent years. The operative technique performed using the Da Vinci Xi robot system is considered ideal for open and laparoscopic surgery.

AIM

To introduce Da Vinci Xi robot-assisted PPG (RAPPG)-based operative procedure and technical points as well as report the initial experience based on the clinical pathology data of eight cases of early GC.

METHODS

Da Vinci Xi robot-assisted pylorus and vagus nerve-preserving gastrectomy (RAPPG) was performed for 11 consecutive patients with middle GC from December 2020 to July 2021. Outcome measures were postoperative morbidity, operative time, blood loss, number of lymph nodes harvested, postoperative hospital stay, time to first flatus, time to diet, and resection margins.

RESULTS

Eight of the 11 patients who were pathologically diagnosed with early GC were enrolled in a retrospective study to assess the feasibility and safety of RAPPG. The mean operative time, mean blood loss, mean number of lymph nodes harvested, length of preserved pylorus canal, distal margin, and proximal margin were 330.63 ± 47.24 min, 57.50 ± 37.70 mL, 18.63 ± 10.57, 3.63 ± 0.88 cm, 3.50 ± 1.31 cm, and 3.63 ± 1.19 cm, respectively. None of the cases required conversion to laparotomy. Postoperative complications occurred in two (25.0%) patients. Post-operative complications were hyperamylasemia and gastric stasis in one case and

incision infection in the other. Time to first flatus was 3.75 ± 2.49 d after the operation, and postoperative hospital stay was 10.13 ± 4.55 d.

CONCLUSION

The core technique in the Da Vinci Xi RAPPG is lymph node dissection and the anatomic method of the nerve. Robotic surgical procedures are feasible and safe. With the progress of surgical technology, optimization of medical insurance structure, and emergence of evidence-based medicine, automated surgery systems will have a broad application in clinical treatment.

Key Words: Da Vinci robotic surgery system; Gastric carcinoma; Vagus nerve; Pylorus; Gastrectomy

Core Tip: The robotic surgery system is widely used in the surgical field. Pylorus and vagus nerve-preserving gastrectomy is a function-preserving surgery for early gastric cancer (GC). We introduced an robot-assisted pylorus and vagus nerve-preserving gastrectomy-based operative procedure and technical points as well as report the initial experience. We analyzed the the mean operative time, mean blood loss, mean number of lymph nodes harvested, length of preserved pylorus canal, distal margin, proximal margin, and postoperative complications of 8 patients with early GC. None of the cases required conversion to laparotomy. The main postoperative complications were hyperamylasemia and gastric stasis. These study results are preliminary, and on establishing a standard surgical treatment, large-sample, multicenter, and prospective clinical trial should be conducted.

Citation: Zhang C, Wei MH, Cao L, Liu YF, Liang P, Hu X. Performing robot-assisted pylorus and vagus nerve-preserving gastrectomy for early gastric cancer: A case series of initial experience. *World J Gastrointest Surg* 2022; 14(10): 1107-1119

URL: https://www.wjgnet.com/1948-9366/full/v14/i10/1107.htm

DOI: https://dx.doi.org/10.4240/wjgs.v14.i10.1107

INTRODUCTION

Gastric cancer (GC) is the most frequent neoplastic diagnosis and the second most common cause of cancer-related deaths worldwide[1]. The incidence of early GC is increasing annually. Function-preserving surgery for GC has been gaining attention in recent years[2]. Pylorus and vagus nerve-preserving gastrectomy (PPG) as a function-preserving surgical treatment has gained gradual acceptance and promotion. Clinical studies have shown that PPG is a safer option with a better oncological prognosis than distal gastrectomy for managing early GC[3,4].

Moreover, PPG can reduce the incidence of cholelithiasis, diarrhea, and dumping syndrome. It is conducive to the recovery of nutritional indicators and body weight, reducing insulin secretion disorders[5]. Although laparoscopic techniques are improving, the "chopstick" effect caused by the parallel arrangement of the instruments in the umbilicus is considered an obstacle in delicate operations. The tremor filter, scale motions, three-dimensional imaging, and dexterous arm of the Da Vinci robot have advantages in localizing the anatomy of the nerves, vessels, and lymph nodes for clearly demarcated dissections. A meta-analysis evaluated the advantages of robotic gastrectomy (RG) *vs* laparoscopic gastrectomy (LG) for GC. The results showed that the operative time of RG was significantly shorter and the cost was relatively higher, but RG had advantages in increasing the number of retrieved lymph nodes and controlling intraoperative blood loss. Although there was no significant difference in overall complications, complications with Clavien–Dindo classification greater than grade 3 in RG were significantly lower than those in LG. Distal and proximal resection margin distance, conversion rate to open surgery, mortality rate, and recurrence rate were not significantly different between them[6]. Han *et al*[7] from South Korea first compared perioperative efficacy and oncologic safety between robot-assisted and laparoscopy-assisted pylorus-preserving gastrectomy in the treatment of middle-third early GC. The operative time of the robot-assisted pylorus-preserving gastrectomy was longer, but there was no significant difference in complications and the number of examined lymph nodes[7].

Experience showed that reasonable surgical process, close cooperation of the surgical team, rational use of energy equipment, and avoidance of surgical risks are key factors to ensure surgical quality. The purpose of this study was to introduce an robot-assisted pylorus and vagus nerve-preserving gastrectomy (RAPPG)-based operative procedure and technical points as well as report the initial experience based on the clinical pathology data of eight cases.

MATERIALS AND METHODS

After introducing the Da Vinci Xi robot system, RAPPG was performed for 11 consecutive patients with middle GC from December 2020 to July 2021. All patients were diagnosed with GC with gastroscopy and histological examination before surgery. Gastroscopy and upper gastrointestinal radiography were performed to locate the lesion. Complemented with computed tomography (CT) examination, nine patients with early middle GC with preoperative stage cT1N0 were treated with PPG according to the Japanese GC Treatment Guidelines 2018 (5th edition). One patient was preoperatively diagnosed with cT2N0 without enlarged lymph nodes in the superior pyloric region on CT. PPG was correspondingly performed upon indication due to the clinical assessment of tumor enlargement. Another patient was preoperatively diagnosed with cT4aN2M0. This patient's case was complicated with chronic obstructive pulmonary disease, and the patient had dyspnea after activity; ASA grade was 3. PPG was performed by a multi-disciplinary team as an extended indication. All patients' treatment protocols were formulated by preoperative discussion without ethical committee involvement. Before surgery, the procedure details were explained to all patients, and appropriate informed consent was obtained.

The inclusion criteria were as follows: (1) ECOG score ≤ 2 points; (2) Histologically confirmed adenocarcinoma (papillary adenocarcinoma, tubular adenocarcinoma, mucinous adenocarcinoma, signet ring cell carcinoma, poorly differentiated adenocarcinoma) with gastroscopic pathological biopsy before operation; (3) No group 1 and 5 lymph node metastasis on abdominal CT; (4) A distance of ≥4 cm from the distal end of the tumor to the pylorus on gastroscopy, abdominal CT, and upper gastrointestinal angiography; (5) Clinical stage of cT1a-1bN0M0 on transabdominal-enhanced CT (AJCC 8th Edition); and (6) Confirmation that the depth of tumor infiltration was limited to the mucosa or submucosa on postoperative pathology.

Operative technique

Patient and robot position and port placement: The patient's position, setting of the trocar puncture sheath, position of the assistant, and choice of the surgical approach play a role in surgical difficulty. R-PPG operation position: the patient was placed in the supine position, the head is held high at 15°, feet are maintained low at 15°, and the assistant is on the right side of the patient. The "Smile" layout was used for the punch card setting (Figure 1).

The coaxial axis was set as the line connecting the umbilicus to the splenic hilum. Arm 3 was used as the central operation hole, and the Maryland bipolar coagulation forceps, ultrasonic scalpel, and Hem-O-lock applier were used. Arm 1 could be inserted with proGrasp forceps and fenestrated bipolar coagulation forceps, whereas Arm 4 could only be inserted with proGrasp forceps. Arm 2 could be used as the endoscope hole (8 mm, 30 ° endoscope). The assistant used the right B hole (12 mm) to assist the operator in exposing the operation field using a Hem-O-lock, aspirator, electrocoagulation rod, and cutting closure device.

Exploration: The pneumoperitoneum was established, abdominal pressure was maintained at 12 mmHg, and the liver was suspended. Tumor location was determined and marked preoperatively and confirmed again by gastroscopy during the procedure.

Treatment of the left part of the greater curvature of the stomach

In the middle of the stomach, Arm 4 used proGrasp forceps to lift the vascular arch of the greater curvature of the stomach and pull it to the ventral wall and cephalic side. Arm 1 used proGrasp forceps to expand the gastrocolic ligament from the right side. The assistant pulled the greater omentum to the right and foot sides to expand the gastrocolic ligament in a bullfight towel style. Focus should be on observing the distribution of the transverse colon and omental branch blood vessels. The transverse colon should not be damaged during the operation. Hemostasis of omental branch blood vessels should be reliable, and the operation field should be kept clean. Arm 3 used an ultrasonic scalpel or Maryland bipolar electrocoagulation to open the gastrocolic ligament and enter the omental sac. The gastrocolic ligament was cut at the center of the resultant force and clamped directly to the inferior pole of the spleen. The pancreatic tail was used as a landmark to expose the left gastroepiploic vessels from the ventral and dorsal sides. At the same time, group 4 Lymph nodes were cleared, the medium-large clip was placed in Arm 3, and the left gastric omental vessels were clamped using an applier (Figure 2A) and cut off using an ultrasonic scalpel. The repair of the greater curvature of the stomach and preparation for gastric disconnection and anastomosis were correspondingly facilitated.

Treatment of the lower pylorus region

Arm 4 used proGrasp forceps to pull the omentum of the greater curvature of the gastric antrum to the left and abdominal wall side, and the assistant pulled the liver region of the transverse colon to the middle and foot side. The duodenum and pancreatic head were transferred to the abdomen's central part by traction, and the descending duodenum and pancreatic head were fully exposed. Arm 1 used proGrasp forceps to assist exposure and lifting, whereas Arm 3 used Maryland bipolar electrocoagulation. First, the omentum was opened along with the descending duodenum. The transverse mesocolon was dissected along the front of the pancreatic head to nearly reach the horizontal part of the

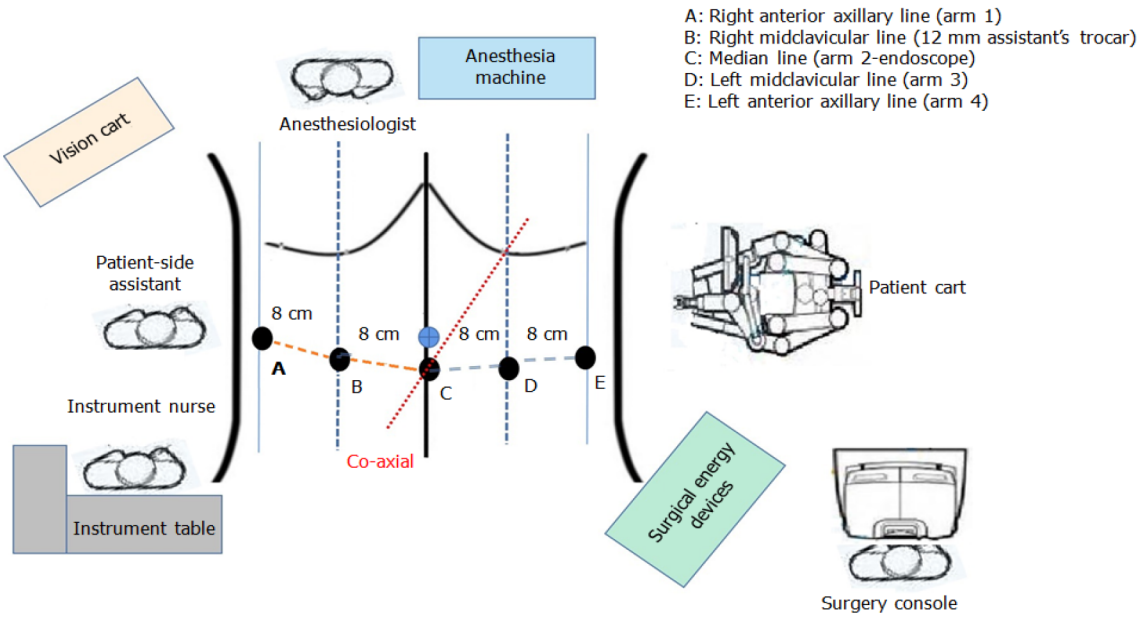

DOI: 10.4240/wjgs.v14.i10.1107 **Copyright** ©The Author(s) 2022.

Figure 1 Smile layout and operation room setting of pylorus and vagus nerve-preserving gastrectomy using the Da Vinci Xi robot system.

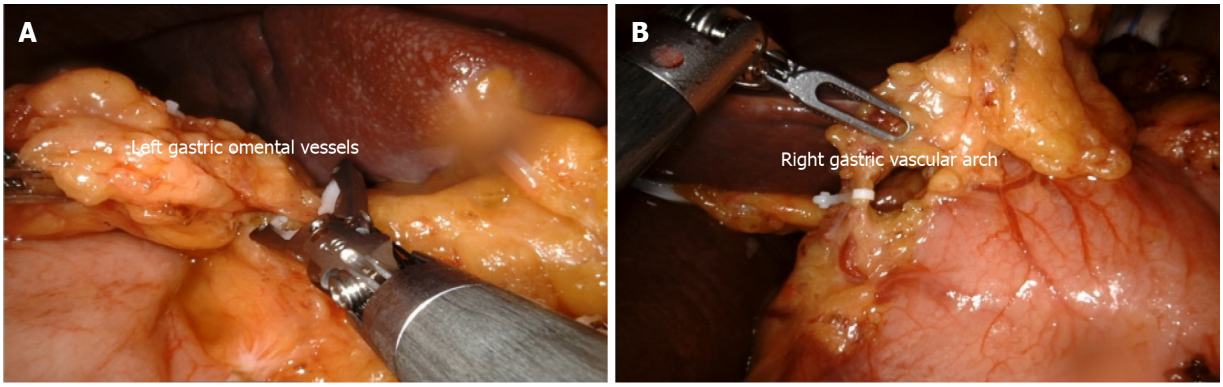

DOI: 10.4240/wjgs.v14.i10.1107 **Copyright** ©The Author(s) 2022.

Figure 2 Hem-O-lock clamping gastric omental vessels. A: Left; B: Right.

descending duodenum. Part of the hepatocolic ligament was opened outside the duodenum to facilitate traction of the colonic liver region and dissociation of the transverse mesocolon. The accessory right colonic vein, superior anterior pancreaticoduodenal vein, and right gastroepiploic vein were exposed on the right side. The operative field was turned to the middle part of the stomach. The gastrocolic ligament incision in the greater curvature of the stomach was dissociated along the transverse colon to the right.

After communicating with the free plane of the descending duodenum, the transverse mesocolon was dissociated from the lower edge of the pancreas to reach the right gastroepiploic vein. The antrum, pylorus, and posterior wall of the duodenum were dissociated to expose the gastroduodenal artery. At this time, the operative field of the area under the pylorus was fully expanded from the right, left, and lower sides. It is safe to dissect the right gastroepiploic vessels and blood vessels under the pylorus and clean the lymph nodes of group 6. First, the lymph nodes in the inferior pylorus region were dissected from the right side along the front of the pancreatic head. The omentum was opened in the avascular area between the inferior pylorus vessel and the first branch of the right gastroepiploic vessel to communicate with the left free plane. The right gastroepiploic vessel branches were cut off one by one along the gastric wall, and the gastric wall of the great curvature of the gastric antrum was exposed by 4–5 cm. The lymph nodes were dissected from the pylorus and duodenum to the bifurcation of the inferior pylorus vessels and right gastroepiploic vessels. Lymph node dissection was performed from the bottom along the root of the right gastroepiploic vein to the top of the bifurcation. Finally, the lymph nodes were dissected from the left side of the pancreas along the blood vessels to reach the bifurcation. The right gastroepiploic vessels were circumscribed 4–5 cm to complete the lymph node dissection in

the lower pylorus region (Figure 3). The inferior pyloric artery and veins were preserved. The right gastroepiploic artery was clamped and severed using a Hem-O-lock near the bifurcation.

Management of the superior pylorus

Arm 4 Lifted the lesser omentum to the oral, left, and abdominal sides, and the assistant pulled the greater curvature of the stomach (the part to be excised) to the left side and under the left side of Arm 3 to fully expose the lesser curvature of the upper pylorus. There was no need to clean group 5 Lymph nodes in the upper pylorus area, and the first to second right gastric vascular branches were preserved. The distance of 4 cm from the lesser curvature to the pylorus was measured as the precut line. Arm 4 Lifted the right gastric artery near the precut line with proGrasp forceps. Arm 3 used an ultrasonic scalpel or Maryland bipolar electrocoagulation. The precut line was close to the gastric wall, and the right gastric vascular arch was circumscribed. Hem-O-lock was used to clamp and disconnect the right gastric vascular arch (Figure 2B). The vascular branches of the gastric wall were cut off one by one along the anterior and posterior wall of the gastric wall to the oral side along the lesser curvature, and the naked gastric wall reached 1 cm distal to the lesion.

Treatment of the superior margin of the pancreas

Arm 4 used proGrasp forceps to lift the descending branch of the left gastric artery and omental adipose tissue together and pull to the abdominal wall, shifting the operation field to the left and right sides to facilitate better exposure. The assistant can carry a piece of gauze to hide the tip of the forceps, press the middle and lower one-third of the pancreatic body, pull the pancreas to the foot side, turn the superior margin of the pancreas outward, and pull the pancreas to the left and right sides with the change in the operative field. Assistant forceps are typically located in the field of operation. Do not use brute force to avoid injury to the pancreas, mesenteric blood vessels, superior mesenteric blood vessels, and intestine. Arm 3 used Maryland bipolar electrocoagulation, which could be operated from a multi-dimensional angle and was convenient for lymph node dissection and nerve exposure at the superior margin of the pancreas. Arm 1 was pulled and exposed with proGrasp forceps.

Left retroperitoneal approach

Arm 4 pulled the stomach to the abdominal wall and right side, while the assistant pulled the pancreas to the foot and right side. The left retroperitoneal approach was performed by double-click electrocoagulation to open the gastropancreatic fold on the upper edge of the pancreas, expose the left edge of the left gastric artery, and continue to expand the gastropancreatic fold up to the main trunk of the left gastric artery to the bifurcation of the descending branch. The left serosa is opened to the posterior wall of the lesser curvature of the stomach and determines the medial edge of the left approach.

The dorsal membrane of the pancreas was opened along the superior margin of the pancreas, and the superficial nerve of the splenic artery was used to clean the lymph nodes of group 11p, which directly contacted the posterior gastric artery. The lower edge of the left approach was determined. An L-shaped section is formed, and along this section, the nerve is dissociated to the direction of the esophageal hiatus to the posterior wall of the lesser curvature of the stomach. The celiac branch of the vagus nerve can be seen behind the left gastric artery (Figure 4A). The nerve is dissociated into the superficial layer without damage.

Right diaphragmatic foot approach

Arm 4 pulled the stomach to the abdominal wall and left side, while the assistant pulled the pancreas to the foot and left side. The right branch of the diaphragmatic foot was exposed and dissociated along with the superficial layer of the nerve bundle on the surface of the common hepatic artery. The portal vein bounded the right side, and the left gastric artery bound the left side. The lymph nodes of groups 8a and 9 were dissected carefully towards the diaphragmatic foot.

The celiac ganglion was not damaged on the left side. The lymphatic vessels in this area were abundant and should be carefully coagulated using the Maryland bipolar coagulation. The serous membrane was opened on the surface of the right branch of the diaphragm crus to reach the cardia from above. From the right surface of the main left gastric artery, the left gastric artery was dissociated to the bifurcation of the cardia branch and descending branch, forming an L-shaped free plane with the right branch of the foot of the diaphragm (Figure 4B). Along this plane, the left gastric artery was pushed along the cardia branch to the lower part of the cardia, and the abdominal branch of the vagus nerve was exposed from the right side.

The transection of the left gastric artery was performed by preserving the abdominal branch of the vagus nerve and the cardia branch of the left gastric artery *via* the esophageal approach.

It is vital to maintain the right surgical field, expose the anterior wall of the lesser curvature of the stomach below the cardia, and determine the cardia branch of the left gastric artery, which should be retained. At the distal end of this branch, the group 1 and 3 Lymph nodes were cleared along the lesser curvature of the gastric wall, and the right branch of the foot of the diaphragm. The distal end of the stomach was dissociated from the lower part of the cardia. The left gastric artery was exposed throughout the entire process, and the esophageal cardia branch went directly to the bifurcation of the

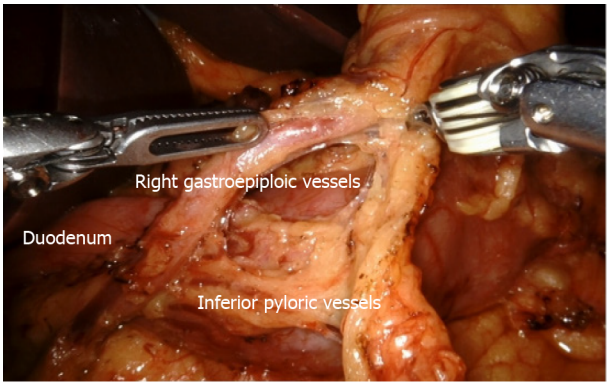

DOI: 10.4240/wjgs.v14.i10.1107 **Copyright** ©The Author(s) 2022.

Figure 3 Lymph node dissection in the inferior pylorus region.

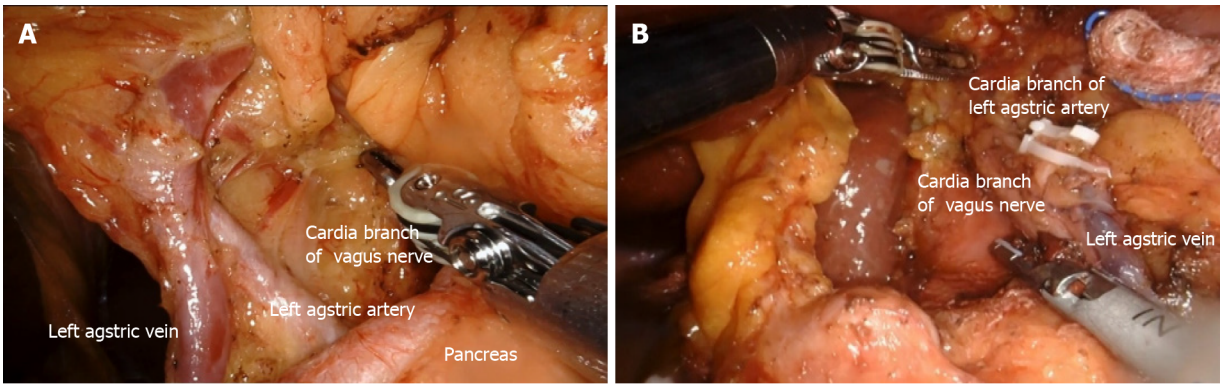

DOI: 10.4240/wjgs.v14.i10.1107 **Copyright** ©The Author(s) 2022.

Figure 4 The celiac branch of the vagus nerve is exposed. A: Through the left approach at the superior margin of the pancreas; B: Through the right approach at the superior margin of the pancreas.

descending branch of the left gastric artery. The left approach can be connected to the descending branch along the bifurcation ring. The descending branch of the left gastric artery can also be seen from the left approach, communicating with the right approach, retaining the abdominal branch of the vagus nerve and the cardia branch of the left gastric artery, and cutting off the left gastric artery (Figure 5).

The gastric wall was repaired, and the stomach was cut 2 cm from the distal and proximal ends of the tumor. The specimens were removed through a small incision in the upper abdomen. Intraoperative pathology confirmed that the cutting edge was negative. Correspondingly, gastrostomy was performed through a small abdominal incision. The length of the pylorus tube was 3–4 cm. No pyloroplasty was performed (Figure 6).

Statistical analysis

Data in the text and tables are presented as mean ± SD. Statistical analysis was performed using the SPSS software ver. 20.0 for Windows.

RESULTS

The clinical data of the 11 patients are shown in Table 1. The postoperative pathological diagnosis results of patients 1, 5, and 8 showed that the depth of tumor infiltration exceeded the submucosa, which represents advanced GC and thus did not meet the inclusion criteria of this study. Therefore, these three patients were excluded. Finally, eight patients remained in this study.

The eight patients had an average BMI of 24.90 ± 2.60 kg/m^2 and successfully underwent RAPPG. Patient characteristics are summarized in Table 2.

There were no laparoscopic conversions or intraoperative complications. The mean intraoperative blood loss was 57.50 ± 37.70 mL, no transfusions were required, and the mean operative time was 330.63 ± 47.24 min (Table 3). Lymph node dissection was D1 + 8a, 9, 11p. Postoperative complications occurred in two patients. The incidence of complications was 25.0%. One patient had gastric stasis and

Table 1 The general clinical data of 11 patients

No.	Sex	Year	Body mass index (kg/m²)	Operative time (min)	Tumor size (cm)	pT	pN	Histology	Number of resected lymph nodes	Number of metastatic lymph nodes
1[1]	M	70	24.20	300	7	3	2	Poorly	29	3
2	M	62	21.70	390	2	1b	0	Well	19	0
3	F	64	20.70	330	3	1a	0	Medium	32	0
4	M	56	27.10	315	3	1a	0	Signet ring cell	8	0
5[1]	M	65	29.50	325	4	4a	3	Poorly	51	13
6	F	72	26.20	410	1.5	1a	0	Well	9	0
7	M	70	26.42	330	2.5	1a	0	Poorly	21	0
8[1]	M	79	28.73	240	3	2	0	Poorly	12	0
9	M	52	28.02	270	3	1a	0	Medium	13	0
10	M	66	23.95	300	2	1a	0	Well	11	0
11	F	66	25.08	300	4	1b	2	Poorly	36	3

[1]Cases do not meet the inclusion criteria, and these case data are excluded from statistics.

Table 2 Patient characteristics

Variables	mean ± SD, *n* = 8
Age (yr)	63.50 ± 6.74 (52.0-72.0)
Sex (male/female)	5/3
Body mass index (kg/m²)	24.90 ± 2.60 (20.70-28.02)
ASA status	
I	7
II	1
Comorbidity	
Chronic obstructive pulmonary dysfunction	0
Diabetes	0
Valvular heart disease	0
Chronic atrial fibrillation	0
Hypertension	1
Occlusive vascular disease	0
History of appendectomy	1

hyperamylasemia postoperatively. The Clavien–Dindo classification of complications was grade 2. The patient had first flatus on day 9, liquid diet on day 11, and semi-liquid diet on day 13 after the operation. On day 1 after the surgery, the blood amylase level increased above 500 U/dL. After the application of somatostatin, the blood amylase level returned to normal. No abdominal infection occurred, and the patient was discharged on day 18 after the operation. The other patient had incision infection about grade 2 of Clavien–Dindo classification.

The pathological data are listed in Table 4. Among the eight patients, one had early GC invading the submucosa; however, three metastatic lymph nodes were found [groups 4d (1/7) and 6 (2/8)]. Pathological diagnosis showed protuberant lesions, invasion of the submucosa, low adhesion carcinoma, and poorly differentiated carcinoma. Immunohistochemistry showed HER-2 (0), Ki67 (+60%), MLH-1 (loss of expression), MSH-2 (expression), MSH-6 (expression), PMS-2 (loss of expression), and EGFR (-). The mean number of resected lymph nodes was 18 in the eight early GC patients.

Table 3 Intraoperative data and early outcome

Variables	mean ± SD, *n* = 8
Operative time (min)	330.63 ± 47.24 (270.0-410.0)
Estimated blood loss (mL)	57.50 ± 37.70 (10.0-100.0)
Postoperative hospital stay (d)	10.13 ± 4.55 (6.0-18.0)
Time to first flatus (d)	3.75 ± 2.49 (2.0-9.0)
Time to diet (d)	
Liquid	5.38 ± 2.56 (3.0-11.0)
Solid	7.63 ± 2.67 (5.0-13.0)
Morbidity	
Stomach stasis	1
Atelectasis	0
Incision infection	1
Anastomotic leakage	0
Hyperamylasemia	1
Valvular heart disease	0
Ascites	0
Trocar bleeding	0
Ileus	0

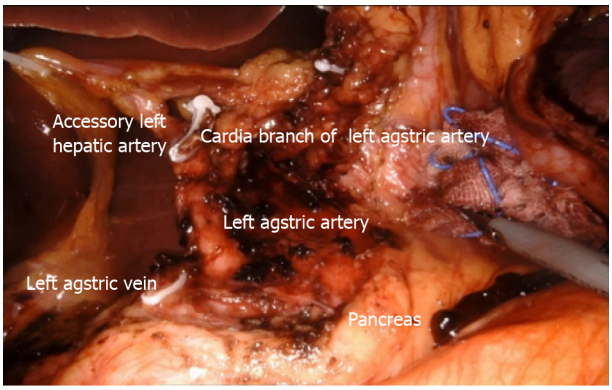

DOI: 10.4240/wjgs.v14.i10.1169

Figure 5 The left gastric artery is cut off by preserving the celiac branch of the vagus nerve and the cardia branch of the left gastric artery.

DISCUSSION

Current scenario of PPG practice

PPG was first proposed by Maki in the 1960s to treat peptic ulcers. At the beginning of the 1990s, lymph node dissection and the applied PPG technology became popular for early GC treatment in Japan. With the increasing incidence of early GC, this technology is widely used in Asian countries, mainly in China, Japan, and South Korea. The 3rd edition of the Japanese guidelines for the treatment of GC (2010) stipulates the indications for PPG. For early middle GC, the distance from the distal part of the tumor to the pylorus was > 4 cm. Group 5 Lymph nodes above the pylorus were not removed, and the hepatic branches and celiac branches of the vagus nerve were preserved. Clinical studies have found that compared with distal gastrectomy, vagus-preserving gastrectomy can reduce postoperative cholelithiasis, diarrhea, and dumping syndrome and is beneficial for recovering postoperative hemoglobin level[8]. Some scholars worry that PPG surgery without thorough lymph node dissection increases the risk of postoperative recurrence. A Japanese study included 3646 cases of T1 GC in the middle of the stomach. The results showed that the rate of upper pyloric lymph node metastasis was only 0.2%[9].

Table 4 Pathologica features

Variables	mean ± SD, *n* = 8
T	
T1a	6
T1b	2
N	
N0	7
N2	1
Stage (8th AJCC TNM staging system for gastric cancer)	
IA	7
IIA	1
Histology	
Well	3
Medium	2
Poorly	2
Signet ring cell	1
Size of tumor (cm)	2.66 ± 0.82 (1.5-4.0)
Distance between anastomosis and pylorus (cm)	3.63 ± 0.88 (2.5-5.0)
Resection margins (cm)	
Proximal	3.63 ± 1.19 (2.0-5.0)
Distal	3.50 ± 1.31 (2.0-5.0)
Mean resected Lymph nodes	18.63 ± 10.57 (8.0-36.0)
Number of metastatic lymph nodes	0.38 ± 1.06 (0-3)

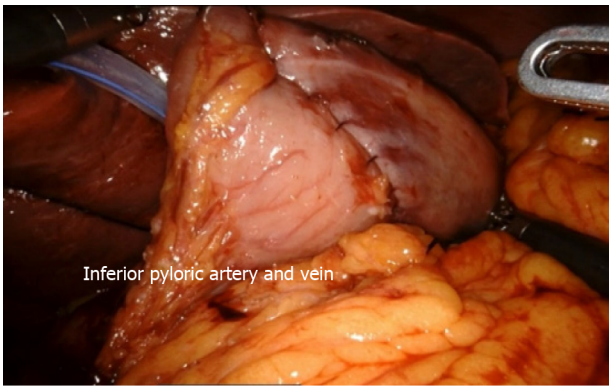

DOI: 10.4240/wjgs.v14.i10.1107

Figure 6 Four cm length of the pylorus canal was preserved.

Tsujiura *et al*[10] reported 465 cases of laparoscopic pylorus-preserving gastrectomy with a 5-year overall and disease-free survival rate of 98%. The recurrence sites of the two cases were not in the remnant stomach and regional lymph nodes, which proved the non-inferiority of PPG in local recurrence and long-term prognosis. The primary complications of PPG are postoperative gastric stasis, such as delayed duodenal discharge, excessive food residue in the remnant stomach, and postprandial nausea or upper abdominal fullness. In South Korea, Oh *et al*[11] found that the incidence of postoperative gastric stasis was 35% in patients with a pylorus tube length of 1.5 cm and 10% in patients with a length of 3.0 cm. Takahashi *et al*[12] found that 68 (7.6%) of 897 PPG patients with pylorus tube preservation of 3–5 cm had postoperative gastric stasis. Multivariate analysis showed that for patients aged > 61 years, diabetes mellitus and abdominal infection were risk factors. The Korean klass-04 trial is a multicenter, prospective randomized controlled trial (RCT) to explore the safety and feasibility of

laparoscopic PPG and provide evidence-based medicine.

Current status of robotic surgery for GC

The Da Vinci robotic surgery system is widely used in the surgical field because of its advantages of high definition, an enlarged 3D field of vision, good stability, and flexibility. In 2002, Hashizume *et al* [13] reported the first Da Vinci robot-assisted radical gastrectomy. A meta-analysis published in 2019 included 8413 patients with GC from 24 non-randomized studies. A total of 2741 cases were treated with RG, and 5672 cases were treated with LG. The results showed that the operative time in the RG group was longer than that in the LG group, but the number of lymph nodes was higher. Complications such as delayed gastric emptying, intestinal obstruction, abdominal infection, incision infection, anastomotic leakage, and pancreatic complications were not significantly different. There were no significant differences in the 3-year and 5-year overall survival rates[14]. Uyama *et al*[15] reported a multicenter, single-arm, prospective study of robot-assisted distal gastrectomy in 253 patients with stage I/II GC. The results showed that the average operative time of robot-assisted distal gastrectomy was 313 min, and blood loss was 20 mL. No 30 d mortality occurred, the incidence of complications was 2.45%, and incidence of complications was lower than that of laparoscopic distal gastrectomy (6.4%). Wang *et al* [16] compared the incidence of complications between the RG and LG groups.

The results showed that the overall incidence of complications and severe complications in the robotic gastric surgery group was 18.8% and 8.9%, respectively, lower than 24.5% and 17.5% in the laparoscopic group. The robot system is safe and feasible for the surgical treatment of GC. The latest Da Vinci robot system is the Da Vinci Xi. A Korean study compared the short-term effects of the Da Vinci Xi System and the Da Vinci Si System on gastrectomy for GC. Early and advanced GCs were included in this study. Surgical methods included distal gastrectomy, total gastrectomy, and proximal gastrectomy. The results showed no significant difference in operative time, intraoperative blood loss, first postoperative exhaust time, hospital stay, and complications between the two groups[17]. At present, there is no evidence-based medicine such as an RCT comparing robotic GC surgery with laparoscopy and laparotomy. Ojima *et al*[18] carried out an RCT on robot-assisted laparoscopic radical gastrectomy in 2018 and planned to include 240 patients with GC of clinical stages I–III. The primary endpoint was to assess the incidence of postoperative complications of intra-abdominal infection, including pancreatic fistula, intra-abdominal abscess, and anastomotic fistula. Secondary endpoints included the incidence of any complications, surgical outcomes, postoperative course of the disease, and oncological outcomes.

Fundamental techniques of robot-assisted PPG surgery

The fundamental techniques of PPG are (1) Group 6 Lymph node dissection with preservation of the inferior pylorus vessels and (2) Treatment of the upper edge of the pancreas with preservation of the abdominal branch of the vagus nerve. Kiyokawa *et al*[19] proposed that the incidence of gastric stasis after PPG with preservation and disconnection of inferior pyloric vein was 5.4% and 23.4% respectively. Based on the concept of structure-determining function, preserving the blood vessels around the pylorus can maintain the basic shape of the pylorus and has minimal effect on the function of the pylorus after PPG. The inferior pylorus artery and vein were preserved during PPG. The lymph nodes in the inferior pylorus region were dissected and exposed from the upper, lower, right, and left directions and from the ventral and dorsal sides by taking the bifurcation of the right gastroepiploic artery and the inferior pylorus artery as the center. Upper part: duodenal bulb, pylorus, significant curvature of the gastric antrum; lower part: root of the right gastroepiploic vein; right side: medial edge of the descending duodenum; left side: right edge of the first branch of the right gastroepiploic vessel; ventral side: the anterior wall of the stomach; dorsal side: the posterior wall of the stomach. The dissociation order can be as follows: right ventral border, lower dorsal upper left border, right ventral border, and upper-lower dorsal left border.

Moreover, preservation of the esophageal branch of the cardia plays a vital role in maintaining the shape and function of the cardia. The right diaphragmatic foot approach was combined with the left retroperitoneal approach to determine the distribution of the vagus nerve. Lymph node dissection outside the nerve fiber membrane is vital to this technique. In addition, Maryland bipolar electrocoagulation is better than ultrasonic scalpel in treating Arm 3 of the superior margin of the pancreas.

The major limitation of this single center is the retrospective design and small sample size. This study aimed to highlight the surgical process, technical details, technical points, and precautions of RAPPG and retrospectively analyze the short-term prognosis of early GC cases. More cases should be accumulated, long-term follow-up should be conducted, and data should be compared with data for LAPPG to gather more data for RAPPG in the treatment of patients with early GC.

Overall, these study results are preliminary, and on establishing a standard surgical treatment, large-sample, multi-center, and prospective clinical trial should be conducted.

CONCLUSION

Laparoscopic PPG for GC management has advanced, but the chopstick effect of laparoscopic surgery

limits its delicate operation. The robot system functions as a high-degree-of-freedom simulation operation instrument, with a high-definition magnified 3D field of vision and tremor elimination, which significantly improves the safety, flexibility, and stability of a more effective operation platform for PPG operation. However, the application of robot systems remains limited due to its bulky volume and high cost, resulting in decreased operation cost and efficiency. In addition, evidence-based medicine is essential to confirm the safety and feasibility of the Da Vinci surgical system in the treatment of GC. However, with the continuous improvement and upgrading of robot systems, advancement of surgical technology, optimization of medical insurance structure, and accumulation of research samples, the robot system will occupy an important position in the minimally invasive treatment of GC in the future.

ARTICLE HIGHLIGHTS

Research background

Pylorus and vagus nerve-preserving gastrectomy (PPG) as a function-preserving surgical treatment has gained gradual acceptance and promotion. Although laparoscopic techniques are improving, the "chopstick" effect caused by the parallel arrangement of the instruments in the umbilicus is considered an obstacle in delicate operations. The results of study showed that operative time of the robot-assisted pylorus-preserving gastrectomy (RAPPG) was longer, but there was no significant difference in complications and the number of examined lymph nodes compared with laparoscopy-assisted pylorus-preserving gastrectomy (LAPPG).

Research motivation

In order to formulate the reasonable surgical process and technical standards for RAPPG.

Research objectives

To introduce Da Vinci Xi RAPPG-based operative procedure and technical points as well as report theinitial experienc.

Research methods

This retrospective analysis of clinical and pathological data of 8 early middle gastric cancer (GC) cases who have performed RAPPG.The fundamental techniques of RAPPG are (1) The inferior pylorus artery and vein were preserved during operation; and (2) The right diaphragmatic foot approach was combined with the left retroperitoneal approach to determine the distribution of the vagus nerve.

Research results

There were no laparoscopic conversions or intraoperative complications. The mean intraoperative blood loss was 57.50 ± 37.70 mL; the mean operative time was 330.63 ± 47.24 min .The incidence of complications was 25.0%.

Research conclusions

The core technique in the RAPPG is lymph node dissection and the anatomic method of the nerve. Robotic surgical procedures are feasible and safe. Reasonable surgical process, close cooperation of the surgical team, rational use of energy equipment, and avoidance of surgical risks are key factors to ensure surgical quality.

Research perspectives

This study aimed to highlight the surgical process, technical details, technical points, and precautions of RAPPG and retrospectively analyze the short-term prognosis of early GC cases. More cases should be accumulated, long-term follow-up should be conducted, and data should be compared with data for LAPPG to gather more data for RAPPG in the treatment of patients with early GC.

ACKNOWLEDGEMENTS

We would like to thank the editors and the reviewers for their useful remarks that improved this paper.

FOOTNOTES

Author contributions: Zhang C performed the surgery and was responsible for manuscript writing, study design, data collection; Hu X performed the surgery and was responsible for study design; Wei MH and Liu YF performed the surgery; Liang P and Cao L performed the statistical analysis and literature review.

Institutional review board statement: The study was reviewed and approved by the ethics committee of First Affiliated Hospital of Dalian Medical University [Approval No. PJ-XJS-2022-02].

Informed consent statement: All study participants, or their legal guardian, provided written informed consent form.

Conflict-of-interest statement: The authors of this manuscript having no conflicts of interest to disclose.

Data sharing statement: There is no additional data available.

Country/Territory of origin: China

ORCID number: Chi Zhang 0000-0003-1408-0841.

S-Editor: Ma YJ
L-Editor: A
P-Editor: Ma YJ

REFERENCES

1 **Joshi SS**, Badgwell BD. Current treatment and recent progress in gastric cancer. *CA Cancer J Clin* 2021; **71**: 264-279 [PMID: 33592120 DOI: 10.3322/caac.21657]
2 **Tsujiura M**, Nunobe S. Functional and nutritional outcomes after gastric cancer surgery. *Transl Gastroenterol Hepatol* 2020; **5**: 29 [PMID: 32258533 DOI: 10.21037/tgh.2019.11.10]
3 **Aizawa M**, Honda M, Hiki N, Kinoshita T, Yabusaki H, Nunobe S, Shibasaki H, Matsuki A, Watanabe M, Abe T. Oncological outcomes of function-preserving gastrectomy for early gastric cancer: a multicenter propensity score matched cohort analysis comparing pylorus-preserving gastrectomy versus conventional distal gastrectomy. *Gastric Cancer* 2017; **20**: 709-717 [PMID: 27672061 DOI: 10.1007/s10120-016-0644-y]
4 **Morita S**, Katai H, Saka M, Fukagawa T, Sano T, Sasako M. Outcome of pylorus-preserving gastrectomy for early gastric cancer. *Br J Surg* 2008; **95**: 1131-1135 [PMID: 18690631 DOI: 10.1002/bjs.6295]
5 **Kojima K**, Yamada H, Inokuchi M, Kawano T, Sugihara K. Functional evaluation after vagus-nerve-sparing laparoscopically assisted distal gastrectomy. *Surg Endosc* 2008; **22**: 2003-2008 [PMID: 18594924 DOI: 10.1007/s00464-008-0016-8]
6 **Guerrini GP**, Esposito G, Magistri P, Serra V, Guidetti C, Olivieri T, Catellani B, Assirati G, Ballarin R, Di Sandro S, Di Benedetto F. Robotic versus laparoscopic gastrectomy for gastric cancer: The largest meta-analysis. *Int J Surg* 2020; **82**: 210-228 [PMID: 32800976 DOI: 10.1016/j.ijsu.2020.07.053]
7 **Han DS**, Suh YS, Ahn HS, Kong SH, Lee HJ, Kim WH, Yang HK. Comparison of Surgical Outcomes of Robot-Assisted and Laparoscopy-Assisted Pylorus-Preserving Gastrectomy for Gastric Cancer: A Propensity Score Matching Analysis. *Ann Surg Oncol* 2015; **22**: 2323-2328 [PMID: 25361887 DOI: 10.1245/s10434-014-4204-6]
8 **Eom BW**, Park B, Yoon HM, Ryu KW, Kim YW. Laparoscopy-assisted pylorus-preserving gastrectomy for early gastric cancer: A retrospective study of long-term functional outcomes and quality of life. *World J Gastroenterol* 2019; **25**: 5494-5504 [PMID: 31576095 DOI: 10.3748/wjg.v25.i36.5494]
9 **Isozaki H**, Okajima K, Momura E, Ichinona T, Fujii K, Izumi N, Takeda Y. Postoperative evaluation of pylorus-preserving gastrectomy for early gastric cancer. *Br J Surg* 1996; **83**: 266-269 [PMID: 8689185 DOI: 10.1002/bjs.1800830239]
10 **Tsujiura M**, Hiki N, Ohashi M, Nunobe S, Kumagai K, Ida S, Hayami M, Sano T, Yamaguchi T. Excellent Long-Term Prognosis and Favorable Postoperative Nutritional Status After Laparoscopic Pylorus-Preserving Gastrectomy. *Ann Surg Oncol* 2017; **24**: 2233-2240 [PMID: 28280944 DOI: 10.1245/s10434-017-5828-0]
11 **Oh SY**, Lee HJ, Yang HK. Pylorus-Preserving Gastrectomy for Gastric Cancer. *J Gastric Cancer* 2016; **16**: 63-71 [PMID: 27433390 DOI: 10.5230/jgc.2016.16.2.63]
12 **Takahashi R**, Ohashi M, Hiki N, Makuuchi R, Ida S, Kumagai K, Sano T, Nunobe S. Risk factors and prognosis of gastric stasis, a crucial problem after laparoscopic pylorus-preserving gastrectomy for early middle-third gastric cancer. *Gastric Cancer* 2020; **23**: 707-715 [PMID: 31916027 DOI: 10.1007/s10120-019-01037-4]
13 **Hashizume M**, Shimada M, Tomikawa M, Ikeda Y, Takahashi I, Abe R, Koga F, Gotoh N, Konishi K, Maehara S, Sugimachi K. Early experiences of endoscopic procedures in general surgery assisted by a computer-enhanced surgical system. *Surg Endosc* 2002; **16**: 1187-1191 [PMID: 11984681 DOI: 10.1007/s004640080154]
14 **Qiu H**, Ai JH, Shi J, Shan RF, Yu DJ. Effectiveness and safety of robotic versus traditional laparoscopic gastrectomy for gastric cancer: An updated systematic review and meta-analysis. *J Cancer Res Ther* 2019; **15**: 1450-1463 [PMID: 31939422 DOI: 10.4103/jcrt.JCRT_798_18]
15 **Uyama I**, Suda K, Nakauchi M, Kinoshita T, Noshiro H, Takiguchi S, Ehara K, Obama K, Kuwabara S, Okabe H, Terashima M. Clinical advantages of robotic gastrectomy for clinical stage I/II gastric cancer: a multi-institutional

prospective single-arm study. *Gastric Cancer* 2019; **22**: 377-385 [PMID: 30506394 DOI: 10.1007/s10120-018-00906-8]

16 **Wang WJ**, Li HT, Yu JP, Su L, Guo CA, Chen P, Yan L, Li K, Ma YW, Wang L, Hu W, Li YM, Liu HB. Severity and incidence of complications assessed by the Clavien-Dindo classification following robotic and laparoscopic gastrectomy for advanced gastric cancer: a retrospective and propensity score-matched study. *Surg Endosc* 2019; **33**: 3341-3354 [PMID: 30560498 DOI: 10.1007/s00464-018-06624-7]

17 **Alhossaini RM**, Altamran AA, Choi S, Roh CK, Seo WJ, Cho M, Son T, Kim HI, Hyung WJ. Similar Operative Outcomes between the da Vinci Xi® and da Vinci Si® Systems in Robotic Gastrectomy for Gastric Cancer. *J Gastric Cancer* 2019; **19**: 165-172 [PMID: 31245161 DOI: 10.5230/jgc.2019.19.e13]

18 **Ojima T**, Nakamura M, Nakamori M, Hayata K, Katsuda M, Kitadani J, Maruoka S, Shimokawa T, Yamaue H. Robotic versus laparoscopic gastrectomy with lymph node dissection for gastric cancer: study protocol for a randomized controlled trial. *Trials* 2018; **19**: 409 [PMID: 30064474 DOI: 10.1186/s13063-018-2810-5]

19 **Kiyokawa T**, Hiki N, Nunobe S, Honda M, Ohashi M, Sano T. Preserving infrapyloric vein reduces postoperative gastric stasis after laparoscopic pylorus-preserving gastrectomy. *Langenbecks Arch Surg* 2017; **402**: 49-56 [PMID: 27815708 DOI: 10.1007/s00423-016-1529-6]

World Journal of Gastrointestinal Surgery

Submit a Manuscript: https://www.f6publishing.com

World J Gastrointest Surg 2022 October 27; 14(10): 1120-1130

DOI: 10.4240/wjgs.v14.i10.1120

ISSN 1948-9366 (online)

ORIGINAL ARTICLE

Retrospective Study

Long-term efficacy and safety of cap-assisted endoscopic sclerotherapy with long injection needle for internal hemorrhoids

Ya-Ting Xie, Yu Yuan, Hui-Min Zhou, Tao Liu, Li-Hao Wu, Xing-Xiang He

Specialty type: Medicine, general and internal

Provenance and peer review: Unsolicited article; Externally peer reviewed.

Peer-review model: Single blind

Peer-review report's scientific quality classification

Grade A (Excellent): 0
Grade B (Very good): 0
Grade C (Good): C, C
Grade D (Fair): 0
Grade E (Poor): 0

P-Reviewer: Elfeki H, Egypt; Gupta R, India

Received: June 24, 2022
Peer-review started: June 24, 2022
First decision: August 1, 2022
Revised: August 19, 2022
Accepted: September 22, 2022
Article in press: September 22, 2022
Published online: October 27, 2022

Ya-Ting Xie, Yu Yuan, Hui-Min Zhou, Tao Liu, Li-Hao Wu, Xing-Xiang He, Department of Gastroenterology, The First Affiliated Hospital of Guangdong Pharmaceutical University, Guangzhou 510080, Guangdong Province, China

Corresponding author: Xing-Xiang He, MD, Chief Physician, Department of Gastroenterology, The First Affiliated Hospital of Guangdong Pharmaceutical University, No. 19 Lower Nonglin Street, Yuexiu District, Guangzhou 510080, Guangdong Province, China.
hexingxiang@gdpu.edu.cn

Abstract

BACKGROUND

Hemorrhoids are a common anal condition and can afflict an individual at any age. Epidemiological survey results in China show that the prevalence of anorectal diseases is as high as 50.1% among which 98.08% of patients have hemorrhoid symptoms.

AIM

To assess long-term efficacy and safety of cap-assisted endoscopic sclerotherapy (CAES) with long injection needle for internal hemorrhoids.

METHODS

This study was retrospective. Data from patients with symptomatic internal hemorrhoids treated with CAES using endoscopic long injection needle from April 2016 to December 2019 were collected. Patients were telephoned and followed at two time points, December 2020 and 2021, to evaluate the improvements in symptoms, complications, recurrence, and satisfaction.

RESULTS

Two hundreds and one patients with internal hemorrhoids underwent CAES with the long needle. The first median follow-up was performed 33 mo post-operatively. Symptoms improved in 87.5% of patients after the first CAES. Efficacy did not decrease with treatment time extension. Fifty-four patients underwent colonoscopy after the first CAES treatment of which 21 underwent CAES again, and 4 underwent hemorrhoidectomy. At the first follow-up, 62.7% of patients had both improved hemorrhoid grades and symptoms, and 27.4% had a significant improvement in both parameters. At the second follow-up, 61.7% of the patients showed satisfactory improvement in their hemorrhoid grade and symptoms when compared with pre-surgery values. 90% of patients reported

CAES was painless, and 85% were satisfied/very satisfied with CAES treatment outcomes.

CONCLUSION

The present study based on the largest sample size reported the long-term follow-up of the treatment for internal hemorrhoid with the CAES using endoscopic long injection needle. Our findings demonstrate that CAES should be a micro-invasive endoscopic technology yields satisfactory long-term efficacy and safety.

Key Words: Hemorrhoids; Cap-assisted endoscopic sclerotherapy; Long injection needle; Efficacy; Prolapse

Core Tip: Cap-assisted endoscopic sclerotherapy (CAES) is a novel procedure to process flexible endoscopic sclerotherapy. Data from patients with symptomatic internal hemorrhoids treated with CAES using endoscopic long injection needle from April 2016 to December 2019 were collected. Patients were telephoned and followed at two time points, December 2020 and 2021, to evaluate the improvements in symptoms, complications, recurrence, and satisfaction. The present study based on the largest sample size reported the long-term follow-up of the treatment for internal hemorrhoid with the CAES using endoscopic long injection needle. Our findings demonstrate that CAES should be a micro-invasive endoscopic technology yields satisfactory long-term efficacy and safety.

Citation: Xie YT, Yuan Y, Zhou HM, Liu T, Wu LH, He XX. Long-term efficacy and safety of cap-assisted endoscopic sclerotherapy with long injection needle for internal hemorrhoids. *World J Gastrointest Surg* 2022; 14(10): 1120-1130

URL: https://www.wjgnet.com/1948-9366/full/v14/i10/1120.htm

DOI: https://dx.doi.org/10.4240/wjgs.v14.i10.1120

INTRODUCTION

Hemorrhoids are a common anal condition that can afflict an individual at any age. Epidemiological survey results in China show that the prevalence of anorectal diseases is as high as 50.1% among which 98.08% of patients have hemorrhoid symptoms. Epidemiological survey results in the United States show that the prevalence rate of hemorrhoids was higher than 50%, and the risk of hemorrhoids was highest among people aged 45-65 with 44.7% of patients affected by bleeding, pain, prolapse, and other symptoms affecting their life quality[1-3].

Injection sclerotherapy is a safe and simple treatment for internal hemorrhoids. However, traditional hardening agent injection therapy is performed *via* an anoscopy, which may present iatrogenic risks due to incorrect injection location[4,5]. Three milestones in the history of flexible endoscopic sclerotherapy have been reported. Ponsky *et al*[6] in 1991 reported the flexible endoscopic injection of 23.4% saline, with 5-mm retractable needle, and retroflexed position for symptomatic hemorrhoids. Tomiki *et al*[7] in 2014 reported the flexible endoscopic injection of aluminum potassium sulfate and tannic acid, with 5-mm retractable needle, retroflexed and anterograde position, and endoscopic cap. Zhang *et al*[5] in 2015 reported cap-assisted endoscopic sclerotherapy (CAES) using a Lauromacrogol injection with a 10-20 mm retractable needle, normal position, endoscopic cap, and proper air delivery for improving endoscopic exposure.

CAES is a novel procedure to process flexible endoscopic sclerotherapy. The special design of the CAES endoscopic needle (generally using a long needle) helps accurately control the injection angle, direction, and depth under direct vision, and avoids iatrogenic injury caused by ectopic injection[5,8]. Although this technique has become a widely used flexible endoscopy procedure in China with expert recommendations[9], few studies have reported long-term follow-up studies of more than one year. This study retrospectively analyzed the clinical data of patients with internal hemorrhoids treated with long needle CAES from April 2016 to December 2019 in our hospital to explore the long-term clinical efficacy and safety of long needle CAES in the treatment of internal hemorrhoids.

MATERIALS AND METHODS

This study was a single-center study. Patients with symptomatic internal hemorrhoids who received CAES treatment at the First Affiliated Hospital of Guangdong Pharmaceutical University from April

2016 to December 2019 were included in this study and followed by telephone.

Inclusion criteria

No gender or age restrictions were placed on study participants. All patients underwent complete bowel preparation and signed an informed consent for colonoscopy diagnosis and treatment.

Exclusion criteria

Patients with external hemorrhoids, asymptomatic internal hemorrhoids, perianal abscesses, anal stenosis, anal fistulas, malignancies involving the anal canal, pregnancy, coagulation dysfunction, decompensated cirrhosis, cerebrovascular accident, and other diseases, such as dementia, stroke, and mental retardation were excluded. Patients who did not comply with follow-ups were also excluded.

Preparation for CAES

All patients completed the coagulation function examination. To prepare for concurrent endoscopic treatments, such as a bowel polypectomy, aspirin is generally discontinued for 5 d and other antiplatelet drugs for 7 d if possible. All patients signed informed consents for colonoscopy diagnosis and treatment. All patients underwent pre-operative intestinal preparation for CAES to meet the requirements of colonoscopy for diagnosis and treatment. If polyps were found during colonoscopy, treatment of polyps was completed before CAES treatment started. The One physician who was familiar with endoscopic operation and two assistants performed the procedures. All endoscopists had experience in with more than 200 endoscopes.

CAES procedure

A short, straight transparent cap was installed at the front end of the endoscope,and an appropriate amount of gas was injected into the rectum. With the help of the transparent cap, the internal hemorrhoids with a blue-purple surface were visible. Under conditions of full exposure, a long needle, such as an injection needle with a diameter of 22 G and a length of 14 mm, was used (DT-EN-W122-14, Detian, Changzhou, China). Lauromacrogol (10 mL:100 mg, 1%, Tianyu, Xi'an, China) was injected into the base of the hemorrhoids. The injection point was located above the dentate line. According to the location of the left, posterior, right, and anterior anus (LPRA), the inclined plane injection was selected for an endoscopic direction of 6 o'clock, and 1-2 mL Lauromacrogol was injected into each injection site (Figure 1). The clockwise order should be followed when choosing the injection sites. The sclerosing agent is injected into submucosal layer within 5 s. After the injection, the needle was left *in situ*, or the needle sheath was pressed for 10 to 20 s to avoid bleeding at the injection site. Very rapid injections and more than a 2 mL injection in one site are not permitted. After retracting the endoscope, a finger massage around the anal ring was performed to help disperse the drug.

Post-operative treatment

Patients were asked to maintain a horizontal position for at least 2 h after surgery, and routine use of antibiotics and hemostatic drugs was not required after surgery. Laxative agents, such as lactulose, were given after surgery to keep the stool soft and thin. The changes in the condition and vital signs were strictly monitored and handle defecation difficulties, bleeding, infection, ulcers, and other issues were addressed in a timely manner.

Overall evaluation of curative effect

Patients self-reported bleeding and other symptoms were taken as the basis for with three classes of evaluation criteria: (1) Excellent, very satisfied no or mild symptoms; (2) good, significant improvement, occasional symptoms; or (3) poor, no improvement, even worse symptoms.

The symptoms and concomitant symptoms before and after treatment, including anal bleeding, anal pain, anal prolapse, defecation difficulties, anal distension, anal pruritus, anal dampness, and others, were evaluated according to the presence/absence of medical records.

Follow-up treatment attitudes after CAES

Several parameters related to satisfaction with the procedure and outcome were rated: (1) Great satisfaction; (2) satisfaction; (3) general; (4) less satisfaction; and (5) very dissatisfied. Pain level of CAES was rated according to certain levels: (1) No pain; (2) mild and tolerable; and (3) serious and intolerable. Patients' recommendations to undergo the procedure (Would you like to recommend it to other patients?) were based on yes or no answers.

Endoscopic findings

The changes in internal hemorrhoids before, after, and before and during the first CAES and follow-up were compared in patients who returned to the hospital for the second CAES.

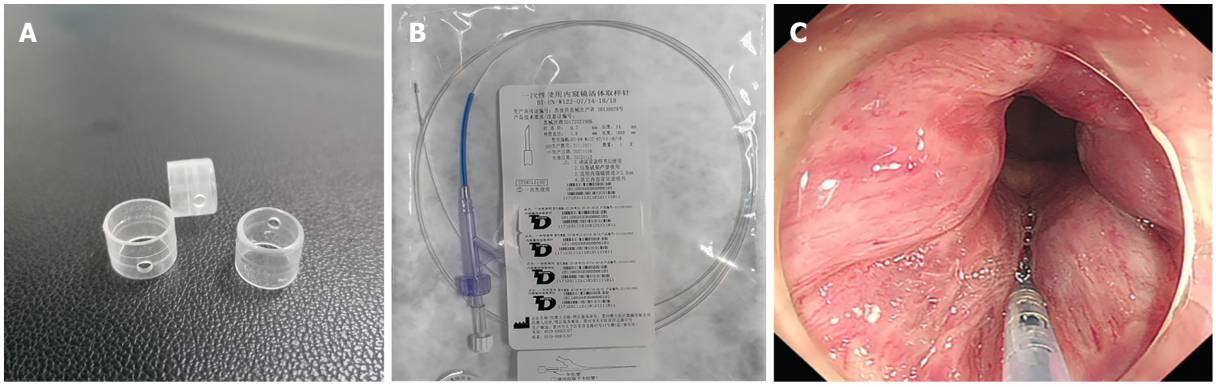

DOI: 10.4240/wjgs.v14.i10.1120

Figure 1 Long needle and the cap used for the procedure. A: The cap; B: Long needle; C: The injection process.

Statistical analysis

SPSS 25.0 was used for systematic analysis of the data, and a chi-squared test was used to analyze the data differences between the two groups before and after treatment. $P < 0.05$ was considered statistically significant.

RESULTS

A total of 201 patients with internal hemorrhoids who underwent CAES treatment were admitted to our hospital from April 2016 to December 2019. These patients were followed by telephone between December 2020 and December 2021. In December 2020, 201 patients were followed, and none were lost to follow-up. In December 2021, 149 patients were followed up of which 52 were lost to follow-up. The patient did not use Ayurveda, Chinese medicine, or herbal medicines during follow-up. Prior to the first treatment, patients with hemorrhoids based on Goligher classification were divided into four stages: (1) 88 patients with stage I hemorrhoids; (2) 53 patients with stage II hemorrhoids; (3) 50 patients with stage III hemorrhoids; and (4) 10 patients with stage IV hemorrhoids (Table 1).

Treatment outcomes

At the first follow-up, 62.7% (126/201) patients showed satisfactory improvement in hemorrhoid grade and symptoms when compared with pre-operative parameters, and 27.4% (55/201) patients had significant improvement in grade and symptoms of hemorrhoids compared with pre-operative parameters but occasionally had symptoms. Twenty out of 201 (9.9%) patients experienced the same grade and/or no improvement or even worsening of symptoms (Table 2).

Fifty-four patients underwent colonoscopy after CAES treatment (Figure 2), and 21 of those patients underwent CAES treatment again. Four additional patients underwent hemorrhoidectomy. At the second follow-up, 61.7% (92/149) of the patients had satisfactory improvement in hemorrhoid grade and symptoms when compared with the pre-operative level, and 33.6% (50/149) of the patients had significant improvement in hemorrhoid grade and symptoms compared with the pre-operative level but occasionally had symptoms. Seven out of 149 patients (4.7%) showed no improvement or even deterioration (Table 3). In our long-term follow-up, we did not identify patients who developed ulcers after treatment.

In terms of internal hemorrhoid improvements, anal bleeding was taken as an example. At the first follow-up, 31 patients had no bleeding either before or after treatment. Bleeding frequency ranged from occasional occurrence in the first defecation samples to asymptomatic after treatment in 107 patients, and 37 patients had no change. Bleeding frequency varied at each defecation before treatment to asymptomatic after treatment in 11 patients, occasionally in nine patients, and no change in four patients after treatment. Bleeding frequency ranged from pretreatment with or without defecation to occasionally in one patient after treatment to asymptomatic in one patient (Figure 3).

126 patients had no anal prolapse either before or after treatment, 57 patients had significant improvement in symptoms, 14 patients had no changes in symptoms either before or after treatment, and 4 patients reported symptom worsening after treatment. 10 patients had stage 4 internal hemorrhoids, 5 patients showed no improvement in prolapse symptoms, 3 patients with less prolapse than before, and 2 patients without prolapse.

131 patients had no pain either before or after treatment, 49 patients had significant improvement in symptoms after treatment, 20 patients had no change in symptoms after treatment, and 1 patient had aggravation of symptoms after treatment. One hundred and forty patients had no distension either

Table 1 Basic patient information and distribution of internal hemorrhoids

Basic situation	Follow-up of 2020 (*n* = 201)	Follow-up of 2021 (*n* = 149)
Median follow-up	33 (24-45)	45 (34-57)
Age	54.71 ± 13.016	54.77 ± 13.495
Gender, *n* (%)		
Male	116 (57.7)	92 (61.7)
Female	85 (42.3)	57 (38.3)
Hemorrhoids installment, *n* (%)		
Stage I	88 (43.8)	67 (45.0)
Stage II	53 (26.4)	38 (25.5)
Stage III	50 (24.8)	37 (24.8)
Stage IV	10 (5.0)	7 (4.7)

Table 2 Long-term efficacy evaluation after cap-assisted endoscopic sclerotherapy treatment (follow-up in 2020, *n* = 201), *n* (%)

Efficacy	Excellent	Good	Poor	χ^2	*P* value
Stage I	54 (61.4)	26 (29.5)	8 (9.1)		
Stage II	35 (66.1)	13(24.5)	5 (9.4)	8.90	0.177
Stage III	34 (68.0)	13 (26.0)	3 (6.0)		
Stage IV	3 (30.0)	3 (30.0)	4 (40.0)		

Table 3 Long-term efficacy evaluation after cap-assisted endoscopic sclerotherapy treatment (follow-up in 2021, *n* = 149), *n* (%)

Efficacy	Excellent	Good	Poor	χ^2	*P* value
Stage I	46 (68.6)	18 (26.9)	3 (4.5)		
Stage II	22 (57.9)	13(34.2)	3 (7.9)	4.78	0.572
Stage III	20 (54.1)	16 (43.2)	1 (2.7)		
Stage IV	4 (57.1)	3 (42.9)	0 (0)		

before or after treatment, 47 patients' symptoms improved significantly after treatment, 12 patients' symptoms did not change after treatment, and 2 patients reported worsening symptoms after treatment. 59 patients had no pruritus either before or after treatment, 28 patients had significant improvement in symptoms after treatment, 11 patients had no change in symptoms after treatment, and 3 patients had aggravation of post-treatment symptoms. 176 patients had no dampness either before or after treatment, 18 patients had significant improvement in symptoms, 5 patients had no changes in symptoms either before or after treatment, and 2 patients had aggravation of symptoms after treatment.

At the second follow-up, 22 patients had no bleeding before or after treatment, 90 patients had significant improvement in symptoms, 35 patients had no change in symptoms before or after treatment, and 2 patients had aggravation of symptoms (Figure 4). 94 patients had no prolapse before and after treatment, 41 patients had significant improvement in prolapse symptoms, 8 patients had no change in symptoms before or after treatment, and 6 patients had symptom worsening. 92 patients had no pain either before or after treatment, 38 patients had significant improvement in pain symptoms after treatment, 10 patients had no change in symptoms after treatment, and 9 patients had aggravation of symptoms after treatment. 94 patients had no distension either before or after treatment, 37 patients had significant improvement in distension symptoms, 8 patients had no change in symptoms either before or after treatment, and 10 patients had symptom aggravation. No pruritus was found in 110 patients either before or after treatment, 25 patients improved significantly after treatment, 5 patients' pruritis symptoms did not change either before or after treatment, and 9 patients' symptoms worsened after treatment. No dampness in 118 patients either before or after treatment was found, 15 patients improved significantly, 4 patients' dampness symptoms did not change either before or after treatment, and 12 patients' symptoms worsened.

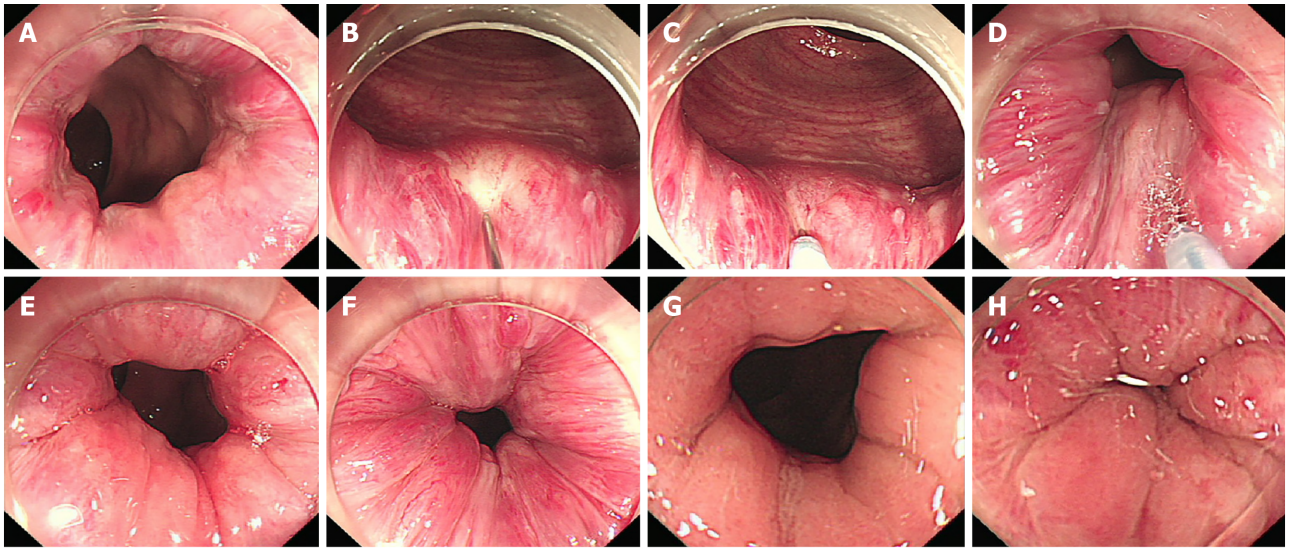

Figure 2 Endoscopic images of the same patient after undergoing one cap-assisted endoscopic sclerotherapy treatment. A: Conditions of internal hemorrhoids and rectal mucosa before surgery; B-D: Intra-operative injection; E and F: Post-operative period; G and H: Re-examination 1 year after treatment (second colonoscopy in 2017).

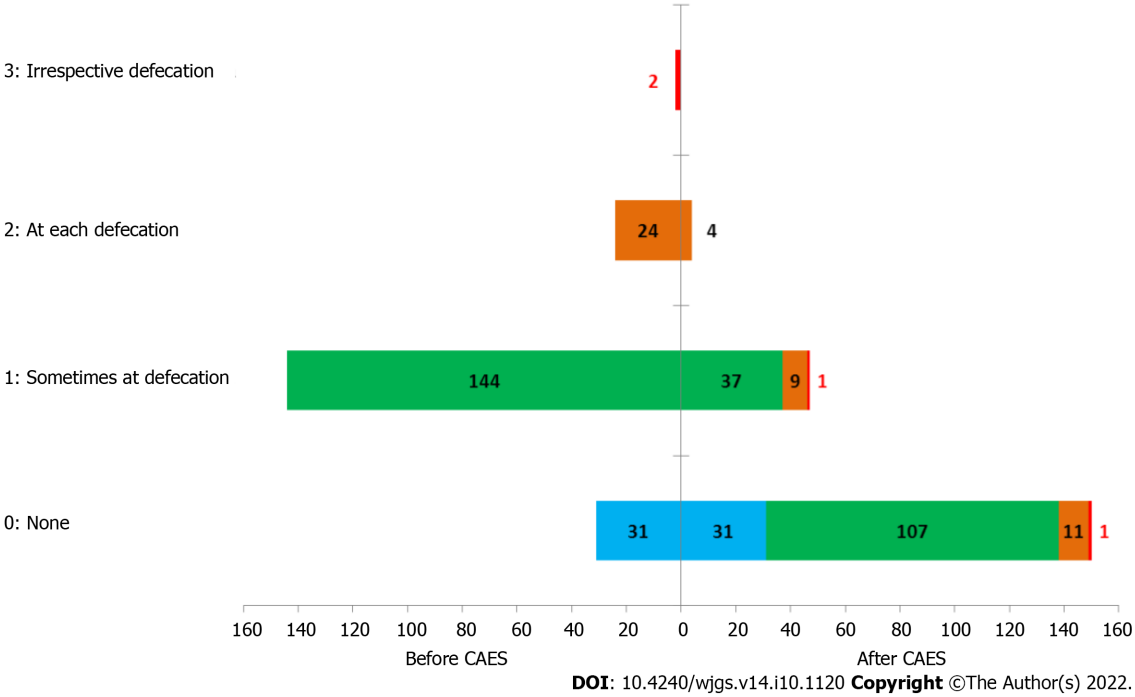

Figure 3 Improvement in anal bleeding after treatment (follow-up in 2020, *n* = 201). CAES: Cap-assisted endoscopic sclerotherapy.

At the second follow-up, 90% of patients reported CAES was painless (Figure 5), and 85% were satisfied/very satisfied with CAES treatment outcomes (Figure 6).

DISCUSSION

As for the pathogenesis of internal hemorrhoids, Thomson[10] proposed the "theory of anal cushion moving down," which has been widely recognized. Internal hemorrhoids are abnormal vascular pads covered by columnar epithelium located in the anal canal above the dentate line. The hemorrhoid pad shrinks during defecation to facilitate stool excretion. During periods of non-defecation, the arterial hemorrhoid pad becomes hyperemic and swollen and then seals the anus[11-13]. The American Society

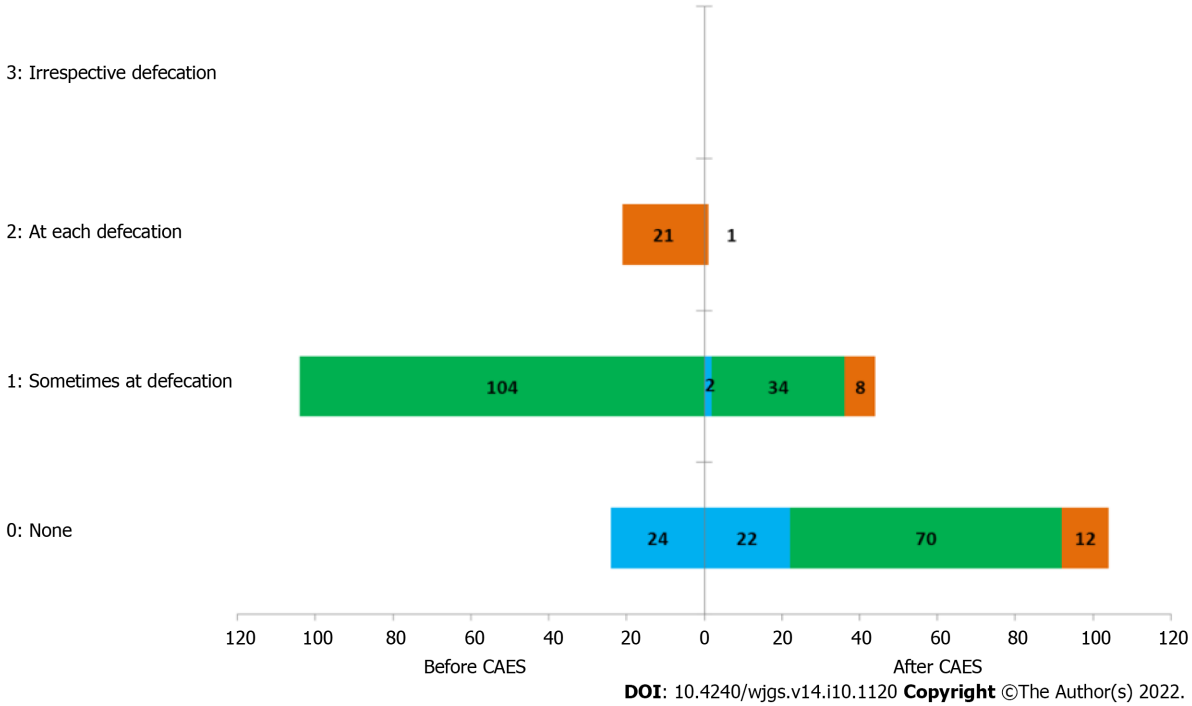

DOI: 10.4240/wjgs.v14.i10.1120 **Copyright** ©The Author(s) 2022.

Figure 4 Improvement in anal bleeding before and after treatment (follow-up in 2021, *n* = 149). CAES: Cap-assisted endoscopic sclerotherapy.

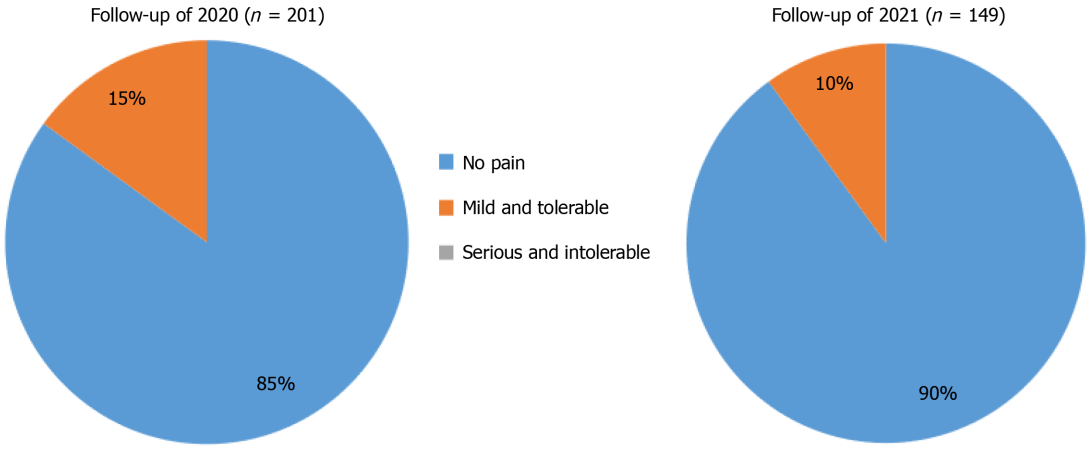

DOI: 10.4240/wjgs.v14.i10.1120 **Copyright** ©The Author(s) 2022.

Figure 5 Patient pain levels during cap-assisted endoscopic sclerotherapy treatment.

of Digestive Endoscopy recommends that endoscopic treatment of hemorrhoids include rubber band ligation (RBL), infrared coagulation, and/or injection sclerotherapy.

Polidocanol is a commonly used injection sclerotherapy that has been widely used for injection sclerotherapy of internal hemorrhoids[14,15]. Polidocanol is injected into the anus mirror or *via* colorectal colonoscopy under direct intravascular injection of pathological changes and causes minimal damage to the mucous membrane tube and anal cushion. However, local intravascular thrombosis resulting from vascular endothelial injury leading to aseptic inflammatory that eventually translates into fiber cords led to occlusion of artery branch blood vessels on rectal hemorrhoids that eventually shrank. In addition, this fibrous action can fix the loose mucous membrane to the anal muscle wall, thereby reducing the symptoms of prolapsed hemorrhoids.

A longer injection needle has advantages as the sclerosing agent injected with short injection needle cannot form hardening pile in the base of hemorrhoids, and the shallow injection depth of the sclerosing agent can easily cause ulcer formation. With the help of a transparent cap, Zhang *et al*[5] used a long needle for submucosal injection and achieved satisfactory efficacy. In 2021, Zhang *et al*[9] on behalf of the CAES-LPRA Study Group released the expert recommendation concerning flexible endoscopic positioning methods. Briefly, endoscopic residual effusion or injected water is the sign for determining the left anus under the left lateral decubitus position. Along the clockwise direction, LPRA are

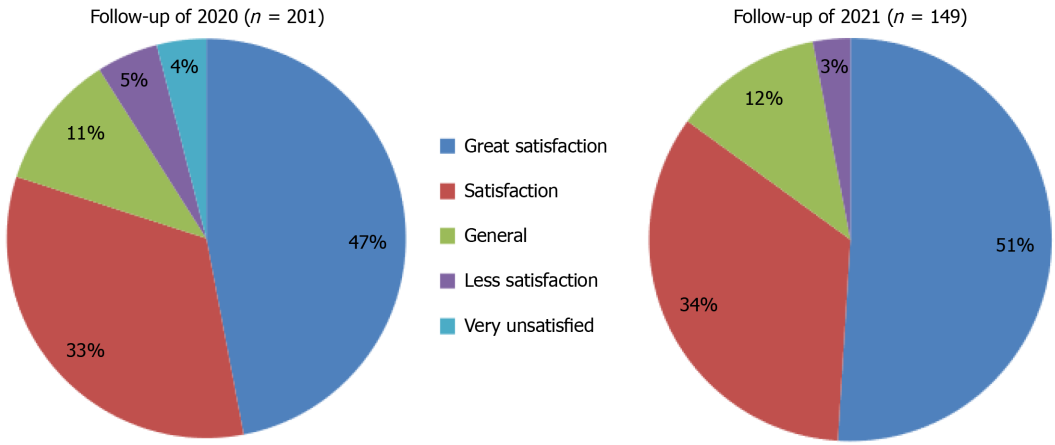

DOI: 10.4240/wjgs.v14.i10.1120

Figure 6 Patient satisfaction with cap-assisted endoscopic sclerotherapy treatment.

recommended to replace the typical lithotomy position for the precise direction description on the anal lesions and for endoscopic therapy.

The LPRA anal positioning method helps the endoscopist distinguish between injected and un-injected sites and avoids the use of tracers[9]. Our group routinely uses long needles for multi-point injection therapy according to the LPRA anal positioning method. This study evaluated the long-term efficacy and safety of long needle CAES for symptomatic internal hemorrhoids. In Zhang's *et al* report[5,8,9,16,17], the follow-up for CAES treatment did not exceed one year. In our study, the time for following CAES treatment was up to 5 years. This study presents the largest sample size reported so far in the treatment of internal hemorrhoids with CAES long needles. In this study, patients treated with CAES were divided into three effect grades: (1) Excellent (no or mild symptoms); (2) good (obviously improved but occasionally symptomatic); and (3) invalid (no improvement, even worse symptoms). In the 2020 follow-up results, 90.1% of patients with internal hemorrhoids, including 94% of patients with stage III internal hemorrhoids, achieved good or excellent results. At the 2021 follow-up, 95.3% of patients with internal hemorrhoids, including 97.3% of patients with stage III internal hemorrhoids achieved good or excellent outcomes. Zhang *et al*'s study found that CAES was effective for stages I and II and a portion of stage III internal hemorrhoids[5]. However, our study found that symptoms improved significantly before and after CAES treatment, and no difference in the long-term efficacy of the treatment in stages I-III was found (Tables 2 and 3). No statistically significant difference in internal hemorrhoid staging between the four groups in 2020 was found. In 2021, no statistically significant differences in the efficacy of CAES in the treatment of stages I-IV internal hemorrhoids were found, that is, it is not considered that CAES produces different long-term efficacies for different stages of internal hemorrhoids. According to the improvement in symptoms and overall evaluation of follow-up, it was found that as the follow-up years increased, no statistically significant difference between the two groups of patients followed up in 2020 and 2021 was noted, indicating that the curative effect of patients treated with CAES did not decline with the extension of treatment years, and the long-term curative effect was stable.

The limitation of this study is the lack of dose difference analysis although the same hardener was used for all patients. Although the operators in the center are experienced, individual technical differences were not considered in this study. Although CAES is a locally minimally invasive treatment, human conditions (such as constipation and advanced age) were not included in the analysis. Since the LPRA method for the location description of anal lesions was published in 2021[9], this study did not analyze the relationship between disease efficacy, safety, and disease site.

In general, post-operative bleeding is the most common complication of hemorrhoids, but in this study, no complications, such as anal bleeding, anal fistula, and anal stenosis occurred after CAES was performed with a long needle. When compared with RBL and hemorrhoidectomy, long-needle CAES appears to be less likely to cause pain. During the follow-up in 2020, 85% of patients believed that long-needle CAES was painless after treatment, and 80% of patients were satisfied or very satisfied with CAES treatment. During the follow-up in 2021, 90% of patients reported that CAES treatment with long needle was painless, and 85% of patients were satisfied or very satisfied with CAES treatment. Patients reported that the pain level during CAES treatment did not increase with the increase in treatment years. This study further confirms that CAES is a simple and effective treatment for internal hemorrhoids that requires no anesthesia and is less painful. Ninety-three percent of patients were willing to recommend CAES treatment to other patients.

CONCLUSION

The present study based on the largest sample size reported the long-term follow-up of the treatment for internal hemorrhoid with the CAES using endoscopic long injection needle. Our findings demonstrate that CAES should be a micro-invasive endoscopic technology yields satisfactory long-term efficacy and safety.

ARTICLE HIGHLIGHTS

Research background

Hemorrhoids are a common anal condition and can afflict an individual at any age. Cap-assisted endoscopic sclerotherapy (CAES) is a novel procedure to process flexible endoscopic sclerotherapy.

Research motivation

There are few previous studies discussing CAES in the treatment of internal hemorrhoids with large sample size and long-term follow-up, so this study can make up for the shortcomings of previous theories.

Research objectives

Long-term efficacy and safety of CAES with long injection needle for internal hemorrhoids were assessed.

Research methods

This retrospective analysis of data from patients with symptomatic internal hemorrhoids treated with CAES using endoscopic long injection needle from April 2016 to December 2019 were collected. Patients were telephoned and followed at two time points, December 2020 and 2021, to evaluate the improvements in symptoms, complications, recurrence, and satisfaction.

Research results

Two hundred and one patients with internal hemorrhoids underwent CAES with the long needle, At the first follow-up, 62.7% of patients had both improved hemorrhoid grades and symptoms, and 27.4% had a significant improvement in both parameters. At the second follow-up, 61.7% of the patients showed satisfactory improvement in their hemorrhoid grade and symptoms when compared with pre-surgery values. 90% of patients reported CAES was painless, and 85% were satisfied/very satisfied with CAES treatment outcomes.

Research conclusions

The present study based on the largest sample size reported the long-term follow-up of the treatment for internal hemorrhoid with the CAES using endoscopic long injection needle. Our findings demonstrate that CAES should be a micro-invasive endoscopic technology yields satisfactory long-term efficacy and safety.

Research perspectives

The improvement of symptoms, complications, recurrence and satisfaction of patients with symptomatic hemorrhoids were cure by CAES.

ACKNOWLEDGEMENTS

We sincerely thank Dr. Fa-Ming Zhang (Nanjing Medical University) for his guidance on this manuscript. We would like to thank all patients in the study.

FOOTNOTES

Author contributions: He XX, Yuan Y and Xie YT designed the concept of the study; Zhou HM, Wu LH and Liu T collected and analyzed the data; Xie YT and Yuan Y wrote the draft manuscript; all authors listed have made a substantial, direct, and intellectual contribution to the work and approved it for publication.

Institutional review board statement: The study was reviewed and approved by the the First Affiliated Hospital of Guangdong Pharmaceutical University Institutional Review Board (No.2016-(33)-01).

Informed consent statement: All study participants or their legal guardian provided informed written consent about personal and medical data collection prior to study enrolment.

Conflict-of-interest statement: All the authors report no relevant conflicts of interest for this article.

Data sharing statement: Technical appendix, statistical code, and dataset available from the corresponding author at hexingxiang@gdpu.edu.cn. Participants gave informed consent for data sharing.

Country/Territory of origin: China

ORCID number: Ya-Ting Xie 0000-0002-8340-8671; Yu Yuan 0000-0002-9536-3167; Hui-Min Zhou 0000-0001-9740-2361; Tao Liu 0000-0003-3572-0134; Li-Hao Wu 0000-0003-4674-8287; Xing-Xiang He 0000-0003-0007-8513.

S-Editor: Gong ZM
L-Editor: A
P-Editor: Gong ZM

REFERENCES

1 **Ray-Offor E**, Amadi S. Hemorrhoidal disease: Predilection sites, pattern of presentation, and treatment. *Ann Afr Med* 2019; **18**: 12-16 [PMID: 30729927 DOI: 10.4103/aam.aam_4_18]
2 **Internal Hemorrhoids Cooperative Group of Chinese Society of Digestive Endoscopology**. Chinese digestive endoscopic practice guidelines and operation consensus for internal hemorrhoids. *Zhonghua Xiaohua Neijing Zazhi* 2021; **38**: 676-687 [DOI: 10.3760/cma.j.cn321463-20210526-00340]
3 **Gallo G**, Martellucci J, Sturiale A, Clerico G, Milito G, Marino F, Cocorullo G, Giordano P, Mistrangelo M, Trompetto M. Consensus statement of the Italian society of colorectal surgery (SICCR): management and treatment of hemorrhoidal disease. *Tech Coloproctol* 2020; **24**: 145-164 [PMID: 31993837 DOI: 10.1007/s10151-020-02149-1]
4 **Jacobs D**. Clinical practice. Hemorrhoids. *N Engl J Med* 2014; **371**: 944-951 [PMID: 25184866 DOI: 10.1056/NEJMcp1204188]
5 **Zhang T**, Xu LJ, Xiang J, He Z, Peng ZY, Huang GM, Ji GZ, Zhang FM. Cap-assisted endoscopic sclerotherapy for hemorrhoids: Methods, feasibility and efficacy. *World J Gastrointest Endosc* 2015; **7**: 1334-1340 [PMID: 26722615 DOI: 10.4253/wjge.v7.i19.1334]
6 **Ponsky JL**, Mellinger JD, Simon IB. Endoscopic retrograde hemorrhoidal sclerotherapy using 23.4% saline: a preliminary report. *Gastrointest Endosc* 1991; **37**: 155-158 [PMID: 2032599 DOI: 10.1016/s0016-5107(91)70675-5]
7 **Tomiki Y**, Ono S, Aoki J, Takahashi R, Sakamoto K. Endoscopic sclerotherapy with aluminum potassium sulfate and tannic acid for internal hemorrhoids. *Endoscopy* 2014; **46** Suppl 1 UCTN: E114 [PMID: 24676816 DOI: 10.1055/s-0034-1364884]
8 **Zhang T**, Long CY, Cui BT, He Z, Peng ZY, Huang GM, Zhang FM. Cap-assisted endoscopic sclerotherapy for hemorrhoids: a prospective study (with video). *Zhonghua Xiaohua Neijing Zazhi* 2017; **34**: 709-712 [DOI: 10.3760/cma.j.issn.1007-5232.2017.10.005]
9 **Zhang FM**, Wu KC, Li JN, Wang X, He XX, Wan R, Chen SY; CAES-LPRA Study Group. Rationale, new anus positioning methods, and updated protocols: Expert recommendations on cap-assisted endoscopic sclerotherapy for hemorrhoids from China Gut Conference. *Chin Med J (Engl)* 2021; **134**: 2675-2677 [PMID: 34711720 DOI: 10.1097/CM9.0000000000001836]
10 **Thomson WH**. The nature of haemorrhoids. *Br J Surg* 1975; **62**: 542-552 [PMID: 1174785 DOI: 10.1002/bjs.1800620710]
11 **Pata F**, Sgró A, Ferrara F, Vigorita V, Gallo G, Pellino G. Anatomy, Physiology and Pathophysiology of Haemorrhoids. *Rev Recent Clin Trials* 2021; **16**: 75-80 [PMID: 32250229 DOI: 10.2174/1574887115666200406115150]
12 **van Tol RR**, Kleijnen J, Watson AJM, Jongen J, Altomare DF, Qvist N, Higuero T, Muris JWM, Breukink SO. European Society of ColoProctology: guideline for haemorrhoidal disease. *Colorectal Dis* 2020; **22**: 650-662 [PMID: 32067353 DOI: 10.1111/codi.14975]
13 **Aoki T**, Hirata Y, Yamada A, Koike K. Initial management for acute lower gastrointestinal bleeding. *World J Gastroenterol* 2019; **25**: 69-84 [PMID: 30643359 DOI: 10.3748/wjg.v25.i1.69]
14 **Watanabe T**, Ohno M, Tahara K, Tomonaga K, Ogawa K, Takezoe T, Fuchimoto Y, Fujino A, Kanamori Y. Efficacy and safety of sclerotherapy with polidocanol in children with internal hemorrhoids. *Pediatr Int* 2021; **63**: 813-817 [PMID: 33045763 DOI: 10.1111/ped.14506]
15 **Mishra S**, Sahoo AK, Elamurugan TP, Jagdish S. Polidocanol versus phenol in oil injection sclerotherapy in treatment of internal hemorrhoids: A randomized controlled trial. *Turk J Gastroenterol* 2020; **31**: 378-383 [PMID: 32519957 DOI: 10.5152/tjg.2020.19276]
16 **ASGE Technology Committee**, Siddiqui UD, Barth BA, Banerjee S, Bhat YM, Chauhan SS, Gottlieb KT, Konda V, Maple JT, Murad FM, Pfau P, Pleskow D, Tokar JL, Wang A, Rodriguez SA. Devices for the endoscopic treatment of

hemorrhoids. *Gastrointest Endosc* 2014; **79**: 8-14 [PMID: 24239254 DOI: 10.1016/j.gie.2013.07.021]

17 **Wu X**, Wen Q, Cui B, Liu Y, Zhong M, Yuan Y, Wu L, Zhang X, Hu Y, Lv M, Wu Q, He S, Jin Y, Tian S, Wan R, Wang X, Xu L, Bai J, Huang G, Ji G, Zhang F. Cap-assisted endoscopic sclerotherapy for internal hemorrhoids: technique protocol and study design for a multi-center randomized controlled trial. *Ther Adv Gastrointest Endosc* 2020; **13**: 2631774520925636 [PMID: 32551439 DOI: 10.1177/2631774520925636]

World Journal of Gastrointestinal Surgery

Submit a Manuscript: https://www.f6publishing.com

World J Gastrointest Surg 2022 October 27; 14(10): 1131-1140

DOI: 10.4240/wjgs.v14.i10.1131

ISSN 1948-9366 (online)

ORIGINAL ARTICLE

Retrospective Study

Reconstructing the portal vein through a posterior pancreatic tunnel: New choice for portal vein thrombosis during liver transplantation

Dong Zhao, Yi-Ming Huang, Zi-Ming Liang, Kang-Jun Zhang, Tai-Shi Fang, Xu Yan, Xin Jin, Yi Zhang, Jian-Xin Tang, Lin-Jie Xie, Xin-Chen Zeng

Specialty type: Gastroenterology and hepatology

Provenance and peer review: Unsolicited article; Externally peer reviewed.

Peer-review model: Single blind

Peer-review report's scientific quality classification

Grade A (Excellent): 0
Grade B (Very good): 0
Grade C (Good): C, C
Grade D (Fair): 0
Grade E (Poor): 0

P-Reviewer: Boteon YL, Brazil; Kumar R, India

Received: July 14, 2022
Peer-review started: July 14, 2022
First decision: July 31, 2022
Revised: August 8, 2022
Accepted: September 21, 2022
Article in press: September 21, 2022
Published online: October 27, 2022

Dong Zhao, Yi-Ming Huang, Zi-Ming Liang, Kang-Jun Zhang, Tai-Shi Fang, Xu Yan, Xin Jin, Yi Zhang, Jian-Xin Tang, Lin-Jie Xie, Xin-Chen Zeng, Department of Liver Surgery and Organ Transplantation Center, The Third People's Hospital of Shenzhen, The Second Affiliated Hospital of Southern University of Science and Technology, National Clinical Research Center for Infectious Disease, Shenzhen 518000, Guangdong Province, China

Corresponding author: Dong Zhao, MD, Professor, Surgeon, Department of Liver Surgery and Organ Transplantation Center, The Third People's Hospital of Shenzhen, The Second Affiliated Hospital of Southern University of Science and Technology, National Clinical Research Center for Infectious Disease, No. 29 Bulan Road, Longgang District, Shenzhen 518000, Guangdong Province, China. zdong1233@126.com

Abstract

BACKGROUND

Thrombectomy and anatomical anastomosis (TAA) has long been considered the optimal approach to portal vein thrombosis (PVT) in liver transplantation (LT). However, TAA and the current approach for non-physiological portal reconstructions are associated with a higher rate of complications and mortality in some cases.

AIM

To describe a new choice for reconstructing the portal vein through a posterior pancreatic tunnel (RPVPPT) to address cases of unresectable PVT.

METHODS

Between August 2019 and August 2021, 245 adult LTs were performed. Forty-five (18.4%) patients were confirmed to have PVT before surgery, among which seven underwent PV reconstruction *via* the RPVPPT approach. We retrospectively analyzed the surgical procedure and postoperative complications of these seven recipients that underwent PV reconstruction due to PVT.

RESULTS

During the procedure, PVT was found in all the seven cases with significant adhesion to the vascular wall and could not be dissected. The portal vein proximal to the superior mesenteric vein was damaged in one case when attempting thrombolectomy, resulting in massive bleeding. LT was successfully performed in

all patients with a mean duration of 585 min (range 491-756 min) and mean intraoperative blood loss of 800 mL (range 500-3000 mL). Postoperative complications consisted of chylous leakage (n = 3), insufficient portal venous flow to the graft (n = 1), intra-abdominal hemorrhage (n = 1), pulmonary infection (n = 1), and perioperative death (n = 1). The remaining six patients survived at 12-17 mo follow-up.

CONCLUSION

The RPVPPT technique might be a safe and effective surgical procedure during LT for complex PVT. However, follow-up studies with large samples are still warranted due to the relatively small number of cases.

Key Words: Liver transplantation; Portal vein thrombosis; Portal vein reconstruction; Retropancreatic tunnel; Computer tomography angiography; Three-dimensional visualization

Core Tip: In the study, we presented a new choice for reconstructing the portal vein through a posterior pancreatic tunnel (RPVPPT) to address the issue of unresectable portal vein thrombosis in adult liver transplantation (LT). Clinical data of seven recipients who had portal vein thrombosis (PVT) and underwent RPVPPT were analyzed. PVT was found in all the seven cases with significant adhesion to the vascular wall and could not be dissected. LT was successfully performed in all patients without serious complications. Six patients survived at 12-17 mo follow-up. The RPVPPT technique may be a safe and effective surgical procedure in LT for complex PVT.

Citation: Zhao D, Huang YM, Liang ZM, Zhang KJ, Fang TS, Yan X, Jin X, Zhang Y, Tang JX, Xie LJ, Zeng XC. Reconstructing the portal vein through a posterior pancreatic tunnel: New choice for portal vein thrombosis during liver transplantation. *World J Gastrointest Surg* 2022; 14(10): 1131-1140
URL: https://www.wjgnet.com/1948-9366/full/v14/i10/1131.htm
DOI: https://dx.doi.org/10.4240/wjgs.v14.i10.1131

INTRODUCTION

Liver transplantation (LT) remains the mainstay treatment for end-stage liver disease. However, the incidence of portal vein thrombosis (PVT) in patients on the waiting list for transplantation has been reported to range from 5% to 26%. Due to the complexity of treatment techniques, PVT has long been regarded as a contraindication of LT until the 1980s[1-3]. However, the past decade has witnessed unprecedented progress achieved in surgical techniques, leading to the advent of many surgical approaches for recipients with PVT, including physiological portal reconstruction (such as thrombectomy, interposition venous grafts, and mesoportal jump grafts) and non-physiological portal reconstruction (such as cavoportal hemitransposition, renoportal anastomosis, and arterialization of PV flow)[4,5]. Importantly, physiological reconstruction can restore the anatomical structure of the portal venous system and ensure adequate blood flow to the graft. In contrast, non-physiological reconstruction exhibits limited ability to resolve portal hypertension due to the inability to drain visceral blood into the liver, resulting in a higher incidence of postoperative complications and mortality than physiological reconstruction[6-10]. Most recipients with PVT can undergo thrombectomy and anatomical anastomosis (TAA), yielding satisfactory results. However, in clinical practice, some patients with PVT present with organized thrombi adhering to vascular walls that cannot be completely removed intraoperatively, compromising blood flow to the graft. Non-physiological reconstruction methods are indicated in such cases, including portal-renal vein anastomosis and bypass, portal vena cava semi-transposition, and portal vein arterialization. An increasing body of evidence suggests that this approach is ineffective and might lead to an insufficient blood supply to the portal vein or postoperative hepatic encephalopathy[10-12].

Kasahara *et al*[13] reported a "pullout technique" for portal vein reconstruction in ten pediatric cases of LT. The portal vein was first pulled out from the back of the pancreas and resected. Then the portal vein reconstruction was completed by bridging the back of the pancreas with allograft or autologous blood vessels. However, this technique has not been widely used, and no relevant reports of its application during adult LT have been documented. Therefore, based on the "pullout technique", our center explored the technique of reconstructing the portal vein through a posterior pancreatic tunnel (RPVPPT) in adult LT recipients where PVT could not be resolved.

MATERIALS AND METHODS

General clinical data

A retrospective analysis was performed on 245 cases of LT at Shenzhen Third People's Hospital from August 2019 to August 2021. PVT was documented in 45 cases, of which 7 underwent RPVPPT for PVT and portal vein reconstruction (6 males, 1 female; age 48-65 years, mean 54 years). All patients in this study underwent LT with the approval of the Ethics Committee of Shenzhen Third People's Hospital, and livers were donated after the death of healthy citizens.

Preoperative assessment method

Before surgery, each patient underwent Doppler ultrasound and abdominal computed tomography angiography (CTA) to determine the incidence of complications such as PVT. Three-dimensional (3D) visualization models were reconstructed according to the DICOM format data of CTA, as previously described in the literature[14], and surgery was simulated on the model.

Main surgical methods of RPVPPT technique

Dissection of the hepatic hilum: First, the varicose veins of the hepatic hilum were separated and ligated successively, the common hepatic artery and the proper hepatic artery were dissected, and the left hepatic artery and the right hepatic artery were separated. The main portal vein was dissected from the caudal to the cephalad direction along the trunk to the left and right branches of the portal vein. Finally, the bile duct was isolated and severed near the hilum.

Establishment of the retropancreatic tunnel: First, the main portal vein was dissected from the cephalad to the caudal direction, and the left gastric vein (coronary vein) and the portal vein branch vessels were ligated successively. When the upper edge of the pancreas was reached, dissection started from the lower edge of the pancreas. The superior mesenteric vein (SMV) and splenic vein (SpV) were first separated and lifted with vascular slings. Then, dissection continued from the back of the pancreas to the cephalic side along the main portal vein to establish a retropancreatic tunnel. Subsequently, the pancreas was lifted with a vascular sling or a fine urinary catheter. Finally, the portal vein and its tributary branches behind the pancreas were completely severed and "naked".

Resection of the main portal vein of the recipient: The severed main portal vein was pulled out from the retropancreatic tunnel to the lower edge of the pancreas. The main portal vein containing the thrombus was removed after interrupting blood flow in the SMV and SpV. If the left gastric vein drained into the SpV or the superior mesenteric-portal vein (SMPV) confluence, it was ligated and severed first to avoid insufficient portal venous flow to the graft due to blood shunting.

Portal vein reconstruction: After the donor-recipient inferior vena cava anastomosis was completed, the donor's portal vein was pulled to the lower edge of the pancreas through the retropancreatic tunnel, and the portal vein reconstruction was conducted at the SMPV confluence (Figure 1).

Main evaluation indicators

The clinical data of each LT recipient with PVT were collected, including the medical history and laboratory, imaging, and 3D reconstruction results. The surgical methods and operation-related indicators were analyzed, including the operation time, bleeding volume, amount of blood transfusion, and surgical complications.

RESULTS

General clinical data

Patients with PVT included in the present study were cases with a preoperative diagnosis of decompensated hepatitis B virus (HBV)-related cirrhosis (n = 3) and hepatocellular carcinoma with decompensated HBV-related cirrhosis (n = 4). Five cases had a history of gastrointestinal bleeding before the operation. All patients underwent preoperative 3D reconstructions to visually assess blood vessels and simulate surgery, and LT was successfully conducted. The mean operation time was 585 min (range 491-756 min), and the mean intraoperative blood loss was 800 mL (range 500-3000 mL). More details are provided in Table 1.

Changes in the structure of the portal vein system

Anatomical structure of the PVT: One patient presented with complete portal vein occlusion with thrombosis proximal to the SMPV confluence, four cases with portal vein stenosis greater than 70% and thrombosis extending to the SMPV confluence, and two cases with portal vein stenosis greater than 70% and thrombosis extending to the proximal segment of the SMV. All seven patients with PVT presented with organized thrombi that could be completely removed intraoperatively during surgery. Moreover,

Table 1 Basic demographics and clinical data of cases with portal vein thrombosis (*n* = 7)

	Gender	Age	Diagnosis	Operation time (s)	Anhepatic stage (s)	Intraoperative blood loss (mL)	Transfusion of red blood cell suspension (U)	Cold ischemia time (s)	Outcome
Case 1	Male	65	HBV-related decompensated liver cirrhosis, HCC	648	34	1300	10	510	Survival
Case 2	Male	48	HBV-related decompensated liver cirrhosis	756	31	1000	6	480	Survival
Case 3	Male	38	HBV-related decompensated liver cirrhosis	564	35	800	0	390	Death
Case 4	Female	64	HBV-related decompensated liver cirrhosis, HCC	585	25	600	0	360	Survival
Case 5	Male	57	HBV-related decompensated liver cirrhosis, HCC	583	47	600	0	360	Survival
Case 6	Male	54	HBV-related decompensated liver cirrhosis	491	30	500	0	360	Survival
Case 7	Male	51	HBV-related decompensated liver cirrhosis, HCC	625	34	3000	20	360	Survival

HBV: Hepatitis B virus; HCC: Hepatocellular carcinoma.

the proximal portal vein was damaged near the SMPV confluence in one case when attempting thrombolectomy, resulting in massive bleeding.

Anatomical structure of varicose vessels: The left gastric vein drained into the main portal vein (*n* = 3), SpV (*n* = 3), and SMPV confluence (*n* = 1), and the maximum diameter of the left gastric vein was greater than 1 cm in four cases. All cases presented with esophageal and gastric fundal varices and splenorenal shunt; the maximum diameter of the splenorenal shunt was 24 mm, and an umbilical vein opening was found in two cases. More details are provided in Table 2.

Surgical results and complications

Portal vein reconstruction and LT were successfully conducted in all cases, with patent and sufficient portal vein flow documented by intraoperative color Doppler ultrasonography. Six patients recovered smoothly after the surgery, and one patient died. The liver and coagulation function indicators are shown in Tables 3 and 4. Postoperative complications consisted of chylous leakage (*n* = 3), insufficient portal venous flow to the graft (*n* = 1), intra-abdominal hemorrhage (*n* = 1), pulmonary infection (*n* = 1), and perioperative death (*n* = 1).

Management of postoperative complications included conservative medical treatment for chylous leaks and antibiotics for pulmonary infection. In cases of insufficient portal venous flow, embolization of splenorenal shunt vessels under digital subtraction angiography (DSA) was used to improve portal venous blood flow (Figure 2). An exploratory laparotomy was performed on a patient with post-operative intra-abdominal bleeding (postoperative day 7) that was attributed to multiple blood vessels at the lower margin of the pancreas. Liver ischemia and hypoxia occurred due to hemorrhagic shock after surgery. The patient died 15 d after LT due to liver failure. At 12-17 mo follow-up, six of the seven cases in this study survived.

DISCUSSION

Management of PVT

PVT refers to thrombosis occurring in the main portal vein and its associated venous system (SMV, inferior mesenteric vein, and SpV). It is one of the most common complications of end-stage liver disease, with an incidence of about 5%-26%[1,15,16]. In the present study, the incidence of PVT was 18.4% (45/245). PVT has long been considered a contraindication for LT due to limited surgical techniques and poor understanding of PVT[17]. With significant inroads achieved in recent years,

Table 2 Vascular anatomical changes in the portal vein system of cases with portal vein thrombosis (*n* = 7)

Case	Left gastric vein (coronary vein)				Esophagogastric fundus vein		Superior mesenteric vein		Splenic vein		Shunt situation		
	Drain into the main portal vein	Drain into the confluence of SMV and SpV	Drain into SpV	Maximum diameter of the blood vessel (mm)	Degree of varicose veins	History of upper gastrointestinal bleeding	With or without thrombus	Maximum diameter (mm)	With or without thrombus	Maximum diameter (mm)	With or without splenorenal shunt	Maximum diameter of the shunt (mm)	With or without umbilical vein opening
1	Yes			30	Severe	Yes	No	18.8	No	21.3	Yes	21	No
2			Yes	10.4	Severe	Yes	Yes	17	No	14.2	Yes	24	Yes
3			Yes	24.2	Severe	Yes	No	15.4	No	12.4	Yes	15.7	No
4			Yes	13.8	Severe	Yes	Yes	10.8	No	10.5	Yes	17.3	No
5	Yes			5.9	Severe	No	No	16.4	No	12.5	Yes	11.2	Yes
6	Yes			6.9	Mild	No	No	11	No	18.4	Yes	15.6	No
7		Yes		8.2	Severe	Yes	No	13.1	No	17.1	Yes	7.6	No

Maximum vessel diameter is measured based on contrast-enhanced computed tomography. SMV: Superior mesenteric vein; SpV: Splenic vein.

various innovative surgical approaches are now available.

Hibi *et al*[10] performed LT in 174 cases of PVT, among which 83 (47.7%) and 91 (52.3%) presented with complete and partial PVT, respectively. In terms of portal vein reconstruction, 149 cases underwent physiological reconstruction [thrombolectomy (n = 123), interposition vein grafts (n = 16), and mesoportal jump grafts (n = 10)]. There were 25 cases of non-physiological reconstruction [cavoportal hemitranspositions (n = 18), renoportal anastomoses (n = 6), and arterialization (n = 1)]. The study found that the non-physiological group suffered a significantly increased incidence of rethrombosis of the portomesenteric veins and gastrointestinal bleeding, with a dismal 10-year overall survival rate of 42% (*vs* no PVT, 61%; P = 0.002 and *vs* PVT: Physiological group, 55%; P = 0.043). Rodríguez-Castro *et al*[12] reported that of 25753 liver transplants, 2004 were performed in patients with PVT (7.78%), and complete thrombosis was observed in nearly 50%. TAA was performed in 75% of patients; other techniques included venous graft interposition and portocaval hemitransposition. It was found that PVT significantly increased post-LT mortality at 30 d (10.5%) and 1 year (18.8%) when compared to patients without PVT (7.7% and 15.4%, respectively). Moreover, rethrombosis occurred in up to 13% of patients with complete PVT, whereby no preventive strategies were used, leading to increased morbidity and mortality. In the present study, there was no recurrence of PVT, but one patient had portal venous insufficiency after LT. Accordingly, the optimal approach for portal vein reconstruction is the restoration of the physiological anatomy of the portal vein system while ensuring adequate portal venous flow[10,18].

Table 3 Laboratory examination indicators on postoperative day 7

	ALB (g/L)	TB (μmol/L)	DB (μmol/L)	ALT (U/L)	AST (U/L)	GGT (U/L)	PT (s)	INR
Case 1	32	98	52	111	43	78	20.4	1.72
Case 2	31.4	11.2	4.9	49	24	85	16.6	1.36
Case 3	38.1	27.8	18.3	204	63	236	18.9	1.61
Case 4	35.1	35.1	22.8	224	175	741	16.4	1.30
Case 5	35.3	39.5	23.1	169	41	89	15.9	1.25
Case 6	50	26.8	14.7	329	62	355	14.8	1.19
Case 7	35	20.1	13.5	48	20	328	15.4	1.21

ALB: Albumin; TB: Total bilirubin; DB: Direct bilirubin; ALT: Alanine aminotransferase; AST: Aspartate aminotransferase; GGT: Gamma-glutamyl transferase; PT: Prothrombin time; INR: International normalized ratio.

Table 4 Laboratory examination indicators on postoperative day 14

	ALB (g/L)	TB (μmol/L)	DB (μmol/L)	ALT (U/L)	AST (U/L)	GGT (U/L)	PT (s)	INR
Case 1	33	66	37	58	21	128	17.6	1.42
Case 2	38.3	12.1	5.2	35	15	75	14	1.09
Case 3	42.1	567	226	246	115	232	52.2	6.0
Case 4	34.3	80	54	135	87	677	15.1	1.18
Case 5	39.1	24.2	13.2	27	21	39	14	1.20
Case 6	39.8	13.8	11.2	57	53	140	13.6	1.12
Case 7	34.5	13.8	8.6	37	15	238	14.7	1.14

ALB: Albumin; TB: Total bilirubin; DB: Direct bilirubin; ALT: Alanine aminotransferase; AST: Aspartate aminotransferase; GGT: Gamma-glutamyl transferase; PT: Prothrombin time; INR: International normalized ratio.

At present, no consensus has been reached on the optimal reconstruction approach for different types of PVT during LT. Some scholars have formulated surgical methods according to Yerdel classification criteria[19-21]. However, in some cases, this classification criteria cannot be used to guide clinical practice since the Yerdel standard is based on the extent that the thrombus occupies the portal vein lumen and does not take into account adhesion to the blood vessel wall.

Application and precautions of RPVPPT

The RPVPPT technique adopted by our team was mainly applied in patients with PVT contraindicated for routine thrombolectomy during the LT surgery. This approach restores the physiological anatomy of the portal vein system while ensuring adequate portal vein blood flow, which is hypothetically ideal for PVT patients. At 12-17 mo follow-up, six of the seven patients survived, preliminarily validating the feasibility and safety of RPVPPT.

However, severe portal hypertension in this patient population accounts for an increase in varicose vessels around the portal vein, or even cavernous transformation of the portal vein, leading to an increased risk of bleeding during the procedure[22,23]. In addition, the RPVPPT technique requires the establishment of a retropancreatic tunnel behind the pancreas in these patients, increasing surgical risks. Accordingly, this surgical approach requires highly skilled surgeons and a transplant team. During the operation, it is recommended to dissect the hepatic hilum along the portal vein to the upper margin of the pancreas and then successively ligate each branch of the portal vein at the lower margin of the pancreas. When separating the lower edge of the pancreas, the SMV and SpV branches should be dissected first, and vascular slings should be placed to lift them for prompt hemostasis during the establishment of the retropancreatic tunnel or the separation of the surrounding tissues of the portal vein. After a successful retropancreatic tunnel is established, lifting the pancreas with a vascular sling or urinary tube is recommended to facilitate portal vein reconstruction (Figure 1).

Intraoperative traction of the pancreas should be as gentle as possible to avoid pancreatic damage and pancreatitis. Based on our experience, we recommend successfully ligating the branches of the blood vessels that merge into the portal vein behind the pancreas. Given that the blood vessels in this

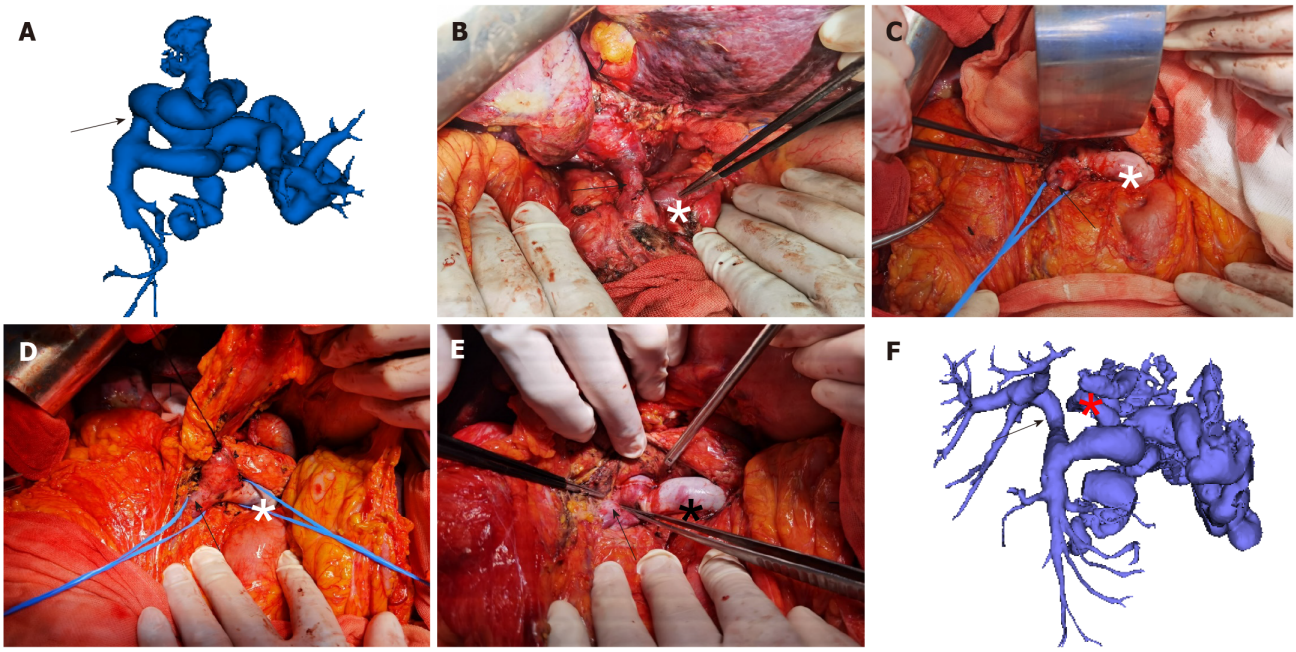

DOI: 10.4240/wjgs.v14.i10.1131

Figure 1 Main steps of reconstructing the portal vein through the posterior pancreatic tunnel technique during portal vein reconstruction in liver transplantation recipients with complex portal vein thrombosis. A: Three-dimensional (3D) visualization model of the portal vein system constructed before surgery showed that the main portal vein was occluded, and the left gastric veins (coronary veins) were visible (arrow); B: After the varicose vessels were severed, the main portal vein (arrow) was exposed, the portal vein was dissected from the cephalic side to the upper edge of the pancreas, and the coronary varicose was ligated (*); C: Dissection started from the lower edge of the pancreas. The superior mesenteric vein (SMV) (arrow) and splenic vein (SpV) (*) were dissected successively, and the rear of the pancreas was separated towards the cephalic side along the main portal vein to establish a retropancreatic tunnel; D: The main portal vein was pulled out from the retropancreatic tunnel, and the main portal vein, SMV (arrow), and SpV (*) presented a triangular structure; E: Blood flow in the SMV and SpV was blocked. After the portal vein containing the thrombus was resected, the portal vein of the donor was pulled to the lower edge of the pancreas through the retropancreatic tunnel, and portal vein reconstruction was completed at the confluence of the SMV (arrow) and SpV (*); F: 3D visualization model of the portal vein system after surgery showed that the main portal vein was unobstructed (arrow), and the original coronary vein was severed (*).

region are very thin, hemostasis can be challenging once bleeding occurs. In this regard, given the narrow surgical view, it can be challenging to perform suture hemostasis, and the effect of electrocoagulation is often not satisfactory. In such circumstances, we can only resort to compression hemostasis. In addition, due to the brittleness of pancreatic tissue in patients with portal hypertension and the increase of surface varicose vessels, the risk of hemorrhagic shock is relatively high. Therefore, it is advisable to dissect the lower edge of the pancreas during surgery to prevent postoperative abdominal bleeding. In our study, one patient developed intra-abdominal hemorrhage on postoperative day 7. Exploratory laparotomy revealed that the source of the hemorrhage was at the lower edge of the pancreas, with multiple hemorrhagic foci observed. This finding could be attributed to postoperative pancreatitis since the amylase level in drain fluid from the lower edge of the pancreas was 700 U/L. It is highly likely that the extravasation of pancreatic fluid corroded the blood vessel, thus leading to rupture and bleeding. The patient died of liver failure due to hemorrhagic shock resulting in liver ischemia and hypoxia. Based on our experience, we recommend that the drainage tube should be indwelled at the lower margin of the pancreas and properly fixed. Importantly, the drain fluid amylase level should be assessed regularly after surgery.

During the establishment of the retropancreatic tunnel, the varicose vessels around the portal vein were ligated to create the posterior pancreatic tunnel and reduce the blood shunt of the portal vein system to avoid insufficient portal venous flow to the graft after surgery. However, it is often difficult to ligate splenorenal shunt vascular branches intraoperatively due to their deep location. In some cases, postoperative intervention may be required to manage shunt vessels. In this study, one patient developed insufficient portal venous flow to the graft after surgery, mainly due to significant splenic-renal shunting. DSA showed that most splenic venous flow drained into the inferior vena cava through the shunt rather than the portal vein. After shunt embolization, an immediate improvement in portal vein blood supply was observed.

CONCLUSION

With the increased number of LT cases, PVT has become a major conundrum that may be solved by

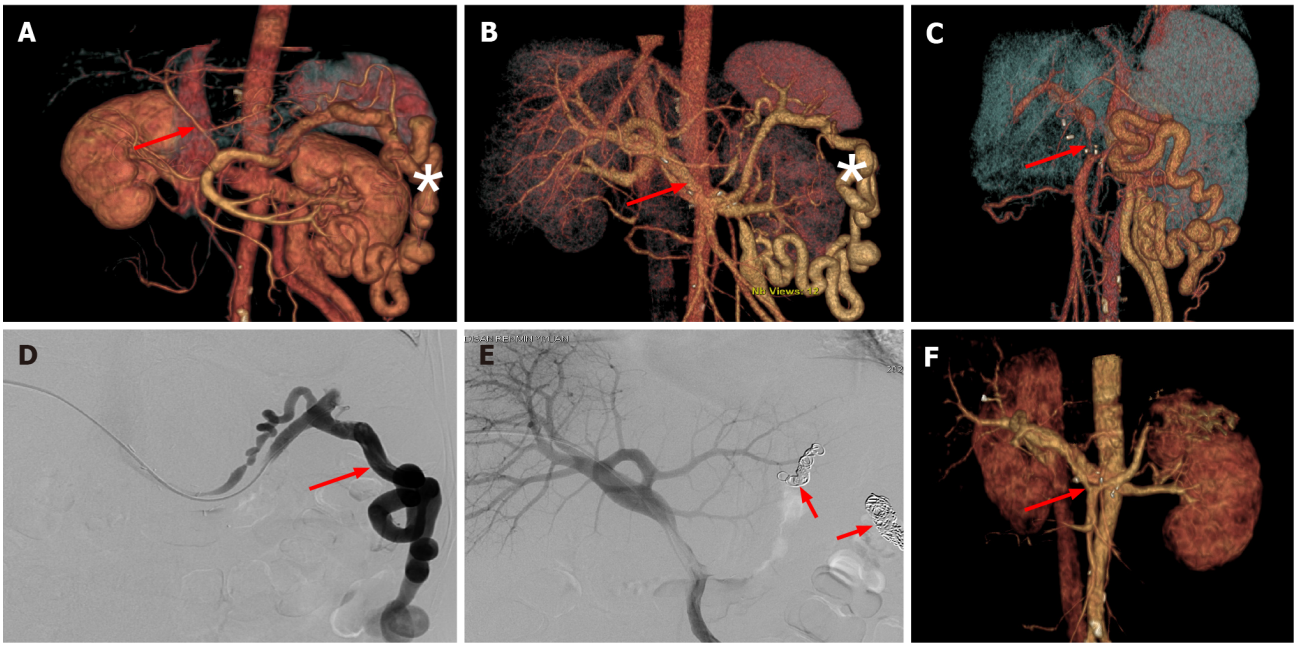

DOI: 10.4240/wjgs.v14.i10.1131 **Copyright** ©The Author(s) 2022.

Figure 2 Embolization of large splenorenal shunt under digital subtraction angiography alleviates portal vein insufficiency after liver transplantation. A: Preoperative three-dimensional (3D) visualization model showed a slender portal vein (arrow) and obvious splenorenal shunt varices (*); B: Postoperative 3D visualization model on day 3 showed a normal portal vein shape and unobstructed blood flow (arrow), and splenorenal shunt varicosity was reduced (*); C: Postoperative 3D visualization model (at 3 wk) showed portal vein stenosis in the initial segment (arrow), and color Doppler ultrasound examination indicated insufficient portal venous blood supply; D: Percutaneous and transhepatic splenic venography showed that most splenic venous flow drained into the inferior vena cava through the splenorenal shunt, but did not drain into the portal vein (arrow); E: After embolization of the splenorenal shunt (arrow), angiography showed that blood flow was mainly present into the portal vein; F: 3D visualization model 1 wk after the vascular intervention showed unobstructed portal vein flow (arrow), and the splenorenal shunt was no longer visible.

portal vein reconstruction. The key point of this technique is to ensure sufficient portal venous blood flow and restore the physiological anatomy of the portal vein system as much as possible. The RPVPPT approach adopted in this study meets the above requirements, and our preliminary assessment yielded good results. We substantiated that the RPVPPT technique is a safe and effective surgical procedure in LT for complex PVT. However, follow-up studies with large samples are warranted due to the relatively small number of cases.

ARTICLE HIGHLIGHTS

Research background

Portal vein thrombosis (PVT) poses a great challenge in liver transplantation (LT). It has been established that thrombectomy and anatomical anastomosis (TAA) can restore the physiological anatomy of the portal vein by complete thrombus excision and has been considered the optimal solution to this problem; however, in some cases, PVT cannot be treated by TAA.

Research motivation

We describe our experience of reconstructing the portal vein through a posterior pancreatic tunnel (RPVPPT) to address the issue of unresectable PVT, which may achieve a similar effect to TAA and provide a new approach to solve this intricate clinical problem.

Research objectives

We sought to describe a new strategy of RPVPPT to address cases of unresectable PVT.

Research methods

A retrospective analysis was performed on 245 adult patients that underwent LT from August 2019 to August 2021. Forty-five (18.4%) patients presented with PVT before surgery, among which seven underwent portal vein reconstruction using RPVPPT. Preoperative clinical data, operation-related indicators, and postoperative complications were statistically analyzed.

Research results

During the operation, PVT was found in all seven cases with significant adhesion to the vascular wall and could not be dissected. LT was successfully performed in all patients without serious postoperative complications. At 12-17 mo follow-up, there were six patients who survived.

Research conclusions

The RPVPPT technique can restore the physiological anatomy of the portal vein system through a retropancreatic tunnel, which might be a safe and effective surgical procedure in LT for complex PVT.

Research perspectives

Due to the relatively small number of cases in the study, follow-up studies with large samples are still required.

ACKNOWLEDGEMENTS

We thank the professor Nan Jiang and the patients for cooperating with our investigation.

FOOTNOTES

Author contributions: Zhao D and Huang YM were involved in the conception and design of this study; Zhao D provided administrative support in this study; Tang JX, Zhang KJ, Fang TS, and Zeng XC contributed to the provision of study materials or patients; Liang ZM, Yan X, Jin X, and Xie LJ were involved in the collection and assembly of data; Zhang Y and Huang YM analysed and interpreted the data; and all authors approved this manuscript to publish.

Supported by the Third People's Hospital of Shenzhen Scientific Research Project, No. G2021008 and No. G2022008; Shenzhen Key Medical Discipline Construction Fund, No. SZXK079; Shenzhen Science and Technology Research and Development Fund, No. JCYJ20190809165813331 and No. JCYJ20210324131809027.

Institutional review board statement: The study was reviewed and approved by the Third People's Hospital of Shenzhen Institutional Review Board (Approval No. 2022-037-02).

Informed consent statement: All cases involved in this study proved written informed consent.

Conflict-of-interest statement: All the authors report no relevant conflicts of interest for this article.

Data sharing statement: No additional data are available.

Country/Territory of origin: China

ORCID number: Dong Zhao 0000-0003-3773-721X; Jian-Xin Tang 0000-0003-4416-5336.

S-Editor: Wang JJ
L-Editor: Wang TQ
P-Editor: Wang JJ

REFERENCES

1 **Chen H**, Turon F, Hernández-Gea V, Fuster J, Garcia-Criado A, Barrufet M, Darnell A, Fondevila C, Garcia-Valdecasas JC, Garcia-Pagán JC. Nontumoral portal vein thrombosis in patients awaiting liver transplantation. *Liver Transpl* 2016; **22**: 352-365 [PMID: 26684272 DOI: 10.1002/lt.24387]

2 **Ponziani FR**, Zocco MA, Senzolo M, Pompili M, Gasbarrini A, Avolio AW. Portal vein thrombosis and liver transplantation: implications for waiting list period, surgical approach, early and late follow-up. *Transplant Rev (Orlando)* 2014; **28**: 92-101 [PMID: 24582320 DOI: 10.1016/j.trre.2014.01.003]

3 **Werner KT**, Sando S, Carey EJ, Vargas HE, Byrne TJ, Douglas DD, Harrison ME, Rakela J, Aqel BA. Portal vein thrombosis in patients with end stage liver disease awaiting liver transplantation: outcome of anticoagulation. *Dig Dis Sci*

2013; **58**: 1776-1780 [PMID: 23314858 DOI: 10.1007/s10620-012-2548-y]
4 **Teng F**, Sun KY, Fu ZR. Tailored classification of portal vein thrombosis for liver transplantation: Focus on strategies for portal vein inflow reconstruction. *World J Gastroenterol* 2020; **26**: 2691-2701 [PMID: 32550747 DOI: 10.3748/wjg.v26.i21.2691]
5 **Turon F**, Hernández-Gea V, García-Pagán JC. Portal vein thrombosis: yes or no on anticoagulation therapy. *Curr Opin Organ Transplant* 2018; **23**: 250-256 [PMID: 29432256 DOI: 10.1097/MOT.0000000000000506]
6 **Lai Q**, Spoletini G, Pinheiro RS, Melandro F, Guglielmo N, Lerut J. From portal to splanchnic venous thrombosis: What surgeons should bear in mind. *World J Hepatol* 2014; **6**: 549-558 [PMID: 25232448 DOI: 10.4254/wjh.v6.i8.549]
7 **Quintini C**, Spaggiari M, Hashimoto K, Aucejo F, Diago T, Fujiki M, Winans C, D'Amico G, Trenti L, Kelly D, Eghtesad B, Miller C. Safety and effectiveness of renoportal bypass in patients with complete portal vein thrombosis: an analysis of 10 patients. *Liver Transpl* 2015; **21**: 344-352 [PMID: 25420619 DOI: 10.1002/lt.24053]
8 **Bhangui P**, Lim C, Salloum C, Andreani P, Sebbagh M, Hoti E, Ichai P, Saliba F, Adam R, Castaing D, Azoulay D. Caval inflow to the graft for liver transplantation in patients with diffuse portal vein thrombosis: a 12-year experience. *Ann Surg* 2011; **254**: 1008-1016 [PMID: 21869678 DOI: 10.1097/SLA.0b013e31822d7894]
9 **Borchert DH**. Cavoportal hemitransposition for the simultaneous thrombosis of the caval and portal systems - a review of the literature. *Ann Hepatol* 2008; **7**: 200-211 [PMID: 18753986]
10 **Hibi T**, Nishida S, Levi DM, Selvaggi G, Tekin A, Fan J, Ruiz P, Tzakis AG. When and why portal vein thrombosis matters in liver transplantation: a critical audit of 174 cases. *Ann Surg* 2014; **259**: 760-766 [PMID: 24299686 DOI: 10.1097/SLA.0000000000000252]
11 **Ghabril M**, Agarwal S, Lacerda M, Chalasani N, Kwo P, Tector AJ. Portal Vein Thrombosis Is a Risk Factor for Poor Early Outcomes After Liver Transplantation: Analysis of Risk Factors and Outcomes for Portal Vein Thrombosis in Waitlisted Patients. *Transplantation* 2016; **100**: 126-133 [PMID: 26050013 DOI: 10.1097/TP.0000000000000785]
12 **Rodríguez-Castro KI**, Porte RJ, Nadal E, Germani G, Burra P, Senzolo M. Management of nonneoplastic portal vein thrombosis in the setting of liver transplantation: a systematic review. *Transplantation* 2012; **94**: 1145-1153 [PMID: 23128996 DOI: 10.1097/TP.0b013e31826e8e53]
13 **Kasahara M**, Sasaki K, Uchida H, Hirata Y, Takeda M, Fukuda A, Sakamoto S. Novel technique for pediatric living donor liver transplantation in patients with portal vein obstruction: The "pullout technique". *Pediatr Transplant* 2018; **22**: e13297 [PMID: 30280455 DOI: 10.1111/petr.13297]
14 **Zhao D**, Lau WY, Zhou W, Yang J, Xiang N, Zeng N, Liu J, Zhu W, Fang C. Impact of three-dimensional visualization technology on surgical strategies in complex hepatic cancer. *Biosci Trends* 2018; **12**: 476-483 [PMID: 30473555 DOI: 10.5582/bst.2018.01194]
15 **Ponziani FR**, Zocco MA, Garcovich M, D'Aversa F, Roccarina D, Gasbarrini A. What we should know about portal vein thrombosis in cirrhotic patients: a changing perspective. *World J Gastroenterol* 2012; **18**: 5014-5020 [PMID: 23049208 DOI: 10.3748/wjg.v18.i36.5014]
16 **Violi F**, Corazza GR, Caldwell SH, Perticone F, Gatta A, Angelico M, Farcomeni A, Masotti M, Napoleone L, Vestri A, Raparelli V, Basili S; PRO-LIVER Collaborators. Portal vein thrombosis relevance on liver cirrhosis: Italian Venous Thrombotic Events Registry. *Intern Emerg Med* 2016; **11**: 1059-1066 [PMID: 27026379 DOI: 10.1007/s11739-016-1416-8]
17 **Shaw BW Jr**, Iwatsuki S, Bron K, Starzl TE. Portal vein grafts in hepatic transplantation. *Surg Gynecol Obstet* 1985; **161**: 66-68 [PMID: 3892734]
18 **D'Amico G**, Tarantino G, Spaggiari M, Ballarin R, Serra V, Rumpianesi G, Montalti R, De Ruvo N, Cautero N, Begliomini B, Gerunda GE, Di Benedetto F. Multiple ways to manage portal thrombosis during liver transplantation: surgical techniques and outcomes. *Transplant Proc* 2013; **45**: 2692-2699 [PMID: 24034026 DOI: 10.1016/j.transproceed.2013.07.046]
19 **Yerdel MA**, Gunson B, Mirza D, Karayalçin K, Olliff S, Buckels J, Mayer D, McMaster P, Pirenne J. Portal vein thrombosis in adults undergoing liver transplantation: risk factors, screening, management, and outcome. *Transplantation* 2000; **69**: 1873-1881 [PMID: 10830225 DOI: 10.1097/00007890-200005150-00023]
20 **Nacif LS**, Zanini LY, Pinheiro RS, Waisberg DR, Rocha-Santos V, Andraus W, Carrilho FJ, Carneiro-D'Albuquerque L. Portal vein surgical treatment on non-tumoral portal vein thrombosis in liver transplantation: Systematic Review and Meta-Analysis. *Clinics (Sao Paulo)* 2021; **76**: e2184 [PMID: 33503185 DOI: 10.6061/clinics/2021/e2184]
21 **Rhu J**, Choi GS, Kwon CHD, Kim JM, Joh JW. Portal vein thrombosis during liver transplantation: The risk of extra-anatomical portal vein reconstruction. *J Hepatobiliary Pancreat Sci* 2020; **27**: 242-253 [PMID: 31945273 DOI: 10.1002/jhbp.711]
22 **Kiyosue H**, Ibukuro K, Maruno M, Tanoue S, Hongo N, Mori H. Multidetector CT anatomy of drainage routes of gastric varices: a pictorial review. *Radiographics* 2013; **33**: 87-100 [PMID: 23322829 DOI: 10.1148/rg.331125037]
23 **Bosch J**, Iwakiri Y. The portal hypertension syndrome: etiology, classification, relevance, and animal models. *Hepatol Int* 2018; **12**: 1-10 [PMID: 29064029 DOI: 10.1007/s12072-017-9827-9]

World Journal of Gastrointestinal Surgery

Submit a Manuscript: https://www.f6publishing.com

World J Gastrointest Surg 2022 October 27; 14(10): 1141-1149

DOI: 10.4240/wjgs.v14.i10.1141

ISSN 1948-9366 (online)

ORIGINAL ARTICLE

Retrospective Study

Topological approach of liver segmentation based on 3D visualization technology in surgical planning for split liver transplantation

Dong Zhao, Kang-Jun Zhang, Tai-Shi Fang, Xu Yan, Xin Jin, Zi-Ming Liang, Jian-Xin Tang, Lin-Jie Xie

Specialty type: Gastroenterology and hepatology

Provenance and peer review: Unsolicited article; Externally peer reviewed.

Peer-review model: Single blind

Peer-review report's scientific quality classification

Grade A (Excellent): 0
Grade B (Very good): 0
Grade C (Good): C
Grade D (Fair): D
Grade E (Poor): 0

P-Reviewer: Aseni P, Italy; Han B, China

Received: August 23, 2022
Peer-review started: August 23, 2022
First decision: September 26, 2022
Revised: September 28, 2022
Accepted: October 17, 2022
Article in press: October 17, 2022
Published online: October 27, 2022

Dong Zhao, Kang-Jun Zhang, Tai-Shi Fang, Xu Yan, Xin Jin, Zi-Ming Liang, Jian-Xin Tang, Lin-Jie Xie, Department of Liver Surgery and Organ Transplantation Center, The Third People's Hospital of Shenzhen, The Second Affiliated Hospital of Southern University of Science and Technology, National Clinical Research Center for Infectious Disease, Shenzhen 518000, Guangdong Province, China

Corresponding author: Dong Zhao, MD, Professor, Department of Liver Surgery and Organ Transplantation Center, The Third People's Hospital of Shenzhen, The Second Affiliated Hospital of Southern University of Science and Technology, National Clinical Research Center for Infectious Disease, No. 29 Bulan Road, Longgang District, Shenzhen 518000, Guangdong Province, China. zdong1233@126.com

Abstract

BACKGROUND

Split liver transplantation (SLT) is a complex procedure. The left-lateral and right tri-segment splits are the most common surgical approaches and are based on the Couinaud liver segmentation theory. Notably, the liver surface following right tri-segment splits may exhibit different degrees of ischemic changes related to the destruction of the local portal vein blood flow topology. There is currently no consensus on preoperative evaluation and predictive strategy for hepatic segmental necrosis after SLT.

AIM

To investigate the application of the topological approach in liver segmentation based on 3D visualization technology in the surgical planning of SLT.

METHODS

Clinical data of 10 recipients and 5 donors who underwent SLT at Shenzhen Third People's Hospital from January 2020 to January 2021 were retrospectively analyzed. Before surgery, all the donors were subjected to 3D modeling and evaluation. Based on the 3D-reconstructed models, the liver splitting procedure was simulated using the liver segmentation system described by Couinaud and a blood flow topology liver segmentation (BFTLS) method. In addition, the volume of the liver was also quantified. Statistical indexes mainly included the hepatic vasculature and expected volume of split grafts evaluated by 3D models, the

actual liver volume, and the ischemia state of the hepatic segments during the actual surgery.

RESULTS

Among the 5 cases of split liver surgery, the liver was split into a left-lateral segment and right tri-segment in 4 cases, while 1 case was split using the left and right half liver splitting. All operations were successfully implemented according to the preoperative plan. According to Couinaud liver segmentation system and BFTLS methods, the volume of the left lateral segment was 359.00 ± 101.57 mL and 367.75 ± 99.73 mL, respectively, while that measured during the actual surgery was 397.50 ± 37.97 mL. The volume of segment IV (the portion of ischemic liver lobes) allocated to the right tri-segment was 136.31 ± 86.10 mL, as determined using the topological approach to liver segmentation. However, during the actual surgical intervention, ischemia of the right tri-segment section was observed in 4 cases, including 1 case of necrosis and bile leakage, with an ischemic liver volume of 238.7 mL.

CONCLUSION

3D visualization technology can guide the preoperative planning of SLT and improve accuracy during the intervention. The simulated operation based on 3D visualization of blood flow topology may be useful to predict the degree of ischemia in the liver segment and provide a reference for determining whether the ischemic liver tissue should be removed during the surgery.

Key Words: Three-dimensional visualization; Couinaud liver segmentation; Blood flow topology liver segmentation; Split liver transplantation; Surgical planning

Core Tip: This is the first study to explore the application of the topological approach of liver segmentation based on 3D visualization technology in surgical planning of split liver transplantation. Clinical data of 10 recipients and 5 donors were analyzed. Couinaud liver segmentation and blood flow topology liver segmentation (BFTLS) methods were used to simulate operation, respectively. The volume of segment IV (the portion of ischemic liver lobes) allocated to the right tri-segment was 136.31 ± 86.10 mL as determined using BFTLS. Results showed that the approach of BFTLS may be useful to predict the range of ischemia in the liver section.

Citation: Zhao D, Zhang KJ, Fang TS, Yan X, Jin X, Liang ZM, Tang JX, Xie LJ. Topological approach of liver segmentation based on 3D visualization technology in surgical planning for split liver transplantation. *World J Gastrointest Surg* 2022; 14(10): 1141-1149

URL: https://www.wjgnet.com/1948-9366/full/v14/i10/1141.htm

DOI: https://dx.doi.org/10.4240/wjgs.v14.i10.1141

INTRODUCTION

The Couinaud liver segmentation is based on the distribution of the Glisson system in the liver and the division of the hepatic vein system. Three hepatic veins are used as vertical planes to form the main longitudinal fissure, and the liver is divided into different liver segments by the left and right branches of the portal vein. This segmentation method provides an anatomical basis for the clinical imaging diagnosis of liver diseases and has been widely used in clinical practice[1-3]. However, only 30%-50% of the segmented results are consistent with the actual anatomy of the liver as the segmented results are derived from the cast liver specimen *ex vivo*, and the variation in hepatic blood vessels is not taken into account[4,5]. The blood flow topology segmentation method is based on the blood flow topology of the hepatic portal vein[6,7]. Therefore, this method can truly reflect the anatomical structure of the liver and is the theoretical basis of anatomical hepatectomy *via* indocyanine green fluorescence imaging[8-10].

Split liver transplantation (SLT) is complex, and the commonly used surgical technique is the left-lateral segment and right tri-segment splits, which are implemented based on the theory of Couinaud liver segmentation. Previous studies uncovered that the right tri-segment liver surface might show different degrees of ischemic changes related to the destruction of the local portal vein blood flow topology following the intervention[11-13].

However, opinions diverge on the management of ischemia found on the surface tissues of the liver segment following SLT, as well as liver tissue necrosis, infection, and bile leakage[11,14]. Some experts postulate that the direct resection of segment IV of the ischemic liver tissue is necessary, while others

believe no treatment is needed. This difference in opinion is due to a lack of preoperative evaluation and predictive strategy for hepatic segmental necrosis after SLT and a dearth of relevant publications worldwide. Therefore, this study aimed to investigate the application value of 3D visualization technology in the surgical planning of SLTs.

MATERIALS AND METHODS

General clinical data

A retrospective analysis was performed on 10 patients who underwent SLT in the Third People's Hospital of Shenzhen from January 2020 to January 2021 and the corresponding data of 5 donors. All cases in this study were performed after the approval of the Hospital Ethics Committee. The livers were donated after the death of the donors.

Pre-operation evaluation

For each organ donor, preoperative blood routine, liver function, kidney function, coagulation function, tumor markers, and infection-related tests, as well as abdominal Doppler ultrasound and liver computed tomography (CT) angiography examination, were performed. A preoperative 3D visualization model of the liver was constructed for each case. The model was acquired by importing high-quality THIN-layer enhanced CT DICOM data into the medical 3D reconstruction software: (1) For organ reconstruction: The region-growing method was used to perform a 3D reconstruction of the liver, tumor, pancreas and spleen; and (2) For vascular reconstruction: The segmentation based on threshold method was used to perform a 3D reconstruction of the portal vein, hepatic artery and hepatic vein[15]. The model was utilized to evaluate the vascular pattern and hepatectomy simulation.

Simulated surgery

(1) The SLT procedure was simulated on a 3D visualization model and included a segment of the hepatic artery, portal vein, and hepatic vein and the disconnection of the liver parenchyma; and (2) The SLT procedure was simulated according to the Couinaud liver segmentation and blood flow topology liver segmentation (BFTLS) methods. The volume of the two liver segments and the ischemic volume were also quantified (Figure 1).

Actual operation

The combination of *in-situ* and *ex vivo* splitting was used for liver splitting. The surgical methods included left-lateral and right tri-segment splits, and left and right hepatic splits. During the operation, Doppler ultrasound was employed to identify and mark the shape of the middle hepatic vein, and a cavitron ultrasonic surgical aspirator and an ultrasonic knife were used to separate the liver parenchyma.

Main statistical indicators

The classification of hepatic vasculatures was based on 3D visualization technology, the hepatic and ischemic volume was estimated using simulated surgery, and hepatic ischemia was measured during the actual surgery.

RESULTS

Preoperative hepatic vascular evaluation and simulated surgical results. The preoperative 3D visualization model revealed that all the donor hepatic portal veins were Cheng *et al*'s type I[16], the hepatic arteries were Michels[17] type I, the middle hepatic vein and left hepatic vein shared trunk in 5 cases, and a single hepatic vein of segment IV directly flowed into the inferior vena cava in 1 case. Among the 5 simulated operations, 4 cases were split into left-lateral segment and right tri-segment; 1 case was split into left and right half liver, and the middle hepatic vein was split by median segmentation.

The results revealed that the resection plane simulated by the Couinaud liver segmentation method or BFTLS method was inconsistent, the former was flat, while the latter was irregularly shaped. 4 cases were simulated using left-lateral and right tri-segment splits. As measured by the above two liver segmentation methods, the volumes of the left-lateral segments were 359.00 ± 101.57 mL and 367.75 ± 99.73 mL, respectively. According to the BFTLS method, the volume of segment IV (*i.e.*, the ischemic part of the liver) cleaving to the right tri-segment was 136.31 ± 86.10 mL. 1 case of left and right liver splitting was simulated, and median segmentation of the middle hepatic vein was performed after strictly evaluating two adult recipients with low body weight. The operation was simulated according to the above two segmentation methods. 99.95 mL of tissues in segment IV was assigned to the left half of the liver according to Couinaud classification; if splitting was carried out according to this method, 99.95 mL of liver tissues might experience postoperative ischemia or even necrosis.

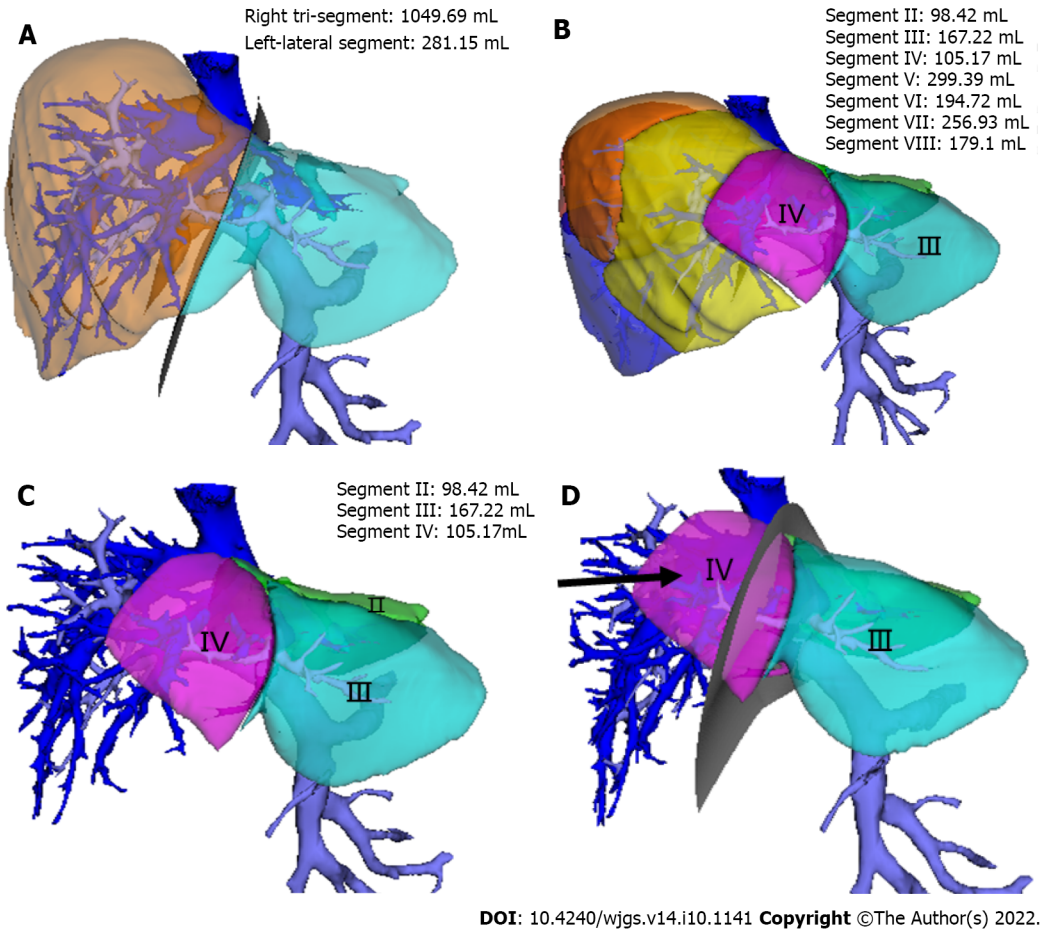

DOI: 10.4240/wjgs.v14.i10.1141

Figure 1 The range of hepatic ischemia was calculated by simulating the left-lateral segment and right tri-segment splitting. A: The simulated operation based on Couinaud liver segmentation; B: The liver segments constructed *via* the topological structural relationship of portal vein blood flow; C: The calculated liver volume of the II/III/IV segments based on the blood flow topology liver segmentation method; D: The volume of ischemic range in the hepatic segment of the right tri-segment after split liver transplantation (black arrow).

Actual surgical results

In practice, *in-situ* and *ex vivo* splits were performed successfully according to the preoperative plan. According to the Couinaud liver segmentation method, left-lateral and right tri-segment splitting was performed in 4 cases. The left branch of the portal vein, the main trunk of the left hepatic artery, and the left branch of the hepatic vein were distributed to the left-lateral segment. The hepatic artery and portal vein branches entering segment IV of the liver were severed. The actual volume of the left-lateral segment was 397.50 ± 37.97 mL. The liver sections of the 4 cases exhibited ischemic changes after the operation (Figure 2). 1 case experienced necrosis of the liver section and bile leakage and underwent reoperation to remove the necrotic tissues. The volume of the ischemic liver calculated before the operation was 238.7 mL.

In the other case, the operation was performed by left and right half liver splitting based on the portal vein BFTLS method. The middle hepatic vein was segmented in the middle, and the donor's external iliac vein was used to reconstruct the middle hepatic vein of the left and right halves of the liver. No apparent changes in hepatic sectional ischemia were detected post-surgery (Figure 3).

Post-transplant outcomes

The operation was successfully completed in all 10 patients corresponding to the split livers, and postoperative biliary leakage occurred in 1 case without small-for-size syndrome. During the perioperative period, 1 patient who underwent a right tri-segment split suffered from a sudden intracerebral hemorrhage on the 7th postoperative day and died on the 18th postoperative day.

DISCUSSION

Couinaud liver segmentation is an artificial segmentation method based on anatomical markers of the liver. Moreover, its segmentation plane limits the drainage area of the hepatic vein and does not

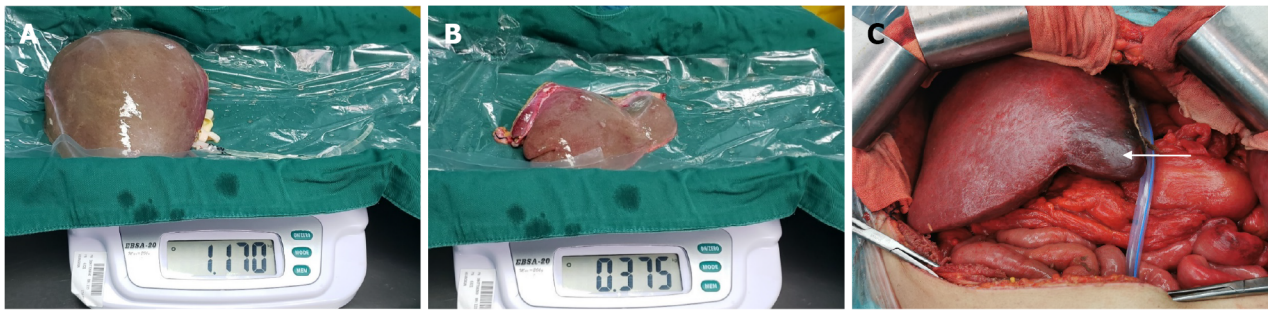

DOI: 10.4240/wjgs.v14.i10.1141 **Copyright** ©The Author(s) 2022.

Figure 2 Based on the Couinaud liver segmentation method, left-lateral segment and right tri-segment splits were performed. During the operation, obvious ischemic changes in the cross-section of the right tri-segment were observed. A: The right tri-segment graft; B: The left-lateral segment graft; C: Cleaved right tri-segment with distinct ischemia in the hepatic segment after hepatic reflow (white arrow).

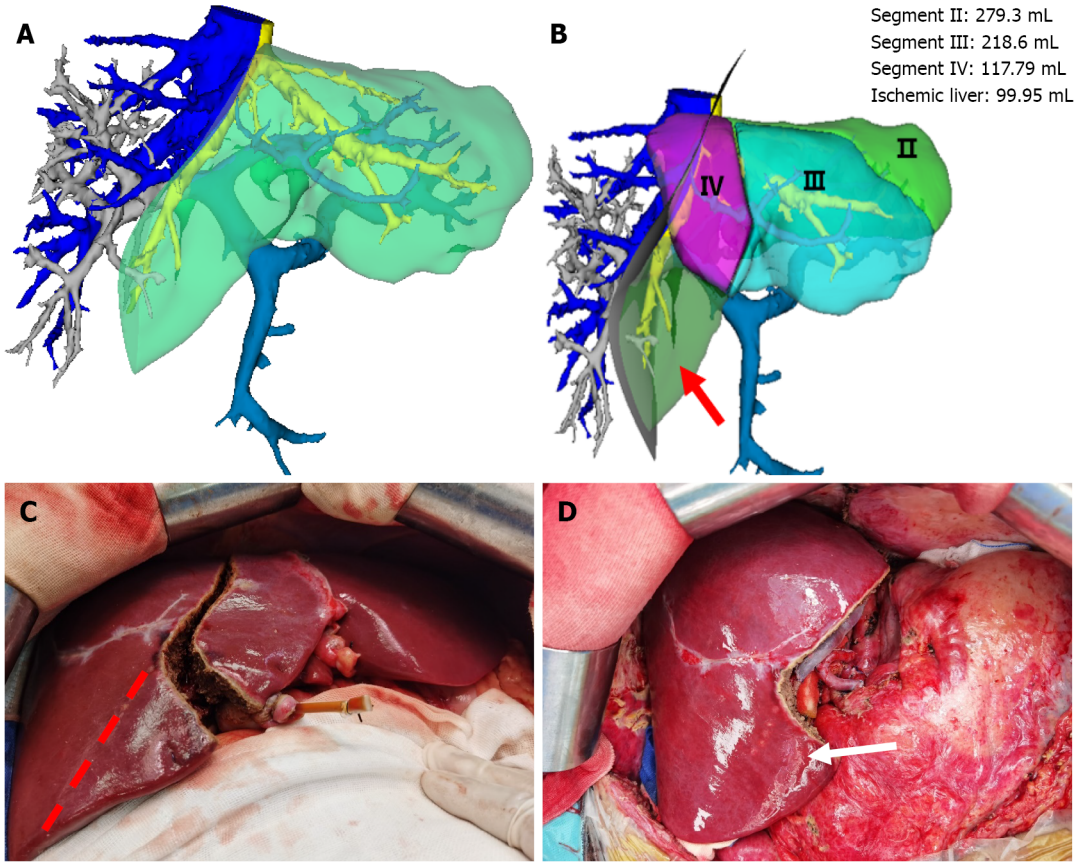

DOI: 10.4240/wjgs.v14.i10.1141 **Copyright** ©The Author(s) 2022.

Figure 3 Left and right half-split liver transplantation was performed according to the portal vein blood flow topology liver segmentation method. There was no ischemic change in the liver segment after reflow. A: Left and right half liver splitting were simulated based on the Couinaud liver segmentation method, while the middle hepatic vein was split in the middle; B: The simulation of left and right half liver splitting based on the portal vein blood flow topology liver segmentation method. It can be seen that a portion of segment V liver tissues (99.95 mL) is partitioned into the left liver (arrow); C: Surgery based on the portal vein blood flow topology liver segmentation method was implemented for left and right half liver splitting instead of the Couinaud liver segmentation method (red dotted line); D: No ischemic changes in the hepatic segment after reflow (white arrow).

consider the topology of portal vein branches in the liver[6,7,18]. For instance, when a vascular variation occurs in the liver, multiple portal or hepatic vein branches may co-exist within the same Couinaud liver segment. However, the BFTLS approach used herein was based on the topological structural relationship of the hepatic portal vein, which can truly display anatomical structural relationships in the liver[6,7]. Indeed, this concept is also widely used in clinical practice[19-21].

The initial aim of SLT is to save two lives with a single liver. However, inappropriate preoperative evaluation of the liver donor or splitting method may bring a well-functional liver into 2 marginal donors, which may delay the recovery of graft function and even lead to graft failure or recipient death

[22,23]. Therefore, compared with other hepatobiliary surgeries, adequate preoperative evaluation of SLT is monumental. At the time of preoperative donor evaluation, enhanced CT of the liver must be performed, with initial vascular and biliary evaluation followed by re-evaluation based on the 3D visual model. If the donor has significant portal vein variation, SLT is not recommended to ensure the safety of both recipients. Herein, only donors with good liver function and no significant anatomical variation were included in the SLT cohort. All the patients undergoing SLT in our center underwent an initial simulation using the 3D visualization model, and the portal vein, hepatic vein, and hepatic artery were segmented accordingly. Furthermore, the liver volume was also calculated so that a detailed preoperative plan could be drawn up.

In this study, all patients underwent simulated surgeries using the Couinaud liver segmentation method and BFTLS method, and the measured volumes of the left-lateral segment were 359.00 ± 101.57 mL and 367.75 ± 99.73 mL, respectively. Moreover, according to the above two methods, the volume of the segment IV (the portion of the ischemic liver lobe) allocated to the right tri-segment was 136.31 ± 86.10 mL, obtained by adding the volume of segments II/III/IV minus the volume of the left-lateral segment. Based on these data, we can obtain a detailed evaluation of the surgery, predict the degree of ischemic tissue changes and necrosis in the liver segments, as well as assess the need to remove ischemic segments during liver transplantation.

Hepatic segmental ischemic necrosis is extremely common following SLT, mainly because the branches of the portal vein[13] and hepatic artery[14,24,25] entering this part of the liver are not connected, and the corresponding hepatic vein[26-28] may also be cut off in some cases. Therefore, this part of the liver may undergo pathological changes such as hepatocyte ischemia, necrosis, fibrosis, and atrophy, and in some cases, tissue necrosis and bile leakage. Indeed, one of the 5 cases in this study suffered from ischemic tissue necrosis and bile leakage on the surface of the right tri-segment. The necrotic tissue was eventually resected by reoperation in that particular case, with a preoperative ischemic liver volume of 238.7 mL. The ischemic areas of the right tri-segment in the other 3 cases, calculated preoperatively, were 76.9 mL, 54.4 mL, and 175.3 mL, respectively. Therefore, we postulate that if the scope of hepatic segmental ischemia can be accurately determined before the operation, hepatic segmental tissue necrosis can be predicted in advance, avoiding reoperation and alleviating the pain and economic burden of patients.

CONCLUSION

In conclusion, in the case of the left-lateral segment and right tri-segment splits, preoperative evaluation based on three-dimensional visualization technology could calculate the ischemic range of the right tri-segment. Judging by the results, the operator could predict the postoperative ischemic range and make clinical judgments accordingly. For instance, when the branches of the hepatic artery and portal vein of segment IV supplying the right tri-segment are disconnected, and the calculated ischemic range is large, the operator can directly remove this section during the operation to avoid further damage to the body due to tissue necrosis, infection or bile leakage. Nevertheless, due to the small number of cases, it was not possible to determine a specific cut-off value to predict the likelihood of postoperative hepatic ischemic necrosis. Therefore, it is imperative to include a large number of cases for future clinical or multi-center research.

ARTICLE HIGHLIGHTS

Research background

Split liver transplantation (SLT) is complex, and the commonly used surgical technique is the left-lateral segment and right tri-segment splits, which is implemented based on Couinaud liver segmentation. The right tri-segment liver surface may have different degrees of ischemic changes after SLT, which was related to the destruction of the local portal vein blood flow topology.

Research motivation

To our best knowledge, opinions diverge on the management of ischemia in surface tissues of the liver segment following SLT and there was no a consensus of pre-operative evaluation and predictive strategy for hepatic segmental necrosis after SLT worldwide.

Research objectives

Herein, we sought to investigate the application of the topological approach of liver segmentation based on 3D visualization technology in the surgical planning of SLT.

Research methods

A retrospective analysis was performed on 10 recipients and 5 donors who underwent SLT from January 2020 to January 2021. All the donor livers were subjected to 3D modeling and evaluation before surgery, based on which the liver splitting procedure was simulated by the Couinaud liver segmentation and blood flow topology liver segmentation (BFTLS) methods respectively, and the volume of the liver was calculated. Clinical data were analyzed, including the hepatic vasculature and expected volume of split grafts evaluated by 3D models, the actual liver volume, and the ischemia state of hepatic section in actual surgery.

Research results

The donor liver was split into a left-lateral segment and right tri-segment in 4 cases, while 1 case was split by left and right half liver splitting. According to Couinaud liver segmentation and BFTLS methods, the volume of the left lateral segment was 359.00 ± 101.57 mL and 367.75 ± 99.73 mL, respectively. The volume of segment IV (the portion of ischemic liver lobes) allocated to the right tri-segment was 136.31 ± 86.10 mL as determined using the topological approach to liver segmentation. Yet, during the actual operations, ischemia of the right tri-segment section was observed in 4 cases, including 1 case of necrosis of the surfaces cut and bile leakage.

Research conclusions

The application of the topological approach of liver segmentation based on 3D visualization technology may be useful to predict the range of ischemia in the liver section and provide a basis for determining whether the ischemic liver tissue should be removed during the surgery.

Research perspectives

However, the follow-up studies with large samples are still warranted due to the relatively small number of cases.

ACKNOWLEDGEMENTS

We thank all the liver donors and patients.

FOOTNOTES

Author contributions: Zhao D conceived and designed, and made contributions to administrative support; Zhang KJ, Fang TS and Tang JX made contributions to providing research materials or patients; Liang ZM, Yan X, Jin X and Xie LJ collected and compiled data; Zhao D, Zhang KJ and Fang TS conducted data analysis and interpretation; All authors wrote the manuscript and contributed to the final approval of manuscript.

Supported by The Third People's Hospital of Shenzhen Scientific Research Project, No. G2021008 and No. G2022008; Shenzhen Key Medical Discipline Construction Fund, No. SZXK079; Shenzhen Science and Technology Research and Development Fund, No. JCYJ20190809165813331 and No. JCYJ20210324131809027.

Institutional review board statement: The study was reviewed and approved by the Third People's Hospital of Shenzhen Institutional Review Board (Approval No. 2022-133).

Informed consent statement: All study participants or their legal guardian provided informed written consent about personal and medical data collection prior to study enrolment.

Conflict-of-interest statement: All the authors report no relevant conflicts of interest for this article.

Data sharing statement: No additional data are available.

Country/Territory of origin: China

ORCID number: Dong Zhao 0000-0003-3773-721X; Jian-Xin Tang 0000-0003-4416-5336.

S-Editor: Fan JR

L-Editor: A
P-Editor: Fan JR

REFERENCES

1 **Couinaud C**. [The anatomy of the liver]. *Ann Ital Chir* 1992; **63**: 693-697 [PMID: 1305370]
2 **Juza RM**, Pauli EM. Clinical and surgical anatomy of the liver: a review for clinicians. *Clin Anat* 2014; **27**: 764-769 [PMID: 24453062 DOI: 10.1002/ca.22350]
3 **Lebre MA**, Vacavant A, Grand-Brochier M, Rositi H, Abergel A, Chabrot P, Magnin B. Automatic segmentation methods for liver and hepatic vessels from CT and MRI volumes, applied to the Couinaud scheme. *Comput Biol Med* 2019; **110**: 42-51 [PMID: 31121506 DOI: 10.1016/j.compbiomed.2019.04.014]
4 **Ortale JR**, Naves De Freitas Azevedo CH, Mello De Castro C. Anatomy of the intrahepatic ramification of the portal vein in the right hemiliver. *Cells Tissues Organs* 2000; **166**: 378-387 [PMID: 10867440 DOI: 10.1159/000016754]
5 **Sakamoto Y**, Kokudo N, Kawaguchi Y, Akita K. Clinical Anatomy of the Liver: Review of the 19th Meeting of the Japanese Research Society of Clinical Anatomy. *Liver Cancer* 2017; **6**: 146-160 [PMID: 28275581 DOI: 10.1159/000449490]
6 **Zahlten C**, Jürgens H, Evertsz CJ, Leppek R, Peitgen HO, Klose KJ. Portal vein reconstruction based on topology. *Eur J Radiol* 1995; **19**: 96-100 [PMID: 7713095 DOI: 10.1016/0720-048x(94)00578-z]
7 **Cho A**, Okazumi S, Miyazawa Y, Makino H, Miura F, Ohira G, Yoshinaga Y, Tohma T, Kudo H, Matsubara K, Ryu M, Ochiai T. Proposal for a reclassification of liver based anatomy on portal ramifications. *Am J Surg* 2005; **189**: 195-199 [PMID: 15720989 DOI: 10.1016/j.amjsurg.2004.04.014]
8 **Wang X**, Teh CSC, Ishizawa T, Aoki T, Cavallucci D, Lee SY, Panganiban KM, Perini MV, Shah SR, Wang H, Xu Y, Suh KS, Kokudo N. Consensus Guidelines for the Use of Fluorescence Imaging in Hepatobiliary Surgery. *Ann Surg* 2021; **274**: 97-106 [PMID: 33351457 DOI: 10.1097/SLA.0000000000004718]
9 **Urade T**, Sawa H, Iwatani Y, Abe T, Fujinaka R, Murata K, Mii Y, Man-I M, Oka S, Kuroda D. Laparoscopic anatomical liver resection using indocyanine green fluorescence imaging. *Asian J Surg* 2020; **43**: 362-368 [PMID: 31043331 DOI: 10.1016/j.asjsur.2019.04.008]
10 **Kim YS**, Choi SH. Pure Laparoscopic Living Donor Right Hepatectomy Using Real-Time Indocyanine Green Fluorescence Imaging. *J Gastrointest Surg* 2019; **23**: 1711-1712 [PMID: 31152351 DOI: 10.1007/s11605-019-04217-w]
11 **Yersiz H**, Renz JF, Farmer DG, Hisatake GM, McDiarmid SV, Busuttil RW. One hundred in situ split-liver transplantations: a single-center experience. *Ann Surg* 2003; **238**: 496-505; discussion 506 [PMID: 14530721 DOI: 10.1097/01.sla.0000089852.29654.72]
12 **Maggi U**, Caccamo L, Reggiani P, Lauro R, Bertoli P, Camagni S, Paterson IM, Rossi G. Hypoperfusion of segment 4 in right in situ split-liver transplantation. *Transplant Proc* 2010; **42**: 1240-1243 [PMID: 20534271 DOI: 10.1016/j.transproceed.2010.03.110]
13 **Maurer R**, Rivoire M, Basso V, Meeus P, Peyrat P, Dupré A. Portal supply of segment IV of the liver based on CT-scan. *Surg Radiol Anat* 2017; **39**: 471-476 [PMID: 27757519 DOI: 10.1007/s00276-016-1761-3]
14 **Alghamdi T**, Viebahn C, Justinger C, Lorf T. Arterial Blood Supply of Liver Segment IV and Its Possible Surgical Consequences. *Am J Transplant* 2017; **17**: 1064-1070 [PMID: 27775870 DOI: 10.1111/ajt.14089]
15 **Zhao D**, Lau WY, Zhou W, Yang J, Xiang N, Zeng N, Liu J, Zhu W, Fang C. Impact of three-dimensional visualization technology on surgical strategies in complex hepatic cancer. *Biosci Trends* 2018; **12**: 476-483 [PMID: 30473555 DOI: 10.5582/bst.2018.01194]
16 **Cheng YF**, Huang TL, Lee TY, Chen TY, Chen CL. Variation of the intrahepatic portal vein; angiographic demonstration and application in living-related hepatic transplantation. *Transplant Proc* 1996; **28**: 1667-1668 [PMID: 8658830]
17 **Michels NA**. Newer anatomy of the liver and its variant blood supply and collateral circulation. *Am J Surg* 1966; **112**: 337-347 [PMID: 5917302 DOI: 10.1016/0002-9610(66)90201-7]
18 **Xiang N**, Fang C, Fan Y, Yang J, Zeng N, Liu J, Zhu W. Application of liver three-dimensional printing in hepatectomy for complex massive hepatocarcinoma with rare variations of portal vein: preliminary experience. *Int J Clin Exp Med* 2015; **8**: 18873-18878 [PMID: 26770510]
19 **Ni ZK**, Lin D, Wang ZQ, Jin HM, Li XW, Li Y, Huang H. Precision Liver Resection: Three-Dimensional Reconstruction Combined with Fluorescence Laparoscopic Imaging. *Surg Innov* 2021; **28**: 71-78 [PMID: 32873180 DOI: 10.1177/1553350620954581]
20 **Nakaseko Y**, Ishizawa T, Saiura A. Fluorescence-guided surgery for liver tumors. *J Surg Oncol* 2018; **118**: 324-331 [PMID: 30098296 DOI: 10.1002/jso.25128]
21 **Terasawa M**, Ishizawa T, Mise Y, Inoue Y, Ito H, Takahashi Y, Saiura A. Applications of fusion-fluorescence imaging using indocyanine green in laparoscopic hepatectomy. *Surg Endosc* 2017; **31**: 5111-5118 [PMID: 28455774 DOI: 10.1007/s00464-017-5576-z]
22 **Reyes J**, Gerber D, Mazariegos GV, Casavilla A, Sindhi R, Bueno J, Madariaga J, Fung JJ. Split-liver transplantation: a comparison of ex vivo and in situ techniques. *J Pediatr Surg* 2000; **35**: 283-9; discussion 289 [PMID: 10693682 DOI: 10.1016/s0022-3468(00)90026-5]
23 **Bowring MG**, Massie AB, Schwarz KB, Cameron AM, King EA, Segev DL, Mogul DB. Survival Benefit of Split-Liver Transplantation for Pediatric and Adult Candidates. *Liver Transpl* 2022; **28**: 969-982 [PMID: 34923725 DOI: 10.1002/lt.26393]
24 **Jin GY**, Yu HC, Lim HS, Moon JI, Lee JH, Chung JW, Cho BH. Anatomical variations of the origin of the segment 4 hepatic artery and their clinical implications. *Liver Transpl* 2008; **14**: 1180-1184 [PMID: 18668651 DOI: 10.1002/lt.21494]
25 **Sommacale D**, Farges O, Ettorre GM, Lebigot P, Sauvanet A, Marty J, Durand F, Belghiti J. In situ split liver

transplantation for two adult recipients. *Transplantation* 2000; **69**: 1005-1007 [PMID: 10755568 DOI: 10.1097/00007890-200003150-00060]

26 **Cheng YF**, Chen CL, Haung TL, Lee TY, Chen TY, Chen YS, Liu PP, Chiang YC, Eng HL, Wang CC, Cheung HK, Jawan B, Goto S. Post-transplant changes of segment 4 after living related liver transplantation. *Clin Transplant* 1998; **12**: 476-481 [PMID: 9787960]

27 **Zhang J**, Guo X, Qiao Q, Zhao J, Wang X. Anatomical Study of the Hepatic Veins in Segment 4 of the Liver Using Three-Dimensional Visualization. *Front Surg* 2021; **8**: 702280 [PMID: 34414210 DOI: 10.3389/fsurg.2021.702280]

28 **Lubezky N**, Oyfe I, Contreras AG, Rocca JP, Rudow DL, Keegan T, Taouli B, Kim-Schluger L, Florman S, Schiano T, Facciuto M. Segment 4 and the left lateral segment regeneration pattern after resection of the middle hepatic vein in a living donor right hepatectomy. *HPB (Oxford)* 2015; **17**: 72-78 [PMID: 25212437 DOI: 10.1111/hpb.12303]

World Journal of Gastrointestinal Surgery

Submit a Manuscript: https://www.f6publishing.com

World J Gastrointest Surg 2022 October 27; 14(10): 1150-1160

DOI: 10.4240/wjgs.v14.i10.1150

ISSN 1948-9366 (online)

ORIGINAL ARTICLE

Observational Study

Can DKI-MRI predict recurrence and invasion of peritumoral zone of hepatocellular carcinoma after transcatheter arterial chemoembolization?

Xin Cao, Hao Shi, Wei-Qiang Dou, Xin-Yao Zhao, Ying-Xin Zheng, Ya-Ping Ge, Hai-Chao Cheng, Dao-Ying Geng, Jun-Ying Wang

Specialty type: Radiology, nuclear medicine and medical imaging

Provenance and peer review: Invited article; Externally peer reviewed.

Peer-review model: Single blind

Peer-review report's scientific quality classification

Grade A (Excellent): A
Grade B (Very good): B, B
Grade C (Good): 0
Grade D (Fair): 0
Grade E (Poor): 0

P-Reviewer: Elpek GO, Turkey; Pham TTT, Viet Nam; Shekouhi R, Iran

Received: April 18, 2022
Peer-review started: April 18, 2022
First decision: July 14, 2022
Revised: July 29, 2022
Accepted: September 21, 2022
Article in press: September 21, 2022
Published online: October 27, 2022

Xin Cao, Hao Shi, Ya-Ping Ge, Hai-Chao Cheng, Jun-Ying Wang, Department of Medical Imaging, The First Affiliated Hospital of Shandong First Medical University & Shandong Province Qianfoshan Hospital, Jinan 250014, Shandong Province, China

Xin Cao, Dao-Ying Geng, Department of Radiology, Huashan Hospital, Fudan University, Shanghai 200040, China

Xin Cao, Dao-Ying Geng, Center for Shanghai Intelligent Imaging for Critical Brain Diseases Engineering and Technology Research, Shanghai 200040, China

Wei-Qiang Dou, MR Research, GE Healthcare, Beijing 10076, China

Xin-Yao Zhao, Department of Radiology, Yantaishan Hospital, Yantai 264001, Shandong Province, China

Ying-Xin Zheng, Department of Magnetic Resonance Imaging, Zhangqiu District People's Hospital, Jinan 250200, Shandong Province, China

Corresponding author: Jun-Ying Wang, MD, Doctor, Department of Medical Imaging, The First Affiliated Hospital of Shandong First Medical University & Shandong Province Qianfoshan Hospital, No. 66 Jingshi Road, Jinan 250014, Shandong Province, China.
jywang1120@163.com

Abstract

BACKGROUND

Hepatocellular carcinoma (HCC) is a major cause of cancer-related mortality worldwide. Transcatheter arterial chemoembolization (TACE) has been performed as a palliative treatment for patients with HCC. However, HCC is easy to recur after TACE. Magnetic resonance imaging (MRI) has clinical potential in evaluating the TACE treatment effect for patients with liver cancer. However, traditional MRI has some limitations.

AIM

To explore the clinical potential of diffusion kurtosis imaging (DKI) in predicting recurrence and cellular invasion of the peritumoral liver zone of HCC after TACE.

METHODS
Seventy-six patients with 82 HCC nodules were recruited in this study and underwent DKI after TACE. According to pathological examinations or the overall modified response evaluation criteria in solid tumors (mRECIST) criterion, 48 and 34 nodules were divided into true progression and pseudo-progression groups, respectively. The TACE-treated area, peritumoral liver zone, and far-tumoral zone were evaluated on DKI-derived metric maps. Non-parametric *U* test and receiver operating characteristic curve (ROC) analysis were used to evaluate the prediction performance of each DKI metric between the two groups. The independent *t*-test was used to compare each DKI metric between the peritumoral and far-tumoral zones of the true progression group.

RESULTS
DKI metrics, including mean diffusivity (MD), axial diffusivity (DA), radial diffusivity (DR), axial kurtosis (KA), and anisotropy fraction of kurtosis (Fak), showed statistically different values between the true progression and pseudo-progression groups ($P < 0.05$). Among these, MD, DA, and DR values were higher in pseudo-progression lesions than in true progression lesions, whereas KA and FAk values were higher in true progression lesions than in pseudo-progression lesions. Moreover, for the true progression group, the peritumoral zone showed significantly different DA, DR, KA, and FAk values from the far-tumoral zone. Furthermore, MD values of the liver parenchyma (peritumoral and far-tumoral zones) were significantly lower in the true progression group than in the pseudo-progression group ($P < 0.05$).

CONCLUSION
DKI has been demonstrated with robust performance in predicting the therapeutic response of HCC to TACE. Moreover, DKI might reveal cellular invasion of the peritumoral zone by molecular diffusion-restricted change.

Key Words: Diffusion kurtosis imaging; Hepatocellular carcinoma; Transcatheter arterial chemoembolization; Recurrence

Core Tip: This study demonstrated feasible performance and advantages of diffusion kurtosis imaging metrics (*i.e.*, mean diffusivity, axial diffusivity, radial diffusivity, axial kurtosis, and anisotropy fraction of kurtosis) in evaluating liver cancer and tumoral cell invasion of peritumoral zone between hepatocellular carcinoma progressive group and pseudo-progressive group after transcatheter arterial chemoembolization treatment.

Citation: Cao X, Shi H, Dou WQ, Zhao XY, Zheng YX, Ge YP, Cheng HC, Geng DY, Wang JY. Can DKI-MRI predict recurrence and invasion of peritumoral zone of hepatocellular carcinoma after transcatheter arterial chemoembolization? *World J Gastrointest Surg* 2022; 14(10): 1150-1160
URL: https://www.wjgnet.com/1948-9366/full/v14/i10/1150.htm
DOI: https://dx.doi.org/10.4240/wjgs.v14.i10.1150

INTRODUCTION

Hepatocellular carcinoma (HCC) is a major cause of cancer-related mortality worldwide[1]. Unfortunately, most patients with HCC are diagnosed at the advanced stage and thus lose the opportunity for surgical resection. Transcatheter arterial chemoembolization (TACE), which blocks local blood supply of cancerous lesions to induce ischemia and necrosis with a mixture of chemotherapeutic agents[2], has been performed as a palliative treatment for patients with advanced stage HCC. With TACE, the survival rate and prognosis of patients with HCC could be significantly improved[3]. However, due to hypervascular feature and possibly established new collateral circulation[4], HCC is prone to being recurrent after TACE treatment. Thus, an accurate evaluation method is essential to help guide subsequent therapeutic planning for patients with HCC after TACE in clinical practice. In addition, after TACE, there may be microscopic changes prior to morphological changes in the peritumoral liver parenchyma zone of the true progression. While, no related studies have been conducted regarding this.

Magnetic resonance imaging (MRI) has clinical potential in evaluating the effect of TACE in patients with liver cancer[5]. However, anatomical MRI has some limitations. These include the following: (1) MRI signals are easily affected by various time points and different treatment methods; (2) para-

magnetic substances, such as hemorrhage, granulation tissue, protein components, and steatosis, present high signal on T1-weighted imaging (T1WI) and may interfere with the enhancement of recurring lesions; and (3) disordered collateral circulation in TACE area can lead to false-negative diagnosis in arterial enhancement measurement.

Diffusion MRI, as a promising method of measuring the diffusion behavior of water molecules, sensitively reflects the physiological and morphological changes of tissues[6]. Diffusion-weighted imaging (DWI) has been relatively stable to different treatment methods[7] and has shown higher diagnostic performance in liver cancer after TACE than contrast-enhanced MRI[8]. However, the DWI metric apparent diffusion coefficient, derived in mono-exponential model, tends to be affected by various factors, such as macromolecule concentration, viscosity, and capillary perfusion[9]. In contrast, diffusion kurtosis imaging (DKI), a relatively novel diffusion imaging technique describing the deviations of water molecules diffusing away from Gaussian distribution, enables the precise depiction of microstructural environment[10]. With the DKI-derived parameter mean kurtosis (MK), HCC lesions can be well distinguished between the true progression and pseudo-progression groups[11]. Moreover, together with another DKI metric, mean diffusivity (MD), MK can assess the therapeutic response to TACE in HCC[12]. Although the effectiveness of both MK and MD has been validated, the remaining DKI parameters including fractional anisotropy of kurtosis (FAk), axial and radial kurtosis (KA and KR), and axial and radial diffusivity (DA and DR) have not yet been investigated for their clinical potential on HCC diagnosis after TACE. In addition, whether there are microscopic or molecular level changes in the liver parenchyma around the surviving lesion needs to be investigated.

Therefore, this study aimed to systematically explore the clinical feasibility of all DKI-derived metrics in predicting recurrence and cellular invasion of the peritumoral liver zone of HCC after TACE.

MATERIALS AND METHODS

Subjects

The local institutional review board approved this study, and each subject provided written informed consent. From January to May 2019, 76 patients (46 males *vs* 30 females; mean age, 55 years ± 12 years) with 82 HCC nodules were recruited in this study after receiving TACE treatment (1.4 mo ± 0.8 mo). Based on the pathological examination or the overall modified response evaluation criteria in solid tumors (mRECIST) criteria, 48 relapse/residual lesions and 34 stable and inactive lesions were divided into true progression and pseudo-progression groups, respective. The true progression was pathologically manifested as viable tumor cells in the foci, including primary liver cancer among the incisions, necrotic material, and granulomatous inflammation. The pseudo-progression was manifested as absence of the cancer cell infiltration in the operation area, only liver cirrhosis nodules, and some fibrous necrosis components (Figure 1).

According to the mRECIST criteria proposed by the American Association for the Study of Liver Diseases and European Association for the Study of the Liver and combined clinical indications, we considered the following lesions as true progression lesions[13]: (1) Progressive disease: Target lesion diameter increased by at least 20% on enhanced imaging compared with previous examination; (2) stable disease: Target lesion did not change; (3) partial response: The sum of initial lesion diameters in all target areas was reduced by at least 30%; (4) digital subtraction angiography (DSA): Lipiodol angiography found tumor staining in the focus area; and (5) alpha-fetoprotein (AFP) was significantly increased. However, if lesions met the following criteria, they were classified into the pseudo-progression group: (1) After TACE, DSA revealed that the focus was stable (no clear tumor blood vessels, tumor staining, clear arterial-venous/portal fistula, or vein-portal fistula); (2) after follow-up for a period of time (7.8 mo ± 0.5 mo), previous foci showed no signs of recurrence (all target lesions disappeared during the arterial enhancement phase of imaging); and (3) AFP was normal.

Imaging acquisition

All MRI studies were performed using a 3T MRI scanner (Discovery MR750, GE, United States), with eight-channel abdomen coils employed. A respiratory-gated spin-echo echo-planar imaging DKI sequence was performed in the axial plane. The corresponding applied scan parameters were as follows: Repetition time (TR), 3333 ms; echo time (TE), 69.4 ms; slice thickness, 6 mm; slice spacing, 2.0 mm; field of view, 360 mm × 288 mm; and matrix size, 128 × 128. In addition, five *b* values (400, 800, 1200, 1600, and 2000 s/mm^2) and 15 directions at each *b* value were used. The total scan time was 10 min. Conventional MRI was also performed, with the following parameters: T1WI: TR 3.7 ms, TE 1.1 ms, and slice thickness 6 mm; T2WI: TR 2319.5 ms, TE 68.0 ms, and slice thickness 6.0 mm; FS-T2WI: TR 9000.0 ms, TE 81.0 ms, and slice thickness 6.0 mm; and DWI sequence: TR 5000 ms and TE 50.8 ms. Dynamic-enhanced MRI with gadopentetate dimeglumine, captured the arterial (20 s), venous (60 s), delayed (2 min) and hepatobiliary (45-120 min) phases. Gadolinium-diethylenetriamine penta-acetic acid of 15-20 mL was injected intravenously through the back of the hand at a rate of 2 mL/s.

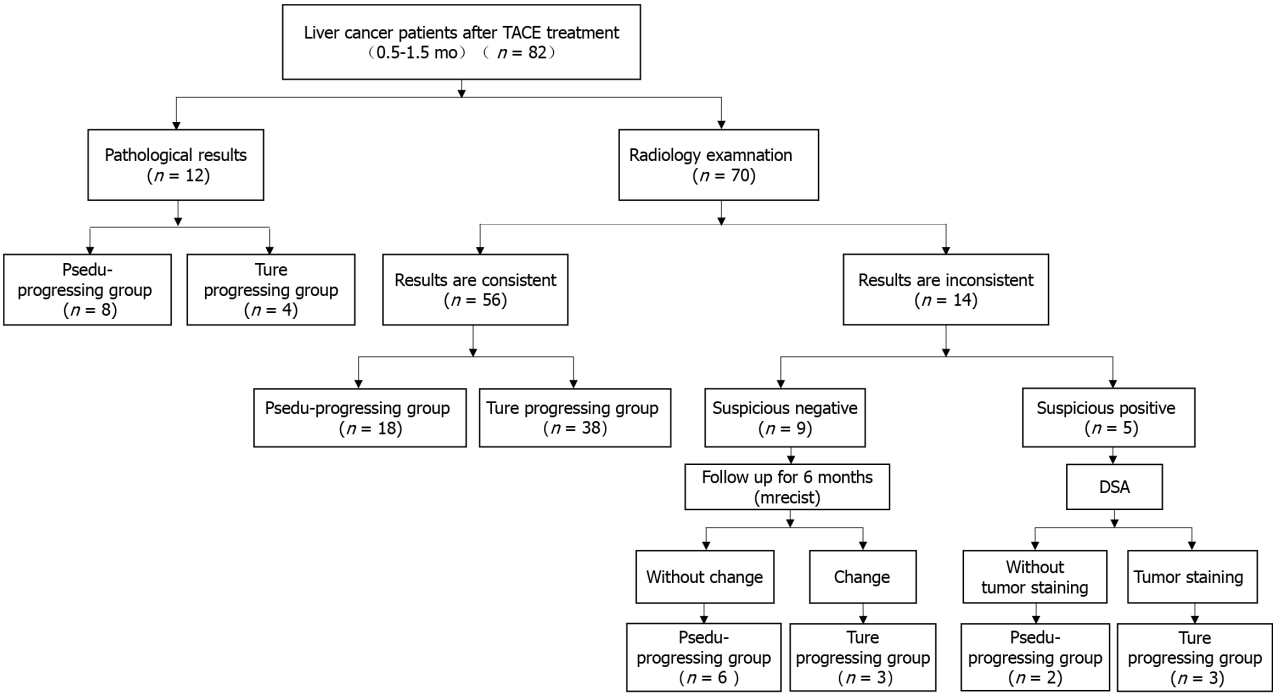

DOI: 10.4240/wjgs.v14.i10.1150

Figure 1 Flowchart of patient enrollment. *n*: Number of cases; TACE: Transcatheter arterial chemoembolization; mRECIST: Modified response evaluation criteria in solid tumors; DSA: Digital subtraction angiography.

DSA was performed under guidance on a Toshiba rotary DSA (GEIGS530, United States) machine. All patients were approached *via* the femoral artery and routinely underwent skin preparation, disinfection, draping, and local anesthesia in the groin area. After the artery was successfully inserted, the guide wire and catheter sheath were sequentially inserted. The Cook 5-F RH tube was introduced to select the abdominal trunk or common hepatic angiography to observe the tumor staining.

Data analysis

Two professional radiologists (Hansen and HC), with 30 and 10 years of experience in MRI assessment, respectively, independently recorded the imaging and clinical data of the true progression and pseudo-progression groups (Table 1). All acquired DKI images were examined on the workstation using vendor-supplied postprocessing software (GE AW4.6 advantage, United States). The corresponding mappings of DKI-derived parameters (*i.e.*, MD, DA, DR, MK, KA, KR, and FAk) were obtained. The two radiologists independently selected the regions of interest (ROIs) for TACE-treated area, peritumoral area (distance < 2 cm to the tumor), and long-distance area (distance > 5 cm) on anatomical DKI image at b = 0 s/mm^2 and then copied them on each of the DKI-derived parametric maps (Figure 2). Each expert selected two different ROIs and calculated the average value. All chosen ROIs of a circular or oval form were selected carefully to avoid necrotic area. Considering the inter-subject variation, all obtained values were standardized based on the following formulas: $Std_{pseudoprogression}$ = ROI (pseudo-progression lesion)/ROI (normal parenchyma) and $Std_{progression}$ = ROI (progression lesion)/ROI (normal parenchyma).

Statistical analysis

All statistical analyses were performed using the Statistical Package for the Social Sciences version 22.0 statistical software. Intra-class correlation coefficient (ICC) analysis was performed to evaluate the inter-agreement of DKI parameter assessment by the two professional experts. The non-parametric U test and receiver operating characteristic (ROC) curve analysis were used to evaluate the differences and prediction performance of the DKI-derived parameters. The independent sample t-test was used to compare all DKI metrics in the peritumoral zone (distance < 2 cm) and the far-tumoral zone (distance > 5 cm) of the true progression group. $P < 0.05$ was considered statistically significant.

Table 1 Summary of clinical data of patients in true and pseudo-progressing groups

Characteristic	All cases (*n* = 82)	True group (*n* = 48)	Pseudo-group (*n* = 34)	*P* value
Age range (yr)	55 ± 12	50 ± 16	53 ± 14	0.745
Male/female (*n*)	46/30	26/18	20/12	0.402
AFP (ng/mL) (+/-)	49/33	47/1	2/32	0.001
	Tumor-related characteristics			
Tumor size (cm)	4.0 ± 1.8	4.2 ± 1.6	2.7 ± 1.3	0.142
Enhancement (+/-)	50/32	46/2	4/30	0.006
DSA (+/-)	42/27	42/2	0/25	< 0.010
Resection (+/-)	10	9	1	-
TACE times (single/repeated)	26/56	4/44	22/12	< 0.011
Follow-up for > 6 mo (+/-)	39/33	39/0	0/33	< 0.001

AFP: Alpha-fetoprotein; DSA: Digital subtraction angiography; TACE: Transcatheter arterial chemoembolization.

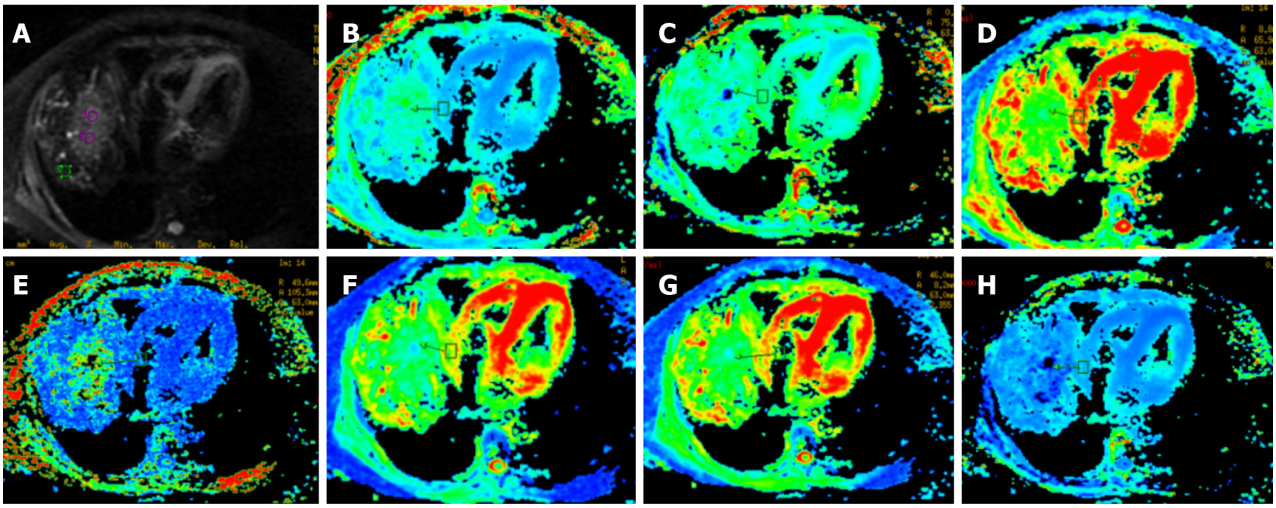

DOI: 10.4240/wjgs.v14.i10.1150

Figure 2 Representative maps of transcatheter arterial chemoembolization-treated and recurrent hepatocellular carcinoma foci. The patient was a 46-year-old man with transcatheter arterial chemoembolization-treated and recurrent hepatocellular carcinoma foci. A: Diffusion map with b = 0 s/mm^2; B: Maps of mean kurtosis (MK); C: Maps of mean diffusivity (MD); D: Maps of radial kurtosis (KR); E: Maps of axial kurtosis (KA); F: Maps of axial diffusivity (DA); G: Maps of radial diffusivity (DR); H: Maps of anisotropy coefficient of kurtosis (FAk). In the first map (A), the region of interest (ROI) (1) corresponds to the arrow pointing to a new lesion. The peritumoral zone (distance < 2 cm) refers to ROI (2) (red circle), and far-tumoral zone (diameter > 5 cm) refers to ROI (3) (green square).

RESULTS

Clinical data analysis

Clinical data, including age, gender, and tumor-related characteristics, of patients in the true progression and pseudo-progression groups are summarized in Table 1. There were significantly more patients in the true progression group than in the pseudo-progression group. Moreover, the true progression group had higher serum AFP level (> 200 ng/mL) (P < 0.05) than the pseudo-progression group. In addition, significantly greater proportions of patients in the progression group showed typical enhancement (95.8%) and more or less tumor staining in lipiodol angiography (95.5%). In contrast, tumor size and age range were similar between the two groups (P > 0.05). Among the 48 nodules in the progression group, 44 received repeated TACE, and the mean number of TACE sessions per nodule was 1-3. Four nodules underwent only a single course of TACE.

Inter-observer agreement analysis

As shown in Table 2, ICC analysis was utilised by two radiologists to assess the inter-agreement of each DKI parameter measurement on the TACE-treated region, peritumoral zone, and far-tumoral zone,

Table 2 Evaluation of inter-observer agreement using intra-class correlation coefficient analysis

	MK	MD	KA	KR	DA	DR	FAk
ROI (T)	0.86	0.85	0.80	0.83	0.76	0.78	0.62
ROI (N)	0.79	0.74	0.71	0.76	0.72	0.75	0.54
ROI (F)	0.70	0.73	0.69	0.68	0.64	0.70	0.50

FAk: Anisotropy coefficient of kurtosis; ROC: Receiver operating characteristic curve; MD: Mean diffusivity; MK: Mean kurtosis; KA: Axial kurtosis; KR: Radial kurtosis; DA: Axial diffusivity; DR: Radial diffusivity.

Table 3 Diffusion kurtosis imaging derived metrics in true and pseudo-progressing lesions

	MK	MD	KR	KA	DR	DA	FAk
N	0.60 ± 0.15	1.90 ± 0.65	0.55 ± 0.16	0.60 ± 0.13	1.88 ± 0.55	2.20 ± 0.63	0.10 ± 0.09
Y	0.71 ± 0.24	1.60 ± 0.45	0.65 ± 0.29	0.70 ± 0.15	1.4 ± 0.38	2.10 ± 0.60	0.32 ± 0.22
Std-N	0.68 ± 0.27	1.89 ± 0.58	0.70 ± 0.31	0.61 ± 0.16	2.01 ± 0.54	1.60 ± 0.42	0.54 ± 0.32
Std-Y	0.81 ± 0.23	0.91 ± 0.18	0.75 ± 0.24	1.03 ± 0.20	0.88 ± 0.22	0.92 ± 0.22	1.07 ± 0.78
P value	0.270	0.009	0.679	0.000	0.003	0.000	0.000

N = pseudo-progressing group; Y = true progressing group. FAk: Anisotropy coefficient of kurtosis; MD: Mean diffusivity; MK: Mean kurtosis; KA: Axial kurtosis; KR: Radial kurtosis; DA: Axial diffusivity; DR: Radial diffusivity.

separately. General excellent inter-agreement was confirmed by high ICC values. Among these, optimal measurement consistency was obtained in TACE-treated area for DKI-derived parameter values showing the best consistency, whereas the worst measurement consistency was found in the far-tumoral zone.

Diffusion kurtosis imaging-derived parameter analysis

Compared to pseudo-progression inactive lesions, true progression recurrence lesions were associated with lower values of MD, DA, and DR (1.60 ± 0.45 × 10^{-3} mm/s *vs* 1.90 ± 0.65 × 10^{-3} mm/s, 2.10 ± 0.60 × 10^{-3} mm/s *vs* 2.29 ± 0.63 × 10^{-3} mm/s, and 1.40 ± 0.38 × 10^{-3} mm/s *vs* 1.88 ± 0.55 × 10^{-3} mm/s, respectively; Table 3). However, higher KA and FA values were found in the foci area of true progression lesions than of pseudo-progression lesions (0.70 ± 0.15 *vs* 0.60 ± 0.13 and 0.32 ± 0.22 *vs* 0.10 ± 0.09, respectively; Table 3). Moreover, ROC curve analysis was performed to compared the DKI-derived metrics in predicting recurrence performance (Figure 3). High AUC values were obtained for the parameters MD (0.80), FAk (0.78), KA (0.82), DA (0.82), and DR (0.80), whereas low ICC values were found in MK (0.6) and KR (0.54).

For the true progression group, DA and DR values were lower in the peritumoral zone (distance < 2 cm) than in the far-tumoral zone (distance > 5 cm) (2.11 ± 0.52 × 10^{-3} mm/s *vs* 2.44 ± 0.59 × 10^{-3} mm/s and 1.382 ± 0.440 × 10^{-3} mm/s *vs* 1.647 ± 0.470 × 10^{-3} mm/s, respectively; Figure 4), whereas FAk and KA values showed opposite trends (0.309 ± 0.110 *vs* 0.228 ± 0.060 and 0.809 ± 0.340 *vs* 0.783 ± 0.120, respectively; Figure 3).

In addition, the MD values of the liver parenchyma (peritumoral and far-tumoral zones) were significantly lower in the true progression group than in the pseudo-progression group (0.866 ± 0.330 × 10^{-3} mm/s *vs* 1.677 ± 0.630 × 10^{-3} mm/s and 0.843 ± 0.170 × 10^{-3} mm/s *vs* 1.569 ± 0.410 × 10^{-3} mm/s, respectively; Figure 4D).

DISCUSSION

In this study, we explored the prediction performance of DKI for recurrence and cellular invasion of the peritumoral liver zone of HCC after TACE and further investigated the characteristics of the DKI-derived metrics between the true progression and pseudo-progression groups. Considering the high data consistency between the two experts, we found that most DKI metrics, including MD, DA, DR, KA, and FAk, showed statistically different values between the true progression and pseudo-progression groups ($P < 0.05$). Moreover, for the true progression group, except the metrics MK and KR, all other parameters of the peritumoral liver zone (distance < 2 cm) were significantly different from those of the far-tumoral liver parenchyma (distance > 5 cm). Therefore, we concluded that DKI with derived

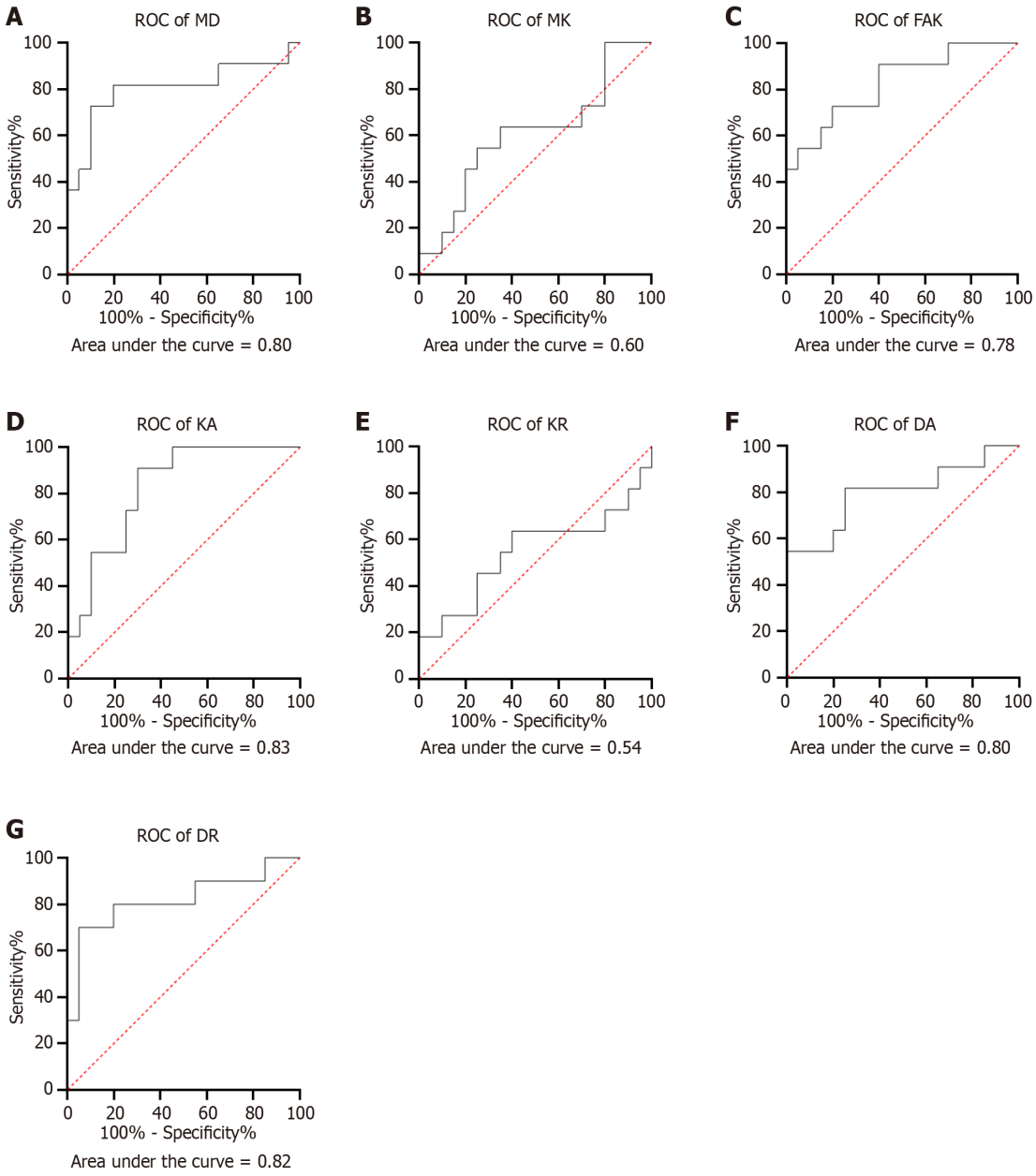

DOI: 10.4240/wjgs.v14.i10.1150

Figure 3 Receiver operating characteristic curves of diffusion kurtosis imaging metric in predicting recurrence. AUC value greater than 0.7 indicates a higher diagnostic value. A: Mean diffusivity; B: Mean kurtosis; C: Anisotropy coefficient of kurtosis; D: Axial kurtosis; E: Radial kurtosis; F: Axial diffusivity; G: Radial diffusivity. FAk: Anisotropy coefficient of kurtosis; ROC: Receiver operating characteristic curve; MD: Mean diffusivity; MK: Mean kurtosis; KA: Axial kurtosis; KR: Radial kurtosis; DA: Axial diffusivity; DR: Radial diffusivity.

functional metrics showed advantages in assessing the therapeutic response of HCC to TACE and also provided robust performance in evaluating peritumoral zone invasion.

Except for FAk, especially in ROI (F) (far-tumoral zone, distance > 5 cm), all other DKI metrics showed excellent consistency measured by two professional experts. FAk has been shown to have a significant benefit in the central nervous system, where the nerve fibre structure exhibits full fractional anisotropy[14]. Nevertheless, the fibre structure in the liver lacks a defined fractional anisotropy, making it difficult to identify the specificity of FAk. Furthermore, Nasu *et al*[15] established the idea of "pseudo-fractional anisotropy artefact of the liver", which asserts that manual selection of ROI (F) is inherently subjective and can be influenced by heartbeat and breathing artifact. This artefact might be another explanation for low consistency of FAk.

Important findings in this study were that DKI parameters, including MD, DA, DR, KA, and FAk, showed statistical differences between the true progression and pseudo-progression groups ($P < 0.05$). MD, DA, and DR values of pseudo-progression lesions were higher than those of true progression lesions, whereas KA and FAk values were higher in true progression lesions than in pseudo-progression lesions. Yuan *et al*[11] showed significant potential of DKI in assessing the therapeutic response of HCC

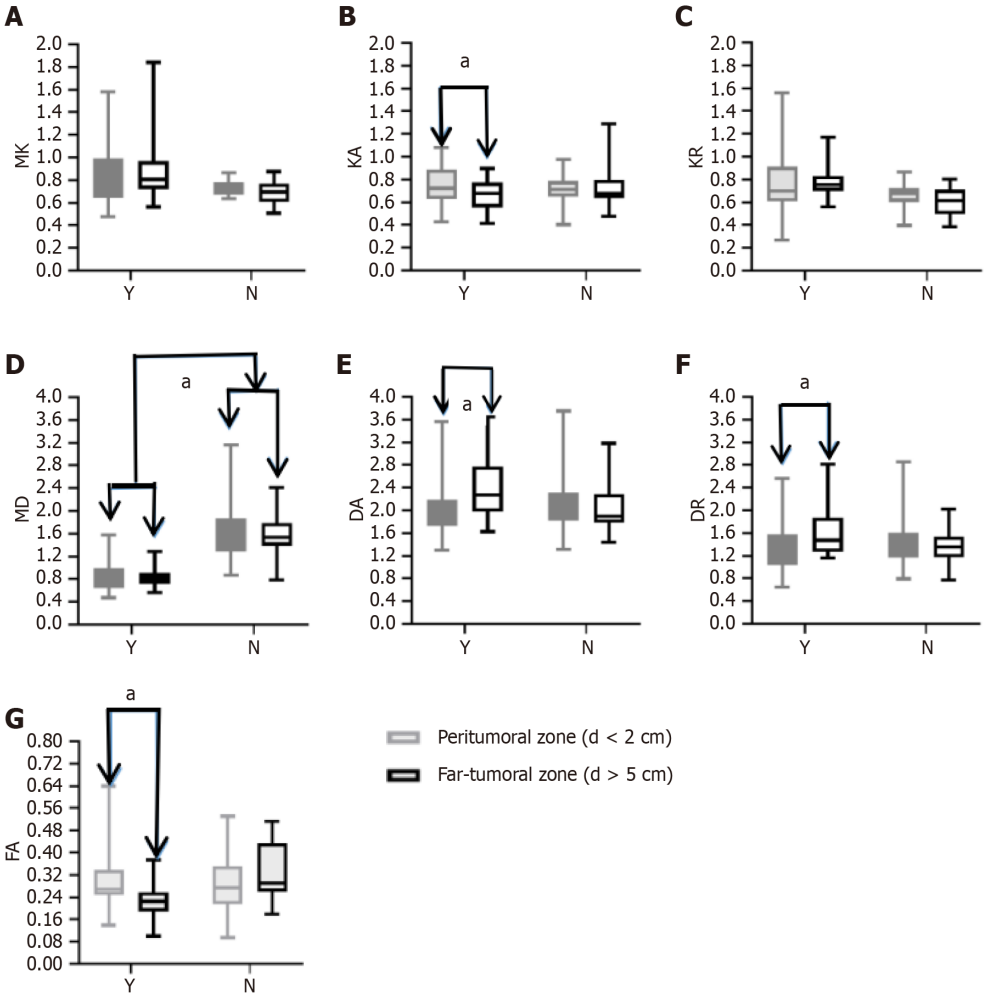

DOI: 10.4240/wjgs.v14.i10.1150

Figure 4 Box plots showing diffusion kurtosis imaging derived metrics of peritumoral zones between true and pseudo-progressing groups. A: Mean kurtosis (MK); B: Axial kurtosis (KA); C: Radial kurtosis (KR); D: Mean diffusivity (MD); E: Axial diffusivity (DA); F: Radial diffusivity (DR); G: Anisotropy coefficient of kurtosis (FAk). $^{a}P < 0.05$; the unit of MD, DA, and DR is 10^{-3} mm^2/s. N = pseudo-progressing group; Y = true progressing group. FAk: Anisotropy coefficient of kurtosis; MD: Mean diffusivity; MK: Mean kurtosis; KA: Axial kurtosis; KR: Radial kurtosis; DA: Axial diffusivity; DR: Radial diffusivity.

to TACE. Thus, they believed that MK is an effective biomarker in the assessment of HCC progression after TACE. This conclusion, however, is not fully consistent with our results. Compared with the pseudo-progression group with inactive foci after TACE, the normalized MK value of the true progression group with residual/recurrent foci was not higher. Since MK can reflect the complexity and density of tissues[16], high cell density usually shows high MK value. We hypothesized that after TACE, foci cells are swelling and experience degeneration or necrosis, while leads to a decreased cell density. Moreover, some low-activity tumor cells have been severely damaged in structure, but still retain the ability to metastasize and recur. This type of condition cannot be effectively screened out based on the characteristics of tissue density, leading to the absence of statistical difference of the MK value between the true progression and pseudo-progression groups. It is worth mentioning that KA in this study revealed certain sensitivity in assessing tumor recurrence. Follow-up studies should be further conducted to explore the underlying mechanism.

Additionally, the clinical potential of DKI in determining the invasion of peritumoral zone of the residual foci for the true progression group was assessed. We discovered that diffusion metrics (DA and DR) differed considerably between the far-tumoral zone (distance > 5 cm) and the peritumoral zone (distance < 2 cm). The peritumoral zone (distance < 2 cm) had lower DA and DR values than the far-tumoral zone (distance > 5 cm), indicating that microenvironmental alterations may occur in the peritumoral zone, which is close to residual/recurrent foci and may be sensitive in representing cancer cell infiltration. However, only KA revealed a larger value in the peritumoral zone than the far-tumoral zone among the three kurtosis coefficients (MK, KR, and KA).

Despite the fact that a variety of DKI implementations have investigated the correlations of MK and MD with fibrosis or liver function[17-20], no similar DKI findings have been published in these studies. Yoshimaru *et al*[17] investigated the relationship between MK and Child-Pugh score in 79 patients with varying degrees of hepatic decompensation and found a minor correlation. In comparison, Goshima *et al*

[18] investigated the relationship between MK and Child-Pugh score but found no association. There was also disagreement about whether MK or MD had a superior diagnostic effectiveness for liver fibrosis. In another study, Hu *et al*[19] concluded that MD correlated strongly with the degrees of liver fibrosis, and the parameter MK may provide complementary information. In contrast, Li *et al*[20] claimed that MK could best predict the liver fibrosis stage. In this study, we did not analyze the relationship between DKI parameters and liver fibrosis or function. However, the MD value of the liver parenchyma (peritumoral and far-tumoral zones) was lower in the true progression group than in the pseudo-progression group. Moreover, the MK value did not show any difference between the two groups. The results obtained in this study were more inclined to the view that MD has a higher sensitivity to detect the degree of fibrosis. We thus hypothesized that poor liver function and high grade of liver fibrosis may lead to poor prognosis and high recurrence rate.

There are some limitations in the present study. First, manual selection of active ROIs is inevitably subjective. According to the results of dynamic enhancement and DSA imaging, independent measurement by two experienced radiologists can minimize measurement errors. Second, DKI with 5 *b* values and 15 directions per *b* value currently takes a long time of 10 min for imaging. Third, each patient showed different fibrosis state and liver function. To minimize this effect, we selected the liver parenchyma far away from the focus area for standardization. Fourth, there was a lack of pathological examination of tumor changes before and after TACE treatment. Further studies with more pathologically confirmed cases are required to be conducted. Fifth, it was difficult to obtain the histological results for each lesion after TACE. Therefore, no pathological support could determine whether the surrounding liver parenchyma was invaded. Relevant pathological study is requested to further explore the relationship among DKI parameters, liver fibrosis, and peripheral infiltration.

CONCLUSION

In conclusion, DKI metrics (MD, DA, DR, KA, and FAk) have been demonstrated with robust performance in predicting the therapeutic response of HCC to TACE and evaluating cellular invasion of the peritumoral zone.

ARTICLE HIGHLIGHTS

Research background

Transcatheter arterial chemoembolization (TACE) has been used to treat patients with hepatocellular carcinoma (HCC) as a palliative therapy. Nevertheless, HCC is prone to recur after TACE. Traditional anatomical MRI has certain limitations in assessing recurrence. Diffusion kurtosis imaging (DKI) provides a detailed depiction of the microstructural environment. Whether DKI-derived metrics can provide clinical feasibility in predicting HCC recurrence and cellular invasion of the peritumoral liver zone after TACE remains to be a concern.

Research motivation

To investigate the clinical use of DKI in predicting recurrence and cellular invasion of HCC in the peritumoral liver zone after TACE.

Research objectives

In this study, 76 patients with 82 hepatic cancer nodules were enrolled and underwent DKI after TACE. Forty-eight and 34 nodules were divided into two groups: True progression and pseudo-progression, respectively.

Research methods

DKI-derived metric maps were used to assess the TACE-treated area, peritumoral liver zone, and far-tumoral zone. To compare the prediction performance of each DKI metric between the true progression and pseudo-progression groups, the non-parametric *U* test and receiver operating characteristic curve (ROC) analysis were performed. The independent *t*-test was utilized to compare each DKI metric between the peritumoral and far-tumoral zones in the true progression group.

Research results

DKI metrics, including mean diffusivity (MD), axial diffusivity (DA), radial diffusivity (DR), axial kurtosis (KA), and anisotropy fraction of kurtosis (Fak), exhibited significantly different values between the true progression and pseudo-progression groups, respectively ($P < 0.05$). Furthermore, the peritumoral zone had substantially different DA, DR, KA, and FAk values than the far-tumoral zone in the true progression group. Additionally, MD values of the liver parenchyma (peritumoral and far-

tumoral zones) were substantially lower in the true progression group compared to the pseudo-progression group ($P < 0.05$).

Research conclusions

DKI has been shown to predict the therapeutic response of HCC to TACE with high accuracy. Furthermore, DKI may indicate cellular invasion of the peritumoral zone by molecular diffusion-restricted change.

Research perspectives

This study systematically investigated the clinical feasibility of all DKI-derived metrics in predicting recurrence and cellular invasion of the peritumoral liver zone of HCC after TACE, providing an accurate evaluation method to help guide subsequent therapeutic planning in clinical practice for patients with HCC after TACE.

FOOTNOTES

Author contributions: Cao X and Wang JY designed and performed the research, and wrote the paper; Shi H designed the research and supervised the report; Zheng YX, Ge YP, and Cheng HC contributed to the analysis; Dou WQ, Zhao XY, and Geng DY provided clinical advice.

Supported by the Greater Bay Area Institute of Precision Medicine, No. KCH2310094; Shanghai Sailing Program, No. 22YF1405000; Research Startup Fund of Huashan Hospital Fudan University, No. 2021QD035; and Clinical Research Plan of SHDC, No. SHDC2020CR3020A.

Institutional review board statement: The study was conducted in accordance with the Declaration of Helsinki, and approved by the Institutional Review Board of Huashan Hospital and First Affiliated Hospital of Shandong First Medical University.

Conflict-of-interest statement: The authors declare no conflicts of interest for this article.

Data sharing statement: The data presented in this study are available on request from the corresponding author. The data are not publicly available due to protecting patient privacy.

Country/Territory of origin: China

ORCID number: Xin Cao 0000-0003-3839-3076; Wei-Qiang Dou 0000-0003-0056-2014; Dao-Ying Geng 0000-0002-3585-6883; Jun-Ying Wang 0000-0003-3839-3207.

S-Editor: Chen YL
L-Editor: Wang TQ
P-Editor: Zhao S

REFERENCES

1 **European Association for the Study of the Liver**. EASL Clinical Practice Guidelines: Management of hepatocellular carcinoma. *J Hepatol* 2018; **69**: 182-236 [PMID: 29628281 DOI: 10.1016/j.jhep.2018.03.019]
2 **Rognoni C**, Ciani O, Sommariva S, Facciorusso A, Tarricone R, Bhoori S, Mazzaferro V. Trans-arterial radioembolization in intermediate-advanced hepatocellular carcinoma: systematic review and meta-analyses. *Oncotarget* 2016; **7**: 72343-72355 [PMID: 27579537 DOI: 10.18632/oncotarget.11644]
3 **Sacco R**, Bertini M, Petruzzi P, Bertoni M, Bargellini I, Bresci G, Federici G, Gambardella L, Metrangolo S, Parisi G, Romano A, Scaramuzzino A, Tumino E, Silvestri A, Altomare E, Vignali C, Capria A. Clinical impact of selective transarterial chemoembolization on hepatocellular carcinoma: a cohort study. *World J Gastroenterol* 2009; **15**: 1843-1848 [PMID: 19370781 DOI: 10.3748/wjg.15.1843]
4 **Ramsey DE**, Geschwind JF. Chemoembolization of hepatocellular carcinoma--what to tell the skeptics: review and meta-analysis. *Tech Vasc Interv Radiol* 2002; **5**: 122-126 [PMID: 12524642 DOI: 10.1053/tvir.2002.36418]
5 **Yu JS**, Kim JH, Chung JJ, Kim KW. Added value of diffusion-weighted imaging in the MRI assessment of perilesional tumor recurrence after chemoembolization of hepatocellular carcinomas. *J Magn Reson Imaging* 2009; **30**: 153-160 [PMID:

19557734 DOI: 10.1002/jmri.21818]
6 **Labeur TA**, Runge JH, Klompenhouwer EG, Klümpen HJ, Takkenberg RB, van Delden OM. Diffusion-weighted imaging of hepatocellular carcinoma before and after transarterial chemoembolization: role in survival prediction and response evaluation. *Abdom Radiol (NY)* 2019; **44**: 2740-2750 [PMID: 31069479 DOI: 10.1007/s00261-019-02030-2]
7 **Yang K**, Zhang XM, Yang L, Xu H, Peng J. Advanced imaging techniques in the therapeutic response of transarterial chemoembolization for hepatocellular carcinoma. *World J Gastroenterol* 2016; **22**: 4835-4847 [PMID: 27239110 DOI: 10.3748/wjg.v22.i20.4835]
8 **Kamel IR**, Bluemke DA, Ramsey D, Abusedera M, Torbenson M, Eng J, Szarf G, Geschwind JF. Role of diffusion-weighted imaging in estimating tumor necrosis after chemoembolization of hepatocellular carcinoma. *AJR Am J Roentgenol* 2003; **181**: 708-710 [PMID: 12933464 DOI: 10.2214/ajr.181.3.1810708]
9 **Taouli B**, Tolia AJ, Losada M, Babb JS, Chan ES, Bannan MA, Tobias H. Diffusion-weighted MRI for quantification of liver fibrosis: preliminary experience. *AJR Am J Roentgenol* 2007; **189**: 799-806 [PMID: 17885048 DOI: 10.2214/AJR.07.2086]
10 **Wang J**, Dou W, Shi H, He X, Wang H, Ge Y, Cheng H. Diffusion kurtosis imaging in liver: a preliminary reproducibility study in healthy volunteers. *MAGMA* 2020; **33**: 877-883 [PMID: 32377906 DOI: 10.1007/s10334-020-00846-4]
11 **Yuan ZG**, Wang ZY, Xia MY, Li FZ, Li Y, Shen Z, Wang XZ. Diffusion Kurtosis Imaging for Assessing the Therapeutic Response of Transcatheter Arterial Chemoembolization in Hepatocellular Carcinoma. *J Cancer* 2020; **11**: 2339-2347 [PMID: 32127960 DOI: 10.7150/jca.32491]
12 **Luo X**, Li Y, Shang Q, Liu H, Song L. Role of Diffusional Kurtosis Imaging in Evaluating the Efficacy of Transcatheter Arterial Chemoembolization in Patients with Liver Cancer. *Cancer Biother Radiopharm* 2019; **34**: 614-620 [PMID: 31560562 DOI: 10.1089/cbr.2019.2878]
13 **Lencioni R**, Llovet JM. Modified RECIST (mRECIST) assessment for hepatocellular carcinoma. *Semin Liver Dis* 2010; **30**: 52-60 [PMID: 20175033 DOI: 10.1055/s-0030-1247132]
14 **Zhuo J**, Keledjian K, Xu S, Pampori A, Gerzanich V, Simard JM, Gullapalli RP. Changes in Diffusion Kurtosis Imaging and Magnetic Resonance Spectroscopy in a Direct Cranial Blast Traumatic Brain Injury (dc-bTBI) Model. *PLoS One* 2015; **10**: e0136151 [PMID: 26301778 DOI: 10.1371/journal.pone.0136151]
15 **Nasu K**, Kuroki Y, Fujii H, Minami M. Hepatic pseudo-anisotropy: a specific artifact in hepatic diffusion-weighted images obtained with respiratory triggering. *MAGMA* 2007; **20**: 205-211 [PMID: 17960439 DOI: 10.1007/s10334-007-0084-0]
16 **Steven AJ**, Zhuo J, Melhem ER. Diffusion kurtosis imaging: an emerging technique for evaluating the microstructural environment of the brain. *AJR Am J Roentgenol* 2014; **202**: W26-W33 [PMID: 24370162 DOI: 10.2214/AJR.13.11365]
17 **Yoshimaru D**, Takatsu Y, Suzuki Y, Miyati T, Hamada Y, Funaki A, Tabata A, Maruyama C, Shimada M, Tobari M, Nishino T. Diffusion kurtosis imaging in the assessment of liver function: Its potential as an effective predictor of liver function. *Br J Radiol* 2019; **92**: 20170608 [PMID: 30358410 DOI: 10.1259/bjr.20170608]
18 **Goshima S**, Kanematsu M, Noda Y, Kondo H, Watanabe H, Bae KT. Diffusion kurtosis imaging to assess response to treatment in hypervascular hepatocellular carcinoma. *AJR Am J Roentgenol* 2015; **204**: W543-W549 [PMID: 25905960 DOI: 10.2214/AJR.14.13235]
19 **Hu G**, Liang W, Wu M, Chan Q, Li Y, Xu J, Luo L, Quan X. Staging of rat liver fibrosis using monoexponential, stretched exponential and diffusion kurtosis models with diffusion weighted imaging- magnetic resonance. *Oncotarget* 2018; **9**: 2357-2366 [PMID: 29416777 DOI: 10.18632/oncotarget.23413]
20 **Li J**, Wang D, Chen TW, Xie F, Li R, Zhang XM, Jing ZL, Yang JQ, Ou J, Cao JM. Magnetic Resonance Diffusion Kurtosis Imaging for Evaluating Stage of Liver Fibrosis in a Rabbit Model. *Acad Radiol* 2019; **26**: e90-e97 [PMID: 30072289 DOI: 10.1016/j.acra.2018.06.018]

World Journal of Gastrointestinal Surgery

Submit a Manuscript: https://www.f6publishing.com

World J Gastrointest Surg 2022 October 27; 14(10): 1161-1168

DOI: 10.4240/wjgs.v14.i10.1161

ISSN 1948-9366 (online)

CASE REPORT

Cecocutaneous fistula diagnosed by computed tomography fistulography: A case report

Tung-Yen Wu, Kuang-Hua Lo, Chao-Yang Chen, Je-Ming Hu, Jung-Cheng Kang, Ta-Wei Pu

Specialty type: Gastroenterology and hepatology

Provenance and peer review: Unsolicited article; Externally peer reviewed.

Peer-review model: Single blind

Peer-review report's scientific quality classification

Grade A (Excellent): A, A
Grade B (Very good): B, B
Grade C (Good): C, C
Grade D (Fair): D
Grade E (Poor): E, E

P-Reviewer: Dai DL, China; Mishra TS, India; Salimi M, Iran; Sica G, Italy; Singh R, India; Vyshka G, Albania

Received: June 21, 2022
Peer-review started: June 21, 2022
First decision: July 12, 2022
Revised: August 8, 2022
Accepted: October 5, 2022
Article in press: October 5, 2022
Published online: October 27, 2022

Tung-Yen Wu, Department of Surgery, Tri-Service General Hospital Songsang Branch, Taipei 105, Taiwan

Kuang-Hua Lo, Department of Surgery, Taipei Veterans General Hospital, Taipei 112, Taiwan

Chao-Yang Chen, Je-Ming Hu, Division of Colon and Rectal Surgery, Department of Surgery, Tri-Service General Hospital, Taipei 114, Taiwan

Jung-Cheng Kang, Division of Colon and Rectal Surgery, Department of Surgery, Taiwan Adventist Hospital, Taipei 105, Taiwan

Ta-Wei Pu, Division of Colon and Rectal Surgery, Department of Surgery, Tri-Service General Hospital Songsang Branch, National Defense Medical Center, Taipei 105, Taiwan

Corresponding author: Ta-Wei Pu, MD, Doctor, Lecturer, Division of Colon and Rectal Surgery, Department of Surgery, Tri-Service General Hospital Songsang Branch, National Defense Medical Center, No. 131 Chien-Kang Road, Taipei 105, Taiwan.
tawei0131@gmail.com

Abstract

BACKGROUND

Enterocutaneous fistula (ECF) is an abnormal communication between the skin and the gastrointestinal tract and is associated with considerable morbidity and mortality. To diagnose ECF, X-ray fistulography and abdominal computed tomography (CT) with intravenous or oral contrast are generally used. If the anatomic details obtained from CT are insufficient, CT fistulography may help diagnose and determine the extent of the abnormal channel. However, CT fistulography is seldom performed in patients with insufficient evidence of a fistula.

CASE SUMMARY

A 35-year-old man with a prior appendectomy presented with purulence over the abdominal wall without gastrointestinal tract symptoms or a visible opening on the abdominal surface. His history and physical examination were negative for nausea, diarrhea, muscle guarding, and bloating. Local abdominal tenderness and redness over a purulent area were noted, which led to the initial diagnosis of cellulitis. He was admitted to our hospital with a diagnosis of cellulitis. We performed a minimal incision on the carbuncle to collect the pus. The bacterial culture of the exudate resulted positive for *Enterococcus* sp. ECF was thus suspected, and we arranged a CT scan for further investigation. CT images before

intravenous contrast administration showed that the colon was in close contact with the abdominal wall. Therefore, we conducted CT fistulography by injecting contrast dye into the carbuncle during the CT scan. The images showed an accumulation of the contrast agent within the subcutaneous tissues, suggesting the formation of an abscess. The contrast dye tracked down through the muscles and peritoneum into the colon, delineating a channel connecting the subcutaneous abscess with the colon. This evidence confirmed cecocutaneous fistula and avoided misdiagnosing ECF without gastrointestinal tract symptoms as cellulitis. The patient underwent laparoscopic right hemicolectomy with re-anastomosis of the ileum and transverse colon.

CONCLUSION
CT fistulography can rule out ECF in cases presenting as cellulitis if examinations are suggestive.

Key Words: Cecocutaneous fistula; Enterocutaneous fistula; Computed tomography fistulography; Laparoscopy; Hemicolectomy; Case report

Core Tip: Computed tomography (CT) fistulography is seldom performed on patients with insufficient evidence of fistula; however, it provides more accurate anatomical details than X-ray fistulography and abdominal CT. A 35-year-old man with swelling and purulence over the abdominal wall was admitted to our hospital under the diagnosis of cellulitis. Serial examinations suggested a possible enterocutaneous fistula (ECF); thus, we performed CT fistulography. Images showed the subcutaneous contrast agent tracked down through the muscle and peritoneum into the cecum, confirming a cecocutaneous fistula. CT fistulography may rule out ECF in patients presenting with cellulitis if examinations are suggestive.

Citation: Wu TY, Lo KH, Chen CY, Hu JM, Kang JC, Pu TW. Cecocutaneous fistula diagnosed by computed tomography fistulography: A case report. *World J Gastrointest Surg* 2022; 14(10): 1161-1168
URL: https://www.wjgnet.com/1948-9366/full/v14/i10/1161.htm
DOI: https://dx.doi.org/10.4240/wjgs.v14.i10.1161

INTRODUCTION

Enterocutaneous fistula (ECF) is an abnormal channel connecting the skin and the gastrointestinal tract. It occurs most often after abdominal surgery (75%-85%), and only 15%-25% of cases occur spontaneously[1,2]. X-ray fistulography with oral contrast and abdominal computed tomography (CT) with intravenous or oral contrast are generally used to diagnose ECF. If radiographic findings from X-ray fistulography and CT scan are insufficient, CT fistulography is a good alternative[3,4]. However, CT fistulography is seldom used without strong evidence of ECF.

Herein, we present the case of a 35-year-old man admitted to the hospital with presumed abdominal wall cellulitis. However, a series of events provided evidence supporting the diagnosis of ECF. Therefore, we elected to conduct CT fistulography, which provides more accurate anatomical details compared to a simple CT scan.

CASE PRESENTATION

Chief complaints

Abdominal wall swelling and pain for a week.

History of present illness

A 35-year-old man presented to the outpatient department with painful swelling and mass formation over the right lower quadrant abdominal wall for one week. No fever or gastrointestinal symptoms were reported. Oral intake and defecation were normal. The patient was hospitalized with a suspected diagnosis of cellulitis.

History of past illness

The patient was diagnosed with acute appendicitis and underwent an appendectomy 15 years ago in 2006. No history of underlying abdominal malignancy, inflammatory bowel disease, abdominal trauma,

or other gastrointestinal diseases was reported.

Personal and family history

There was no family history of abdominal neoplasms, inflammatory bowel disease, or ECF. The patient exhibited normal social functioning and self-care.

Physical examination

The vital signs, including body temperature, were within the normal ranges. Abdominal palpation revealed a mass over the right lower abdominal wall without visible opening and suspected abscess formation. Local abdominal tenderness and redness over purulence were noted. No nausea, diarrhea, muscle guarding, or bloating was observed, which led to the initial diagnosis of cellulitis.

Laboratory examinations

In outpatient department, we performed a minimal incision of the lesion to collect discharge for bacterial culture and blood analysis was also performed. Lab reports revealed a white blood cell count of 20.17 × 10^3/μL, 79.9% neutrophils and 12.4% lymphocytes, and a serum C-reactive protein concentration of 19.60 mg/dL. The bacterial culture of the lesion pus revealed the presence of *Enterococcus* sp. Based on these results, ECF was suspected.

Imaging examinations

We performed a colonoscopy and observed inflammation in the ileocecal valve region (Figure 1). CT of the abdomen in the axial view suggested that the colon was in close contact with the abdominal wall (Figure 2A), highly suggestive of ECF. We conducted CT fistulography by injecting contrast dye into the carbuncle for a more detailed radiographic view and a definitive diagnosis. Images after contrast administration showed the presence of contrast dye in both the abdominal wall and the colon (Figure 2B). Coronal images showed contrast dye retention in the subcutaneous area (Figure 2C) with penetration through the abdominal wall (Figure 2D) into the colon (Figure 2E).

FURTHER DIAGNOSTIC WORK-UP

The laboratory results and the imaging examinations indicated the existence of a cecocutaneous fistula. Therefore, we performed a diagnostic laparoscopy, during which we could observe severe adhesion of the colon to the abdominal wall. This evidence allowed us to formulate the final diagnosis of the cecocutaneous fistula.

TREATMENT

The patient underwent laparoscopic right hemicolectomy, reanastomosis of ileum and transverse colon, and peritoneal repair. During surgery, severe adhesion of the colon to the abdominal wall was noted (Figure 3A). After tissue adhesiolysis (Figure 3B), colon resection, and reanastomosis, a peritoneal defect was reported. We thus performed peritoneal repair with a V-LOC suture line (COVIDIEN™ 1-0 V-LOC, Medtronic, Ireland) to prevent hernia and adhesion (Figure 3C). Upon debridement of the infected abdominal wall, a fascial defect due to the outer opening of the fistula was noted (Figure 4A). Finally, a Penrose drainage tube was placed (Figure 4B). The surgical specimen consisted of the resected colon with attached peritoneum (Figure 4C). The histopathological results suggested a fistula with multifocal chronic inflammation. Microscopically, abscess formation with focal regeneration atypia of the soft tissue were found, with no granulomatous inflammation.

OUTCOME AND FOLLOW-UP

After surgery, we kept administering antibiotics with Ampicillin 1g + Sulbactam 0.5g IV Q6H and used chlorhexidine gluconate 2% solution for daily skin surface disinfection. The wound remained stable without contracting infections. Swelling and redness over the abdominal wall gradually improved. The highest temperature during the hospital stay was 37.3C on the fourth day after the operation. The final data before discharging were a white blood cell count of 11.44 × 103/μL, 68.9% neutrophils and 22.1% lymphocytes, and a serum C-reactive protein concentration of 1.99 mg/dL. The patient was discharged from the hospital one week after surgery. No wound infection or gastrointestinal symptoms were noted during outpatient follow-up 6 mo after surgery. The patient's oral intake recovered due to the short course of treatment and the absence of any further surgical operation. The patient was satisfied with the treatment outcome, and further hospitalization was not required. The treatment timeline from

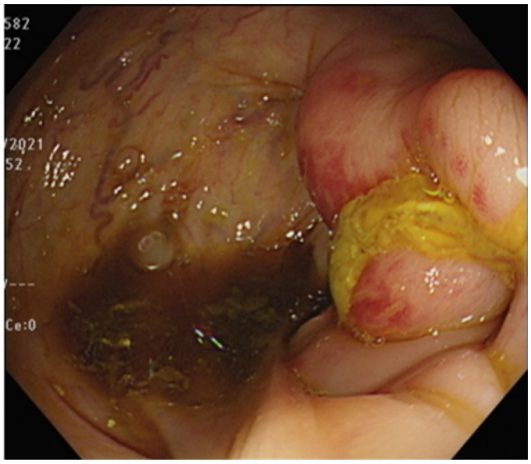

DOI: 10.4240/wjgs.v14.i10.1161 **Copyright** ©The Author(s) 2022.

Figure 1 Colitis in the ileocecal valve region.

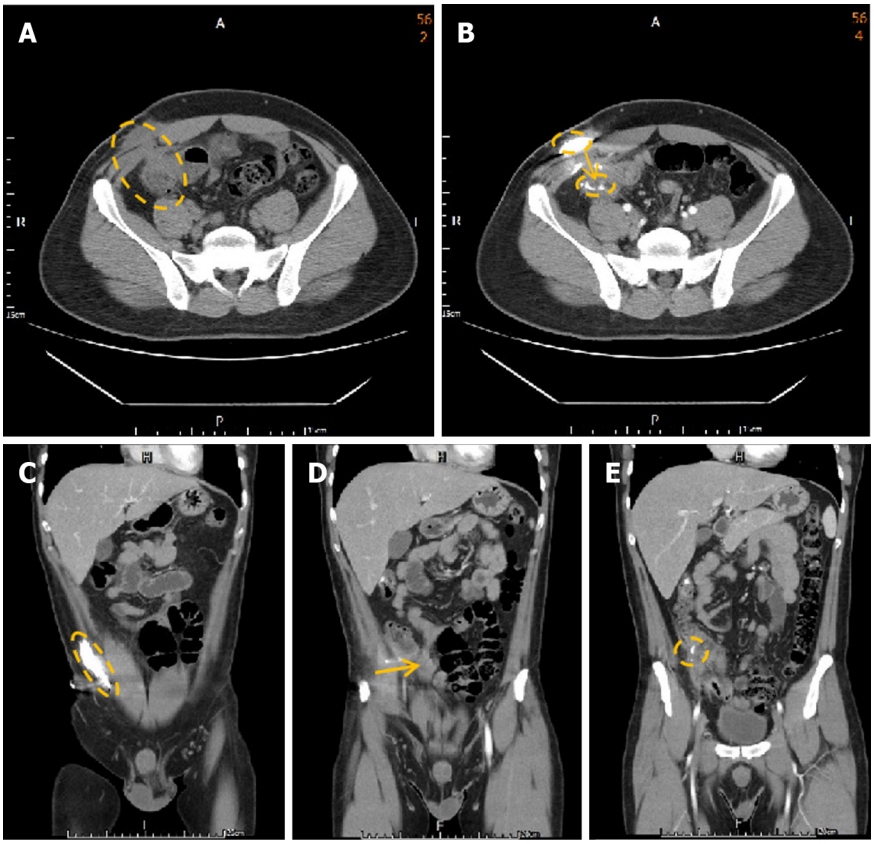

DOI: 10.4240/wjgs.v14.i10.1161 **Copyright** ©The Author(s) 2022.

Figure 2 Abdominal computed tomography with contrast injection from the abdominal opening. A: The axial computed tomography (CT) demonstrates the colon in close contact with the abdominal wall; B: The axial CT with contrast injection into the abdominal carbuncle demonstrates the canal between the abdominal wall and colon; C: Contrast was injected from the carbuncle and accumulated in the subcutaneous area, indicating abscess formation; D: Contrast dye extended through the canal between the abdominal wall and colon; E: Contrast finally arrived at the colon.

admission to discharge is shown in Figure 5.

DISCUSSION

Although cecocutaneous fistulae are rare, they still contribute to considerable morbidity and mortality. Major etiological factors of cecocutaneous fistula include abdominal tuberculosis, neoplasm of the appendix or cecum, leakage from the appendiceal stump, and inflammatory bowel disease[1,5]. In

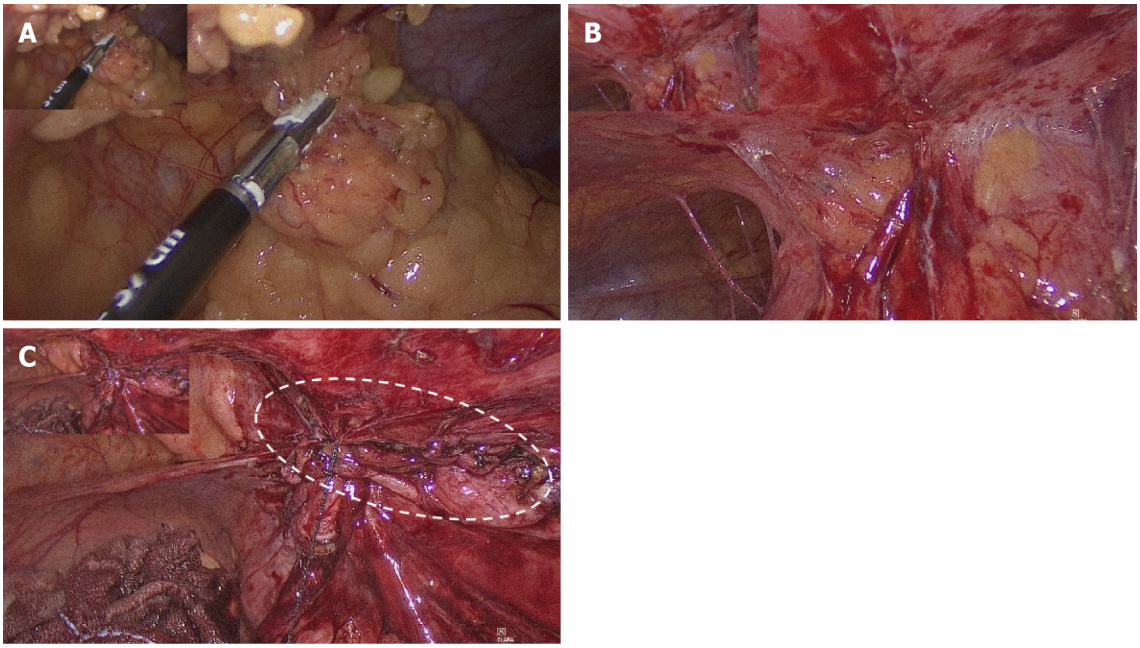

DOI: 10.4240/wjgs.v14.i10.1161 **Copyright** ©The Author(s) 2022.

Figure 3 Intraoperative laparoscopic images. A: Severe adhesion of the colon with the abdominal wall; B: After tissue adhesiolysis, severe peritoneal adhesion was noted; C: After colon resection and re-anastomosis, a peritoneal defect was found; peritoneal repair with V-LOC suture line was thus performed to prevent hernia and adhesion.

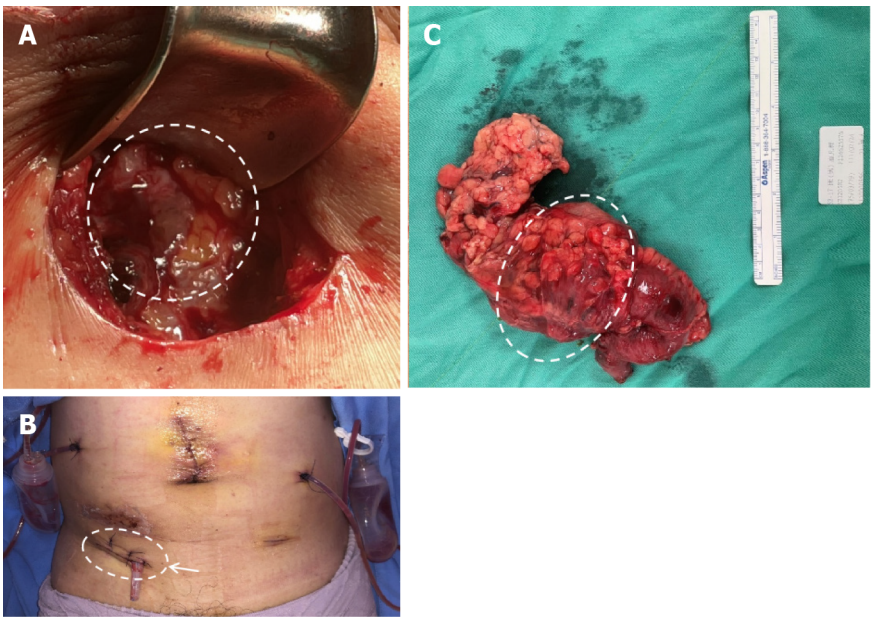

DOI: 10.4240/wjgs.v14.i10.1161 **Copyright** ©The Author(s) 2022.

Figure 4 Postoperative image. A: Fascia defect due to infection caused by the external opening of the fistula into the subcutaneous layer; B: Fascia defect post debridement and closure and Penrose drainage tube placement; C: Specimen including the resected colon with the attached peritoneum.

addition, some cases of cecocutaneous fistula were reported as related to a previous appendectomy[6], while some others were related to an underlying stump appendix[7]. Investigation of the patient's history was negative for abdominal malignancy, inflammatory bowel disease, abdominal trauma, or any other gastrointestinal disease. The histopathological report of the resected colon showed a fistula with multifocal chronic inflammation. Microscopically, it evidenced abscess formation with focal regeneration atypia of the soft tissues, with no granulomatous inflammation. The single abnormal finding in the history was the appendectomy in 2006, which was preliminarily compatible with the result of the diagnostic laparoscopy (cecum attached to the peritoneum). Appendectomy might have been a possible reason for the fistula.

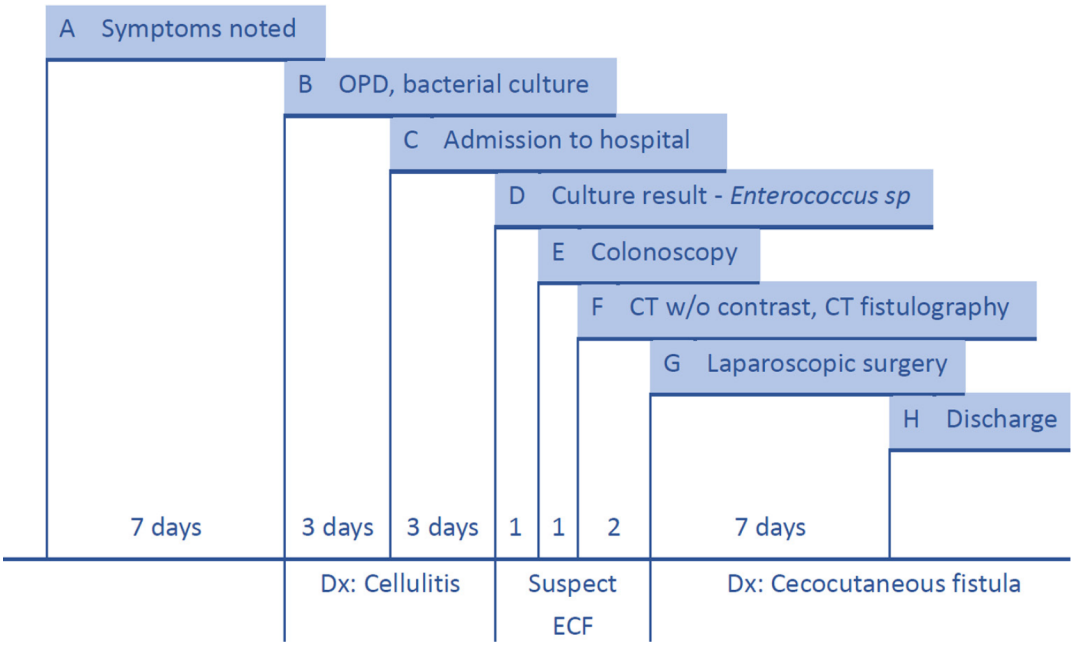

DOI: 10.4240/wjgs.v14.i10.1161 **Copyright** ©The Author(s) 2022.

Figure 5 Timeline. A: Redness and swelling over the right lower quadrant abdominal wall were noted; B: The patient came to the outpatient department for help; discharge from the carbuncle abscess was collected for bacterial culture. Blood analysis was performed; C: The patient was admitted to our hospital under the diagnosis of cellulitis (redness and a mass formation over the abdominal wall without visible opening or intestinal tract symptoms); D: The bacterial culture of the discharge produced Enterococcus sp. Enterocutaneous fistula was suspected; E: We performed a colonoscopy and observed inflammation in the ileocecal valve region; F: Abdominal computed tomography (CT) without contrast suggested that the colon was in close contact with the abdominal wall. We thus performed CT fistulography; G: Diagnostic laparoscopy showed severe adhesion of the colon to the abdominal wall. We conducted laparoscopic right hemicolectomy and reanastomosis; H: The patient was discharged from the hospital one week after surgery.

Different protocols and modalities for the treatment of ECF have been reported in the literature[3,8,9]. Most of them include four phases: Treatment of sepsis, nutrition support, definition of fistula anatomy, and definitive intervention. Surgical intervention is not necessary in all cases; some fistulae close spontaneously. Patients with ECF associated with independent adverse factors conditioning non-spontaneous closure (including sepsis, high output, and multiple fistulae) may need surgical treatment [10]. Besides surgery, there are several other methods for the management of ECF, including negative pressure wound therapy (NPWT), stent placement, fibrin glues, and endoscopic management[5]. Stent placement plays an important role in the drainage of sepsis[11]. Recently, a 3D-printed patient-personalized fistula stent was successfully implanted in patients, reducing the fistula output[12]. NPWT has the advantage of lowering the effluent volume of enteric fistulae, in some cases leading to spontaneous closure; however, it often entails a longer treatment time. Fibrin glues are an option when the fistula has low-to-medium effluent volume, surgery is not possible, the fistula has complex branching, or is only accessible from a small external orifice[13,14]. Endoscopic minimally invasive management is emerging as a choice for gastrointestinal fistulae, and it may be safer and more effective than surgery[15,16]. Surgery is usually time-consuming and requires extensive adhesiolysis[17].

In this case, we suspected adhesions of the colon and peritoneum. The patient opted for a treatment that would ensure low recurrence and a prompt resolution. Considering his young age and his relatively stable condition, we finally opted for surgery rather than endoscopic management or conservative treatment. We performed laparoscopic resection with reanastomosis, which has a lower recurrence rate than oversewing surgery[18].

Despite the wealth of treatments for ECF, diagnosis has always been challenging. The diagnostic process generally includes X-ray fistulography and abdominal CT with intravenous contrast. X-ray fistulography has recently been replaced by abdominal CT, which better reveals the anatomy of the gastrointestinal tract and provides more information about the associated pathology. If anatomical details obtained using X-ray fistulography and CT are insufficient, CT fistulography helps to identify and determine the extent of the abnormal channel[3,4].

In this case, physical examination revealed a mass over the right lower abdominal wall without visible opening and suspected abscess formation. Absence of nausea, diarrhea, abdominal tenderness, muscle guarding, or bloating led to the initial diagnosis of cellulitis. Bacterial culture revealed *Enterococcus* sp., and CT images before administering the contrast agent showed that the colon was in close contact with the abdominal wall. ECF was thus highly suspected. Because CT with intravenous contrast agent may provide insufficient anatomical details concerning fistulae, we conducted CT fistulography by injecting contrast dye into the carbuncle. The resulting images showed definitive evidence of a

cecocutaneous fistula.

Though CT fistulography is an option that provides more detailed anatomical information, it is still seldom utilized in patients with insufficient evidence of fistula[3]. ECF without gastrointestinal symptoms may mimic cellulitis. Once a fistula is suspected according to our diagnostic evaluation (*e.g.*, bacterial culture, X-ray fistulography, CT without contrast), CT fistulography can be used to diagnose or rule out ECF.

A significant problem with CT fistulography is that the contrast agent sometimes cannot be administered through the fistula because of adhesions and continuous purulent discharge; in such cases, magnetic resonance imaging (MRI) may be considered. MRI has superior soft tissue discrimination. Magnetic resonance enterography (which is a variant of MRI, has been used to rule out small bowel pathology and delineate fistula anatomy. Magnetic resonance enterography has also been used to detect colon disease[19], but it was initially used for small bowel investigation. Therefore, its application as diagnostic imaging of the colon still warrants further evidence.

The current challenge is that a simple CT scan may provide insufficient anatomical details of the fistula[3]. Furthermore, most advanced examinations, including CT and MRI, are expensive. Thus, a fistula may get neglected following a plain CT scan, and CT fistulography/MRI may not be arranged. In this case, we suspected ECF due to the positive bacterial culture and performed CT fistulography. However, most physicians may not perform advanced examinations without evidence suggesting fistula. Therefore, several ECF cases may be neglected or misdiagnosed. Despite the availability of various diagnostic methods, the indications for performing further examinations are pivotal in the process and require adequate discussion.

CONCLUSION

ECF without gastrointestinal symptoms or visible openings may be misdiagnosed as cellulitis. X-ray fistulography and abdominal CT sometimes provide insufficient anatomical details, thus leading to misdiagnosis. CT fistulography may rule out ECF in patients presenting with cellulitis if examinations are suggestive.

ACKNOWLEDGEMENTS

The authors wish to acknowledge the assistance of the people at the Department of Surgery, Tri-Service General Hospital Songsang Branch. This report would not have been possible without their efforts in data collection and interprofessional collaboration in treating this patient.

FOOTNOTES

Author contributions: Wu TY, Pu TW, Lo KH, Chen CY, Hu JM, and Kang JC designed and performed the research; Wu TY and Pu TW analyzed the data and wrote the manuscript.

Informed consent statement: Informed written consent was obtained from the patient to publish this report and any accompanying images.

Conflict-of-interest statement: The authors declare no conflict of interest.

CARE Checklist (2016) statement: The authors have read the CARE Checklist (2016), and the manuscript was prepared and revised according to it.

Country/Territory of origin: Taiwan

ORCID number: Tung-Yen Wu 0000-0003-3645-7830; Kuang-Hua Lo 0000-0002-8661-8842; Chao-Yang Chen 0000-0002-2246-7635; Je-Ming Hu 0000-0002-7377-0984; Jung-Cheng Kang 0000-0001-7511-5337; Ta-Wei Pu 0000-0002-0538-407X.

S-Editor: Ma YJ
L-Editor: A
P-Editor: Ma YJ

REFERENCES

1 **Kumar P**, Maroju NK, Kate V. Enterocutaneous fistulae: etiology, treatment, and outcome - a study from South India. *Saudi J Gastroenterol* 2011; **17**: 391-395 [PMID: 22064337 DOI: 10.4103/1319-3767.87180]

2 **Falconi M**, Pederzoli P. The relevance of gastrointestinal fistulae in clinical practice: a review. *Gut* 2001; **49** Suppl 4: iv2-i10 [PMID: 11878790 DOI: 10.1136/gut.49.suppl_4.iv2]

3 **Schecter WP**, Hirshberg A, Chang DS, Harris HW, Napolitano LM, Wexner SD, Dudrick SJ. Enteric fistulas: principles of management. *J Am Coll Surg* 2009; **209**: 484-491 [PMID: 19801322 DOI: 10.1016/j.jamcollsurg.2009.05.025]

4 **Agrawal V**, Prasad S. Appendico-cutaneous fistula: a diagnostic dilemma. *Trop Gastroenterol* 2003; **24**: 87-89 [PMID: 14603830]

5 **Ghimire P**. Management of Enterocutaneous Fistula: A Review. *JNMA J Nepal Med Assoc* 2022; **60**: 93-100 [PMID: 35199684 DOI: 10.31729/jnma.5780]

6 **Genier F**, Plattner V, Letessier E, Armstrong O, Heloury Y, Le Neel JC. [Post-appendectomy fistulas of the cecum. Apropos of 22 cases]. *J Chir (Paris)* 1995; **132**: 393-398 [PMID: 8550699]

7 **Agostinho N**, Bains HK, Sardelic F. Enterocutaneous Fistula Secondary to Stump Appendicitis. *Case Rep Surg* 2017; **2017**: 6135251 [PMID: 28473939 DOI: 10.1155/2017/6135251]

8 **Datta V**, Engledow A, Chan S, Forbes A, Cohen CR, Windsor A. The management of enterocutaneous fistula in a regional unit in the United kingdom: a prospective study. *Dis Colon Rectum* 2010; **53**: 192-199 [PMID: 20087095 DOI: 10.1007/DCR.0b013e3181b4c34a]

9 **Gribovskaja-Rupp I**, Melton GB. Enterocutaneous Fistula: Proven Strategies and Updates. *Clin Colon Rectal Surg* 2016; **29**: 130-137 [PMID: 27247538 DOI: 10.1055/s-0036-1580732]

10 **Martinez JL**, Luque-de-Leon E, Mier J, Blanco-Benavides R, Robledo F. Systematic management of postoperative enterocutaneous fistulas: factors related to outcomes. *World J Surg* 2008; **32**: 436-43; discussion 444 [PMID: 18057983 DOI: 10.1007/s00268-007-9304-z]

11 **Alexander RJ**, Nash GF. Enterocutaneous fistula stent. *Ann R Coll Surg Engl* 2009; **91**: 619-620 [PMID: 19842252 DOI: 10.1308/rcsann.2009.91.7.619b]

12 **Huang JJ**, Ren JA, Wang GF, Li ZA, Wu XW, Ren HJ, Liu S. 3D-printed "fistula stent" designed for management of enterocutaneous fistula: An advanced strategy. *World J Gastroenterol* 2017; **23**: 7489-7494 [PMID: 29151703 DOI: 10.3748/wjg.v23.i41.7489]

13 **Assenza M**, Rossi D, De Gruttola I, Ballanti C. Enterocutaneous fistula treatment: case report and review of the literature. *G Chir* 2018; **39**: 143-151 [PMID: 29923483]

14 **Avalos-González J**, Portilla-deBuen E, Leal-Cortés CA, Orozco-Mosqueda A, Estrada-Aguilar Mdel C, Velázquez-Ramírez GA, Ambriz-González G, Fuentes-Orozco C, Guzmán-Gurrola AE, González-Ojeda A. Reduction of the closure time of postoperative enterocutaneous fistulas with fibrin sealant. *World J Gastroenterol* 2010; **16**: 2793-2800 [PMID: 20533600 DOI: 10.3748/wjg.v16.i22.2793]

15 **Rogalski P**, Daniluk J, Baniukiewicz A, Wroblewski E, Dabrowski A. Endoscopic management of gastrointestinal perforations, leaks and fistulas. *World J Gastroenterol* 2015; **21**: 10542-10552 [PMID: 26457014 DOI: 10.3748/wjg.v21.i37.10542]

16 **Cereatti F**, Grassia R, Drago A, Conti CB, Donatelli G. Endoscopic management of gastrointestinal leaks and fistulae: What option do we have? *World J Gastroenterol* 2020; **26**: 4198-4217 [PMID: 32848329 DOI: 10.3748/wjg.v26.i29.4198]

17 **Bhama AR**. Evaluation and Management of Enterocutaneous Fistula. *Dis Colon Rectum* 2019; **62**: 906-910 [PMID: 31283590 DOI: 10.1097/DCR.0000000000001424]

18 **Lynch AC**, Delaney CP, Senagore AJ, Connor JT, Remzi FH, Fazio VW. Clinical outcome and factors predictive of recurrence after enterocutaneous fistula surgery. *Ann Surg* 2004; **240**: 825-831 [PMID: 15492564 DOI: 10.1097/01.sla.0000143895.17811.e3]

19 **Somwaru AS**, Khanijow V, Katabathina VS. Magnetic resonance enterography, colonoscopy, and fecal calprotectin correlate in colonic Crohn's disease. *BMC Gastroenterol* 2019; **19**: 210 [PMID: 31805875 DOI: 10.1186/s12876-019-1125-7]

World Journal of Gastrointestinal Surgery

Submit a Manuscript: https://www.f6publishing.com

World J Gastrointest Surg 2022 October 27; 14(10): 1169-1178

DOI: 10.4240/wjgs.v14.i10.1169

ISSN 1948-9366 (online)

CASE REPORT

Immunoglobulin G4-related disease in the sigmoid colon in patient with severe colonic fibrosis and obstruction: A case report

Wen-Li Zhan, Liang Liu, Wei Jiang, Fang-Xun He, Hai-Tao Qu, Zhi-Xin Cao, Xiang-Shang Xu

Specialty type: Gastroenterology and hepatology

Provenance and peer review: Unsolicited article; Externally peer reviewed.

Peer-review model: Single blind

Peer-review report's scientific quality classification

Grade A (Excellent): 0
Grade B (Very good): 0
Grade C (Good): C, C, C
Grade D (Fair): D
Grade E (Poor): 0

P-Reviewer: Ashihara N, Japan; Cai W, China; Vujasinovic M, Sweden;

Received: July 10, 2022
Peer-review started: July 10, 2022
First decision: August 19, 2022
Revised: September 3, 2022
Accepted: October 18, 2022
Article in press: October 18, 2022
Published online: October 27, 2022

Wen-Li Zhan, Liang Liu, Wei Jiang, Fang-Xun He, Zhi-Xin Cao, Xiang-Shang Xu, Department of Gastrointestinal Surgery, Tongji Hospital, Huazhong University of Science and Technology, Wuhan 430030, Hubei Province, China

Hai-Tao Qu, Anorectal Disease Center, The First Affiliated Hospital of Henan University of Traditional Chinese Medicine, Zhengzhou 450000, Henan Province, China

Corresponding author: Xiang-Shang Xu, MD, PhD, Associate Professor, Doctor, Department of Gastrointestinal Surgery, Tongji Hospital, Huazhong University of Science and Technology, No. 1095 Jiefang Avenue, Wuhan 430030, Hubei Province, China. xsxu@tjh.tjmu.edu.cn

Abstract

BACKGROUND

Immunoglobulin G4-related disease (IgG4-RD) is an immune-mediated condition characterized by abundant IgG4 positive plasma cells and fibrosis in the affected tissues. It affects most parts of the body; however, there are not many reports on IgG4-RD involving the colon.

CASE SUMMARY

A 50-year-old man complaining of intermittent fever for more than two years was referred to our hospital. Based on various investigations before surgery, we diagnosed him with chronic perforation of the sigmoid colon caused by inflammatory change or tumor. IgG blood tests before the operation suggested IgG4-RD, and postoperative pathology confirmed this prediction.

CONCLUSION

We present a patient with IgG4-RD with colon involvement, which is an uncommon site. This report will expand the understanding of IgG4-RD in unknown tissues.

Key Words: Immunoglobulin G4-related disease; Chronic colon disease; Plasma cells; Fibrosis; Obstruction; Case report

Core Tip: Immunoglobulin G4-related disease (IgG4-RD) is characterized by abundant IgG4 positive plasma cells and fibrosis in the affected tissues. It can affect most parts of the body, but there were not many reports of IgG4-RD in the intestines. This patient was an IgG4-RD case to be reported in the colon, which was identified by computed tomography, magnetic resonance imaging, pathology and blood tests of IgGs. This case report will help expand the understanding of IgG4-RD in some unknown tissues.

Citation: Zhan WL, Liu L, Jiang W, He FX, Qu HT, Cao ZX, Xu XS. Immunoglobulin G4-related disease in the sigmoid colon in patient with severe colonic fibrosis and obstruction: A case report. *World J Gastrointest Surg* 2022; 14(10): 1169-1178
URL: https://www.wjgnet.com/1948-9366/full/v14/i10/1169.htm
DOI: https://dx.doi.org/10.4240/wjgs.v14.i10.1169

INTRODUCTION

Immunoglobulin G4-related disease **(**IgG4-RD) is an immune-mediated condition characterized by infiltration of IgG4 positive plasma cells and fibrosis in the affected tissues[1]. It was first identified as a distinct disease in 2003[2]. Due to lack of understanding in the past, this condition was misdiagnosed or could not be diagnosed. In recent years, awareness of the disease has increased over the past 20 years. The American College of Rheumatology (ACR) and European League Against Rheumatism (EULAR) IgG4-RD criteria were also formed and published[3]. Hence, many patients were diagnosed with IgG4-RD and received personalized treatment. Although it can affect almost any part of the body, it shows a strong preference for some organs (Figure 1), including salivary glands, lacrimal glands and orbitals, pancreas and biliary ducts, lungs, kidneys, aorta and retroperitoneum, meninges, and thyroid gland[4,5]. Typical manifestations of IgG4-RD are enlarged salivary and lacrimal glands, orbital pseudotumor, pancreatitis, sclerosing cholangitis, retroperitoneal fibrosis, tubular interstitial nephritis, and Liddell's thyroiditis[6].

Histopathology is still required to confirm the diagnosis, with the main histological features being IgG4-positive plasma cell infiltration, storiform fibrosis, and obliterative phlebitis[1]. Increased IgG4-positive plasma cells are seen in nearly all affected tissues; however, there is no specific clinical manifestation. Certain diseases such as lymphoma, vasculitis, and inflammatory bowel disease may also exhibit increased IgG4-positive plasma cells without storiform fibrosis and obliterative phlebitis[7,8]. In addition, the latter two features are not evident in the bone marrow and lymph nodes, making these two sites undesirable for histopathological investigations[9]. Additionally, the imaging features of IgG4-RD are as follows: A diffusely enlarged pancreas surrounded by capsule-like edema ("sausage-shaped" pancreas) and the anterolateral aorta wrapped by soft tissue in the case of retroperitoneal fibrosis[10-12]. However, isolated radiological findings are insufficient for diagnosis. ^{18}Fluorodeoxyglucose-positron emission tomography (PET) can scan the entire body for staging and help find the sampling site[13].

IgG4-RD's incidence is still underestimated because the disease is not clinically manifested and rarely leads to immediate organ failure[14]. Many patients are diagnosed accidentally or through histopathology after surgical resection[15]. IgG4-RD is a multi-organ disease that can easily be confused with malignancies, infections, or other conditions. It is also characterized by slow disease progression, but exacerbations to fibrotic disease often lead to irreversible organ dysfunction[8]. Therefore, early recognition and diagnosis are of vital importance.

Intestinal involvement is not common in IgG4-RD, although sporadic reports have been published [16-19]. Therefore, more cases are needed to demonstrate that IgG4-RD can involve the gut. In this article, we will report the data of a patient with IgG4-RD involving the sigmoid colon, hoping to increase the understanding of IgG4-RD disease.

CASE PRESENTATION

Chief complaints

A 50-year-old man presented with intermittent fever for more than two years.

History of present illness

Intermittent fever occurred for more than two years. The body temperature remained at approximately 37.5 °C, and the fever usually occurred in the afternoon for 3–4 d a week. The fever was rarely high and often resolved without any treatment. The patient had been to the department of infectious diseases for treatment; however, no specific infection was found.

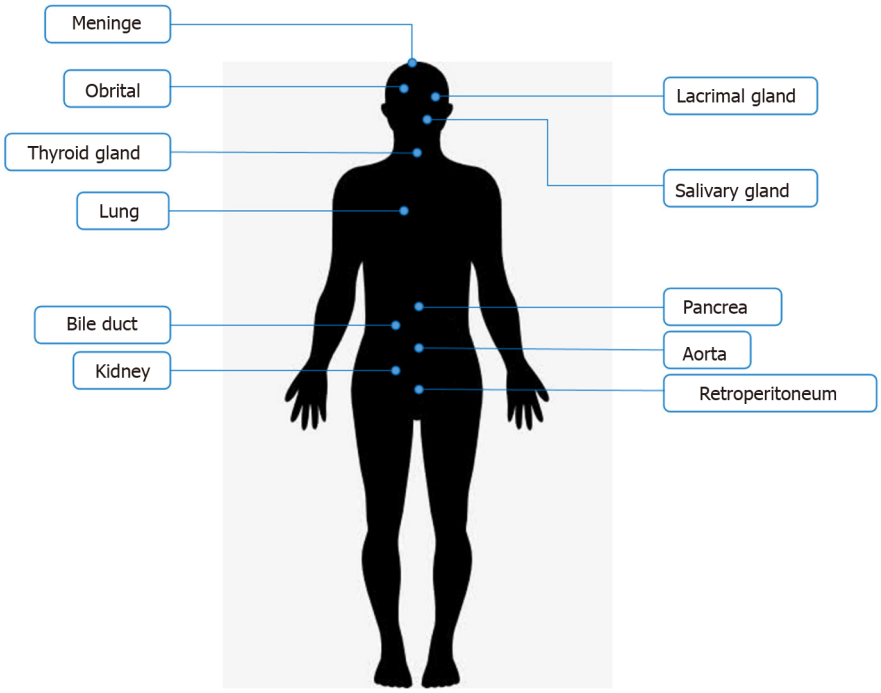

DOI: 10.4240/wjgs.v14.i10.1169

Figure 1 Commonly affected organs in immunoglobulin G4-related disease. Immunoglobulin G4-related disease often appears in salivary glands, lacrimal glands, pancreas, and biliary tract.

Six months ago, he had frequent and urgent micturition and increased nocturia. He went to the urology department, where prostatic hyperplasia was considered after ultrasound detection, but there was no cystoscopy or biopsy to be done. Then he was treated with tamsulosin hydrochloride and the symptoms, although partially alleviated, did not disappear fully.

Two months ago, he began to experience increased bowel movements and a feeling of incomplete bowel movements, accompanied by a bloated lower abdomen. So he came to the Gastrointestinal Surgery Clinic, and we ordered a colonoscopy and admitted him to the hospital.

History of past illness

Our patient had a 30-year-old history of hepatitis B without blatant virus replication. He also had allergic rhinitis for > 20 years, with the onset usually in August and September every year and relieved by itself after the season. He was allergic to ragweed pollen in 2017 and was cured by mometasone furoate nasal spray combined with cetirizine hydrochloride. He has never developed sinusitis.

Personal and family history

The main drugs used in the patient's medical records were interferon, cetirizine hydrochloride, mometasone furoate, and tamsulosin hydrochloride. He did not have a smoking and alcohol consumption history.

His family had no apparent history of colon tumors and autoimmune disease. Both his father and mother had died of cardiovascular diseases. Additionally, his mother had a history of hepatitis B.

Physical examination

Physical examination showed mild tenderness above the symphysis pubis in the lower abdomen without rebound pain. No other abnormality was seen.

Laboratory examinations

The white blood cells count was normal as the baseline level, and hemoglobin was 92 g/L. The biochemical blood tests were within the normal range, including transaminases, bilirubin, amylase, and lipase. The tumor markers carcinoembryonic assay, cancer antigen 19-9, cancer antigen 72-4, and prostate-specific antigen were normal, while the urine culture and tuberculosis screening tests were negative. Nevertheless, this patient had a positive fecal occult blood test.

Imaging examinations

PET/computed tomography (CT) revealed a thick-walled cystic structure above the bladder, which was approximately 8.1 cm × 7.1 cm in size with increased radioactive uptake, and the maximum standard

uptake value (SUVmax) was 6.0. Thus, a diagnosis of a tumor or chronic infection-related mass was made. PET-CT examination did not find high uptake in the parotid gland, pancreas, biliary tract, and prostate (Figure 2).

An enhancement CT scan of the entire abdomen showed a noticeable expansion of the proximal sigmoid colon with significant intestinal content. The intestinal wall was thickened with contrast enhancement, and the boundary between the sigmoid colon and bladder was not evident in the apparent bladder compression (Figure 3). Hence, the possibility of the colonic diverticulum with infection or tumor was considered. We scanned the pancreas by CT and magnetic resonance imaging (Figure 4) and found an enlarged pancreas similar to the "sausage-shaped" pancreas finding in IgG4-RD.

Endoscopy and biopsy pathology

In the electronic colonoscopy, the lesion was located at the sigmoid colon. It was about 40 cm away from the anus with a blind cavity of 6 cm in diameter. The intestinal cavity is next to the blind hole with a large number of feces. Therefore, the colonoscope could no longer observe upwards (Figure 5).

A tissue biopsy was performed on the thickened and enlarged part of the sigmoid colon. While the intestinal wall of the biopsy was hard, the bleeding was negligible. The biopsy pathology chiefly showed inflammatory necrotic and granulomatous tissue; no defined tumorous cells were seen (Figure 6).

Initial diagnosis

Based on all the preoperational investigations, the initial diagnosis was an inflammatory disease of the sigmoid colon with chronic intestinal perforation, with a localized pelvic abscess formed between the sigmoid colon and bladder. However, the possibility of sigmoid colon tumors could not be ruled out.

Further diagnostic work-up

After the operation, pathological results (Figure 7) showed multiple ulcers distributed in the diseased intestinal wall. The ulcers were surrounded by obliterative phlebitis, widespread inflammatory granulation, and fibrous tissue. Many plasma cells and neutrophils infiltrated the lesion tissues. Furthermore, immunohistochemistry showed high IgG4-positive cells in the diseased tissues ($IgG4^+/IgG^+$ ratio was about 60%, $IgG4^+$/HPF was about 110 cells). Therefore, the pathological diagnosis was IgG4-RD in the sigmoid colon.

Immunology-related blood indices (Tables 1 and 2) showed that the IgG4 level was 1. 830 g/L, which was higher than normal (for IgG4-RD, the cut-off value is > 1. 35 g/L).

FINAL DIAGNOSIS

Combined with pathology results, immunohistochemistry, and blood IgG indices, we diagnosed this patient with IgG4-RD involved sigmoid colon and pancreas.

TREATMENT

After signing the informed consent from the patient, we performed exploratory laparoscopic surgery, and during the surgery, we found that the patient's sigmoid colon was too long, and the proximal sigmoid colon moved down and attached to the left side of the bladder, forming a 6 cm × 6 cm mass. There were no apparent abnormalities in the stomach, small intestine, and the rest of the colon and rectum. We tried to separate the periphery of the mass with a harmonic ultrasonic knife; however, the mass was very hard and closely adherent to the bladder. Therefore, the separation could not be completed under laparoscopy (Figure 8). We then switched to open surgery and used an electric knife to separate the sigmoid colon and mass from the bladder carefully. However, the electrosurgical resection was extremely difficult because the mass's boundary was unclear. Unlike the wall in common chronic abscesses, it was tough and similar to severe fibrotic tissue. After careful separation, we performed sigmoid resection plus descending colorectal anastomosis, and in order to prevent anastomotic leakage, we also performed transverse colostomy. The mass (mainly was the thicken colon wall, about 6 cm × 6 cm) and approximately 20 cm sigmoid colon were removed; however, many feces remained in the proximal colon, which might be caused by stenosis of the intestinal cavity and incomplete obstruction due to the lesion mass compression.

Table 1 Rheumatism immunoassay results

Test items	Results	Reference interval
Antinuclear antibody	Negative	Negative
Anti-nuclear chromatin antibody	1.0	≤ 4.0 negative
Anti-RNP-A antibody	< 0.2	< 1.0 negative
Anti-RNP-68 antibody	< 0.2	< 1.0 negative
Anti-Sm/nRNP antibody	< 0.2	< 1.0 negative
Anti-Sm antibody	< 0.2	< 1.0 negative
Anti-SS-A antibody	< 0.2	< 1.0 negative
Anti-Ro-52 antibody	< 0.2	< 1.0 negative
Anti-SS-B antibody	< 0.2	< 1.0 negative
Anti-Sci-70 antibody	< 0.2	< 1.0 negative
Anti-Jo-1 antibody	< 0.2	< 1.0 negative
Anti-ribosomal p protein antibody	< 0.2	< 1.0 negative
Anti-centromere b protein antibody	< 0.2	< 1.0 negative
Antineutrophil cytoplasmic antibody	Negative	Negative
Anti-protease 3 antibody	< 0.2	< 1.0 negative
Anti-myeloperoxidase antibody	< 0.2	< 1.0 negative
Anti-glomerular basement membrane antibody	< 0.2	< 1.0 negative

Table 2 Immunoglobulin G related indexes detection

Test items	Results	Reference interval
IgG	19.2	7.51-15.6
IgA	3.23	0.82-4.53
IgM	0.64	0.46-3.04
Complement 3	0.89	0.65-1.39
Complement 4	0.24	0.16-0.38
IgG1	10.20	4.05-10.11
IgG2	8.26	1.69-7.86
IgG3	0.368	0.11-0.85
IgG4	1.890	0.03-2.01 for IgG4-RD, cutoff value > 1.35

IgG4-RD: Immunoglobulin G4-related disease.

OUTCOME AND FOLLOW-UP

The patient recovered quickly after the operation and underwent a transverse colostomy three months later. We asked the rheumatology department and immunology doctors to provide a glucocorticoid treatment plan as follow-up treatment. After three months of treatment, the serum IgG4 level decreased to near the normal level. The patient did not have any abdominal discomfort and urination problems and also gained 5 kg in weight relative to before the operation.

DISCUSSION

The 2019 ACR and EULAR classification criteria for IgG4-RD (2019 ACR/EULAR IgG4-RD Criteria) are essential in understanding and treating IgG4-RD[3]. Although they list intestinal involvement as an

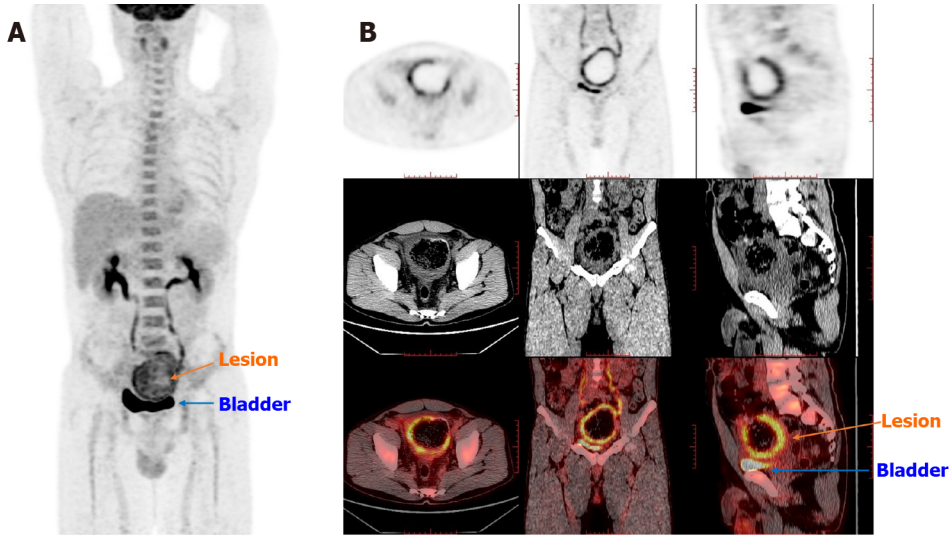

DOI: 10.4240/wjgs.v14.i10.1169 **Copyright** ©The Author(s) 2022.

Figure 2 Positron emission tomography/computed tomography findings. The thick-walled cystic structure above the bladder could be seen, the radioactive uptake was significantly increased, and the maximum standard uptake value reached 6.5. The diagnosis was considered inflammatory or a neoplastic lesion on the sigmoid colon adherent to the bladder. A: Coronal whole-body imaging showing high uptake values at the lesion site; B: Detailed imaging pictures of the lesion, including horizontal, sagittal and coronal.

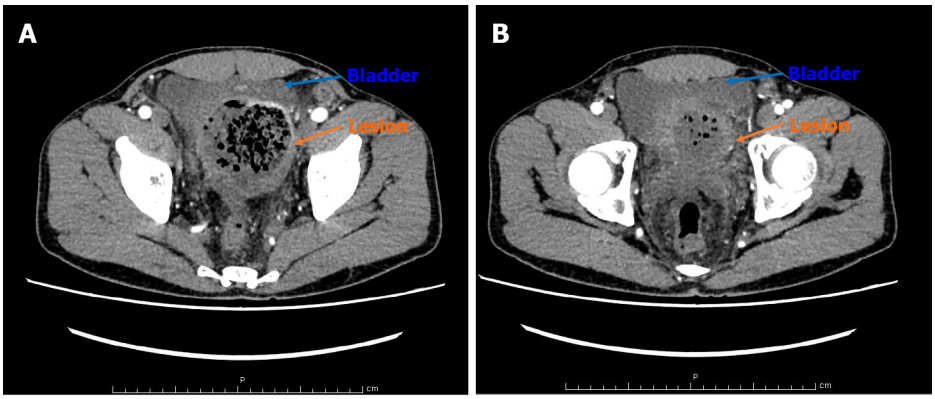

DOI: 10.4240/wjgs.v14.i10.1169 **Copyright** ©The Author(s) 2022.

Figure 3 Contrast-enhanced computed tomography scan of the abdomen findings. A: The proximal sigmoid colon was dilated. The middle colon wall was thickened. It was markedly enhanced in the arterial phase, representing the characteristics of neoplastic lesions or chronic abscesses; B: The sigmoid colon mass compressed the bladder, and the boundary between the bladder and the mass was unclear.

exclusion criterion[3], we reported colonic involvement, which is a unique finding in our patient. Although the patient had a history of allergic rhinitis, the IgG4 level in the blood was increased, exceeding the critical value for IgG4-RD. In the histochemistry detection, we found the plasma cells and IgG4-positive cells infiltration, $IgG4^+/IgG^+$ ratio up to 60%, 110 $IgG4^+$/HPF cells, obliterative phlebitis, and fibrous tissue in the lesion colon. According to the 2019 ACR/EULAR IgG4-RD Criteria[3], if case meets entry criteria and does not meet any exclusion criteria, proceed to step 3 evaluation, this patient could get a score of 42 (Dense lymphocytic infiltrate and storiform fibrosis with or without obliterative phlebitis, +13; Immunostaining, the $IgG4^+$:IgG^+ ratio is 41%–70% and $IgG4^+$ cells/HPF is ≥ 10, +14; Serum IgG4 concentration, > Normal but < 2× upper limit of normal, +4; Diffuse pancreas enlargement and capsule-like rim with decreased enhancement, +11). Therefore, this patient could be diagnosed as IgG4-RD is involved in the colon and pancreas.

When considering IgG4-RD, serum protein electrophoresis and IgG subclass tests should be used as initial investigations because approximately 70% of patients showed elevated serum IgG4 levels[7]. However, since IgG4 levels are not necessary for diagnosing IgG4-RD[8], serological testing, a simple, non-invasive method, can provide essential clues.

Steroids are the first-line treatment for IgG4-RD, and most patients respond well to glucocorticoid therapy[20]. In the 2019 ACR/EULAR IgG4-RD Criteria, failure to respond to glucocorticoids is a vital exclusion criterion for IgG4-RD, which illustrates their significance[3]. However, patients with incomplete remission and recurrence do exist[21]. Additionally, some patients' glucocorticoid-induced

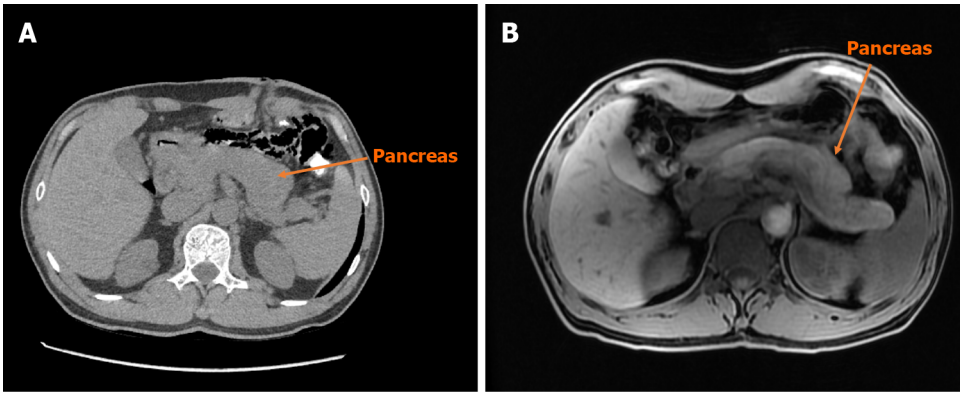

DOI: 10.4240/wjgs.v14.i10.1169 **Copyright** ©The Author(s) 2022.

Figure 4 Computed tomography and magnetic resonance imaging scan of the pancreas. A: The pancreas of the patient is diffusely enlarged, surrounded by capsule-like edema in computed tomography (CT) image; B: Magnetic resonance imaging image of the patient's pancreas is similar to CT.

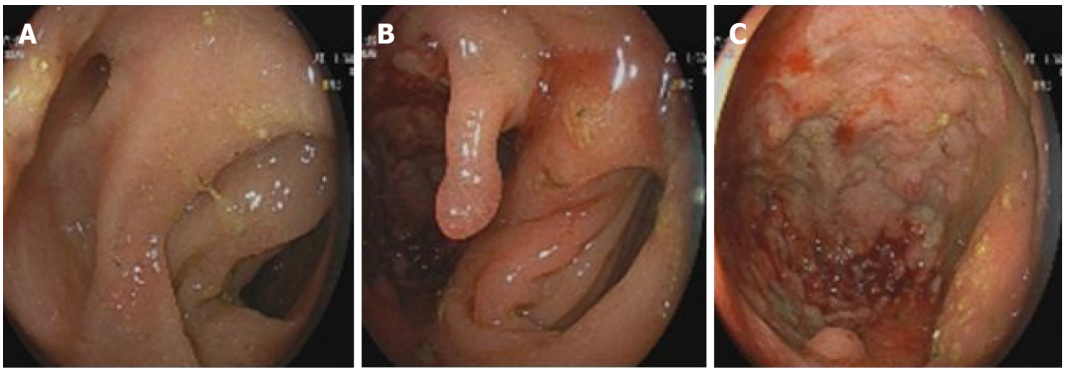

DOI: 10.4240/wjgs.v14.i10.1169 **Copyright** ©The Author(s) 2022.

Figure 5 Findings of the colonoscopy. A and B: From different angles, it could be seen that there were two cavities in the sigmoid colon, one of which was a blind cavity; C: It could be seen that the diseased colon was thickened and rough, and the tissue was so hard to do a biopsy.

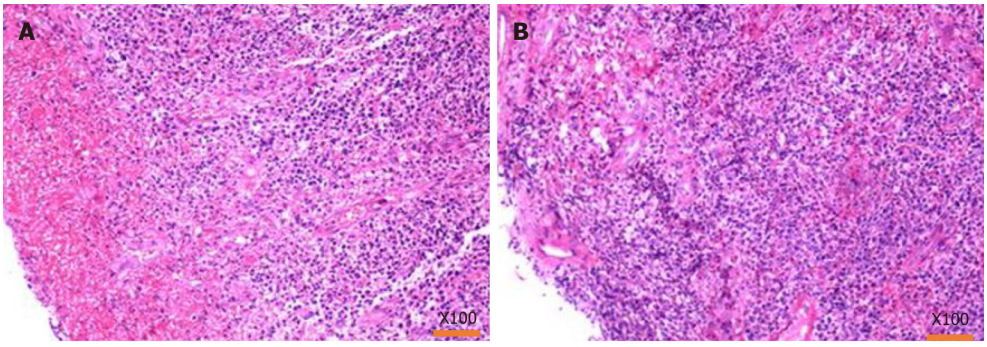

DOI: 10.4240/wjgs.v14.i10.1169 **Copyright** ©The Author(s) 2022.

Figure 6 Pathology of the biopsy by colonoscopy. A: Hematoxylin-eosin staining showed that the tissues were inflammatory hyperplasia changes, and a large number of inflammatory cells were infiltrated; however, there were no tumor cells; B: Results from different sampling sites.

hyperglycemia coupled with secondary pancreatic fibrosis complicates the treatment due to these toxic effects[22].

Significantly, due to hypergammaglobulinemia and plasma cell amplification in IgG4-RD, the clinical efficacy of rituximab (which targets CD20 and depletes B cells) was also remarkable[23]. The use of immunosuppressive drugs such as cyclophosphamide, mycophenolate, leflunomide, and tacrolimus and their combination with glucocorticoids in IgG4-RD remains to be further studied[24-27]. Early identification of IgG4-RD and treatment with glucocorticoids, rituximab, or other immunosuppressive therapies are critical because patients usually respond well to these treatments in the early stages of the disease. Importantly, when chronic pancreatitis and fibrotic disease occur, they are often irreversible [28].

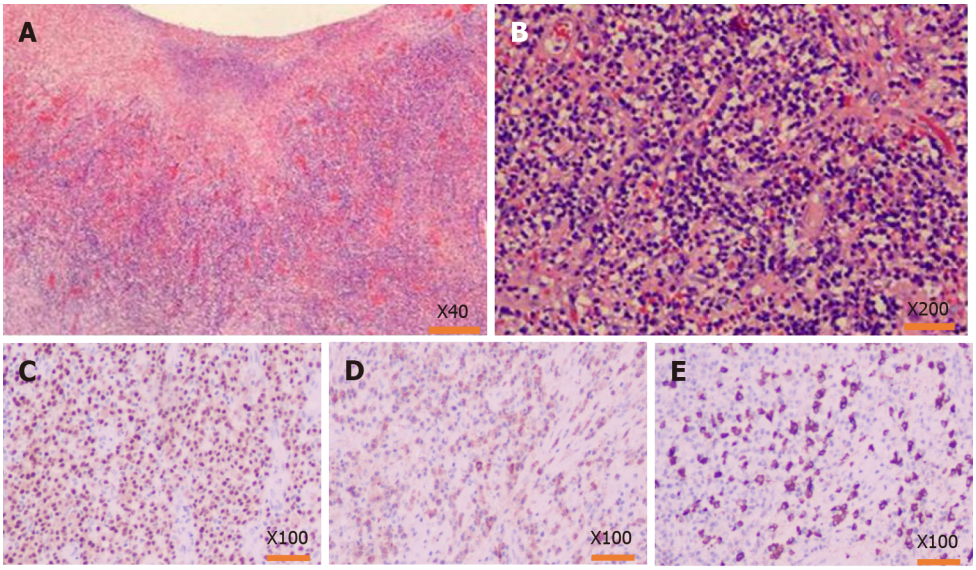

DOI: 10.4240/wjgs.v14.i10.1169 **Copyright** ©The Author(s) 2022.

Figure 7 Pathology findings after the operation. A and B: Hematoxylin-eosin staining of the lesion tissues, inflammatory cell infiltration with plasma cells and neutrophils and increased immunoglobulin G4 (IgG4) positive cells could be seen in the resection colonic mass, accompanied by tissue fibrosis and obliterative phlebitis; C: MMU1 staining showed a high expression state, suggesting a large number of plasma cells infiltration; D: Immunohistochemistry showed a lot of positive IgG staining in the lesion area; E: IgG4 also showed much positive staining in the lesion area, and the number of IgG4-positive cells in the main core area was as high as 110/HPF.

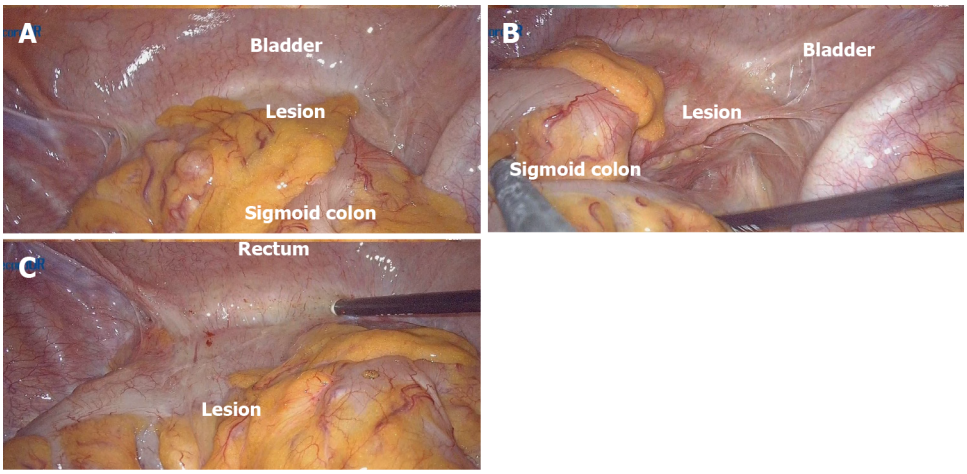

DOI: 10.4240/wjgs.v14.i10.1169 **Copyright** ©The Author(s) 2022.

Figure 8 Operation images from laparoscopy. A: Explore its relationship to surrounding tissue: Dense adhesion of the sigmoid colon to the bladder was observed during the laparoscopic surgery, and it was tough to separate the adhesion; the mass was on the sigmoid colon wall between the bladder and colon; B and C: View the location of the lesion from different angles.

CONCLUSION

In summary, this is a patient with colonic involvement with IgG4-RD. However, recognizing a disease is a gradual process, and the appearance of the disease in rare locations should not be ignored. Since the IgG4 levels in the resected tissue and serological tests were significantly increased, coupled with fibrosis and obliterative phlebitis in the resected colon, the diagnosis of IgG4-RD is reliable. Treatment of IgG4-RD with other immunosuppressive drugs should be further researched. This patient thus provided a rare aspect of IgG4-RD, which may help us further understand this disease.

FOOTNOTES

Author contributions: Zhan WL and Xu XS contributed to conceptualization, data curation, formal analysis, investigation, and methodology; Zhan WL, Liu L, and Jiang W contributed to visualization, roles/writing-original

draft, and writing-review & editing; Cao ZX and Xu XS contributed to conceptualization, project administration, supervision, and writing - review & editing; Qu HT and He FX contributed to investigation; methodology and validation.

Supported by Tongji Hospital Foundation, No. 2021HGRY012; and The Chen Xiao-Ping Foundation for the Development of Science and Technology of Hubei Province, No. CXPJJH121003-2104.

Informed consent statement: Informed written consent was obtained from the patient and her family for publication of this report and any accompanying images.

Conflict-of-interest statement: All the authors report no relevant conflicts of interest for this article.

CARE Checklist (2016) statement: The authors have read the CARE Checklist (2016), and the manuscript was prepared and revised according to the CARE Checklist (2016).

Country/Territory of origin: China

ORCID number: Wen-Li Zhan 0000-0002-5612-8391; Zhi-Xin Cao 0000-0001-9419-5539; Xiang-Shang Xu 0000-0003-3978-401X.

S-Editor: Liu GL
L-Editor: A
P-Editor: Liu GL

REFERENCES

1 **Deshpande V**, Zen Y, Chan JK, Yi EE, Sato Y, Yoshino T, Klöppel G, Heathcote JG, Khosroshahi A, Ferry JA, Aalberse RC, Bloch DB, Brugge WR, Bateman AC, Carruthers MN, Chari ST, Cheuk W, Cornell LD, Fernandez-Del Castillo C, Forcione DG, Hamilos DL, Kamisawa T, Kasashima S, Kawa S, Kawano M, Lauwers GY, Masaki Y, Nakanuma Y, Notohara K, Okazaki K, Ryu JK, Saeki T, Sahani DV, Smyrk TC, Stone JR, Takahira M, Webster GJ, Yamamoto M, Zamboni G, Umehara H, Stone JH. Consensus statement on the pathology of IgG4-related disease. *Mod Pathol* 2012; **25**: 1181-1192 [PMID: 22596100 DOI: 10.1038/modpathol.2012.72]

2 **Kamisawa T**, Funata N, Hayashi Y, Eishi Y, Koike M, Tsuruta K, Okamoto A, Egawa N, Nakajima H. A new clinicopathological entity of IgG4-related autoimmune disease. *J Gastroenterol* 2003; **38**: 982-984 [PMID: 14614606 DOI: 10.1007/s00535-003-1175-y]

3 **Wallace ZS**, Naden RP, Chari S, Choi HK, Della-Torre E, Dicaire JF, Hart PA, Inoue D, Kawano M, Khosroshahi A, Lanzillotta M, Okazaki K, Perugino CA, Sharma A, Saeki T, Schleinitz N, Takahashi N, Umehara H, Zen Y, Stone JH; Members of the ACR/EULAR IgG4-RD Classification Criteria Working Group. The 2019 American College of Rheumatology/European League Against Rheumatism classification criteria for IgG4-related disease. *Ann Rheum Dis* 2020; **79**: 77-87 [PMID: 31796497 DOI: 10.1136/annrheumdis-2019-216561]

4 **Sekiguchi H**, Horie R, Kanai M, Suzuki R, Yi ES, Ryu JH. IgG4-Related Disease: Retrospective Analysis of One Hundred Sixty-Six Patients. *Arthritis Rheumatol* 2016; **68**: 2290-2299 [PMID: 26990055 DOI: 10.1002/art.39686]

5 **Wallace ZS**, Deshpande V, Mattoo H, Mahajan VS, Kulikova M, Pillai S, Stone JH. IgG4-Related Disease: Clinical and Laboratory Features in One Hundred Twenty-Five Patients. *Arthritis Rheumatol* 2015; **67**: 2466-2475 [PMID: 25988916 DOI: 10.1002/art.39205]

6 **Mahajan VS**, Mattoo H, Deshpande V, Pillai SS, Stone JH. IgG4-related disease. *Annu Rev Pathol* 2014; **9**: 315-347 [PMID: 24111912 DOI: 10.1146/annurev-pathol-012513-104708]

7 **Cheuk W**, Chan JK. Lymphadenopathy of IgG4-related disease: an underdiagnosed and overdiagnosed entity. *Semin Diagn Pathol* 2012; **29**: 226-234 [PMID: 23068302 DOI: 10.1053/j.semdp.2012.07.001]

8 **Chang SY**, Keogh KA, Lewis JE, Ryu JH, Cornell LD, Garrity JA, Yi ES. IgG4-positive plasma cells in granulomatosis with polyangiitis (Wegener's): a clinicopathologic and immunohistochemical study on 43 granulomatosis with polyangiitis and 20 control cases. *Hum Pathol* 2013; **44**: 2432-2437 [PMID: 23993777 DOI: 10.1016/j.humpath.2013.05.023]

9 **Chen LYC**, Mattman A, Seidman MA, Carruthers MN. IgG4-related disease: what a hematologist needs to know. *Haematologica* 2019; **104**: 444-455 [PMID: 30705099 DOI: 10.3324/haematol.2018.205526]

10 **Chari ST**. Diagnosis of autoimmune pancreatitis using its five cardinal features: introducing the Mayo Clinic's HISORt criteria. *J Gastroenterol* 2007; **42** Suppl 18: 39-41 [PMID: 17520222 DOI: 10.1007/s00535-007-2046-8]

11 **Perugino CA**, Stone JH. IgG4-related disease: an update on pathophysiology and implications for clinical care. *Nat Rev Rheumatol* 2020; **16**: 702-714 [PMID: 32939060 DOI: 10.1038/s41584-020-0500-7]

12 **Perugino CA**, Wallace ZS, Meyersohn N, Oliveira G, Stone JR, Stone JH. Large vessel involvement by IgG4-related disease. *Medicine (Baltimore)* 2016; **95**: e3344 [PMID: 27428181 DOI: 10.1097/MD.0000000000003344]

13 **Ebbo M**, Grados A, Guedj E, Gobert D, Colavolpe C, Zaidan M, Masseau A, Bernard F, Berthelot JM, Morel N, Lifermann F, Palat S, Haroche J, Mariette X, Godeau B, Bernit E, Costedoat-Chalumeau N, Papo T, Hamidou M, Harlé JR, Schleinitz N. Usefulness of 2-[18F]-fluoro-2-deoxy-D-glucose-positron emission tomography/computed tomography for staging and evaluation of treatment response in IgG4-related disease: a retrospective multicenter study. *Arthritis Care Res (Hoboken)* 2014; **66**: 86-96 [PMID: 23836437 DOI: 10.1002/acr.22058]

14 **Masamune A**, Kikuta K, Hamada S, Tsuji I, Takeyama Y, Shimosegawa T, Okazaki K; Collaborators. Nationwide epidemiological survey of autoimmune pancreatitis in Japan in 2016. *J Gastroenterol* 2020; **55**: 462-470 [PMID: 31872350 DOI: 10.1007/s00535-019-01658-7]

15 **Kamisawa T**, Zen Y, Pillai S, Stone JH. IgG4-related disease. *Lancet* 2015; **385**: 1460-1471 [PMID: 25481618 DOI: 10.1016/S0140-6736(14)60720-0]

16 **Ciccone F**, Ciccone A, Di Ruscio M, Vernia F, Cipolloni G, Coletti G, Calvisi G, Frieri G, Latella G. IgG4-Related Disease Mimicking Crohn's Disease: A Case Report and Review of Literature. *Dig Dis Sci* 2018; **63**: 1072-1086 [PMID: 29417330 DOI: 10.1007/s10620-018-4950-6]

17 **Fujita K**, Naganuma M, Saito E, Suzuki S, Araki A, Negi M, Kawachi H, Watanabe M. Histologically confirmed IgG4-related small intestinal lesions diagnosed *via* double balloon enteroscopy. *Dig Dis Sci* 2012; **57**: 3303-3306 [PMID: 22695887 DOI: 10.1007/s10620-012-2267-4]

18 **Notohara K**, Kamisawa T, Uchida K, Zen Y, Kawano M, Kasashima S, Sato Y, Shiokawa M, Uehara T, Yoshifuji H, Hayashi H, Inoue K, Iwasaki K, Kawano H, Matsubayashi H, Moritani Y, Murakawa K, Oka Y, Tateno M, Okazaki K, Chiba T. Gastrointestinal manifestation of immunoglobulin G4-related disease: clarification through a multicenter survey. *J Gastroenterol* 2018; **53**: 845-853 [PMID: 29222587 DOI: 10.1007/s00535-017-1420-4]

19 **Abe A**, Manabe T, Takizawa N, Ueki T, Yamada D, Nagayoshi K, Sadakari Y, Fujita H, Nagai S, Yamamoto H, Oda Y, Nakamura M. IgG4-related sclerosing mesenteritis causing bowel obstruction: a case report. *Surg Case Rep* 2016; **2**: 120 [PMID: 27797069 DOI: 10.1186/s40792-016-0248-0]

20 **Masaki Y**, Matsui S, Saeki T, Tsuboi H, Hirata S, Izumi Y, Miyashita T, Fujikawa K, Dobashi H, Susaki K, Morimoto H, Takagi K, Kawano M, Origuchi T, Wada Y, Takahashi N, Horikoshi M, Ogishima H, Suzuki Y, Kawanami T, Kawanami Iwao H, Sakai T, Fujita Y, Fukushima T, Saito M, Suzuki R, Morikawa Y, Yoshino T, Nakamura S, Kojima M, Kurose N, Sato Y, Tanaka Y, Sugai S, Sumida T. A multicenter phase II prospective clinical trial of glucocorticoid for patients with untreated IgG4-related disease. *Mod Rheumatol* 2017; **27**: 849-854 [PMID: 27846767 DOI: 10.1080/14397595.2016.1259602]

21 **Inoue D**, Yoshida K, Yoneda N, Ozaki K, Matsubara T, Nagai K, Okumura K, Toshima F, Toyama J, Minami T, Matsui O, Gabata T, Zen Y. IgG4-related disease: dataset of 235 consecutive patients. *Medicine (Baltimore)* 2015; **94**: e680 [PMID: 25881845 DOI: 10.1097/MD.0000000000000680]

22 **Omar D**, Chen Y, Cong Y, Dong L. Glucocorticoids and steroid sparing medications monotherapies or in combination for IgG4-RD: a systematic review and network meta-analysis. *Rheumatology (Oxford)* 2020; **59**: 718-726 [PMID: 31511884 DOI: 10.1093/rheumatology/kez380]

23 **Khosroshahi A**, Bloch DB, Deshpande V, Stone JH. Rituximab therapy leads to rapid decline of serum IgG4 levels and prompt clinical improvement in IgG4-related systemic disease. *Arthritis Rheum* 2010; **62**: 1755-1762 [PMID: 20191576 DOI: 10.1002/art.27435]

24 **Buechter M**, Klein CG, Kloeters C, Schlaak JF, Canbay A, Gerken G, Kahraman A. Tacrolimus as a reasonable alternative in a patient with steroid-dependent and thiopurine-refractory autoimmune pancreatitis with IgG4-associated cholangitis. *Z Gastroenterol* 2014; **52**: 564-568 [PMID: 24905108 DOI: 10.1055/s-0034-1366331]

25 **Wang Y**, Li K, Gao D, Luo G, Zhao Y, Wang X, Zhang J, Jin J, Zhao Z, Yang C, Zhu J, Huang F. Combination therapy of leflunomide and glucocorticoids for the maintenance of remission in patients with IgG4-related disease: a retrospective study and literature review. *Intern Med J* 2017; **47**: 680-689 [PMID: 28321964 DOI: 10.1111/imj.13430]

26 **Yunyun F**, Yu C, Panpan Z, Hua C, Di W, Lidan Z, Linyi P, Li W, Qingjun W, Xuan Z, Yan Z, Xiaofeng Z, Fengchun Z, Wen Z. Efficacy of Cyclophosphamide treatment for immunoglobulin G4-related disease with addition of glucocorticoids. *Sci Rep* 2017; **7**: 6195 [PMID: 28733656 DOI: 10.1038/s41598-017-06520-5]

27 **Yunyun F**, Yu P, Panpan Z, Xia Z, Linyi P, Jiaxin Z, Li Z, Shangzhu Z, Jinjing L, Di W, Yamin L, Xiaowei L, Huadan X, Xuan Z, Xiaofeng Z, Fengchun Z, Yan Z, Wen Z. Efficacy and safety of low dose Mycophenolate mofetil treatment for immunoglobulin G4-related disease: a randomized clinical trial. *Rheumatology (Oxford)* 2019; **58**: 52-60 [PMID: 30124952 DOI: 10.1093/rheumatology/key227]

28 **El Euch M**, Hddad S, Mahfoudhi M, Maktouf H, Ben Hamida F, Jaziri F, Ben Abdelghani K, Turki S, Ben Abdallah T. A Case of Type 1 Autoimmune Pancreatitis (AIP), a Form of IgG4-Related Disease (IgG4-RD). *Am J Case Rep* 2017; **18**: 822-825 [PMID: 28736430 DOI: 10.12659/ajcr.904263]

Published by **Baishideng Publishing Group Inc**
7041 Koll Center Parkway, Suite 160, Pleasanton, CA 94566, USA
Telephone: +1-925-3991568
E-mail: bpgoffice@wjgnet.com
Help Desk: https://www.f6publishing.com/helpdesk
https://www.wjgnet.com